

From reverse to structural vaccinology: profiling of CyRPA as new *Plasmodium falciparum* malaria vaccine candidate antigen

Inauguraldissertation

Zur Erlangung der Würde eines Doktors der Philosophie
vorgelegt der Philosophisch-Naturwissenschaftlichen Fakultät der Universität
Basel

von

Paola Favuzza

aus Italien

Basel, 2017

Original document stored on the publication server of the University of Basel
edoc.unibas.ch



This work is licensed under a [Creative Commons Attribution 4.0 International License](https://creativecommons.org/licenses/by/4.0/).

Genehmigt von der Philosophisch-Naturwissenschaftlichen Fakultät auf Antrag von:

Prof. Dr. Gerd Pluschke

Prof. Dr. Ulrich Certa

Basel, 08 December 2015

Prof. Dr. Jörg Schibler

Dekan

Dedicated to my family

I am among those who think that science has great beauty. A scientist in his laboratory is not only a technician: he is also a child placed before natural phenomena which impress him like a fairy tale.

(Marie Curie)

Acknowledgements

These 4.5 years of my PhD have been challenging and draining but also exciting and rewarding. I have enjoyed wonderful support from my family, friends and colleagues who helped me through this path by inspiring me and getting me to the finish line.

First and foremost, I would like to thank Professor Gerd Pluschke for his expertise, advice, and guidance. I am heartily grateful to Gerd for fostering me in the ability for independent research, for his confidence in me, and for having unconditionally supported me in tough times – not only at work. *Gerd, once again: thank you very much!*

I would also like to thank Professor Ulrich Certa for being the co-referee of my PhD thesis, supporting me along the way and for taking the time to read my PhD thesis.

A special thanks goes to Hugues Matile for his precious advices, constant help, and endless support, and for being a continuous source of inspiration. His guidance allowed me to go on with my research when I was ‘stuck’.

This thesis would not have been possible without the collaboration of many people that have shared their extensive knowledge and experience with me. *Thank you Dr. Ralf Thoma and Dr. Joerg Benz for welcoming me with open arms to your team and for the fruitful collaboration, which moved my research project forward.* And, of course, a huge thank you goes to Dr. Markus Rudolph, who mounted hundreds of tiny crystals, processed and analyzed all the data and kept working with me on the CyRPA project despite frustrating results.

A big thank you goes also to all the people who helped me at Roche – not only with my experiments: Doris Zulauf and Berdard Rutten who taught me how to handle fusions and antibodies, and made my first months at Roche so enjoyable; Dr. Jean-Philippe Carralot, Angelika Schuler and Nicole Soder for their courtesy and unconditional support; Catherine Joseph and Andreas Ehler for introducing me to the awesome world of crystallization and always helping and encouraging me; Elena Guffart for the precious help during the last stages of the crystallization project; and last, but certainly not least, Bernard Gsell who shared with me his deep knowledge and enthusiasm for protein science – and mushrooms!

I could never thank you all enough for your unstinting support, trust and encouragement.

At the Swiss TPH, I owe a big thank you to many people. I would like to thank the entire Molecular Immunology group, including current and former members. Thanks for making my time in the lab pleasant, supporting me when I was frustrated and being very close friends when I was sick.

A special thanks goes to Anita Dreyer who has identified CyRPA and handed over this exciting project to me. *Anita, you introduced me into the lab, shared with me all your knowledge and expertise, taught me how to handle parasites and our 'special protein', and always supported me also from the other side of the world: I'm sincerely thankful to you, without you all this work would have never been possible.*

I also want to thank my master students Simon Blaser and Bianca Scherer for their precious collaboration: *I enjoyed working with you and profit a lot from these teaching experiences!* Many thanks also to Marco Tamborrini for his constant support and invaluable scientific discussions, and for the precious advices on my manuscripts; and, of course, to Arianna Andreoli, a good colleague and a real friend who shared with me the fears and the stress for the final PhD exam.

Further, I would like to thank Dr. Sergio Wittlin and members of his group for the fruitful collaboration on the malaria mouse model.

I would also like to thank all my great friends for their patience, their tireless comfort and optimism in my recurrent ups and downs during the challenging times of my PhD, for having been there and still being here.

Finally, but most importantly, I extend my deepest gratitude to my family – especially to my parents – for their endless love, support and encouragement. They allowed me to pursue my dreams and interests, and encouraged me the whole way in all my decisions.

It is to them that I would like to dedicate this thesis.

Table of Contents

Summary	2
Introduction	5
Global epidemiology of Malaria and control strategies	5
<i>Plasmodium falciparum</i> life cycle.....	7
Malaria: pathophysiology and control interventions.....	8
Immune responses to malaria infections	10
Malaria vaccine development: challenges and progress	11
Objectives	19
References	20
Results	27
Part 1 Passive immunoprotection of <i>Plasmodium falciparum</i> infected mice designates the Cysteine-Rich Protective Antigen as candidate malaria vaccine antigen	27
Part 2 Generation of <i>Plasmodium falciparum</i> parasite-inhibitory antibodies by immunization with recombinantly expressed CyRPA	71
Part 3 Structure of the malaria vaccine candidate antigen CyRPA and its complex with a parasite invasion inhibitory antibody	105
Part 4 Evaluation of the conserved <i>Plasmodium falciparum</i> merozoite antigen PF14_0044 as candidate vaccine antigen	149
Discussion	181
Towards an effective malaria vaccine	183
Subunit vaccines: implication for malaria vaccine development.....	185
Developing malaria vaccines in the –omics era	187
From reverse to structural vaccinology: a perspective for malaria vaccine development.....	189
Prospects for a CyRPA-based malaria vaccine	190
Conclusions	193
References	194
Curriculum Vitae	201

Summary

Malaria is one of the most important and life-threatening infectious diseases worldwide. In 2015 malaria claimed about 429 000 lives, mostly among children below five year of age in sub-Saharan Africa, and caused 212 million clinical episodes in a population of approximately 3.3 billion people living in regions at risk of infection. The development of an effective malaria vaccine is recognized as one of the most promising approaches for preventing infections and reducing transmission. To date, there is no vaccine on the market for prevention of malaria and only a few candidate vaccines were able to induce some protective efficacy. Thus, there is an urgent need to accelerate the pace of design and development of new malaria vaccine candidates that induce broad and long-lasting protective immunity. Reverse vaccinology and structural vaccinology are two complementary techniques that hold much promise in this regard.

The pathogenesis of malaria is primarily associated with blood-stage infection and there is strong evidence that antibodies specific for parasite blood-stage antigens can control parasitemia. This provides a strong rationale for incorporation of asexual blood-stage antigen components into an effective multivalent malaria subunit vaccine.

In this thesis, we exploited the great potential of the ‘omics’ sciences for the selection of hypothetical surface-exposed protein and the evaluation of their potential as vaccine candidate antigens. For the characterization of selected antigens we have exploited an entirely cell-based, rapid and reliable approach for the generation of antigen-specific and parasite cross-reactive monoclonal antibodies (mAbs): (I) generation of mammalian cell lines expressing high levels of the selected predicted malaria antigens as transmembrane proteins; (II) living-cell immunization of mice; (III) generation of hybridoma cell lines producing mAbs capable of recognizing the endogenous antigen in its native context.

This strategy has led us to the identification of the *Plasmodium falciparum* Cysteine-Rich Protective Antigen (PfCyRPA) as promising blood-stage malaria vaccine candidate: (I) PfCyRPA has limited natural immunogenicity, (II) is highly conserved among *P. falciparum* isolates and (III) forms together with the Reticulocyte-binding Homolog 5 (PfRH5) and the PfRH5-interacting Protein (PfRipr) a multiprotein complex crucial for *P. falciparum* erythrocyte invasion; (IV) PfCyRPA-specific mAbs showed parasite *in vitro* growth-inhibitory activity due to inhibition of merozoite invasion; (V) passive immunization

experiments in *P. falciparum* infected NOD-*scid* *IL2R γ ^{null}* mice engrafted with human erythrocytes demonstrated *in vivo* growth-inhibitory activity of PfCyRPA specific mAbs.

To investigate whether growth inhibitory anti-PfCyRPA and anti-PfRH5 Abs can be induced by active immunization with the adjuvanted recombinant proteins, PfCyRPA and PfRH5 were recombinantly expressed as soluble protein in mammalian and insect cells respectively, purified from culture supernatant and employed for immunization of mice. mAbs raised against recombinant PfCyRPA and PfRH5 proteins showed potent parasite growth-inhibitory activity both *in vitro* and *in vivo*. Furthermore, both *in vitro* and *in vivo* anti-PfCyRPA and anti-PfRH5 antibodies showed more potent parasite growth inhibitory activity in combination than on their own, supporting a combined delivery of PfCyRPA and PfRH5 in a vaccine.

To examine the 3D structure of PfCyRPA and to explore the dynamics of its surface loops, we generated co-crystals of it in complex with an inhibitory mAb and elucidated the 3D structure of PfCyRPA and of the epitope–paratope interface by X-ray crystallography. Elucidation of the structure of the epitope recognized by the protective mAb will strongly facilitate design of peptidomimetics in a structural vaccinology approach. The overall structure of PfCyRPA is a six-bladed β -propeller with each blade of the propeller being a four-stranded anti-parallel β -sheet. The five disulfide bonds of the protein are located within blades 1-5, stabilizing each individual blade. Since the 6th blade is composed of β -strands both from the N- and the C-terminus and has no disulfide bond, PfCyRPA has the potential to undergo large conformational changes by disassembly of blade 6.

Among additional hypothetical antigens investigated in the framework of this thesis, PF14_0044 showed interesting features: while none of the generated PF14_0044-specific mAbs significantly inhibited parasite growth, a synergistic *in vitro* inhibitory activity was observed when anti-PF14_0044 mAbs were combined with anti-PfCyRPA mAbs. Applying the principle of reverse vaccinology, we thus identified PfCyRPA and PF14_0044 as targets of merozoite invasion-inhibitory antibodies.

Taken together results show how a combination of reverse and structural vaccinology approaches can enable the identification of new target antigens for incorporation into subunit vaccines.

Introduction

Global epidemiology of Malaria and control strategies

Malaria is an infectious disease of humans and other animals caused by parasitic protozoans belonging to the genus *Plasmodium* and transmitted by female *Anopheles* mosquitoes (1). There are four different malaria species (*P. falciparum*, *P. vivax*, *P. malariae* and *P. ovale*) infecting humans, of which *P. falciparum* and *P. vivax* are the most prevalent and *P. falciparum* is the most dangerous. *P. knowlesi* is a zoonotic plasmodium that is also known to infect humans.

Despite being preventable and treatable, malaria still represents a massive global public health problem, threatening the lives of nearly half the world's population.

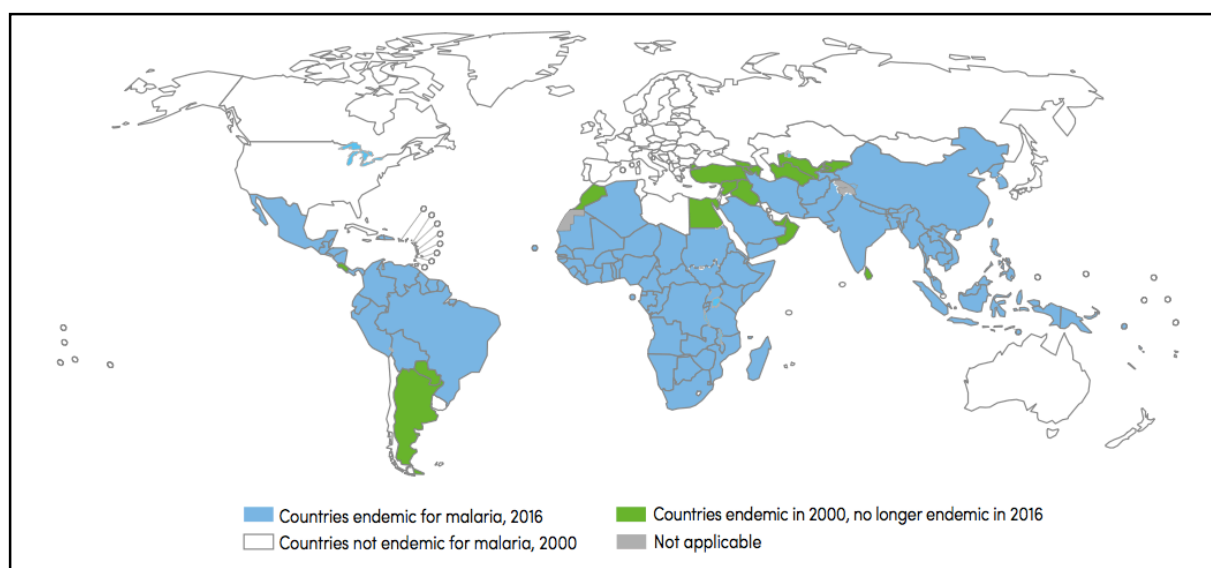


Figure 1. Countries endemic for malaria in 2000 and 2016.

Countries with 3 consecutive years of zero indigenous cases are considered to have eliminated malaria. No country in the WHO European region reported indigenous cases in 2015 but Tajikistan has not yet had 3 consecutive years of zero indigenous cases, its last case being reported in July 2014. Source: WHO database

According to latest available data, an estimated 212 million cases occurred (range: 148 million–304 million) in 2015. In the same year, the disease killed about 429 000 people (range: 235 000–639 000). Approximately 90% of malaria cases and 92% of malaria deaths occurred in Africa, with children aged under 5 years and pregnant women most severely affected (2). Between 2010 and 2015, an expansion of malaria interventions helped to reduce malaria incidence by 21% globally and in Africa. During the same period, malaria mortality rates decreased by an estimated 29% worldwide and by 31% in the African Region.

In the under-five age group, mortality rates have declined by 29% since 2010, but malaria remains a major killer of children, taking the life of a child every 2 minutes. The prevalence of malaria parasite infection (including both symptomatic and asymptomatic infections) has decreased significantly in Africa since 2000: the number of people infected fell from 173 million in 2000 to 114 million in 2015 – a reduction of 34%.

In 2000, malaria was identified as one of the biggest impediments to global development and selected as a critical global target of the Millennium Development Goals (MDGs) (3).

The target to halt and begin to reverse the incidence of malaria by 2015 has been reached: at the beginning of 2016, malaria was considered to be endemic in 91 countries and territories, of the 108 countries that had malaria transmission in 2000 (4–6).

Despite this tremendous progress, a lot still needs to be done: millions of people at risk of malaria still do not have access to interventions such as insecticide-treated mosquito nets (ITNs), diagnostic testing and artemisinin-based combination therapies (ACTs). There is an urgent need to further scale up and sustain malaria control efforts, and ensure that the most vulnerable populations have access to life-saving interventions. The WHO-recommended package of core interventions to prevent infection and reduce morbidity and mortality comprises vector control, chemoprevention, diagnostic testing and treatment.

In May 2015, the World Health Assembly adopted the *Global Technical Strategy for Malaria 2016–2030* (7): the strategy set ambitious yet achievable targets for 2030; namely, to reduce malaria incidence and mortality rates globally by at least 90% by 2030, with a milestone of at least a 40% reduction by 2020. The GTS also set a target to eliminate malaria from at least 35 countries by 2030 (with a milestone of elimination in at least 10 countries by 2020), and simultaneously to prevent the re-establishment of malaria in all countries that were malaria free in 2015. Progress towards the GTS country elimination milestone is on track however, progress towards other GTS targets must be accelerated to meet the GTS milestone of a 40% reduction in malaria case incidence by 2020.

***Plasmodium falciparum* life cycle**

The life cycle of *Plasmodium* is extraordinarily complex involving both invertebrate (mosquito) and vertebrate (mammalian) hosts, multiple parasites stages (asexual and sexual), different infected cell types within the hosts, and numerous intracellular and extracellular environments in which the parasite develops.

During a blood meal, a malaria-infected female *Anopheles* mosquito inoculates sporozoites (a motile infective form) into the human host, thus acting as a transmission vector. Sporozoites travel through the blood vessels to liver cells, where they reproduce asexually (tissue schizogony) maturing into schizonts, which rupture and release thousands of merozoites in the blood stream (over 5-16 days)*. Merozoites infect red blood cells and initiate a series of asexual multiplication cycles (blood schizogony). Within erythrocytes, merozoites develop from ring- to trophozoite-stages, and mature into schizonts that produce up to 36 new infective merozoites, at which point the cells burst and the infective cycle begins anew. In non-immune humans, the infection is amplified about 20-fold each cycle, which takes approximately 48h.

Some of the merozoites leave the cycle of asexual multiplication and develop into immature sexual stages (gametocytes). The gametocytes, male (microgametocytes) and female (macrogametocytes), are ingested by *Anopheles* mosquitos during a blood meal, where they grow and reproduce sexually (sporogonic cycle). In the mosquito gut, gametocytes develop into mature sex cells (gametes). Male and female gametes fuse to form ookinetes — fertilized, motile zygotes that invade the midgut wall and develop into oocysts. The oocysts undergo massive schizogony, rupture and release thousands of sporozoites (after ca. 8-15 days), which eventually migrate to the salivary glands. Inoculation of the sporozoites into a new human host, during a subsequent blood meal, perpetuates the malaria life cycle (8).

* Of note, in *P. vivax* and *P. ovale* a dormant stage (hypnozoites) can persist in the liver and cause relapses by invading the bloodstream weeks, or even years later.

Malaria: pathophysiology and control interventions

Malaria infections may result in a wide variety of symptoms and the disease can be categorized as uncomplicated or severe. In general, malaria is curable if diagnosed and treated promptly and correctly. All the clinical symptoms associated with the disease are caused by the asexual blood-stage parasites. When the parasite develops within the erythrocytes, numerous waste substances, such as hemozoin and other toxic factors, accumulate in the infected red blood cells. Upon schizonts burst, together with the newly formed merozoites, these toxins are dumped into the bloodstream and stimulate host cells to produce cytokines and other soluble factors that produce fever, and probably influence other severe pathophysiology associated with malaria.

Typically, following the infective bite by the *Anopheles* mosquito, the incubation period varies from 7 to 30 days. The first clinical signs are chills, fever, headache, muscle ache, nausea, vomiting, diarrhea, and abdominal cramps. Fever occurs in periodic attacks that last 6 to 10 hours and recur at intervals of approximately 48 hours (tertian malaria – *P. falciparum*, *P. vivax*, and *P. ovale*) or 72 hours (quartan malaria – *P. malarie*), in conjunction with the synchronized release of each new generation of merozoites into the bloodstream.

Besides febrile attacks, malaria patients commonly have anemia (owing to the destruction of red blood cells by the parasites) and splenomegaly (enlargement of the spleen, the organ responsible for ridding the body of degenerate red blood cells).

Infections due to *P. falciparum* are by far the most dangerous: patients may deteriorate rapidly from mild symptoms to coma and death unless they are diagnosed and treated promptly and properly. The greater virulence of *P. falciparum* is associated with the high levels of parasitemia (compared to the other three human malaria species) and the tendency to clump together and adhere to endothelial cells of capillaries. This results in obstruction of the blood flow in various organs, leading to serious organ failure. When the sequestration of infected erythrocytes occurs in the vessels of the brain, it causes the severe disease syndrome known as cerebral malaria, which is associated with high mortality (9–13).

In countries where cases of malaria are infrequent, the symptoms may be attributed to influenza or other common infections resulting in misdiagnosis or delayed diagnosis. Conversely, in highly endemic countries, residents often recognize the symptoms as malaria and treat themselves without diagnostic confirmation ("presumptive treatment").

WHO recommends malaria diagnosis either by microscopy or rapid diagnostic test (RDT) in all patients with suspected malaria before any treatment is administered (14).

According to the WHO guidelines (15), uncomplicated *P. falciparum* malaria cases should be treated with orally administered artemisinin-based combination therapies (ACTs). The combination of two active ingredients with different mode of action is the most effective antimalarial first-line treatment and is thought to delay the emergence of artemisinin resistances. *P. vivax* infections should be treated with chloroquine instead.

Infants, children under five years of age, pregnant women, patients with HIV/AIDS, as well as non-immune migrants, mobile populations and travelers, are at considerably higher risk of contracting malaria, and developing a severe disease progression. Special measures should be taken to protect these population groups from malaria infection: WHO recommends preventive therapies including intermittent preventive treatment of pregnant women (IPTp), intermittent preventive treatment of infants (IPTi), and seasonal malaria chemoprevention (SMC) in children under five years of age in areas with highly seasonal malaria transmission (15). For non-immune travelers, preventive measures against mosquito bites are the first line of defense against malaria. Depending on the malaria risk in the area to be visited, preventive medication (chemoprophylaxis) might be required and should be chosen according to local recommendations.

Together with proper diagnosis and treatment, vector control is a central, critical component of all malaria control strategies. Vector control interventions have proven to successfully reduce or interrupt disease transmission, particularly in areas of high endemicity. Insecticide-treated mosquito nets (ITNs) have been shown to reduce the incidence of malaria cases by 50% in a variety of settings (16, 17). Remarkably, during the past 10 years, coverage with vector control interventions increased substantially in sub-Saharan Africa. Indoor residual spraying (IRS) and long-lasting insecticidal nets (LLINs) are the two most important measures that protect humans from the bite of malaria-infected mosquitoes (18). Of the 65 countries reporting monitoring data for 2010–2013, 53 reported resistance to at least one insecticide class. Therefore, endemic countries are urged to draw up and implement comprehensive insecticide resistance management strategies and ensure entomological and resistance monitoring (19).

Immune responses to malaria infections

Adults living in malaria endemic areas rarely experience malaria episodes: partial protection of adults is mediated by naturally acquired immunity (NAI) and protects against symptomatic disease and high-density parasitemia, but is not effective in offering sterile immunity (20).

Natural immunity to malaria is initially mediated by maternal IgG antibodies, which are acquired by the fetus in utero during the third trimester of pregnancy. Infants remain remarkably resistant to high parasitemia, fever, and severe disease until about 6 months of age. Maternal IgG levels decrease from birth over the first year of life and, as consequence, the prevalence of parasitemia start to increase at about 5 months of age (21). Subsequently, active immunity slowly develops as a result of repeated exposure to malaria, and children gradually develop clinical protection against mild disease (22). The development of clinical and parasitological immunity to malaria is marked by the ability to control disease and parasite density, but require continuous re-exposure. Nonetheless, sterilizing immunity against infection is never fully achieved, and an asymptomatic carrier status is the rule among adults. Conversely, in naïve individuals of any age, *P. falciparum* infection is almost always symptomatic and clinical symptoms can be observed even at very low parasitemia.

Protective immunity against malaria involves both the branches of the immune system and requires a well-coordinated “cross-talk” between the innate and adaptive immunity, involving dendritic cells (DCs), natural killer cells (NKs), B cells, CD4⁺, CD8⁺ and CD3⁺γδ T cells. However, despite intense research efforts, our knowledge about the acquired immunity developed against the disease remains limited and incomplete.

The protective role of antibodies was first demonstrated in 1961 by Cohen et al., showing that passive transfer of immunoglobulins from immune adults to naïve, infected children resulted in rapid reduction of parasitemia and cease of clinical symptoms (23). B cells secreting pathogen-specific antibodies, with CD4⁺ T helper cells enhancement, are essential for clearance of the parasitemia (24). Indeed, merozoite-specific antibodies can prevent erythrocytes invasion and mediate clearance of infected red blood cells by phagocytic cells via antibody-dependent cellular inhibition (22).

In addition to the humoral arm of adaptive immunity, cell-mediated immune responses are also crucial for protection against malaria. CD8⁺ and CD4⁺ T cells kill infected hepatocytes

through diverse mechanisms and induce sterile protection in mouse models (25). Sterile protection, involving both sporozoite-specific antibodies and T cells, has also been observed in humans in sporozoite challenge experiments following vaccination with whole sporozoites (26).

Malaria vaccine development: challenges and progress

Successful vaccinations have proven to prevent infectious diseases by reducing both incidence and mortality, and to significantly contribute to improve public health worldwide. Despite tremendous efforts, many infections that represent a major cause of mortality worldwide are still not vaccine-preventable. Until now, vaccines against certain infections that fail to induce sterilizing immunity upon natural infection (i.e., malaria and respiratory syncytial virus – RSV), those that lead to persistent or latent infection (i.e., HIV-1 and hepatitis C virus – HCV), or those with high degrees of variability (i.e., malaria, dengue and HIV-1) have not been developed (27).

Despite the remarkable improvements achieved in malaria control, emerging antimalarial drug resistances, along with reported insecticide resistances, underline the need of new tools to control and prevent malaria (22, 28). From that perspective, the development of an effective malaria vaccine is recognized as a most promising tool for preventing and controlling malaria. However, complexity of the *Plasmodium* spp. parasite as well as the host response to the parasite has hindered the development of a highly effective vaccine until now. From the immunological point of view, the *Plasmodium* genus presents to the host immune system a myriad of antigens, mostly highly polymorphic, which vary throughout the different stages of the life cycle and successive waves of parasitemia, and against which sequential consecutive immune responses are required. This peculiar antigenic variability, together with the ability of the parasite to hide within host cells (including the MHC class I and II deficient erythrocytes) significantly contributes to immune evasion and appears to be critical for the parasite's survival.

Moreover, no appropriate animal model exists and the only way of testing the efficacy of a candidate vaccine depends on clinical trials being carried out in malaria endemic areas. The high cost of developing a malaria vaccine candidate (e.g., the development of the RTS,S vaccine has received more than \$550 million from the Bill & Melinda Gates Foundation and GSK to date, and another \$260 million are expected to be invested before the completion of the project - (29)) and the length of the process before it can be marketed (up to 10–12 years),

has discouraged pharmaceutical companies from extensively investing in vaccines destined to a market too poor in resources to pay for them.

So far, no surrogate of immunity has been found and there is neither certainty about which specific antigens are relevant for the development of immunity, nor which immune effector mechanisms play the most important role in the immunity developed against the disease.

In spite of these challenges, field and clinical studies showed that some degree of clinical immunity can be acquired naturally with age and exposure or induced by passive or active immunization (23, 30, 31). Those studies support the idea that a malaria vaccine is feasible and pointed out the importance of antibodies as crucial components of the immune response against blood stage parasites. Antimalarial vaccines can break the parasite life cycle at different stages: infection-blocking vaccines targeting hepatic stages, anti-morbidity vaccines targeting the asexual blood stages, and transmission-blocking vaccines targeting the sexual stages. To achieve effective protection, the ideal malaria vaccine is thought to target several steps of the parasite life-cycle in a multistage combination vaccine (32).

Currently, with more than 20 projects in clinical trial phase or advanced preclinical development (33–35), three candidate vaccines are in Phase IIB clinical trials and one, the pre-erythrocytic subunit vaccine RTS,S/AS01, has completed Phase III clinical testing (36).

The updated Malaria Vaccine Roadmap has called for the development and licensing, by 2030, of malaria vaccines, targeting both *P. falciparum* and *P. vivax*, with protective efficacy of at least 75% (37). As new technologies emerged and our understanding of host-pathogen interactions and immunity constantly grows, the achievement of such an ambitious goal may become realistically possible.

Pre-erythrocytic vaccines

Effective immune responses targeting pre-erythrocytic stages would eliminate the parasites before they leave the liver and enter the blood-stream, leading both to protection from clinical disease and to transmission-blocking effects. T cell-mediated responses, specific for liver-stage antigens and able to interfere with the intra-hepatic schizogony, may further limit the infection intensity.

Whole Sporozoite Vaccination

Immunization with attenuated whole parasites, already in late 1960s, has shown to confer highly effective and long-lasting pre-erythrocytic stage immunity against sporozoites challenge in animal models and in humans (26, 38–40). These first clinical trials unequivocally demonstrated the feasibility of vaccination as protection against malaria and made the radiation-attenuated sporozoites (RAS) approach the gold standard for malaria vaccine development.

In 2002, Stephen L. Hoffman founded Sanaria, a biotechnology company, with the mission to develop and commercialize radiation-attenuated, purified and cryopreserved *P. falciparum* sporozoites (PfSPZ). After many technical and quality manufacturing hurdles were overcome (41, 42), a Phase I/IIa clinical trial in 40 adults showed that radiation-attenuated PfSPZ can be highly efficacious if administered intravenously (IV) (43). The vaccine was safe and well tolerated, and induced sterile protection against CHMI (controlled human malaria infection) in six out of six volunteers who received 5 doses of 1.35×10^5 PfSPZ.

Genetically attenuated parasites (GAP), with selected genes crucial for liver-stage development knocked out, have also been investigated. In general, GAP-based vaccines have the advantage of being genetically defined and homogenous, however absolute attenuation is essential and need always to be proved (44). Since the first knockout parasites that cause early liver-stage arrest were described (45, 46), a number of parasite genes involved in the liver-stage development were identified and tested in animal model and humans (47–50). Parasites that are capable of developing into late liver stages, when compared to early-stage-arresting parasites, have been shown to induce a superior effector and memory CD8⁺ T cell response and confer higher levels of protective immunity (51).

Administration of non-attenuated sporozoites under chemoprophylaxis regimen has also been tested and successfully established. In the first human clinical trials (52, 53) all the volunteers exposed to *P. falciparum* infected mosquitoes under chloroquine treatment (leading to elimination of blood-stage trophozoites without any effect on liver-stages parasites)

developed long lasting, sterile protection against homologous CHMI. Currently, other antimalarial drugs and antibiotics are being investigated (54–56).

Pre-erythrocytic subunit vaccines

The development of a pre-erythrocytic (targeting sporozoites and/or liver-stage parasites) subunit vaccine capable of inducing sterile protection would prevent both disease and transmission associated with blood stage infections. The limited antigenic variation (in comparison to blood-stage parasites) certainly represents strength and prospects the possibility of raising strain-transcending immunity. However, pre-erythrocytic subunit vaccines need to be broadly and highly effective because parasites escape from the immune surveillance in the liver, would lead to the onset of blood-stage infection and eventually malaria disease and transmission. Several pre-erythrocytic antigens have been investigated, but the main focus was laid on the circumsporozoite protein (CSP), the most prominent surface antigen on sporozoites, well known to play an important role in the attachment to the hepatocytes and invasion (57). Initial vaccine formulations based on soluble CSP protein failed to provide substantial protection (58, 59). Based on the first genetically engineered hepatitis B vaccine, GlaxoSmithKline (GSK) developed the RTS,S, the most advanced pre-erythrocytic vaccine candidate, and the only malaria vaccine candidate that has proven efficacy, albeit limited, in malaria-naïve, semi-immune adults, as well as children and infants living in endemic regions.

The RTS,S contains the repeat region (R) and T cell epitopes (T) of the *P. falciparum* CSP fused to the hepatitis-B virus surface antigen – HBsAg – (S) and additional unfused copies of HBsAg (S) (60). HBsAg, and derived fusion proteins, are capable of spontaneous assembly into virus-like particles (VLPs) that stimulate strong humoral and cellular immune responses and exhibit self-adjuvanting capabilities. Encouraging results in Phase II clinical trials in African countries, confirmed that both the adult and pediatric doses vaccine conferred partial protection against malaria (61, 62). In 2009, the first Phase III malaria vaccine trial was initiated: a multicenter study of RTS,S/AS01 was undertaken in 11 research centers across 7 countries with various patterns of malaria transmission. Results, including the effect of a booster dose at month 20, have now been published (36). Overall, protection against clinical and severe malaria was 36% and 32%, respectively. When considering infants aged 6-12 weeks at first vaccination, estimates of vaccine efficacy were lower if compared to the older age category. Vaccine efficacy against clinical malaria, over the whole study (average follow-up 38 months) was 18% without a booster dose, and 26% with a booster dose. There was no

evidence for protection against severe malaria. Although RTS,S/AS01 Phase III results showed the potential for a significant impact on the malaria burden, a vaccine with higher levels of efficacy, broader age target and duration of vaccination-induced protection, would be needed to fulfill the ambitious goals fixed by the Malaria Vaccine Roadmap (37).

In July 2015, the European Medicine Agency (EMA) has adopted a positive scientific opinion for the RTS,S/AS01 in children aged 6 weeks to 17 months and, in October 2015, two independent WHO advisory groups recommended the pilot implementation of RTS,S/AS01 in parts of 3 to 5 sub-Saharan African countries. WHO has adopted these recommendations and is strongly supportive of the need to proceed with the pilots as the next step for the world's first malaria vaccine (63). RTS,S/AS01 is being evaluated in a Phase IV pharmacovigilance baseline study (the study is currently recruiting participants - [Clinicaltrials.gov: NCT02374450](https://clinicaltrials.gov/ct2/show/study/NCT02374450)) as a complementary malaria control measure that could be added to – but not replace – the core package of proven malaria preventive, diagnostic and treatment tools.

Viral vectors have also been investigated for delivering the DNA sequence of vaccine antigens and promoting strong cellular immune responses (the antigen of interest is produced within the host cells, processed and then presented on MHC I/II molecules to induce T cell responses) (64). The most advanced viral vectored malaria vaccine is based on the thrombospondin-related adhesive protein (TRAP), a surface sporozoite protein essential for motility and infectivity (65, 66). Immunization with plasmid DNA followed by a recombinant replication-deficient modified vaccinia virus Ankara (MVA), both expressing ME-TRAP, showed promising results both in animal models and humans (67, 68). The use of more potent recombinant replication-deficient adenoviral vectors (HAdV5, HAdV35, ChAd63) coding different malaria antigens (PfTRAP, PvTRAP, CSP, AMA-1, MSP-1- alone and in different combinations) was also considered. Encouraging immunogenicity data (both high antibodies titers and strong T cell responses) have been shown (69–71) and are being evaluated ([Clinicaltrials.gov: NCT01366534](https://clinicaltrials.gov/ct2/show/study/NCT01366534), [NCT01635647](https://clinicaltrials.gov/ct2/show/study/NCT01635647), [NCT02083887](https://clinicaltrials.gov/ct2/show/study/NCT02083887)). Of particular interest is the combination of anti-sporozoite and anti-liver-stage subunit vaccines to assess eventual benefits rising from synergistic vaccine efficacy (72). The initial results of the first clinical trial combining RTS,S/AS01B and ChAd63-MVA ME-TRAP showed an 82% (14/17) sterile protection achieved in a Phase IIa CHMI study ([NCT01883609](https://clinicaltrials.gov/ct2/show/study/NCT01883609)). In this perspective, numerous on-going efforts are trying to identify novel antigens: the combination of new functional and bioinformatic approaches holds significant promise for the identification and clinical development of novel pre-erythrocytic vaccine antigen targets in the near future.

Asexual blood stage vaccines

Although the acquisition of protective anti-disease immunity in endemic populations (naturally acquired immunity – NAI) has been largely reported and associated with antibody responses against blood-stage parasites, the development of vaccines against the asexual blood-stage parasite has been extremely challenging and has not reported significant efficacy. However, sterilizing immunity is not absolutely essential for an effective blood-stage vaccine: if the parasitemia can be contained during the early growth cycles, then disease severity and mortality would still be prevented, whilst allowing for induction of additional naturally acquired responses. Moreover, the reduction of infected red blood cells (iRBC) density would also affect gametocyte availability and, in turn, malaria transmission. Blood-stage vaccines are also regarded as crucial components for the development of a multi-component/multi-stage malaria vaccine, especially in the context of partially effective pre-erythrocytic vaccines.

Despite the broad number of antigens expressed by blood-stage parasites, most efforts in vaccine research have focused on a few antigens implicated in the invasion of red blood cells (RBC) by the merozoites, in particular the *P. falciparum* merozoite surface protein 1, 2 and 3 (MSP1, MSP2, MSP3) (73–75), apical membrane antigen 1 (AMA1) (76), glutamate-rich protein (GLURP) (77), serine repeat antigen 5 (SERA5) (78), and the erythrocyte-binding antigen 175 kDa (EBA-175) (79).

One of the major problems associated with these vaccine candidates, which have mainly been investigated and tested as recombinant protein-in-adjuvant formulations, has been the extensive antigenic polymorphism exhibited (80), coupled with the high titers of antigen-specific antibodies required to achieve protective effects (81).

Prime-boost regimes using replication-deficient adenoviruses and poxviruses encoding blood-stage antigens have been investigated and shown to be favorable compared to protein-in-adjuvant formulations in terms of inducing both antibody and T cell responses in mice and NHPs (82, 83). However, clinical trials (Phase I and II) conducted with MSP1, AMA1 and their combination (ChAd63-MVA prime-boost regime), failed to provide any convincing evidence that cellular immunity induced by viral vectors can impart blood-stage protection in malaria-naïve individuals (84–86).

Despite disappointing efficacy levels of MSP1- and AMA1-based vaccines, the recent identification and assessment of novel merozoites target antigens has rose encouraging optimism (87–90). Since the full genome of *P. falciparum* 3D7 was sequenced and annotated in 2002 (91), large-scale genomic, proteomic, transcriptomic and comparative data, including

different *P. falciparum* strains, field isolates, and other *Plasmodium* species have become available (92). These extensive data sets offer valuable and powerful tools for rational search for new candidate antigens, and have made reverse vaccinology the most promising strategy for vaccine development (93, 94). Based on these dataset, large libraries of merozoites proteins have been compiled (87–90) and new antigens with great potential as blood-stage vaccine candidates have been discovered (95).

On the basis of available genome-wide transcriptomic and proteomic data, Dreyer et al. (89) have selected uncharacterized surface proteins, with specific expression in extracellular parasite stages, to evaluate their potential as vaccine candidate antigens. This strategy has led to the identification of the *Plasmodium falciparum* Cysteine-Rich Protective Antigen (PfCyRPA). PfCyRPA forms together with the Reticulocyte-binding Homolog 5 (PfRH5) and the PfRH5-interacting Protein (PfRipr) a multiprotein complex crucial for *P. falciparum* erythrocyte invasion (96). PfRH5 has been shown to play a key role in the attachment of merozoites to the erythrocyte surface via the interaction with the host receptor basigin (97, 98). PfRH5 is currently regarded as a leading blood-stage malaria vaccine candidate: it demonstrated poor natural immunogenicity and has been shown to induce invasion-inhibitory antibodies that are effective across common PfRH5 genetic variants and PfRH5-based vaccines can protect *Aotus* monkeys against virulent vaccine-heterologous *P. falciparum* challenges (87, 99–101). Interestingly, PfCyRPA and PfRH5 genes are located in close proximity in the genome and have no substantial sequence polymorphisms. Also, Reddy et al. (96) reported a synergistic *in vitro* inhibitory activity for the combination of polyclonal anti-PfCyRPA and anti-PfRH5 antibodies. These findings suggest that additional investigation is needed for an in depth characterization of the invasion complex, and make CyRPA and PfRH5 appealing candidates for the development of new antimalarial vaccine strategies. The first RH5 clinical trial using the ChAd63-MVA platform was initiated in Oxford in 2014 (NCT02181088), the results of which are eagerly awaited.

To date, only one clinical trial has been conducted for *P. vivax* (NCT01816113) – a ChAd63-MVA viral vectored vaccine targeting region II of the Duffy-binding protein, largely reported to be essential for reticulocyte invasion by this parasite (102). Results remain awaited.

Transmission blocking vaccines

Transmission-blocking vaccines (TBV) target sexual blood-stage gametocyte or mosquito-stage parasite antigens to induce antibodies in human hosts, which are ingested by *Anopheles* mosquitoes during blood meals and, eventually, inhibit parasite development in the mosquito midgut (103). Vaccinated individuals would not gain direct benefit or protection but, in the context of community vaccination campaigns, reduced transmission rates would instead confer indirect protection from becoming infected. These vaccines, which include also pre-erythrocytic and asexual blood-stage vaccines capable of reducing gametocyte densities, are described as ‘community-acquired vaccines’ and ‘vaccines that interrupt malaria transmission’ (VIMT) (104).

P. falciparum surface protein 25 (Pfs25), Pfs48/45, and Pfs230 (105) are the most studied and most advanced TBV antigens (106). To date the only TBV antigens evaluated in human clinical trials are Pfs25 and its orthologue in *P. vivax*, Pvs25. These antigens are exclusively expressed on zygote and ookinete stages of parasites within the mosquito, but not in the human host. As not under human immune selection pressure, the antigens are extremely conserved between field isolates however, after vaccination the antibody response cannot be boosted through natural infection.

A Phase Ia clinical trial with recombinant Pvs25 protein in combination with Alhydrogel® showed modest transmission blocking activity, correlated with limited antibody titers (107). To improve immunogenicity, different adjuvant system (108), conjugates to *Pseudomonas aeruginosa* ExoProtein (109, 110), virus-like particle containing a Pfs25 recombinant protein fused to the Alfalfa Mosaic Virus coat protein (NCT02013687), and recombinant replication-deficient viral vectors in prime-boost regimes (111) have been evaluated. The first human clinical trial with ChAd63-MVA vectors encoding Pfs25 fused to IMX313 (heptamerization domain (112)) is currently recruiting patients (NCT02532049).

A number of additional candidates are under intensive investigation at the preclinical stage and/or are progressing towards clinical trials (i.e. Pfs230, Pfs48/45-GLURP fusion protein, Pfs28, PfHAP2).

Objectives

Plasmodium falciparum has a 23-megabase genome that contains an estimated 5,300 predicted proteins, many of which are expressed in different stages of the parasite life cycle. However, so far only a small handful of historical candidate antigens have been extensively investigated as malaria vaccine components, and the results from human clinical trials have been discouraging.

The last 15 years have seen the publication of the genomic sequences of the parasite *Plasmodium falciparum* (91), the mosquito vector *Anopheles gambiae* (113) and the human host (114). Clearly, the onset of the –omics era combined with the advent of new strategies (e.g. reverse and structural vaccinology) creates an unprecedented potential to revolutionize the malaria vaccine field.

In fact, many novel antigens are already being identified from the parasite’s genome (87, 88, 90), renewing hope that more effective antigens can be developed as vaccine formulations and offer higher levels of protection at multiple stages of the parasite’s complex life cycle.

In this thesis, we applied reverse vaccinology (Obj. 1–3) and structural vaccinology (Obj. 4) strategies for the rational discovery and optimization of novel malaria subunit vaccine candidates. Our strategy is based on the selection of uncharacterized parasite proteins that are predicted to be accessible to immune surveillance by antibodies, and their subsequent functional characterization using specific monoclonal antibodies.

Within the framework of this PhD project, specific objectives were:

1. Identification of novel vaccine candidates and characterization of selected antigens exploiting a rapid and efficient mammalian cell-based approach for the generation of monoclonal antibodies (mAbs) capable of recognizing endogenous antigens in their native context;
2. Functional characterization and assessment of their potential as malaria subunit vaccine components by *in vitro* and *in vivo* functional assays with generated antigen-specific mAbs;
3. Active immunization in mice with purified recombinant proteins and evaluation of their immunogenicity in protein-in-adjuvant vaccine formulations.
4. Elucidation of the 3D structure of the *Plasmodium falciparum* Cysteine-Rich Protective antigen (PfCyRPA), to identify the protective B-cell epitopes targeted by parasite growth inhibitory antibodies.

References

1. WHO | Malaria *WHO*. Available at: <http://www.who.int/mediacentre/factsheets/fs094/en/> [Accessed October 14, 2015].
2. WHO | World Malaria Report 2016 Available at: <http://www.who.int/malaria/publications/world-malaria-report-2016/en/> [Accessed February 1, 2017].
3. WHO | MDG 6: combat HIV/AIDS, malaria and other diseases *WHO*. Available at: http://www.who.int/topics/millennium_development_goals/diseases/en/ [Accessed October 14, 2015].
4. World Health Organization (2005) WHO | Resolution WHA58.2 on malaria control. Fifty-eighth World Health Assembly, Geneva, 2005. Available at: http://apps.who.int/gb/ebwha/pdf_files/WHA58-REC1/english/A58_2005_REC1-en.pdf [Accessed October 14, 2015].
5. Achieving the malaria MDG target: reversing the incidence of malaria 2000-2015 - 9789241509442_eng.pdf Available at: http://apps.who.int/iris/bitstream/10665/184521/1/9789241509442_eng.pdf [Accessed October 14, 2015].
6. Bhatt S, et al. (2015) The effect of malaria control on Plasmodium falciparum in Africa between 2000 and 2015. *Nature* 526(7572):207–211.
7. WHO | Global Technical Strategy for Malaria 2016–2030 *WHO*. Available at: <http://www.who.int/malaria/publications/atoz/9789241564991/en/> [Accessed October 9, 2015].
8. CDC - DPDx - Malaria Available at: <http://www.cdc.gov/dpdx/malaria/index.html> [Accessed October 14, 2015].
9. Crutcher JM, Hoffman SL (1996) Malaria. *Medical Microbiology*, ed Baron S (University of Texas Medical Branch at Galveston, Galveston (TX)). 4th Ed. Available at: <http://www.ncbi.nlm.nih.gov/books/NBK8584/> [Accessed October 15, 2015].
10. malaria | pathology *Encycl Br*. Available at: <http://www.britannica.com/science/malaria> [Accessed October 15, 2015].
11. Miller LH, Good MF, Milon G (1994) Malaria pathogenesis. *Science* 264(5167):1878–1883.
12. Miller LH, Baruch DI, Marsh K, Doumbo OK (2002) The pathogenic basis of malaria. *Nature* 415(6872):673–679.
13. Trampuz A, Jereb M, Muzlovic I, Prabhu RM (2003) Clinical review: Severe malaria. *Crit Care* 7(4):315.
14. World Health Organization, World Health Organization, Global Malaria Programme (2011) *Universal access to malaria diagnostic testing an operational manual* (World Health Organization, Geneva).
15. 9789241549127_eng.pdf.
16. Eisele TP, Larsen D, Steketee RW (2010) Protective efficacy of interventions for preventing malaria mortality in children in Plasmodium falciparum endemic areas. *Int J Epidemiol* 39(suppl 1):i88–i101.
17. Lengeler C (2004) Insecticide-treated bed nets and curtains for preventing malaria. *Cochrane Database of Systematic Reviews*, ed The Cochrane Collaboration (John Wiley & Sons, Ltd, Chichester, UK). Available at: <http://doi.wiley.com/10.1002/14651858.CD000363.pub2> [Accessed October 17, 2015].
18. Pluess B, Tanser FC, Lengeler C, Sharp BL (2010) Indoor residual spraying for preventing malaria. *Cochrane Database of Systematic Reviews*, ed The Cochrane

- Collaboration (John Wiley & Sons, Ltd, Chichester, UK). Available at: <http://doi.wiley.com/10.1002/14651858.CD006657.pub2> [Accessed October 17, 2015].
19. World Health Organization, World Health Organization eds. (2012) *Global plan for insecticide resistance management in malaria vectors* (World Health Organization, Geneva, Switzerland).
 20. Doolan DL, Dobaño C, Baird JK (2009) Acquired immunity to malaria. *Clin Microbiol Rev* 22(1):13–36, Table of Contents.
 21. Akum AE, Minang JT, Kuoh AJ, Ahmadou MJ, Troye-Blomberg M (2005) Plasmodium falciparum inhibitory capacities of paired maternal-cord sera from south-west province, Cameroon. *J Trop Pediatr* 51(3):182–190.
 22. Marsh K, Kinyanjui S (2006) Immune effector mechanisms in malaria. *Parasite Immunol* 28(1–2):51–60.
 23. Cohen S, McGregor IA, Carrington S (1961) Gamma-globulin and acquired immunity to human malaria. *Nature* 192(4804):733–737.
 24. Langhorne J, Ndungu FM, Sponaas A-M, Marsh K (2008) Immunity to malaria: more questions than answers. *Nat Immunol* 9(7):725–732.
 25. Doolan DL, Hoffman SL (2000) The Complexity of Protective Immunity Against Liver-Stage Malaria. *J Immunol* 165(3):1453–1462.
 26. Hoffman SL, et al. (2002) Protection of Humans against Malaria by Immunization with Radiation-Attenuated Plasmodium falciparum Sporozoites. *J Infect Dis* 185(8):1155–1164.
 27. Loomis R, Johnson P (2015) Emerging Vaccine Technologies. *Vaccines* 3(2):429–447.
 28. Crompton PD, Pierce SK, Miller LH (2010) Advances and challenges in malaria vaccine development. *J Clin Invest* 120(12):4168–4178.
 29. PATH Malaria Vaccine Initiative Available at: <http://www.malariavaccine.org/> [Accessed November 14, 2015].
 30. Sabchareon A, et al. (1991) Parasitologic and clinical human response to immunoglobulin administration in falciparum malaria. *Am J Trop Med Hyg* 45(3):297–308.
 31. Moreno A, Joyner C (2015) Malaria vaccine clinical trials: what’s on the horizon. *Curr Opin Immunol* 35:98–106.
 32. Doolan DL, Hoffman SL (1997) Multi-gene vaccination against malaria: A multistage, multi-immune response approach. *Parasitol Today Pers Ed* 13(5):171–178.
 33. WHO | Malaria vaccine development WHO. Available at: <http://www.who.int/malaria/areas/vaccine/en/> [Accessed February 14, 2017].
 34. WHO | Tables of malaria vaccine projects globally WHO. Available at: http://www.who.int/immunization/research/development/Rainbow_tables/en/ [Accessed February 14, 2017].
 35. Schwartz L, Brown GV, Genton B, Moorthy VS (2012) A review of malaria vaccine clinical projects based on the WHO rainbow table. *Malar J* 11(11):10–1186.
 36. RTS,S Clinical Trials Partnership (2015) Efficacy and safety of RTS,S/AS01 malaria vaccine with or without a booster dose in infants and children in Africa: final results of a phase 3, individually randomised, controlled trial. *Lancet Lond Engl* 386(9988):31–45.
 37. WHO | Malaria vaccine technology roadmap WHO. Available at: http://www.who.int/immunization/topics/malaria/vaccine_roadmap/en/ [Accessed November 8, 2015].
 38. Nussenzweig RS, Vanderberg J, Most H, Orton C (1967) Protective immunity produced by the injection of x-irradiated sporozoites of plasmodium berghei. *Nature* 216(5111):160–162.

39. Clyde DF, Most H, McCarthy VC, Vanderberg JP (1973) Immunization of man against sporozite-induced falciparum malaria. *Am J Med Sci* 266(3):169–177.
40. Rieckmann KH, Carson PE, Beaudoin RL, Cassells JS, Sell KW (1974) Letter: Sporozoite induced immunity in man against an Ethiopian strain of Plasmodium falciparum. *Trans R Soc Trop Med Hyg* 68(3):258–259.
41. Hoffman SL, et al. (2010) Development of a metabolically active, non-replicating sporozoite vaccine to prevent Plasmodium falciparum malaria. *Hum Vaccin* 6(1):97–106.
42. Epstein JE, et al. (2011) Live attenuated malaria vaccine designed to protect through hepatic CD8⁺ T cell immunity. *Science* 334(6055):475–480.
43. Seder RA, et al. (2013) Protection against malaria by intravenous immunization with a nonreplicating sporozoite vaccine. *Science* 341(6152):1359–1365.
44. Doll KL, Harty JT (2014) Correlates of protective immunity following whole sporozoite vaccination against malaria. *Immunol Res* 59(1–3):166–176.
45. Mueller A-K, Labaied M, Kappe SHI, Matuschewski K (2005) Genetically modified Plasmodium parasites as a protective experimental malaria vaccine. *Nature* 433(7022):164–167.
46. van Dijk MR, et al. (2005) Genetically attenuated, P36p-deficient malarial sporozoites induce protective immunity and apoptosis of infected liver cells. *Proc Natl Acad Sci U S A* 102(34):12194–12199.
47. Labaied M, et al. (2007) Plasmodium yoelii sporozoites with simultaneous deletion of P52 and P36 are completely attenuated and confer sterile immunity against infection. *Infect Immun* 75(8):3758–3768.
48. Finney OC, et al. (2014) Immunization with genetically attenuated P. falciparum parasites induces long-lived antibodies that efficiently block hepatocyte invasion by sporozoites. *Vaccine* 32(19):2135–2138.
49. Spring M, et al. (2013) First-in-human evaluation of genetically attenuated Plasmodium falciparum sporozoites administered by bite of Anopheles mosquitoes to adult volunteers. *Vaccine* 31(43):4975–4983.
50. Mikolajczak SA, et al. (2014) A next-generation genetically attenuated Plasmodium falciparum parasite created by triple gene deletion. *Mol Ther J Am Soc Gene Ther* 22(9):1707–1715.
51. Butler NS, et al. (2011) Superior antimalarial immunity after vaccination with late liver stage-arresting genetically attenuated parasites. *Cell Host Microbe* 9(6):451–462.
52. Roestenberg M, et al. (2009) Protection against a Malaria Challenge by Sporozoite Inoculation. *N Engl J Med* 361(5):468–477.
53. Roestenberg M, et al. (2011) Long-term protection against malaria after experimental sporozoite inoculation: an open-label follow-up study. *Lancet Lond Engl* 377(9779):1770–1776.
54. Bijker EM, et al. (2014) Sporozoite immunization of human volunteers under mefloquine prophylaxis is safe, immunogenic and protective: a double-blind randomized controlled clinical trial. *PloS One* 9(11):e112910.
55. Friesen J, et al. (2010) Natural immunization against malaria: causal prophylaxis with antibiotics. *Sci Transl Med* 2(40):40ra49.
56. Pfeil J, et al. (2014) Protection against malaria by immunization with non-attenuated sporozoites under single-dose piperazine-tetraphosphate chemoprophylaxis. *Vaccine* 32(45):6005–6011.
57. Hollingdale MR, Nardin EH, Tharavanij S, Schwartz AL, Nussenzweig RS (1984) Inhibition of entry of Plasmodium falciparum and P. vivax sporozoites into cultured cells; an in vitro assay of protective antibodies. *J Immunol Baltim Md* 1950 132(2):909–913.

58. Brown AE, et al. (1994) Safety, immunogenicity and limited efficacy study of a recombinant *Plasmodium falciparum* circumsporozoite vaccine in Thai soldiers. *Vaccine* 12(2):102–108.
59. Sherwood JA, et al. (1996) *Plasmodium falciparum* circumsporozoite vaccine immunogenicity and efficacy trial with natural challenge quantitation in an area of endemic human malaria of Kenya. *Vaccine* 14(8):817–827.
60. Cohen J, Nussenzweig V, Nussenzweig R, Vekemans J, Leach A (2010) From the circumsporozoite protein to the RTS, S/AS candidate vaccine. *Hum Vaccin* 6(1):90–96.
61. Agnandji ST, et al. (2010) Evaluation of the safety and immunogenicity of the RTS,S/AS01E malaria candidate vaccine when integrated in the expanded program of immunization. *J Infect Dis* 202(7):1076–1087.
62. Asante KP, et al. (2011) Safety and efficacy of the RTS,S/AS01E candidate malaria vaccine given with expanded-programme-on-immunisation vaccines: 19 month follow-up of a randomised, open-label, phase 2 trial. *Lancet Infect Dis* 11(10):741–749.
63. WHO | Malaria vaccine: WHO position paper – January 2016 - 29 January 2016, vol. 91, 4 (pp. 33–52) WHO. Available at: <http://www.who.int/wer/2016/wer9104/en/> [Accessed February 14, 2017].
64. Liu MA (2010) Immunologic basis of vaccine vectors. *Immunity* 33(4):504–515.
65. Robson KJ, et al. (1988) A highly conserved amino-acid sequence in thrombospondin, properdin and in proteins from sporozoites and blood stages of a human malaria parasite. *Nature* 335(6185):79–82.
66. Sultan AA, et al. (1997) TRAP is necessary for gliding motility and infectivity of *Plasmodium* sporozoites. *Cell* 90(3):511–522.
67. Schneider J, et al. (1998) Enhanced immunogenicity for CD8+ T cell induction and complete protective efficacy of malaria DNA vaccination by boosting with modified vaccinia virus Ankara. *Nat Med* 4(4):397–402.
68. McConkey SJ, et al. (2003) Enhanced T-cell immunogenicity of plasmid DNA vaccines boosted by recombinant modified vaccinia virus Ankara in humans. *Nat Med* 9(6):729–735.
69. Chuang I, et al. (2013) DNA prime/Adenovirus boost malaria vaccine encoding *P. falciparum* CSP and AMA1 induces sterile protection associated with cell-mediated immunity. *PLoS One* 8(2):e55571.
70. Padte NN, et al. (2013) A glycolipid adjuvant, 7DW8-5, enhances CD8+ T cell responses induced by an adenovirus-vectored malaria vaccine in non-human primates. *PLoS One* 8(10):e78407.
71. Reyes-Sandoval A, et al. (2010) Prime-boost immunization with adenoviral and modified vaccinia virus Ankara vectors enhances the durability and polyfunctionality of protective malaria CD8+ T-cell responses. *Infect Immun* 78(1):145–153.
72. Hutchings CL, Birkett AJ, Moore AC, Hill AVS (2007) Combination of Protein and Viral Vaccines Induces Potent Cellular and Humoral Immune Responses and Enhanced Protection from Murine Malaria Challenge. *Infect Immun* 75(12):5819–5826.
73. Holder AA (2009) The carboxy-terminus of merozoite surface protein 1: structure, specific antibodies and immunity to malaria. *Parasitology* 136(12):1445–1456.
74. McCarthy JS, et al. (2011) A Phase 1 Trial of MSP2-C1, a Blood-Stage Malaria Vaccine Containing 2 Isoforms of MSP2 Formulated with Montanide® ISA 720. *PLoS ONE* 6(9):e24413.
75. Sirima SB, et al. (2009) Safety and immunogenicity of the malaria vaccine candidate MSP3 long synthetic peptide in 12-24 months-old Burkinabe children. *PLoS One* 4(10):e7549.
76. Remarque EJ, Faber BW, Kocken CHM, Thomas AW (2008) Apical membrane antigen 1: a malaria vaccine candidate in review. *Trends Parasitol* 24(2):74–84.

77. Mordmüller B, et al. (2010) Safety and immunogenicity of the malaria vaccine candidate GMZ2 in malaria-exposed, adult individuals from Lambaréné, Gabon. *Vaccine* 28(41):6698–6703.
78. Palacpac NMQ, et al. (2013) Phase 1b Randomized Trial and Follow-Up Study in Uganda of the Blood-Stage Malaria Vaccine Candidate BK-SE36. *PLoS ONE* 8(5):e64073.
79. El Sahly HM, et al. (2010) Safety and immunogenicity of a recombinant nonglycosylated erythrocyte binding antigen 175 Region II malaria vaccine in healthy adults living in an area where malaria is not endemic. *Clin Vaccine Immunol CVI* 17(10):1552–1559.
80. Takala SL, et al. (2009) Extreme Polymorphism in a Vaccine Antigen and Risk of Clinical Malaria: Implications for Vaccine Development. *Sci Transl Med* 1(2):2ra5.
81. Thera MA, et al. (2011) A field trial to assess a blood-stage malaria vaccine. *N Engl J Med* 365(11):1004–1013.
82. Douglas AD, et al. (2010) Tailoring subunit vaccine immunogenicity: maximizing antibody and T cell responses by using combinations of adenovirus, poxvirus and protein-adjuvant vaccines against *Plasmodium falciparum* MSP1. *Vaccine* 28(44):7167–7178.
83. Draper SJ, et al. (2010) Enhancing blood-stage malaria subunit vaccine immunogenicity in rhesus macaques by combining adenovirus, poxvirus, and protein-in-adjuvant vaccines. *J Immunol Baltim Md 1950* 185(12):7583–7595.
84. Sheehy SH, et al. (2012) Phase Ia clinical evaluation of the safety and immunogenicity of the *Plasmodium falciparum* blood-stage antigen AMA1 in ChAd63 and MVA vaccine vectors. *PloS One* 7(2):e31208.
85. Sheehy SH, et al. (2011) Phase Ia clinical evaluation of the *Plasmodium falciparum* blood-stage antigen MSP1 in ChAd63 and MVA vaccine vectors. *Mol Ther J Am Soc Gene Ther* 19(12):2269–2276.
86. Sheehy SH, et al. (2012) ChAd63-MVA-vectored blood-stage malaria vaccines targeting MSP1 and AMA1: assessment of efficacy against mosquito bite challenge in humans. *Mol Ther J Am Soc Gene Ther* 20(12):2355–2368.
87. Douglas AD, et al. (2011) The blood-stage malaria antigen PfrH5 is susceptible to vaccine-inducible cross-strain neutralizing antibody. *Nat Commun* 2:601.
88. Crosnier C, et al. (2013) A Library of Functional Recombinant Cell-surface and Secreted *P. falciparum* Merozoite Proteins. *Mol Cell Proteomics MCP* 12(12):3976–3986.
89. Dreyer AM, Beauchamp J, Matile H, Pluschke G (2010) An efficient system to generate monoclonal antibodies against membrane-associated proteins by immunisation with antigen-expressing mammalian cells. *BMC Biotechnol* 10:87.
90. Zenonos ZA, Rayner JC, Wright GJ (2014) Towards a comprehensive *Plasmodium falciparum* merozoite cell surface and secreted recombinant protein library. *Malar J* 13(1):93.
91. Gardner MJ, et al. (2002) Genome sequence of the human malaria parasite *Plasmodium falciparum*. *Nature* 419(6906):498–511.
92. PlasmoDB: The *Plasmodium* genome resource Available at: <http://plasmodb.org/plasmo/> [Accessed April 8, 2015].
93. Rappuoli R (2000) Reverse vaccinology. *Curr Opin Microbiol* 3(5):445–450.
94. Donati C, Rappuoli R (2013) Reverse vaccinology in the 21st century: improvements over the original design: Reverse vaccinology in the 21st century. *Ann N Y Acad Sci* 1285(1):115–132.
95. Proietti C, Doolan DL (2014) The case for a rational genome-based vaccine against malaria. *Front Microbiol* 5:741.

96. Reddy KS, et al. (2015) Multiprotein complex between the GPI-anchored CyRPA with PfRH5 and PfRipr is crucial for *Plasmodium falciparum* erythrocyte invasion. *Proc Natl Acad Sci* 112(4):1179–1184.
97. Baum J, et al. (2009) Reticulocyte-binding protein homologue 5 – An essential adhesin involved in invasion of human erythrocytes by *Plasmodium falciparum*. *Int J Parasitol* 39(3):371–380.
98. Crosnier C, et al. (2011) Basigin is a receptor essential for erythrocyte invasion by *Plasmodium falciparum*. *Nature*. Available at: http://www.nature.com/nature/journal/vaop/ncurrent/full/nature10606.html?WT.mc_id=FBK_NPG [Accessed January 21, 2013].
99. Bustamante LY, et al. (2013) A full-length recombinant *Plasmodium falciparum* PfRH5 protein induces inhibitory antibodies that are effective across common PfRH5 genetic variants. *Vaccine* 31(2):373–379.
100. Douglas AD, et al. (2014) Neutralization of *Plasmodium falciparum* Merozoites by Antibodies against PfRH5. *J Immunol* 192(1):245–258.
101. Douglas AD, et al. (2015) A PfRH5-Based Vaccine Is Efficacious against Heterologous Strain Blood-Stage *Plasmodium falciparum* Infection in Aotus Monkeys. *Cell Host Microbe* 17(1):130–139.
102. Chitnis CE, Sharma A (2008) Targeting the *Plasmodium vivax* Duffy-binding protein. *Trends Parasitol* 24(1):29–34.
103. Lavazec C, Bourgoignie C (2008) Mosquito-based transmission blocking vaccines for interrupting *Plasmodium* development. *Microbes Infect Inst Pasteur* 10(8):845–849.
104. malERA Consultative Group on Vaccines (2011) A research agenda for malaria eradication: vaccines. *PLoS Med* 8(1):e1000398.
105. Renner J, Graves PM, Carter R, Williams JL, Burkot TR (1983) Target antigens of transmission-blocking immunity on gametes of *Plasmodium falciparum*. *J Exp Med* 158(3):976–981.
106. Sinden RE, Carter R, Drakeley C, Leroy D (2012) The biology of sexual development of *Plasmodium*: the design and implementation of transmission-blocking strategies. *Malar J* 11:70.
107. Malkin EM, et al. (2005) Phase 1 vaccine trial of Pvs25H: a transmission blocking vaccine for *Plasmodium vivax* malaria. *Vaccine* 23(24):3131–3138.
108. Wu Y, et al. (2008) Phase 1 trial of malaria transmission blocking vaccine candidates Pfs25 and Pvs25 formulated with montanide ISA 51. *PloS One* 3(7):e2636.
109. Qian F, et al. (2007) Conjugating recombinant proteins to *Pseudomonas aeruginosa* ExoProtein A: a strategy for enhancing immunogenicity of malaria vaccine candidates. *Vaccine* 25(20):3923–3933.
110. Qian F, et al. (2008) Addition of CpG ODN to recombinant *Pseudomonas aeruginosa* ExoProtein A conjugates of AMA1 and Pfs25 greatly increases the number of responders. *Vaccine* 26(20):2521–2527.
111. Goodman AL, et al. (2011) A viral vectored prime-boost immunization regime targeting the malaria Pfs25 antigen induces transmission-blocking activity. *PloS One* 6(12):e29428.
112. Forbes EK, et al. (2012) T Cell Responses Induced by Adenoviral Vectored Vaccines Can Be Adjuvanted by Fusion of Antigen to the Oligomerization Domain of C4b-Binding Protein. *PLoS ONE* 7(9). doi:10.1371/journal.pone.0044943.
113. Holt RA, et al. (2002) The genome sequence of the malaria mosquito *Anopheles gambiae*. *Science* 298(5591):129–149.
114. Venter JC, et al. (2001) The sequence of the human genome. *Science* 291(5507):1304–1351.

Results Part 1

Passive immunoprotection of *Plasmodium falciparum* infected mice designates the Cysteine-Rich Protective Antigen as candidate malaria vaccine antigen

Journal of Immunology 2012, 188:6225-6237

Anita M Dreyer^{*,†}, Hugues Matile[‡], Petros Papastogiannidis^{*,†}, Jolanda Kamber^{*,†},
Paola Favuzza^{*,†}, Till Voss^{*,†}, Sergio Wittlin^{*,†}, Gerd Pluschke^{*,†,§}

* Molecular Immunology, Swiss Tropical and Public Health Institute, CH-4051 Basel, Switzerland

† University of Basel, CH-4003 Basel, Switzerland

‡ Pharma Research Basel, F. Hoffmann-La Roche Ltd., CH-4070 Basel, Switzerland

§ Corresponding author

Abstract

An effective malaria vaccine could prove to be the most cost-effective and efficacious means of preventing severe disease and death from malaria. In an endeavor to identify novel vaccine targets, we tested predicted *Plasmodium falciparum* open reading frames for proteins that elicit parasite-inhibitory Abs. This has led to the identification of the cysteine-rich protective Ag (CyRPA). CyRPA is a cysteine-rich protein harboring a predicted signal sequence. The stage-specific expression of CyRPA in late schizonts resembles that of proteins known to be involved in merozoite invasion. Immunofluorescence staining localized CyRPA at the apex of merozoites. The entire protein is conserved as shown by sequencing of the CyRPA encoding gene from a diverse range of *P. falciparum* isolates. CyRPA-specific mAbs substantially inhibited parasite growth *in vitro* as well as in a *P. falciparum* animal model based on NOD-*scid* *IL2Rg*^{null} mice engrafted with human erythrocytes. In contrast to other *P. falciparum* mouse models, this system generated very consistent results and evinced a dose-response relationship and therefore represents an unprecedented *in vivo* model for quantitative comparison of the functional potencies of malaria-specific Abs. Our data suggest a role for CyRPA in erythrocyte invasion by the merozoite. Inhibition of merozoite invasion by CyRPA-specific mAbs *in vitro* and *in vivo* renders this protein a promising malaria asexual blood-stage vaccine candidate Ag.

Introduction

Although preventable and curable, malaria was estimated to have claimed 781,000 lives in 2009 (1). Besides other control measures, implementation of an effective vaccine against malaria is regarded as a cost-effective measure to reduce mortality and morbidity. Three different malaria vaccine strategies can be distinguished: infection-blocking vaccines targeting pre-erythrocytic stages, anti-morbidity vaccines targeting the erythrocytic stages, and transmission-blocking vaccines targeting the sexual stages. It is assumed that a highly effective malaria vaccine needs to target multiple stages of the parasite life cycle (2, 3).

The importance of a parasite blood-stage component in a malaria subunit vaccine is evident, as clinical symptoms of malaria are mainly attributed to asexual blood stages. In exposed humans, protection from symptomatic disease is acquired after repeated exposure over years (4). This naturally acquired immunity is attributed at least in part to Ab responses targeting blood-stage Ags. This was demonstrated by passive immunotherapy studies, in which transfer of Igs from immune individuals to malaria patients led to very substantial reductions of parasitemia and clinical symptoms (5–7).

The feasibility of an asexual blood-stage vaccine is supported by studies in humans and animal models (8–13). To date, research in this field has focused on a few protein candidates including merozoite surface protein (MSP)-1 (14), MSP-2 (8), MSP-3 (15– 18), apical membrane Ag 1 (AMA-1) (19), erythrocyte binding Ag 175 (EBA-175) (20), glutamate-rich protein (GLURP) (15, 21), and serine repeat Ag 5 (SERA5) (22). These Ags are all merozoite proteins, either located on the merozoite surface or contained within apical invasion organelles. In contrast to intraerythrocytic stages, which are largely hidden within the RBCs, free merozoites are directly accessible to Abs. Abs are thought to interfere with the invasion of erythrocytes by binding to merozoite surface proteins or proteins released from apical organelles. Merozoite invasion involves a complex series of orchestrated molecular interactions but nevertheless takes less than a minute to be completed (23, 24). After low-affinity attachment of a freshly released merozoite to an erythrocyte, the merozoite reorients to its apical pole. Released microneme and rhoptry neck resident proteins mediate high-affinity attachment by the establishment of a tight junction. This in turn initiates the release of rhoptry bulb resident proteins, which are involved in the formation of a membrane to surround the parasitophorous vacuole. Mediated by an actomyosin motor complex, the tight junction is then moved toward the anterior pole, terminating with the sealing of the parasitophorous vacuole membrane at the posterior pole of the merozoite (for a review, see

reference 25). Most proteins currently regarded as key malaria blood-stage vaccine candidate Ags were shown or are thought to be involved in the invasion process. These Ags are targets of invasion inhibitory Abs, which interfere with different steps of the invasion process. Parasite growth inhibitory Abs specific for MSP-1, the most abundant protein on the surface of merozoites assumed to be involved in the initial attachment, were for example shown to inhibit merozoite invasion either by preventing MSP-1 processing or by agglutination preventing the dispersal of released merozoites (26, 27). By contrast, inhibitory Abs specific for AMA-1, a micronemal protein and constituent of the tight junction, were shown to interfere sterically with the assembly of the protein complex forming the tight junction (28). The modes of action of all invasion inhibitory Abs have not been identified, but suggested mechanisms also include opsonization and destruction of merozoites by phagocytic cells (29, 30), complement activation (31), or neutrophil respiratory bursts (32).

To date, relatively few blood-stage Ags are in clinical development as vaccine components (33). Unfortunately, the most advanced blood-stage vaccine Ags, AMA-1 and MSP-1, have not demonstrated efficacy in African children to date (14, 34, 35). However, a multistage vaccine comprising an AMA-1 component showed a 50% reduced incidence rate of clinical malaria episodes in child vaccinees compared with that of control children (36). But whether protection is associated with AMA-1-specific responses remains to be shown. The extensive polymorphisms of current candidate Ags is deemed to be a major hurdle for blood-stage vaccine development (37–41). Hence, although a couple of bloodstage Ags are under vaccine development, it is possible to search for more vaccine candidates. The comparison of a large range of protein Ags in preclinical assays would allow a more rational prioritization of candidates for inclusion into a vaccine. Since the availability of the *Plasmodium falciparum* genome in 2002, reverse vaccinology is considered an opportunity to identify novel vaccine candidates in a more rational way (42–50). On the basis of the genome-wide transcriptomic and proteomic information generated since 2002, we selected the *P. falciparum* open reading frame (ORF) PFD1130w for further characterization. PFD1130w was selected because the available information suggested that the protein is a merozoite protein involved in erythrocyte invasion: 1) transcription has been shown to be upregulated in late asexual blood stages (46, 47); 2) the encoded protein is predicted to contain a N-terminal secretion signal peptide (51); 3) a genomewide in silico study based on gene coexpression, sequence homology, and domain–domain and yeast two-hybrid interaction data showed that PFD1130w clustered into an interaction network implicated in merozoite invasion (48); and 4) the pfd1130w gene lies

in close proximity to genes encoding proteins known to be involved in RBC invasion, such as reticulocyte-binding homolog 4 (RH4) and reticulocyte-binding homolog 5 (RH5) proteins, SURFIN4.2, and glideosome-associated protein with multiple membrane spans 2 (GAPM2) (Fig. 1) (52–55). On the basis of these data, we selected PFD1130w for generation of mouse mAbs (56), which allowed us further to characterize the protein and to perform functional assays.

In this study we carried out an in-depth characterization of PFD1130w and demonstrate its potential as a malaria asexual blood-stage vaccine candidate. PFD1130w is a conserved cysteine-rich protein that we designated cysteine-rich protective Ag (CyRPA). Our data on localization, stage-specific expression pattern, and functional assays suggest a role of CyRPA in erythrocyte invasion by the merozoite. Importantly, CyRPA elicits Abs that inhibit merozoite invasion *in vitro* and *in vivo*. Furthermore, our passive immunization studies in *P. falciparum*-infected NOD-*scid* *IL2Rg*^{null} mice with anti-CyRPA mAbs identified this animal model as an unprecedented system to quantitatively evaluate functional potencies of malaria-specific Abs.

Materials and Methods

Ethics statement

This study was carried out in strict accordance with the Rules and Regulations for the Protection of Animal Rights (Tierschutzverordnung) of the Swiss Bundesamt für Veterinärwesen. The protocol was ethically approved by the Ethikkommission beider Basel (Permit Number 2375). Human sera were obtained from adult volunteers after receiving written informed consent. Ethical clearance was obtained from the institutional ethical review board of the Navrongo Health Research Center (Navrongo, Ghana).

Culture of parasites

P. falciparum strains 3D7, 7G8, D6, W2mef, and K1 were cultured essentially as described previously (57). The culture medium was supplemented with 0.5% AlbuMAX (Life Technologies) as a substitute for human serum (58). Cultures were synchronized by sorbitol treatment (59). Erythrocytes for passages were obtained from the Swiss Red Cross (Basel, Switzerland).

Isolation of free merozoites

To obtain *P. falciparum* merozoites, erythrocytes infected with highly synchronous schizont-stage parasites were centrifuged at 700 \times g for 5 min to separate released merozoites from unruptured schizonts and uninfected erythrocytes. Supernatants containing free merozoites were centrifuged at 3000 \times g for 10 min to collect merozoites.

Western blot analysis

Blood-stage parasite lysates were prepared essentially as described previously by saponin lysis of *P. falciparum* 3D7-infected erythrocytes (57). In brief, cultured parasites were washed once with PBS. Pelleted infected RBCs were lysed in 20 volumes of 0.06% (w/v) saponin in PBS for 20 min. Parasites were washed, and the final pellet was resuspended in 3 volumes of PBS and stored at 280 °C until further use.

Cell lysate of transfected HEK cells was prepared as described previously (56).

For SDS-PAGE, cell or parasite lysate was resolved on precast 4–12% gradient gels (NuPAGE Novex 4–12% Bis-Tris Gel; Invitrogen) with MES running buffer according to the manufacturer's directions. The proteins were electrophoretically transferred to nitrocellulose

membrane using a dry-blotting system (iBlot; Invitrogen). After blocking the membrane, specific proteins were detected with appropriate dilutions of anti-CyRPA mAbs (56) or anti-hexa-his tag mAb (56) followed by HRP-conjugated goat anti-mouse IgG mAb (Kirkegaard & Perry Laboratories). Blots were developed using ECL Western blotting detection reagents (ECL Western Blotting Substrate; Pierce).

Immunofluorescence staining of infected erythrocytes and free merozoites

For indirect immunofluorescence microscopy, smears of infected RBCs were fixed in 60% methanol and 40% acetone for 2 min at 220°C and blocked with 1% BSA in PBS. Isolated free merozoites were spotted and fixed onto L-lysine-coated multitest glass slides as described previously (60). Cells were probed with the following primary or secondary Abs: biotin-labeled mouse anti-CyRPA mAb c06 (56), Alexa 488-labeled mouse anti-RAP-1 5-2 mAb (61), Alexa 488-labeled mouse anti-AMA-1 DV5a mAb (60), Alexa 488-labeled mouse anti-MSP-1 MC7.2 mAb (G. Pluschke, unpublished observations), Alexa 488-labeled mouse anti-GAPDH 1.4a mAb (62), anti-MSP-2 rabbit serum (MRA-318; Malaria Research and Reference Reagent Resource Center), anti-MSP-4 rabbit serum (63), anti-MSP-5 rabbit serum (64), Alexa 568-labeled streptavidin (Invitrogen), and Alexa 488-labeled chicken anti-rabbit IgG (H+L) (Invitrogen). The slides were mounted in mounting medium containing DAPI (ProLong Gold antifade reagent with DAPI; Invitrogen). Fluorescence microscopy was performed on a Leica DM-5000B using a 360 oil immersion objective lens and documented with a Leica DFC300FX digital camera system. Images were processed using Leica Application Suite and Adobe Photoshop CS3.

Immunofluorescence staining of live versus fixed merozoites

Isolated merozoites were incubated with Alexa 488-labeled mouse anti-MSP-1 MC7.2 mAb (G. Pluschke, unpublished observations), Alexa 488-labeled mouse anti-GAPDH 1.4a mAb (62), or biotin-labeled mouse anti-CyRPA mAb c06 (56) and Alexa 568-labeled streptavidin (Invitrogen) diluted in parasite culture medium. Thereafter, cells were washed two times with PBS and then fixed 30 min in 4% PFA in PBS. For staining of fixed merozoites, cells were first incubated for 30 min in 4% PFA and thereafter immunofluorescence-stained as described earlier. Cells were mounted in mounting medium containing DAPI (ProLong Gold antifade reagent with DAPI; Invitrogen). Fluorescence microscopy was performed as described earlier.

***In vitro* growth inhibition assay**

In vitro growth inhibition assays with *P. falciparum* strains 3d7, 7G8, D6, W2mef, and K1 were conducted essentially as described (60). Each culture was set up in triplicate in 96-well flat-bottom culture plates. Viable parasites were stained with hydroethidine and analyzed in a FACScan flow cytometer (Becton Dickinson, San Jose, CA) using CellQuest software. A total of 30,000 cells per sample were analyzed. Percent inhibition was calculated from the mean parasitemia of triplicate test and control wells as follows: percent inhibition = (control – test)/(control/100).

***In vivo* growth inhibition assay**

Abs were tested in the murine *P. falciparum* model essentially as described (65). The only modification implemented was that daily human blood injections (0.75 ml) were administered by the i.v. route instead of the i.p. route. Once parasitemia reached .05%, mice received a single dose of 0.5, 2.5, or 5 mg mAb in PBS by i.v. injection. Thereafter, parasitemia was measured for the next 5 d. To monitor serum levels of administered Abs, serum samples were taken just before, 1 d, and 5 d after mAb injection.

For the transfer experiment, blood cells of mice having previously received 2.5 mg anti-CyRPA mAb c12 were washed with 0.9% NaCl and used to infect naive human erythrocyte engrafted NOD-*scid* *IL2Rg*^{null} mice.

ELISA

Detection of CyRPA-specific and MSP-1-specific Abs in human sera by ELISA. Human serum samples were derived from healthy Swiss adults with no history of malaria exposure (66) and from healthy individuals between 5 and 20 y of age living in the malaria endemic (67) Kassena-Nankana District in northern Ghana. ELISA plates (Maxisorp; Nunc) were coated with 10 mg/ml purified recombinant CyRPA protein produced in HEK cells or purified recombinant MSP-1 (aa 34–595) or MSP-1 (aa 1250– 1563) produced in *Escherichia coli* (68). After blocking, plates were incubated with dilutions of human serum. Alkaline phosphatase-conjugated goat anti-human IgG F(ab₂)₂ (Jackson ImmunoResearch Laboratories) was used as secondary Ab and p-nitrophenyl phosphate was used as substrate (Sigma). The OD of the reaction product was recorded at 405 nm with a microplate absorbance reader (Sunrise Absorbance Reader; Tecan).

Ab competition ELISA. Plates were coated with 10 mg/ml purified recombinant CyRPA protein produced in *E. coli*. After blocking, plates were incubated with 10 mg/ml, 1 mg/ml, or 0 mg/ml of different anti-CyRPA mAbs (c02, c04, c05, c06, c08, c09, c10, c12, c13). After 30 min, different biotinylated anti-CyRPA mAbs (c02, c04, c05, c06, c08, c09, c10, c12, c13) were added to each well resulting in a concentration of 1 mg/ml of labeled Abs. HRP-conjugated streptavidin (GenScript) was used as detecting agent, and tetramethylbenzidine substrate (Pierce Western Blotting Substrate; Pierce) was used for development. The reaction was stopped with 0.5 M H₂SO₄, and the OD was measured at 450 nm.

Culture of eukaryotic cells

The human embryonic kidney cell line 293 HEK was obtained from the American Type Culture Collection (ATCC CRL-1573). 293 HEK cells were cultured in IMDM supplemented with 10% FCS, glutamine, and penicillin/ streptomycin at 37 °C in a humidified incubator.

Expression of CyRPA protein fragments on HEK cell surface

DNA sequences that encode fragments of CyRPA protein were amplified by PCR from a plasmid containing the codon-optimized sequence of PFD1130w. Primers used for amplification were as follows: Fr26-251, 3910 (59-CCAATgctagcGGCATAAATTG-39) and 3913 (59-ATAAGAATgcggccgcTTTCACATTATTGATGTTGTCTCCA-39); Fr127-352, 3912 (59-ATACTAgctagcCGTAAGAAGGATATGACTTGTCACAG-39) and 3905 (59-TCGGTACCTCGCGAATGC-39); Fr26-142, 3910 and 3911 (59-ATAAGATAgcggccgcCTTACCGTCATTTGAATAGAACCT-39); Fr127-251, 3912 and 3913; Fr236-352, 3886 (59-gctagcGACCTGTCCTTTCACCTTTATGTTG-39) and 3887 (59-gcggccgcGTTGTAAATGCCCTGGGATG-39); Fr26-181, 3910 and 3939 (59-ATAAGAATgcggccgcCCCGCAGATGAGGAAGTAC-39); Fr74-181, 3938 (59-ATACTAgctagcGAGACCCATATCTACGTGCAG-39) and 3939; Fr74-251, 3938 and 3913. Amplifications were performed using FIREPol DNA polymerase (Solis Biodyne) according to the manufacturer's protocol with the following profile: 5 min, 95 °C; 30 s, 95 °C; 30 s, 60 °C; 2 min, 72 °C; 6 min, 72 °C. The amplicons were digested with restriction endonucleases *NheI* and *NotI* (New England Biolabs) and then ligated into a pcDNA3.1-based expression vector (56). This expression vector allows surface expression of a protein of interest. It contains the secretion signal of bee-venom melittin, a cloning site for the protein of interest, a FLAG tag, a transmembrane domain of mouse glycoporphin-A, and a hexa-his tag. The 293 HEK cells were transfected with the different expression vectors using

JetPEI transfection reagent (PolyPlus) according to the manufacturer's protocol. One to two days later, transient transfectants were used for Western blot analysis or immunofluorescence staining

Immunofluorescence staining of living transfected HEK cells

Immunofluorescence staining of live HEK cells was performed in chamber slides (8-well chamber-slide, Lab-Tek; Nunc). HEK cells (12,000 cells/ well) were seeded and 4 d later transfected with different expression vectors. The following day, immunofluorescence stainings were performed by incubating the wells with 100 mg/ml anti-CyRPA mAb diluted in IMDM for 30 min on ice. After washing, cells were fixed for 30 min with 4% formaldehyde in PBS. After washing, cells were incubated for 30 min with Cy3-labeled goat anti-mouse IgG F(ab₂)₂ (Jackson ImmunoResearch Laboratories) diluted in PBS and washed four times with PBS. Slides were mounted with mounting solution containing DAPI (ProLong Gold antifade reagent with DAPI; Invitrogen). Stainings were assessed by fluorescence microscopy as described earlier.

Bacterial strains and media

E. coli strain Top10 (TOP10 Chemically Competent *E. coli* Cells; Invitrogen) was used for the amplification of plasmids. *E. coli* strain BL 21 Star (DE3) (Invitrogen) was used for recombinant expression of CyRPA protein. Bacteria were grown in lysogen broth medium containing 100 mg/ ml ampicillin.

Recombinant protein expression and purification

CyRPA (aa 26–352) was recombinantly expressed in *E. coli* using the pET28a expression system (Novagen, modified to contain an ampicillin selection cassette). Briefly, a PCR product of CyRPA was generated from a plasmid containing the sequence of PFD1130w using primer 59-ATGCCATGGGCATAAATTGTGACAGCC-39 and 59-CCGCTCGAGGTTGTAAATGCCCTGGGA-39. The amplicon was digested with restriction endonucleases NcoI and XhoI (New England Biolabs) and cloned into NcoI and XhoI sites of pET28a. Protein expression in *E. coli* BL 21 Star (DE3) (Invitrogen) was induced by addition of 1 mM isopropyl thiogalactoside (Calbiochem) for 2 h at 37°C. The recombinant protein was purified from inclusion bodies using denaturing conditions (8 M urea, 500 mM NaCl, 20 mM Tris-HCl, 5 mM imidazole) by Ni-NTA chromatography. The purity and integrity of the

purified protein was analyzed by SDS-PAGE, and the protein concentration was determined by measuring OD₂₈₀. The purified recombinant protein was identified as the expected CyRPA protein by Western blot analysis with CyRPA-specific mAbs.

Hexa-his-tagged recombinant proteins corresponding to aa 34–595 and aa 1250–1563 of MSP-1 of *P. falciparum* MAD20 were a kind gift of Bela Takacs (Pharma Research Basel, F. Hoffmann-La Roche, Basel, Switzerland [retired]). Proteins were produced in *E. coli* and purified by Ni-NTA chromatography (68).

CyRPA was recombinantly expressed in HEK cells. The codon-optimized sequence of PFD1130w corresponding to aa 22–362 was cloned into a pcDNA3.1-based expression vector. This expression vector allows secretion of the protein of interest. It contains the secretion signal of bee-venom melittin, a cloning site for the protein of interest, and a C-terminal hexa-his tag. 293 HEK cells were stably transfected with the expression vector using JetPEI transfection reagent (PolyPlus) according to the manufacturer's protocol, and clones were generated by limiting dilution. For recombinant protein production, transfected cells were cultured in serum-free medium (Panserin 293A; PAN Biotech). The recombinant protein was purified from culture supernatant by Ni-NTA chromatography. The purity and integrity of the purified protein was analyzed by SDS-PAGE. The purified recombinant protein was identified as the expected CyRPA protein by Western blot analysis with CyRPA-specific mAbs.

Analysis for binding of soluble CyRPA to RBCs by flow cytometry

Human RBCs were incubated with 100, 20, 4, or 0 mg/ml purified recombinant CyRPA (produced in HEK cells) diluted in PBS, 1% BSA. Surface-bound protein was detected by incubating cells with 100 mg/ml anti-hexa-his tag mAb 6/9 (56) and subsequently with Alexa Fluor 568 donkey anti-mouse IgG (H+L) conjugate. FACS analysis was performed on a FACScan (Becton Dickinson) using CellQuest software (Becton Dickinson), and 30,000 events were collected for each sample.

Analysis for binding of human RBCs to CyRPA expressed on HEK cells

Human RBCs were incubated with 50% confluent stably transfected HEK cells expressing recombinant CyRPA on the cell surface (56) for 2 or 24 h. After repeated washing with culture medium, RBCs attached to HEK cells were assessed by microscopy.

Surface plasmon resonance analysis of anti-CyRPA mAb– CyRPA interaction

The affinities of the anti-CyRPA mAbs for CyRPA were determined with an optical biosensor using the real-time surface plasmon resonance (SPR) technology (BIAcore 3000; Pharmacia Biacore) at 35 °C. About 2000 response units of goat anti-mouse IgG (H+L) (Jackson ImmunoResearch) were coupled to CM5 sensor chip by using N-hydroxysuccinimide and 1-ethyl-3-(3-dimethylaminopropyl)-carbodiimide. Approximately 350 response units of anti-CyRPA mAbs in PBS were captured onto the surface. The purified recombinant CyRPA produced in HEK cells at concentrations ranging from 400 to 3.1 nM was injected for 2 min using a flow rate of 50 ml/min. Dissociation of bound Ag in PBS was followed for 5 min. The surfaces were regenerated after each cycle. Equilibrium dissociation constant (KD) was calculated from the ratio of the dissociation and association rate constants obtained with the BIAevaluation 2.1 software using a 1:1 binding model with mass transfer.

Sequencing the CyRPA gene of different strains

Genomic DNA was prepared from *P. falciparum* strains 3D7, MAD20, FC27, RFCR3, W2met, Hb3, Ro-33, 7G8, K1 FCR3, ITG2F6, FVO, IFA4, IFA6, IFA10, IFA12, IFA18, and IFA19 and used for PCR amplification of PFD1130w. PFD1130w was amplified in three overlapping fragments with the following primer combinations: 5'-AAAATTTTGTAGGAAATGTTGAGAA-3' and 5'-AAAACGATGACAAGTCATATCCTTC-3'; 5'-TGTTCCCTTGTATTCGTGATATGTTTT-3' and 5'-TCATCATTTAATGTAGAAACATCTTGA-3'; 5'-TGACAATTACAAATTAGGTGTGCAA-3' and 5'-CAAATATGATGATTGTTGAATGGTT-3'. Amplifications were performed using DreamTaq DNA polymerase (Fermentas Life Sciences) according to the manufacturer's protocol with the following profile: 5 min, 95 °C; 35 3 (30 s, 95 °C; 30 s, 60 °C; 2 min, 72 °C); 6 min, 72 °C. Amplicons were purified and subjected to direct sequencing (Macrogen, Seoul, South Korea). Sequences were analyzed using AutoAssembler 1.4.0 software (Applied Biosystems, PerkinElmer).

Accession numbers for all genes and proteins mentioned in this study

Sequences of genes and proteins mentioned in this study can be found on PlasmoDB (<http://plasmodb.org/plasmo/>) with the following accession numbers: *P. falciparum* CyRPA (PFD1130w), *P. vivax* CyRPA (PVX_090240), *P. knowlesi* CyRPA (PKH_052740), *P. falciparum* MSP-1 (PFI1475w), *P. falciparum* MSP-2 (PFB0300c), *P. falciparum* MSP-3 (PF10_0345), *P. falciparum* MSP-4 (PFB0310c), *P. falciparum* MSP-5 (PFB0305c), *P.*

falciparum AMA-1 (PF11_0344), *P. falciparum* EBA-175 (MAL7P1.176), *P. falciparum* GLURP (PF10_0344), *P. falciparum* SERA5 (PFB0340c), *P. falciparum* RH4 (PFD1150c), *P. falciparum* RH5 (PFD1145c), *P. falciparum* SURFIN4.2 (PFD1160c), *P. falciparum* GAPM2 (PFD1110w), *P. falciparum* PSOP12 (PFE0680), and *P. falciparum* GAPDH (PF14_0598).

Results

Sequence analysis of *P. falciparum* CyRPA

pfd1130w/cyrpa is 1188 bp long with a 99-bp intron and is localized in the subtelomeric region of chromosome 4 in close proximity to genes encoding proteins known to be involved in RBC invasion, such as RH4 and RH5, SURFIN4.2, and GAPM2 (Fig. 1) (52–55).

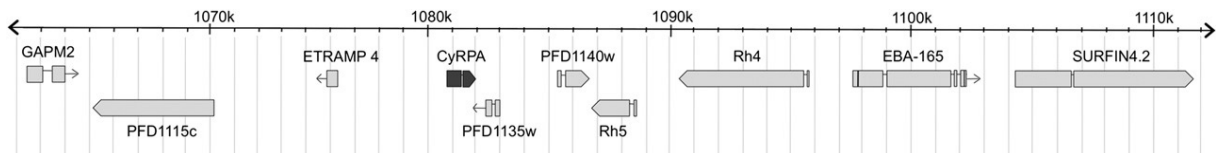


FIGURE 1. The CyRPA encoding gene (dark gray) is positioned in the subtelomeric region of chromosome 4. ORFs in close proximity include genes encoding GAPM2, RH4 and RH5, and SURFIN4.2. These proteins are known or presumed to be involved in merozoite invasion (52–55). Positional data were obtained from PlasmoDB (<http://www.plasmoDB.org>).

The hypothetical protein encoded by *pfd1130w* is predicted to contain an N-terminal secretion signal peptide. Orthologs of CyRPA are only present in the genomes of *P. knowlesi* (PKH_052740) and *P. vivax* (PVX_090240) and are absent in *Plasmodium* species infecting rodents. Comparison of these protein sequences revealed conservation with 36% and 38% identity of *P. falciparum* CyRPA with the *P. knowlesi* and the *P. vivax* orthologs, respectively. Furthermore, cysteine residues in the orthologs are positionally conserved (Fig. 2). BLAST search identified the mosquito-stage protein PSOP12 (PFE0680) as paralog of CyRPA (69). This protein shares nine positionally conserved cysteine residues in the homologous N-terminal part, but additionally has a 6-cysteine-protein domain at the C terminus (70).

CyRPA is nonpolymorphic

To assess potential sequence diversity of the CyRPA protein, *cyrpa* genes of 12 *P. falciparum* standard strains from different geographical origin (3D7, K1, MAD20, FC27, FCR3, RFCR3, W2met, Hb3, Ro-33, 7G8, ITG2F6, and FVO) and six field isolates from Tanzania (IFA4, IFA6, IFA10, IFA12, IFA18, and IFA19) were amplified by PCR and sequenced. Apart from one nonsynonymous single nucleotide polymorphism (SNP) at base pair position 1116 in *P. falciparum* strains K1, FCR3, ITG2F6, and FVO, all sequences obtained were identical to the *P. falciparum* 3D7 reference sequence. In the protein sequence, this SNP results in an arginine/serine dimorphism at amino acid position 339 (Fig. 2).

CLUSTAL W (1.83) multiple sequence alignment

```

pfal|PFD1130w      MIIPFHKKFISFFQIVLVLLLCRSINCDSRHVFI-RTELSFIKNNVPCI 49
pviv|PVX_090240   MIVTKIAIFLFFF---LFSFLRCLSTNTQSKNIIILNDEITTIKSPIHCI 47
pkno|PKH_052740   MIVAKIAI-LFFF---LLSCPTYLTTNEESKQVIILNDEITTTITSPVHCI 46
**:.      : **  * .      : * :*:*: * . *: : *.. : **

pfal|PFD1130w      RDMFFIYKRELYNICLDDDLKGEEDETHIYVQKKVKDSWITLNDLFKETDL 99
pviv|PVX_090240   TDIYFLFRNELYKTCIQHVIKGRTEIHVLVQKKINSTWETQTTLFKDHMW 97
pkno|PKH_052740   ADTYFIFRNELYKICIQHVNKGRTIEHVIVQKKAKNKWETKQKLFEDKMW 96
* :*:*:*:*:*: *::: . * * : * * * * :..* * **::

pfal|PFD1130w      TGRPHIFAYVDVEEIIILLCEDEEFSNRKKDMTCHRFYSNDGKEYNNSEI 149
pviv|PVX_090240   FELPSVFNFIHNDEIIIVICRYKQRSKR-EGTICKRWNSVTGTIYQKEDV 146
pkno|PKH_052740   FHLPFVFNFVQND EIIILVCRYKGMTKG-EGVACDRWSSTTGTNYNKGNI 145
* : * : : . : * * * : * . : : : . * : * * * . * : : :

pfal|PFD1130w      TISDYILKDKLLSSYVSLPLKIENREYFLICGVSPYKFKDDNKDDILCM 199
pviv|PVX_090240   QIDKEAFANKNLESYQSVPLTVKNKKFLICGILSYEYKTANKDNFISCV 196
pkno|PKH_052740   NIDAQALTKMNLDSYASFPIPIKDKAIIHICGVHSYEYQNVNQNNFISCL 195
* .      : . * . * * * . * : : : : : * * * : . * : : * : : * *

pfal|PFD1130w      ASHDKGETWG-TKIVIKYDNYKLGVQYFFLRPYISKNDLSFHFYVGDNIN 248
pviv|PVX_090240   ASEDKGRTWG-TKILINYEELQKGVPHYLRPIIFGDEFGFYFYSRISTN 245
pkno|PKH_052740   ASEDKGTWGDIKIHIYYDQFQEGVPYFYLRPLVFNDEFGFYLYSRISN 245
** . * * * * * * * * * : : * * * * : * * * : : : : * : * . *

pfal|PFD1130w      NV-KNVNFIECT-----HEKDLEFVCSNRDFLKDNKVLQDVSTLNDEYI 291
pviv|PVX_090240   NTARGGNMYTCTLDVTNEGKKEYKFKCKHVSLIKPDKSLQNVTKLNGYYI 295
pkno|PKH_052740   NADRGGKYMKCIILNPTNSRNKEYTFKCTNVNLIKEDKSLQNI TKLNGYYV 295
* . : . : : *      : * : * * . : : : * : * * * : : * * *

pfal|PFD1130w      VSYGNDNNFAECYIFFNENSILIKPEKYGNTTAGCYGGTFVKIDENRITL 341
pviv|PVX_090240   TSYVKKDNFNECYLYYTEQNAIVVKPKVQNDLNGCYGGSFVKLDESKAL 345
pkno|PKH_052740   TSYAKNNFNECYLYYTENNAIVVKPKVQNYELNGCYGGSFVKFNESKAL 345
. * * : . : * * * * : : : : * : * : * * : * * * : * : : *

pfal|PFD1130w      FIYSSSQGIYNIHTIYYANYE 362
pviv|PVX_090240   FIYSTGYGVQNIHTLYYTRYD 366
pkno|PKH_052740   FIYSTGHGVQNIHTLHYARYE 366
* * * * : . * : * * * * : * : * :

```

FIGURE 2. Amino acid sequence alignment of *P. falciparum* CyRPA with orthologs in *P. knowlesi* and *P. vivax*. Full-length putative orthologs of *P. falciparum* CyRPA are only found in the genomes of *P. vivax* (PVX_090240) and *P. knowlesi* (PKH_052740). Sequence identities are 38 and 36%, respectively. Asterisk (*), identical; colon (:), conservation between groups of strongly similar properties; period (.), conservation between groups of weakly similar properties substitution. Ten of twelve cysteine residues are positionally conserved (shaded in gray). Amino acid residues of the predicted secretion signal sequences are indicated in boldface. DNA-sequencing of the *cyrpa* gene of a set of *P. falciparum* strains revealed one nonsynonymous SNP at base pair position 1116. Hence, at amino acid residue 339 (framed), the strains 3D7 (airport malaria), MAD20 (PNG), FC27 (PNG), RFCR3 (The Gambia), W2met (Indochina), Hb3 (Honduras), Ro-33 (Ghana), 7G8 (Brazil), IFA4 (Tanzania), IFA6 (Tanzania), IFA10 (Tanzania), IFA12 (Tanzania), IFA18 (Tanzania), and IFA19 (Tanzania) encode an arginine residue, whereas strains K1 (Thailand), FCR3 (The Gambia), ITG2F6 (Brazil), and FVO (Vietnam) encode a serine residue.

Stage-specific expression of CyRPA in schizonts and free merozoites

The PFD1130w gene encodes a 362-aa-long protein with a predicted molecular mass of 42.8 kDa. Using highly synchronized asexual blood-stage parasite cultures, we assessed the expression profile of CyRPA in *P. falciparum* across the intraerythrocytic developmental cycle at the protein level by Western blot analysis with CyRPA-specific mAbs at 8-h intervals. A discrete band of 36 kDa was detected in schizont stages, free merozoites, and very early ring stages but not in late ring and early trophozoite stages (Fig. 3A). Stage-specific expression of CyRPA in schizont stages and free merozoites was affirmed by indirect immunofluorescence staining of synchronized blood-stage parasites with anti-CyRPA mAbs (Fig. 3B). These results are in agreement with transcriptional data for PFD1130w, showing elevated transcript levels in late stages of the asexual blood cycle of *P. falciparum* with maximal expression measured at 40 to 48 h postinvasion (46, 47, 71). Additionally, mass spectrometry-based evidence for expression of PFD1130w was reported in schizont stages (72).

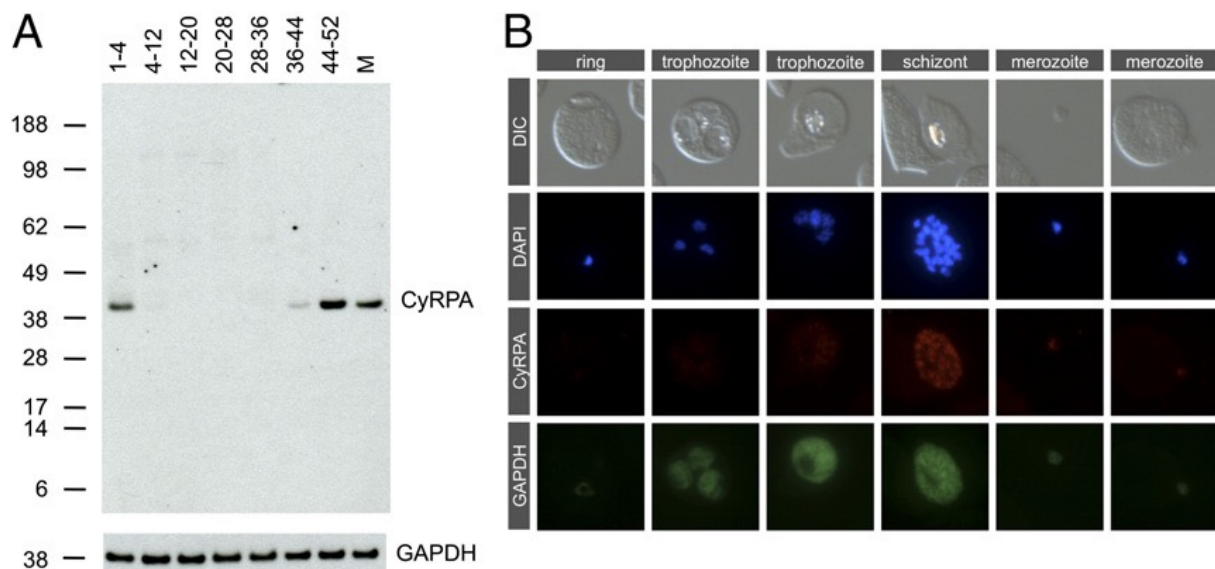


FIGURE 3. Stage-specific expression of CyRPA in late asexual blood-stage parasites. **(A)** Western blot analysis with lysates of tightly synchronized *P. falciparum* 3D7 blood-stage parasites with anti-CyRPA mAb c12 (upper panel). The blot was probed for equal loading with an anti-GAPDH mAb (lower panel). 1-4, 4-12, 12-20, 20-28, 28-36, 36-44, 44-52: hours postinvasion. M: free merozoites. **(B)** Indirect immunofluorescence stainings of asexual blood-stage parasites confirmed stage-specific expression in schizont stages and free merozoites. Methanol/acetone fixed *P. falciparum* 3D7 parasites were probed with anti-CyRPA mAb c06 (red) and anti-GAPDH mAb (green). Exposure times were identical for all pictures of the same channel. Nuclei were stained with DAPI (blue). Original magnification 31008.

CyRPA is localized at the merozoite apex

CyRPA has a putative N-terminal secretion signal sequence and is cysteine-rich (Fig. 2). In contrast to fixed merozoites, CyRPA could not be stained with specific mAbs in live merozoites, indicating that the Ag is located intracellularly in free merozoites (Supplemental Fig. 1). To determine the localization of CyRPA in schizont stages and free merozoites more accurately, we performed colocalization studies using Abs specific for the cytosol (GAPDH), the micronemes (AMA-1) (73), the rhoptry bulb (RAP-1) (74), and the merozoite surface [MSP-1 (75) and MSP-5 (64)] (Fig. 4). The pattern of CyRPA staining in free merozoites included a dot toward the merozoite apical end and a weaker staining dispersed over the anterior pole of the merozoite. The apical dot did not colocalize with micronemes or rhoptry bulbs. But stainings of CyRPA resembled MSP-5–specific stainings. Apical dots of MSP-5 and CyRPA largely overlaid, but the degree of additional faint staining of the merozoite body differed, being spread over the anterior part for CyRPA and just at the apical pole for MSP-5. Accordingly, schizonts were stained by CyRPA-specific mAbs in a patchy to dotted manner, not colocalizing with rhoptry bulbs or micronemes. CyRPA-specific and MSP-5–specific stainings showed a relatively similar pattern. Hence, CyRPA localizes to an apical structure distinct from rhoptry bulbs and micronemes.

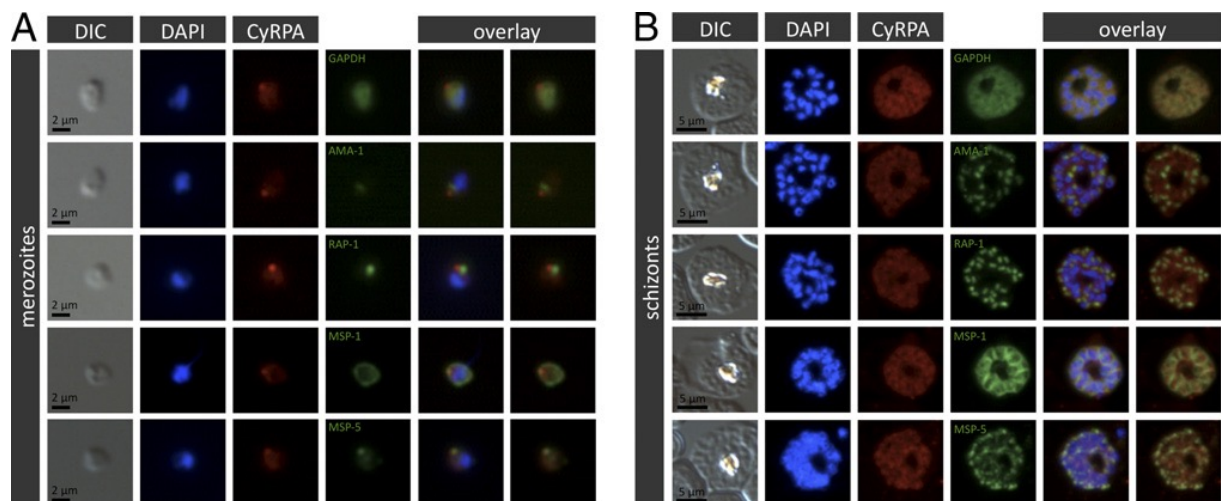


FIGURE 4. Localization of CyRPA to the merozoite apex by immunofluorescence staining. *P. falciparum* 3D7 merozoites (A) or schizont stages (B) were coimmunostained with anti-CyRPA mAb c06 (red) and anti-GAPDH Abs (marker for cytosol), AMA-1 (marker for micronemes), RAP-1 (marker for rhoptry bulbs), MSP-1 (marker for merozoite surface), or MSP-5 (green). Nuclei were stained with DAPI (blue). Original magnification 31008.

Anti-CyRPA mAbs inhibit merozoite invasion *in vitro*

Considering the apical localization of CyRPA, and as CyRPA was predicted to be implicated in merozoite invasion (48), we assessed anti-CyRPA mAbs for *in vitro* parasite growth inhibitory activity. Growth inhibition assays were conducted for two cycles of merozoite invasion. Of the anti-CyRPA mAbs tested, seven out of nine consistently inhibited growth of all five tested *P. falciparum* strains in a concentration-dependent manner (Fig. 5A, Supplemental Fig. 2). At a concentration of 1000 mg/ml, the anti-CyRPA mAb c12 inhibited parasite growth by 58.0 ± 2.8%. In contrast, anti-CyRPA mAb c05 had no effect on parasite growth, and anti-CyRPA mAb c13 exerted only marginal growth inhibitory activity even at high concentrations (Fig. 5A). All mAbs tested were produced and purified in parallel in the same manner, and results were reproducible with independent mAb production batches (data not shown).

To identify the step at which the anti-CyRPA mAbs exert their effect, parasite growth was compared in the presence or absence of inhibitory mAbs during one blood-stage cycle of highly synchronized parasites. Anti-CyRPA mAb c12 (250 mg/ml) was added to early ring stages, and parasitemia was monitored after 13, 27, and 31 h by flow cytometry. No significant difference in the development of trophozoites from ring stages was observed at any time point compared with the PBS control (Fig. 5C). When the anti-CyRPA mAb c12 was added to a synchronized parasite culture at the schizont stage and parasitemia was monitored during development into new ring and subsequently into trophozoite stages, a significant reduction in parasitemia compared with the PBS control was measured (Fig. 5C). This reduction emerged as soon as the parasitized erythrocytes had ruptured and the released merozoites had infected new erythrocytes ($p = 0.0283$ for the difference in parasitemia of PBS versus anti-CyRPA mAb samples at time point +15 h; two-sided t test). In contrast, the subsequent development of the intraerythrocytic parasites from ring stages into trophozoites was not affected by the mAbs. These results verify that the parasite growth inhibitory activity of anti-CyRPA mAbs is not due to inhibition of intracellular parasite development but due to specific inhibition of merozoite invasion.

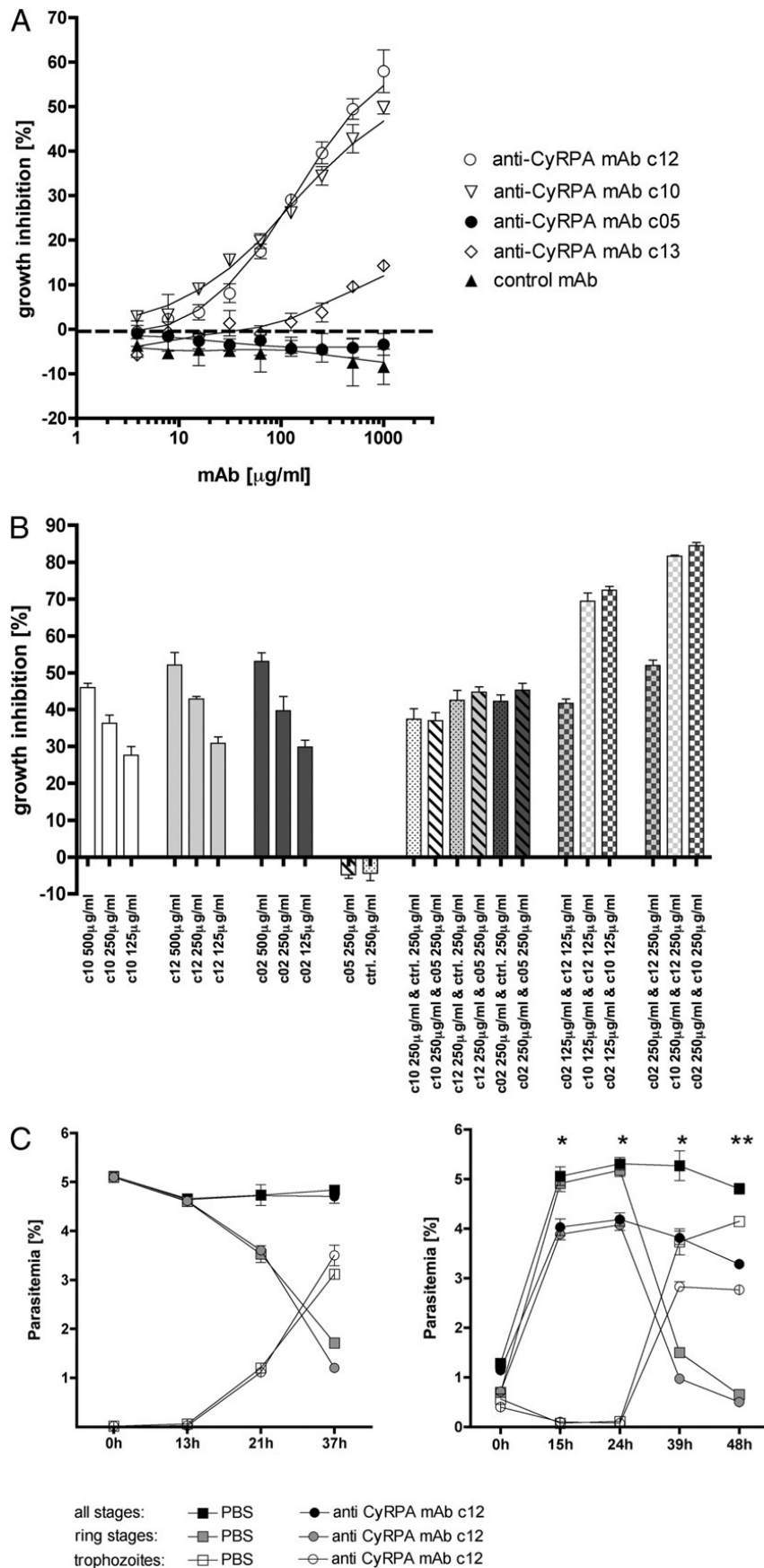


FIGURE 5. CyRPA-specific mAbs inhibit parasite growth *in vitro*. (A) Synchronized *P. falciparum* 3D7 blood-stage parasites were cultured for two cycles in the presence of different concentrations of purified anti-CyRPA mAbs c05, c10, c12, and c13. Percent parasite growth inhibition was calculated against the parasitemia of PBS control wells. Anti-hexa-his

tag mAb was used as negative control mAb. Each symbol represents the mean of a triplicate experiment, and error bars indicate the SD. **(B)** Synchronized *P. falciparum* 3D7 blood-stage parasites were cultured for two cycles in the presence of various combinations of different anti-CyRPA mAbs. Percent parasite growth inhibition was calculated against the parasitemia of PBS control wells. Anti-6xHis tag mAb was used as negative control mAb. Each symbol represents the mean of a triplicate experiment, and error bars indicate the SD. **(C)** Left: Anti-CyRPA mAb c12 (circles) was added to highly synchronous early ring stages, and parasitemia was monitored during development into trophozoite stages and compared with PBS controls (squares). Parasitemia was measured after 0, 13, 21, and 37 h. Right: Anti-CyRPA mAb c12 (circles) was added to highly synchronous schizont stages, and parasitemia was monitored during the infection of new erythrocytes and the development into ring and trophozoite stages and compared with the PBS control (squares). Parasitemia was measured after 0, 15, 24, 39, and 48 h. Each symbol represents the mean of a duplicate experiment, and error bars indicate the SD. Black symbols, total parasitemia; gray symbols, ring stages; white symbols, trophozoite stages. Asterisks indicate significant differences in total parasitemia between Ab-treated cultures and control cultures (unpaired t test); *p , 0.05, **p , 0.05.

Anti-CyRPA mAbs inhibit parasite growth *in vivo*

CyRPA has no orthologs in the rodent malarial species and therefore cannot be studied with conventional mouse models with rodent parasites. Therefore, we evaluated the *in vivo* parasite inhibitory activity of anti-CyRPA mAbs in a *P. falciparum* SCID mouse model. This model uses nonmyelodepleted NOD-*scid IL2Rg^{null}* mice engrafted with human erythrocytes to allow the growth of *P. falciparum* (65). Groups of three mice with a parasitemia of 0.87 ± 0.12% were injected once with 0.5, 2.5, or 5 mg anti-CyRPA mAb c12, respectively. The control group received 2.5 mg subclass-matched control mAb (hexa-his tag-specific). Parasitemia of all mice was monitored for the next 5 d (Fig. 6A). In mice that had received the control mAb, a sigmoidal increase in parasitemia was measured, reaching 21.0 ± 3.6% on day 6. Parasitemia in mice having received 2.5 mg anti-CyRPA mAb 13, which has shown a very weak *in vitro* growth inhibitory effect, increased similarly. In contrast, parasitemia of mice having received 2.5 or 5 mg anti-CyRPA mAb c12 increased only marginally, reaching 3.5 ± 1.2% and 3.7 ± 1.1% on day 6. The difference in parasitemia on day 6 in mice receiving 2.5 mg mAb c12 compared with the negative control group was highly significant (two-sided t test; p = 0.0013). Also, a five times lower dose of mAb c12 (0.5 mg) still reduced parasite growth (15.0 ± 1.2% parasitemia on day 6). Titration of mAbs in the circulation of the passively protected mice by ELISA showed that Ab levels remained high over the entire study period, ranging from 57 to 117% on day 6 compared with day 2, and immunofluorescence staining of persisting parasites showed that they still expressed CyRPA (data not shown).

On day 6, blood cells of mice having received 2.5 mg anti-CyRPA mAb c12 were used in a follow-up experiment to infect three naive groups of NOD-*scid IL2Rg^{null}* mice engrafted with human erythrocytes (Fig. 6B). A rapid and continuous increase in parasitemia indicated good viability of the transferred parasites (14.7 ± 1.3% parasitemia on day 6 in the untreated group). To assess if parasites growing in anti-CyRPA mAb c12-treated mice (Fig. 6A) have

developed resistance to Ab inhibition, recipient mice were treated with a single i.v. injection of 2.5 mg anti-CyRPA mAb c12 (Fig. 6B). Again, parasitemia was significantly reduced in comparison with mice treated with an isotype-matched control mAb (two-sided t test day 6, $p = 0.0001$).

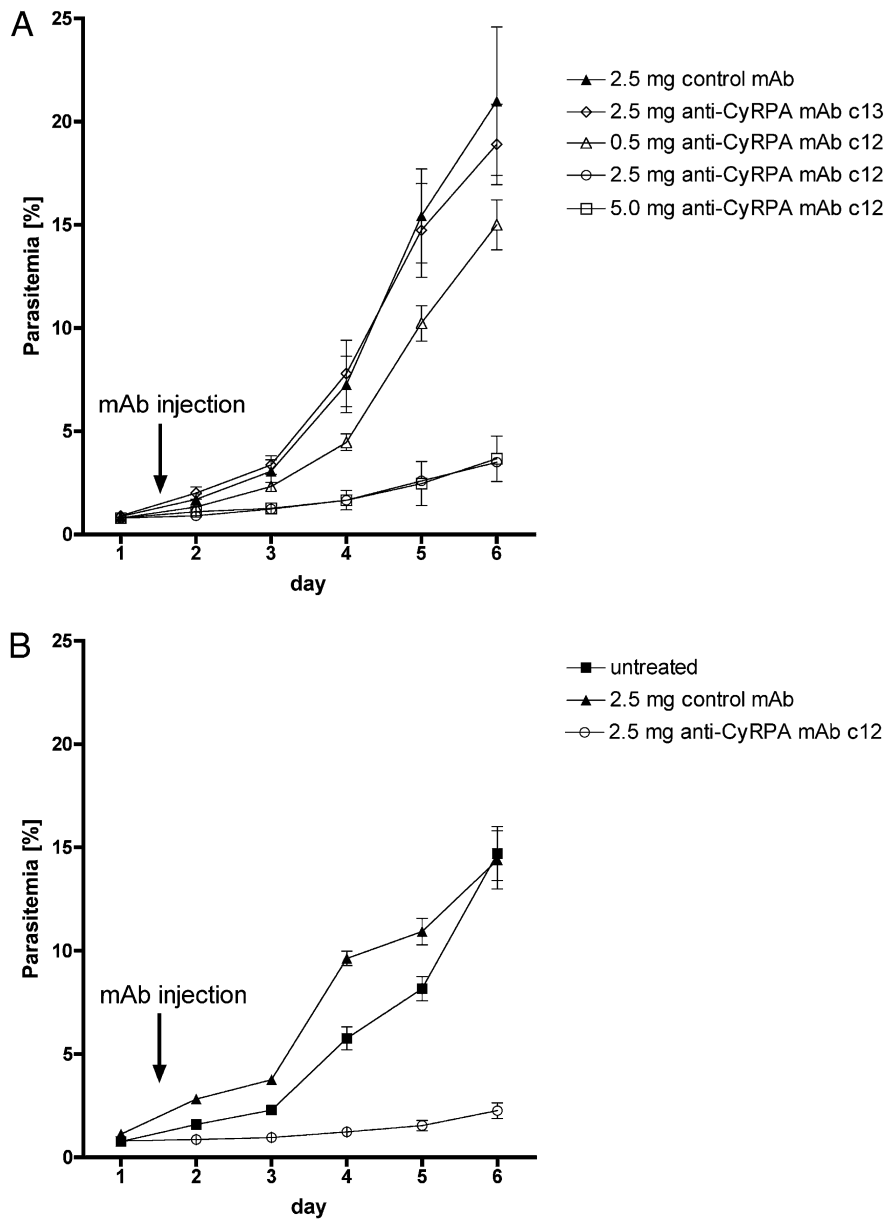


FIGURE 6. CyRPA-specific mAbs inhibit parasite growth in the NOD-*scid* *IL2Rg*^{null} mouse model. **(A)** *P. falciparum*-infected NOD-*scid* *IL2Rg*^{null} mice received purified anti-CyRPA mAbs or isotype/subclass-matched control mAbs by i.v. injection. The arrow indicates the day of mAb injection, and values are the mean parasitemia in peripheral blood of three mice per group. Data are means \pm 6 SD. **(B)** On day 6, blood cells of mice having received 2.5 mg anti-CyRPA mAb c12 were used to infect fresh NOD-*scid* *IL2Rg*^{null} mice. Once parasitemia exceeded 0.5%, mice received a single dose of 2.5 mg anti-CyRPA mAb c12 or control mAb by i.v. injection. Parasitemia was monitored over the next 5 d. Data are mean parasitemia of three mice per group \pm 6 SD.

Fine specificity of anti-CyRPA mAbs

Of nine CyRPA-specific mAbs analyzed, two (c05 and c13) showed no or borderline growth inhibitory effect, and seven (c02, c04, c06, c08, c09, c10, and c12) showed inhibitory activity. To explain these differences in biological activity, affinities as well as fine specificities of the anti-CyRPA mAbs were assessed.



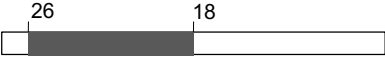

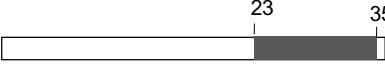


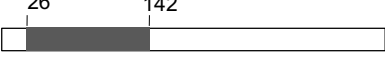

SPR with immobilized anti-CyRPA mAbs and recombinant CyRPA injected at various concentrations was used to analyze binding association and dissociation (Supplemental Fig. 3). All mAbs showed similar on-rates and slightly varying off-rates resulting in KDs ranging from low nanomolar to low picomolar. However, no correlation between affinity and growth inhibitory activity was observed.

Additionally, the fine specificities of the different mAbs were analyzed. First, Ab–Ab competition experiments were performed by ELISA using plates coated with recombinant CyRPA protein expressed in *E. coli* (Table I). mAbs c02, c04, c06, c08, c09, and c12 competed against each other. These mAbs did not compete with and were not competed by mAbs c05, c10, and c13. Whereas mAbs c05 and c13 competed with each other, mAb c10 did not compete with and was not competed by any of the other anti-CyRPA mAbs. According to these results, the nine mAbs were grouped into three epitope groups (I, II, III), with the two non-inhibitory mAbs forming epitope group III.

Second, the anti-CyRPA mAbs were tested for their reactivity with overlapping protein fragments of CyRPA. For this purpose, HEK cells transiently transfected with expression plasmids encoding fragments of CyRPA comprising aa 26–352, 26–251, 26–181, 127–352, 236–352, 74–251, 74–181, 26–142, and 127–251 were analyzed by Western blot analysis and live cell staining. In Western blot analysis, CyRPA-specific mAbs bound to fragments 26–181, 26–251, and 26–352 but not to the two overlapping subfragments 26–141 and 74–181. This indicates that all nine mAbs recognize conformational epitopes that are present in fragment 26–181 but not formed in subfragments 26–141 and 74–181 (Supplemental Fig. 4 and data not shown). Live cell staining of HEK cells expressing the protein fragments on their cell surface with different anti-CyRPA mAbs revealed five distinctive reactivity patterns (A, B, C, D, E) (Table I). When combining results from Ab–Ab competition experiments and epitope mapping, the seven growth inhibitory anti-CyRPA mAbs were classified into three fine specificity groups. These were distinctive from the fine specificities of the two noninhibitory mAbs c05 and c13, which were the only mAbs reacting with the N-terminally truncated fragment comprising aa 74–251 (Table I). The identified dimorphism at amino acid

position 339 does not lie within the sequence stretch aa 26–181 relevant for binding of the analyzed anti-CyRPA mAbs (Table I). Accordingly, anti-CyRPA mAb 12 inhibited growth of *P. falciparum* strains expressing either variant (3D7 versus K1) (Supplemental Fig. 2B).

TABLE 1. Fine specificity of anti-CyRPA mAbs.

Anti-CyRPA mAb	c10	c02	c06	c08	c09	c12	c04	c05	c13
Parasite growth inhibition	yes	yes	yes	yes	yes	yes	yes	no	no
A Antibody-antibody competition ELISA									
Competing anti-CyRPA mAb	c10	c02	c06	c08	c09	c12	c04	c05	c13
c10	x	–	–	–	–	–	–	–	–
c02	–	x	x	x	x	x	x	–	–
c06	–	x	x	x	x	x	x	–	–
c08	–	x	x	x	x	x	x	–	–
c09	–	x	x	x	x	x	x	–	–
c12	–	x	x	x	x	x	x	–	–
c04	–	x	x	x	x	x	x	–	–
c05	–	–	–	–	–	–	–	x	x
c13	–	–	–	–	–	–	–	x	x
epitope group	I	II	II	II	II	II	II	III	III
B Reactivity of anti-CyRRPA mAbs with CyRPA fragments									
CyRPA fragment	Anti-CyRPA mAb							c05	c13
	C10	c02	c06	c08	c09	c12	c04		
	x	x	x	x	x	x	x	x	x
	–	x	x	x	x	x	x	x	x
	–	x	x	x	x	x	x	x	x
	–	–	–	–	–	–	x*	–	–
	–	–	–	–	–	–	x*	–	–
	–	–	–	–	–	–	–	x*	x*
	–	–	–	–	–	–	–	–	x*
	–	–	–	–	–	–	–	–	–
	–	–	–	–	–	–	–	–	–
epitope group	A	B	B	B	B	B	C	D	E

(A) Ab–Ab competition ELISA results of nine anti-CyRPA mAbs. According to their competition pattern, mAbs were assigned to epitope groups I, II, or III. x, Ab competition; 2, no Ab competition.

(B) Capability of nine anti-CyRPA mAbs to bind to fragments of CyRPA expressed on the cell surface of HEK cells assessed by live-cell immunofluorescence staining. According to their reactivity pattern, mAbs were assigned to epitope groups A, B, C, D, or E. x, Staining; 2, no staining.

^aNo reactivity in Western blot analysis of HEK cell lysates (data not shown).

Synergistic inhibitory activity of anti-CyRPA mAbs

In vitro growth inhibition assays with combinations of anti-CyRPA mAbs were performed to assess whether different mAbs functionally interfere with each other (Fig. 5B). The functional activity of inhibitory anti-CyRPA mAbs was not affected by the addition of the noninhibitory anti-CyRPA mAb c05 or a malaria-unrelated control mAb. A synergistic inhibitory activity was measured when combining two inhibitory anti-CyRPA mAbs, which bind to distinct epitopes: 46.0 \pm 1.1% and 52.1 \pm 3.4% growth inhibition was measured for 500 mg/ml of anti-CyRPA mAb c10 or c12, respectively, but combining 250 mg/ml of either mAb inhibited parasite growth by 81.6 \pm 0.3%. In contrast, when combining two inhibitory anti-CyRPA mAbs with the same fine specificity, only an additive but no synergistic inhibitory effect was observed.

Natural immunogenicity of CyRPA

To examine if natural exposure to *P. falciparum* leads to the development of anti-CyRPA Abs, human sera were analyzed by ELISA for their reactivity with purified recombinant CyRPA expressed in HEK cells (Fig. 7). Sera were collected from healthy individuals between 5 and 20 y of age living in the Kassena-Nankana District in northern Ghana where *P. falciparum* is highly endemic (67). Sera from healthy Swiss adults without any history of malaria served as negative control. Whereas sera from malaria-exposed individuals readily contained IgG specific for two MSP-1–derived recombinant protein fragments (mean OD 0.61 \pm 0.03 and mean OD 0.50 \pm 0.02, respectively, at 1:200 serum dilution), basically no CyRPA-specific IgG was measured (mean OD 0.07 \pm 0.00 at 1:200 serum dilution).

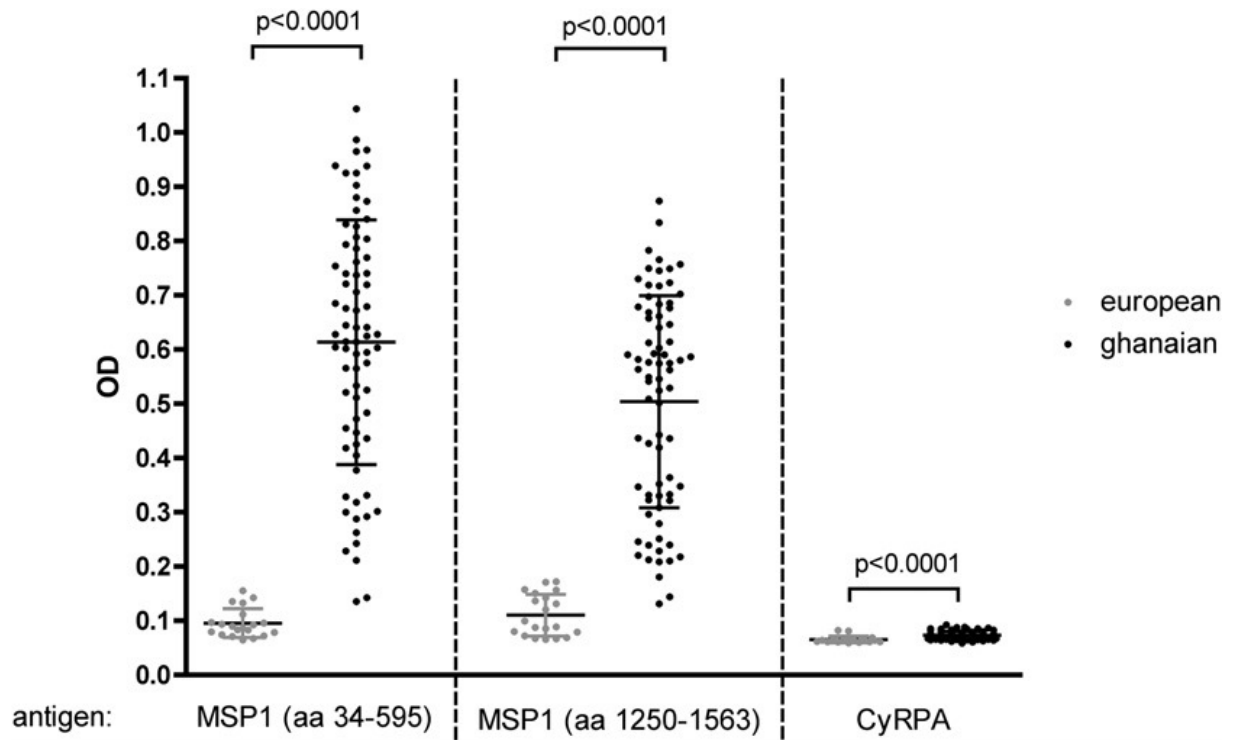


FIGURE 7. Analysis of serum from malaria-exposed individuals for presence of CyRPA-specific IgG. Reactivity of human sera from healthy European adults with no history of malaria exposure or from healthy individuals between 5 and 20 y of age living in the Kassena-Nankana District in northern Ghana (malaria exposed) with recombinant CyRPA and two recombinant MSP-1 fragments assessed by ELISA. Shown are IgG levels expressed as OD at 405 nm of serum samples diluted 1:200. Horizontal lines designate means and SDs of responses.

Discussion

With the release of the fully annotated genome of *P. falciparum* in 2002, genome-wide searches for potential vaccine candidate Ags have become possible (44, 45). On the basis of published transcriptome and proteome data, suggesting expression in extracellular stages and surface localization, we have selected sets of uncharacterized ORFs for evaluation of their potential as vaccine candidate Ags (Refs. 46–48, 51, 56 and A. Dreyer, G. Pluschke, unpublished observations). Among the proteins characterized, CyRPA exhibited outstanding properties, demonstrating the utility of systematic genome-wide approaches for vaccine Ag selection. However, for each individual Ag, detailed evaluations, including functional assays, remain indispensable to evaluate its potential as a vaccine candidate.

One major problem in the development of a malaria asexual blood-stage vaccine is the lack of functional assays with proven predictive potential. Established assays only assess certain potential Ab-mediated effector functions against blood-stage parasites (18, 76–78); that is, growth inhibition by Abs alone or Ab-dependent cellular inhibition. Still, these assays can provide valuable information on the protein function. Abs against CyRPA on its own showed a strong parasite growth inhibitory activity. This activity targeted the process of merozoite invasion into RBCs but not the development of intraerythrocytic stages. These results point toward a complement- and leukocyte-independent mode of action, such as blocking of molecular interactions involved in merozoite invasion (26, 28).

Plasmodium in vitro cultures are very sensitive to physiological changes. Thus, the *in vitro* growth inhibition assay is criticized for being very sensitive to impurities of Ab preparations tested. We addressed this by testing more than one independently produced batch of the individual mAbs and obtained consistent results. Importantly, the mouse *in vivo* model offers the advantage of a constant physiological environment given that factors like nutrient supply, electrolyte balance, and pH are very well controlled by the animal (79). Because *P. falciparum* cannot infect rodent erythrocytes and rodent malaria parasites lack many Ags of *P. falciparum*, including CyRPA, nonhuman primates or SCID-mice engrafted with human erythrocytes are the only *in vivo* models available to study growth inhibitory effects of CyRPA-specific Abs. It was previously shown that the *P. falciparum* model in NOD-SCID mice genetically deficient in IL-2R γ -chain (NOD-*scid* *IL2Rg*^{null}) engrafted with human erythrocytes is a reliable test system for drug evaluation *in vivo* (65, 80). Also in our hands, parasite growth in infected NOD-*scid* *IL2Rg*^{null} mice was very consistent and reproducible. However, this model has never been used previously for passive immunization studies. Anti-

CyRPA mAbs administered at the beginning of the exponential growth phase exerted a strong, dose-dependent parasite growth inhibitory effect. To the best of our knowledge, our study describes the first Ig transfer assay using a *P. falciparum* murine model in which a dose-response relationship has been reported. In contrast to the previously described model (79), this system therefore permits comparison of the relative inhibitory potency of malaria-specific Abs *in vivo*. Thus, we propose this model as a reliable *in vivo* model to test protective efficacy of vaccine Ags against *P. falciparum* blood stages.

The NOD/scid-IL2R β null mouse model is restricted to passive immunization as mice lack the adaptive immune system and additionally have deficiencies in the innate immune system (83, 84). However, besides passive immunization with Abs, adoptive transfer of specific effector immune cells may potentially be studied in this model. Another question left unanswered is whether this model can be used for the assessment of the other Ab-mediated effector mechanisms apart from plain neutralization that have been described for blood-stage-specific Abs (26, 27, 29–32, 81, 82). Such studies may shed light into the relevance of different Ab-mediated effector mechanisms for *in vivo* protection.

Growth inhibitory capacities of different anti-CyRPA mAbs assessed in the *in vivo* model correlate with the results obtained in the *in vitro* assays, strengthening credibility of both systems. The inhibitory effect of CyRPA-specific Abs seen *in vivo* can well be ascribed to the same effector mechanisms as *in vitro*; namely, blocking of invasion-relevant processes. Yet, we cannot exclude involvement of additional immune effector mechanisms. NOD-*scid* IL2R β ^{null} mice are incapable of mounting adaptive immune responses and additionally lack a functional common IL-2R β -chain, which is required for high-affinity binding of IL-2, IL-4, IL-7, IL-9, IL-15, and IL-21 to their receptor (83). As a consequence, NOD-*scid* IL2R β ^{null} mice have no NK cells and show additional defects in innate immunity. Involvement of complement or cellular effector mechanisms in the observed protection is nevertheless possible, as in these mice the percentage of macrophages/monocytes and granulocytes is normal or even increased (84).

Although it has been demonstrated that very high titers of specific Abs can be induced by appropriate vaccine formulations (85), the high Ab concentration required for *in vivo* protection may represent a hurdle for the development of a CyRPA-based vaccine. However, a substantial synergistic growth inhibitory effect was observed when combining two inhibitory anti-CyRPA mAbs with different fine specificity. Hence, stronger inhibitory activities may be achieved if active immunizations with CyRPA induce Abs specific for more

than one inhibitory epitope. If so, lower titers of total CyRPA-specific Abs may be required to confer protection.

Anti-CyRPA mAbs inhibited, but did not completely block, parasite growth. The multiplication rate *in vivo* was much reduced but remained above one, leading to a very slow rise in parasitemia. Increasing the applied dose from 2.5 to 5 mg per mouse did not reduce multiplication further, indicating a saturation of the inhibitory mechanism. From our functional data, we deduce that anti-CyRPA mAbs reduce parasite growth by partially inhibiting some processes crucial for invasion of erythrocytes by merozoites, be it a specific protein interaction or processing of invasion-relevant proteins. However, RBCs did not bind to HEK cells that express CyRPA on their cell surface, and purified recombinant CyRPA did not specifically bind to the erythrocyte surface (data not shown). These results indicate that CyRPA, at least on its own, is no ligand for erythrocyte surface receptors.

P. falciparum merozoites are described to use alternative invasion pathways to evade Ab-mediated immunity (86). Use of a CyRPA-independent invasion pathway of limited efficiency could explain persistence of infection associated with a reduced multiplication rate. Because parasites that survived treatment with anti-CyRPA mAb showed normal multiplication rates when transferred into naive mice and remained sensitive to re-exposure to anti-CyRPA mAbs, no rigid switch to an alternative invasion pathway seems to occur. The fact that, at least over a short time period, no CyRPA-Ab-resistant parasites were selected is of importance when considering the inclusion of CyRPA into a malaria subunit vaccine.

Notably, among a set of nine mAbs specific for CyRPA, seven mAbs showed a parasite growth inhibiting effect whereas two did not. The growth inhibitory activity of the Abs was not determined by their affinity for the target Ag, but by their fine specificity. No confined CyRPA sequence stretch could be defined as epitope, as all mAbs seem to recognize conformational epitopes not present in short CyRPA sequence stretches. However, the fine specificity of inhibitory anti-CyRPA mAbs was distinct from the fine specificity of noninhibitory anti-CyRPA mAbs. The fact that only anti-CyRPA Abs of a certain fine specificity showed invasion inhibitory activity demonstrates once more the shortcoming of assessing immunity or vaccine potential of Ags by solely measuring Ab titers by ELISA. Besides CyRPA, a range of other blood-stage Ags, including AMA-1 and MSP-1, were shown to induce inhibitory as well as noninhibitory or even inhibition-blocking Abs (87, 88). ELISA cannot differentiate between functional and nonfunctional Abs. For the same reason, it is favorable to perform passive immunoprotection experiments with mAbs in animal models

to identify novel vaccine targets rather than using active immunization. MAbs represent highly defined agents with a distinct fine specificity and affinity, whereas immunization induces Abs with a wide range of binding properties. Hence, functional assays with polyclonal Abs pose the risk of generating misleading results due to interference or masking of functional by nonfunctional Abs.

Most merozoite Ags associated with protection identified to date are located on the merozoite surface or within apical organelles. From a gene interaction network associated with invasion constructed from gene coexpression, sequence homology, domain– domain, and yeast two-hybrid data, CyRPA was selected as one of the genes to be expressed as a GFP-fusion protein to validate functional annotations (48). In that study, expression of CyRPA as a GFP-fusion protein in transgenic parasites was shown to result in a predominantly apical distribution. Consistent with this finding, we showed by indirect immunofluorescence staining with CyRPA-specific mAbs that CyRPA localizes intracellularly at the merozoite apex. Additionally, we could show that CyRPA does not localize to micronemes or rhoptry bulbs. The CyRPA-specific staining showed similarity to the staining of MSP-5, possibly indicating that CyRPA shares the same subcellular localization as MSP-5, a protein considered as a blood-stage vaccine candidate (89, 90). Although MSP-5 is described as a merozoite surface protein, its exact localization is sparsely characterized, and immunofluorescence staining of schizonts with MSP-5–specific Abs was shown previously to result in a rather dotted staining pattern (64, 91). The exact subcellular structure at the merozoite apex to which CyRPA localizes and how this structure is implicated in merozoite invasion remain to be investigated. *P. falciparum* is a highly polymorphic organism. This is particularly the case for many surface Ags as a result of natural selective pressure by the human immune responses (92). Most of the asexual blood-stage vaccine candidates evaluated to date, including AMA-1, MSP-1, and MSP-2, therefore have substantial polymorphisms (39–42). Immunodominance of the polymorphic and variant epitopes may explain the need for repeated exposure over several years to achieve clinical immunity against the natural polymorphic parasite populations (93). Malaria vaccines based on polymorphic Ags run the risk of compromised efficacy due to selection of vaccine-resistant variants (8). Therefore, it may be desirable to focus on Ags and protein domains with limited polymorphism. Sera of malaria-exposed adults tested here basically contained no CyRPA-specific Abs; natural immunogenicity of CyRPA thus appears to be very low. Our sequence analysis indicates that CyRPA has no substantial sequence polymorphisms. Only a single nonsynonymous SNP was detected among a range of

P. falciparum isolates. This, together with the low immunogenicity, is an indication that CyRPA is not a major target of naturally acquired immune responses. A possible explanation for the low immunogenicity of CyRPA may be the intracellular localization of CyRPA in released merozoites. Hence, CyRPA may only be accessible to the humoral immune surveillance during the short period of invasion. Other reasons may be a critical function of CyRPA prohibiting variation or hindered accessibility of CyRPA in its native context.

Furthermore, we could demonstrate that the identified SNP-associated amino acid dimorphism is not located within the epitope of the growth inhibitory anti-CyRPA mAbs and that parasites harboring sequence variants are likewise affected by growth inhibitory anti-CyRPA mAbs, indicating that this dimorphism is of no functional importance. From these results, we deduce that the protection-associated epitopes of CyRPA are likely to be free of sequence polymorphisms, suggesting that a CyRPA-based vaccine would target the entire *P. falciparum* population. This represents a clear advantage compared with polymorphic vaccine Ags like AMA-1, where several studies showed significant allele specificity in the inhibitory activity of anti-AMA-1 Abs (94–96).

Our data show that CyRPA clearly fulfills three key criteria applied to select asexual blood-stage Ags as vaccine candidates (97): 1) the protein is conserved; 2) Abs against the Ag inhibit parasite growth *in vitro* and 3) are protective in animal models. To validate further CyRPA as a blood-stage vaccine Ag, one ought to demonstrate that 1) CyRPA is essential for parasite survival, 2) growth inhibitory anti-CyRPA Abs can be induced by active immunization with recombinant CyRPA, 3) immunization is safe, and 4) growth inhibitory anti-CyRPA Abs confer protection against clinical malaria in humans.

In summary, we have identified a conserved merozoite protein that induces Abs that inhibit parasite growth *in vitro* and *in vivo*. We suggest evaluating its suitability as a candidate Ag for inclusion into a multivalent malaria subunit vaccine. In addition, we adopted the improved *P. falciparum* mouse model based on NOD-*scid* *IL2Rg*^{null} mice for functional analysis of malaria blood-stage-specific Abs. This model now allows a more systematic and quantitative comparison of the *in vivo* functionality of malaria Ag-specific Abs.

Acknowledgments

We thank Bernard Rutten for Ab purification, Dr. Walter Huber for SPR analysis, Bela Takacs for providing recombinant MSP-1, and Dr. Caroline Kulangara for providing extracted DNA from different *P. falciparum* strains.

Disclosures

The authors have no financial conflicts of interest.

Footnotes

This work was supported by a research grant from the Swiss National Science Foundation (310000-116337/1) and by the Unisciencia Foundation.

Abbreviations

AMA-1 apical membrane Ag 1; **CyRPA** cysteine-rich protective Ag; **EBA-175** erythrocyte binding Ag 175; **GAPM2** glideosome-associated protein with multiple-membrane spans 2; **GLURP** glutamate-rich protein; **MSP** merozoite surface protein; **ORF** open reading frame; **RH4** reticulocyte-binding homolog 4; **RH5** reticulocyte-binding homolog 5; **SERA5** serine repeat Ag 5; **SNP** single nucleotide polymorphism; **SPR** surface plasmon resonance.

References

1. World Health Organisation (2010) **World Malaria Report 2010**.
2. Doolan DL, Hoffman SL (1997) Multi-gene vaccination against malaria: **A multistage, multi-immune response approach**. *Parasitol. Today (Regul. Ed.)* 13: 171-178.
3. Patarroyo ME, Patarroyo MA (2008) **Emerging rules for subunit-based, multiantigenic, multistage chemically synthesized vaccines**. *Acc. Chem. Res* 41: 377-386. doi:10.1021/ar700120t
4. Marsh K, Kinyanjui S (2006) **Immune effector mechanisms in malaria**. *Parasite Immunol* 28: 51-60.
5. Cohen S, McGregor IA, Carrington S (1961) **Gamma-globulin and acquired immunity to human malaria**. *Nature* 192: 733-737.
6. McGregor IA (1964) **The passive transfer of human malarial immunity**. *Am. J. Trop. Med. Hyg* 13: SUPPL 237-239.
7. Sabchareon A, Burnouf T, Ouattara D, Attanath P, Bouharoun-Tayoun H, et al. (1991) **Parasitologic and clinical human response to immunoglobulin administration in falciparum malaria**. *Am. J. Trop. Med. Hyg* 45: 297-308.
8. Genton B, Betuela I, Felger I, Al-Yaman F, Anders RF, et al. (2002) **A recombinant blood-stage malaria vaccine reduces density and exerts selective pressure on parasite populations in a phase 1-2b trial in Papua New Guinea**. *J. Infect. Dis* 185: 820-827.
9. Mitchell GH, Butcher GA, Voller A, Cohen S (1976) **The effect of human immune IgG on the in vitro development of *Plasmodium falciparum***. *Parasitology* 72: 149-162.
10. Ling IT, Ogun SA, Momin P, Richards RL, Garçon N, et al. (1997) **Immunization against the murine malaria parasite *Plasmodium yoelii* using a recombinant protein with adjuvants developed for clinical use**. *Vaccine* 15: 1562-1567.
11. Perera KL, Handunnetti SM, Holm I, Longacre S, Mendis K (1998) **Baculovirus merozoite surface protein 1 C-terminal recombinant antigens are highly protective in a natural primate model for human *Plasmodium vivax* malaria**. *Infect. Immun* 66: 1500-1506.
12. Crewther PE, Matthew ML, Flegg RH, Anders RF (1996) **Protective immune responses to apical membrane antigen 1 of *Plasmodium chabaudi* involve recognition of strain-specific epitopes**. *Infect. Immun* 64: 3310-3317.
13. Collins WE, Pye D, Crewther PE, Vandenberg KL, Galland GG, et al. (1994) **Protective immunity induced in squirrel monkeys with recombinant apical membrane antigen-1 of *Plasmodium fragile***. *Am. J. Trop. Med. Hyg* 51: 711-719.

14. Ogutu BR, Apollo OJ, McKinney D, Okoth W, Siangla J, et al. (2009) **Blood stage malaria vaccine eliciting high antigen-specific antibody concentrations confers no protection to young children in Western Kenya.** PLoS ONE 4: e4708.
15. Esen M, Kremsner PG, Schleucher R, Gässler M, Imoukhuede EB, et al. (2009) **Safety and immunogenicity of GMZ2 - a MSP3-GLURP fusion protein malaria vaccine candidate.** Vaccine 27: 6862-6868.
16. Audran R, Cachat M, Lurati F, Soe S, Leroy O, et al. (2005) **Phase I malaria vaccine trial with a long synthetic peptide derived from the merozoite surface protein 3 antigen.** Infect. Immun 73: 8017-8026.
17. Sirima SB, Tiono AB, Ouédraogo A, Diarra A, Ouédraogo AL, et al. (2009) **Safety and immunogenicity of the malaria vaccine candidate MSP3 long synthetic peptide in 12-24 months-old Burkinabe children.** PLoS ONE 4: e7549.
18. Druilhe P, Spertini F, Soesoe D, Corradin G, Mejia P, et al. (2005) **A malaria vaccine that elicits in humans antibodies able to kill *Plasmodium falciparum*.** PLoS Med 2: e344.
19. Sagara I, Ellis RD, Dicko A, Niambele MB, Kamate B, et al. (2009) **A randomized and controlled Phase 1 study of the safety and immunogenicity of the AMA1-C1/Alhydrogel + CPG 7909 vaccine for *Plasmodium falciparum* malaria in semi-immune Malian adults.** Vaccine 27: 7292-7298.
20. El Sahly HM, Patel SM, Atmar RL, Lanford TA, Dube T, et al. (2010) **Safety and immunogenicity of a recombinant nonglycosylated erythrocyte binding antigen 175 Region II malaria vaccine in healthy adults living in an area where malaria is not endemic.** Clin. Vaccine Immunol 17: 1552-1559.
21. Hermsen CC, Verhage DF, Telgt DSC, Teelen K, Bousema JT, et al. (2007) **Glutamate-rich protein (GLURP) induces antibodies that inhibit in vitro growth of *Plasmodium falciparum* in a phase 1 malaria vaccine trial.** Vaccine 25: 2930-2940.
22. Horii T, Shirai H, Jie L, Ishii KJ, Palacpac NQ, et al. (2010) **Evidences of protection against blood-stage infection of *Plasmodium falciparum* by the novel protein vaccine SE36.** Parasitol. Int 59: 380-386.
23. Dvorak JA, Miller LH, Whitehouse WC, Shiroishi T (1975) **Invasion of erythrocytes by malaria merozoites.** Science 187: 748-750.
24. Gilson PR, Crabb BS (2009) **Morphology and kinetics of the three distinct phases of red blood cell invasion by *Plasmodium falciparum* merozoites.** Int. J. Parasitol 39: 91-96. doi:10.1016/j.ijpara.2008.09.007
25. Persson KEM (2010) **Erythrocyte invasion and functionally inhibitory antibodies in *Plasmodium falciparum* malaria.** Acta Trop 114: 138-143. doi:10.1016/j.actatropica.2009.05.017

26. Blackman MJ, Scott-Finnigan TJ, Shai S, Holder AA (1994) **Antibodies inhibit the protease-mediated processing of a malaria merozoite surface protein.** J. Exp. Med 180: 389-393.
27. Epstein N, Miller LH, Kaushel DC, Udeinya IJ, Rener J, et al. (1981) **Monoclonal antibodies against a specific surface determinant on malarial (*Plasmodium knowlesi*) merozoites block erythrocyte invasion.** J. Immunol 127: 212-217.
28. Collins CR, Withers-Martinez C, Bentley GA, Batchelor AH, Thomas AW, et al. (2007) **Fine mapping of an epitope recognized by an invasion-inhibitory monoclonal antibody on the malaria vaccine candidate apical membrane antigen 1.** J. Biol. Chem 282: 7431-7441. doi:10.1074/jbc.M610562200
29. Druilhe P, Khusmith S (1987) **Epidemiological correlation between levels of antibodies promoting merozoite phagocytosis of *Plasmodium falciparum* and malaria-immune status.** Infect. Immun 55: 888-891.
30. Kumaratilake LM, Ferrante A (2000) **Oponization and phagocytosis of *Plasmodium falciparum* merozoites measured by flow cytometry.** Clin. Diagn. Lab. Immunol 7: 9-13.
31. Ramasamy R, Rajakaruna R (1997) **Association of malaria with inactivation of [alpha]1,3-galactosyl transferase in catarrhines.** Biochimica et Biophysica Acta (BBA) - Molecular Basis of Disease 1360: 241-246. doi:16/S0925-4439(97)00005-7
32. Joos C, Marrama L, Polson HEJ, Corre S, Diatta A-M, et al. (2010) **Clinical protection from falciparum malaria correlates with neutrophil respiratory bursts induced by merozoites opsonized with human serum antibodies.** PLoS ONE 5: e9871. doi:10.1371/journal.pone.0009871
33. Crompton PD, Pierce SK, Miller LH (2010) **Advances and challenges in malaria vaccine development.** J. Clin. Invest 120: 4168-4178. doi:10.1172/JCI44423
34. Sagara I, Dicko A, Ellis RD, Fay MP, Diawara SI, et al. (2009) **A randomized controlled phase 2 trial of the blood stage AMA1-C1/Alhydrogel malaria vaccine in children in Mali.** Vaccine 27: 3090-3098. doi:10.1016/j.vaccine.2009.03.014
35. Spring MD, Cummings JF, Ockenhouse CF, Dutta S, Reidler R, et al. (2009) **Phase 1/2a study of the malaria vaccine candidate apical membrane antigen-1 (AMA-1) administered in adjuvant system AS01B or AS02A.** PLoS ONE 4: e5254. doi:10.1371/journal.pone.0005254.
36. Cech PG, Aebi T, Abdallah MS, Mpina M, Machunda EB, et al. (2011) **Virosome-Formulated *Plasmodium falciparum* AMA-1 & CSP Derived Peptides as Malaria Vaccine: Randomized Phase 1b Trial in Semi-Immune Adults & Children.** PLoS ONE 6: e22273. doi:10.1371/journal.pone.0022273
37. Takala SL, Plowe CV (2009) **Genetic diversity and malaria vaccine design, testing and efficacy: preventing and overcoming “vaccine resistant malaria.”** Parasite Immunology 31: 560-573. doi:10.1111/j.1365-3024.2009.01138.x

38. Polley SD, Conway DJ (2001) **Strong diversifying selection on domains of the *Plasmodium falciparum* apical membrane antigen 1 gene.** Genetics 158: 1505-1512.
39. Miller LH, Roberts T, Shahabuddin M, McCutchan TF (1993) **Analysis of sequence diversity in the *Plasmodium falciparum* merozoite surface protein-1 (MSP-1).** Mol. Biochem. Parasitol 59: 1-14.
40. Smythe JA, Peterson MG, Coppel RL, Saul AJ, Kemp DJ, et al. (1990) **Structural diversity in the 45-kilodalton merozoite surface antigen of *Plasmodium falciparum*.** Mol. Biochem. Parasitol 39: 227-234.
41. Volkman SK, Hartl DL, Wirth DF, Nielsen KM, Choi M, et al. (2002) **Excess polymorphisms in genes for membrane proteins in *Plasmodium falciparum*.** Science 298: 216-218.
42. Gardner MJ, Hall N, Fung E, White O, Berriman M, et al. (2002) **Genome sequence of the human malaria parasite *Plasmodium falciparum*.** Nature 419: 498-511.
43. Rappuoli R (2000) **Reverse vaccinology.** Curr. Opin. Microbiol 3: 445-450.
44. Chaudhuri R, Ahmed S, Ansari FA, Singh HV, Ramachandran S (2008) **MalVac: database of malarial vaccine candidates.** Malar. J 7: 184.
45. Doolan DL, Mu Y, Unal B, Sundares S, Hirst S, et al. (2008) **Profiling humoral immune responses to *P. falciparum* infection with protein microarrays.** Proteomics 8: 4680-4694.
46. Le Roch KG, Zhou Y, Blair PL, Grainger M, Moch JK, et al. (2003) **Discovery of gene function by expression profiling of the malaria parasite life cycle.** Science 301: 1503-1508.
47. Bozdech Z, Llinás M, Pulliam BL, Wong ED, Zhu J, et al. (2003) **The transcriptome of the intraerythrocytic developmental cycle of *Plasmodium falciparum*.** PLoS Biol 1: E5.
48. Hu G, Cabrera A, Kono M, Mok S, Chahal BK, et al. (2010) **Transcriptional profiling of growth perturbations of the human malaria parasite *Plasmodium falciparum*.** Nat. Biotechnol 28: 91-98.
49. Florens L, Washburn MP, Raine JD, Anthony RM, Grainger M, et al. (2002) **A proteomic view of the *Plasmodium falciparum* life cycle.** Nature 419: 520-526.
50. Lasonder E, Ishihama Y, Andersen JS, Vermunt AMW, Pain A, et al. (2002) **Analysis of the *Plasmodium falciparum* proteome by high-accuracy mass spectrometry.** Nature 419: 537-542.
51. **SignalP 3.0 Server** (n.d.). Available: <http://www.cbs.dtu.dk/services/SignalP/>. Accessed 3 Jun 2010.
52. Gaur D, Singh S, Singh S, Jiang L, Diouf A, et al. (2007) **Recombinant *Plasmodium falciparum* reticulocyte homology protein 4 binds to erythrocytes and blocks invasion.** Proc. Natl. Acad. Sci. U.S.A 104: 17789-17794.

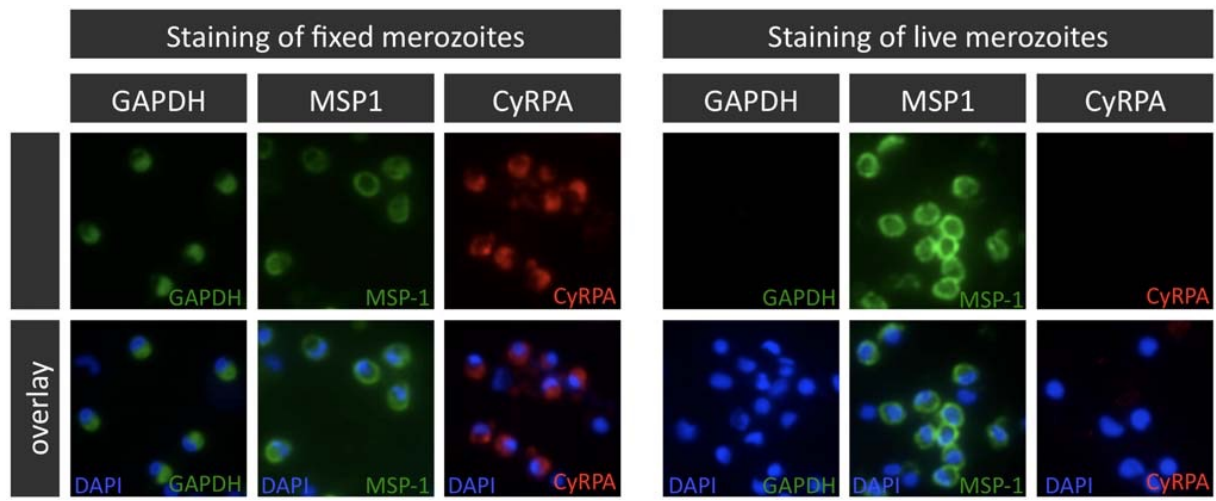
53. Baum J, Chen L, Healer J, Lopaticki S, Boyle M, et al. (2009) **Reticulocyte-binding protein homologue 5 - an essential adhesin involved in invasion of human erythrocytes by *Plasmodium falciparum***. *Int. J. Parasitol* 39: 371-380.
54. Winter G, Kawai S, Haeggström M, Kaneko O, von Euler A, et al. (2005) **SURFIN is a polymorphic antigen expressed on *Plasmodium falciparum* merozoites and infected erythrocytes**. *J. Exp. Med* 201: 1853-1863.
55. Bullen HE, Tonkin CJ, O'Donnell RA, Tham W-H, Papenfuss AT, et al. (2009) **A Novel Family of Apicomplexan Glideosome-associated Proteins with an Inner Membrane-anchoring Role**. *J Biol Chem* 284: 25353-25363.
56. Dreyer AM, Beauchamp J, Matile H, Pluschke G (2010) **An efficient system to generate monoclonal antibodies against membrane-associated proteins by immunisation with antigen-expressing mammalian cells**. *BMC Biotechnol* 10: 87.
57. Matile, H., and J. R. Pink. 1990. ***Plasmodium falciparum* malaria parasite cultures and their use in immunology**. In *Immunological Methods*. Volume IV. I. Lefkovits, and B. Pernis, eds. Academic Press, San Diego, CA, p. 221–234.
58. Dorn, A., R. Stoffel, H. Matile, A. Bubendorf, and R. G. Ridley. 1995. **Malarial haemozoin/beta-haematin supports haem polymerization in the absence of protein**. *Nature* 374: 269–271. 510.
59. Lambros, C., and J. P. Vanderberg. 1979. **Synchronization of *Plasmodium falciparum* erythrocytic stages in culture**. *J. Parasitol.* 65: 418–420.
60. Mueller, M. S., A. Renard, F. Boato, D. Vogel, M. Naegeli, R. Zurbriggen, J. A. Robinson, and G. Pluschke. 2003. **Induction of parasite growth-inhibitory antibodies by a virosomal formulation of a peptidomimetic of loop I from domain III of *Plasmodium falciparum* apical membrane antigen 1**. *Infect. Immun.* 71: 4749–4758.
61. Moreno, R., F. Poitl-Frank, D. Stuber, H. Matile, M. Mutz, N. A. Weiss, and G. Pluschke. 2001. **Rhoptry-associated protein 1-binding monoclonal antibody raised against a heterologous peptide sequence inhibits *Plasmodium falciparum* growth in vitro**. *Infect. Immun.* 69: 2558–2568.
62. Daubenberger, C. A., E. J. Tisdale, M. Curcic, D. Diaz, O. Silvie, D. Mazier, W. Eling, B. Bohrmann, H. Matile, and G. Pluschke. 2003. **The N^o-terminal domain of glyceraldehyde-3-phosphate dehydrogenase of the apicomplexan *Plasmodium falciparum* mediates GTPase Rab2-dependent recruitment to membranes**. *Biol. Chem.* 384: 1227–1237.
63. Wang, L., C. G. Black, V. M. Marshall, and R. L. Coppel. 1999. **Structural and antigenic properties of merozoite surface protein 4 of *Plasmodium falciparum***. *Infect. Immun.* 67: 2193–2200.

64. Marshall VM, Tiegiao W, Coppel RL (1998) **Close linkage of three merozoite surface protein genes on chromosome 2 of *Plasmodium falciparum***. *Molecular and Biochemical Parasitology* 94: 13-25. doi:16/S0166-6851(98)00045-0.
65. Jiménez-Díaz MB, Mulet T, Viera S, Gómez V, Garuti H, et al. (2009) **Improved murine model of malaria using *Plasmodium falciparum* competent strains and non-myelodepleted NOD-scid IL2Rgammanull mice engrafted with human erythrocytes**. *Antimicrob. Agents Chemother* 53: 4533-4536.
66. Genton, B., G. Pluschke, L. Degen, A. R. Kammer, N. Westerfeld, S. L. Okitsu, S. Schroller, P. Vounatsou, M. M. Mueller, M. Tanner, and R. Zurbriggen. 2007. **A randomized placebo-controlled phase Ia malaria vaccine trial of two virosome-formulated synthetic peptides in healthy adult volunteers**. *PLoS ONE* 2: e1018.
67. Appawu, M., S. Owusu-Agyei, S. Dadzie, V. Asoala, F. Anto, K. Koram, W. Rogers, F. Nkrumah, S. L. Hoffman, and D. J. Fryauff. 2004. **Malaria transmission dynamics at a site in northern Ghana proposed for testing malaria vaccines**. *Trop. Med. Int. Health* 9: 164–170.
68. Müller, H. M., K. Früh, A. von Brunn, F. Esposito, S. Lombardi, A. Crisanti, and H. Bujard. 1989. **Development of the human immune response against the major surface protein (gp190) of *Plasmodium falciparum***. *Infect. Immun.* 57: 3765–3769.
69. Ecker, A., E. S. C. Bushell, R. Tewari, and R. E. Sinden. 2008. **Reverse genetics screen identifies six proteins important for malaria development in the mosquito**. *Mol. Microbiol.* 70: 209–220.
70. Gerloff DL, Creasey A, Maslau S, Carter R (2005) **Structural models for the protein family characterized by gamete surface protein Pfs230 of *Plasmodium falciparum***. *Proc. Natl. Acad. Sci. U.S.A* 102: 13598-13603. doi:10.1073/pnas.0502378102
71. Llinás M, Bozdech Z, Wong ED, Adai AT, DeRisi JL (2006) **Comparative whole genome transcriptome analysis of three *Plasmodium falciparum* strains**. *Nucleic Acids Res* 34: 1166-1173.
72. Bowyer PW, Simon GM, Cravatt BF, Bogyo M (2011) **Global profiling of proteolysis during rupture of *Plasmodium falciparum* from the host erythrocyte**. *Mol. Cell Proteomics* 10: M110.001636. doi:10.1074/mcp.M110.001636
73. Healer J, Crawford S, Ralph S, McFadden G, Cowman AF (2002) **Independent translocation of two micronemal proteins in developing *Plasmodium falciparum* merozoites**. *Infect. Immun* 70: 5751-5758.
74. Howard RF, Narum DL, Blackman M, Thurman J (1998) **Analysis of the processing of *Plasmodium falciparum* rhoptry-associated protein 1 and localization of Pr86 to schizont rhoptries and p67 to free merozoites**. *Mol. Biochem. Parasitol* 92: 111-122.
75. Pirson PJ, Perkins ME (1985) **Characterization with monoclonal antibodies of a surface antigen of *Plasmodium falciparum* merozoites**. *J. Immunol* 134: 1946-1951.

76. Bouharoun-Tayoun H, Oouvray C, Lunel F, Druilhe P (1995) **Mechanisms underlying the monocyte-mediated antibody-dependent killing of *Plasmodium falciparum* asexual blood stages.** J. Exp. Med 182: 409-418.
77. Tippet E, Fernandes LA, Rogerson SJ, Jaworowski A (2007) **A novel flow cytometric phagocytosis assay of malaria-infected erythrocytes.** J. Immunol. Methods 325: 42-50. Sugamura K, Asao H, Kondo M, Tanaka N, Ishii N, et al. (1996) **The interleukin-2 receptor gamma chain: its role in the multiple cytokine receptor complexes and T cell development in XSCID.** Annu. Rev. Immunol 14: 179-205.
78. Bouharoun-Tayoun H, Attanath P, Sabchareon A, Chongsuphajaisiddhi T, Druilhe P (1990) **Antibodies that protect humans against *Plasmodium falciparum* blood stages do not on their own inhibit parasite growth and invasion in vitro, but act in cooperation with monocytes.** J. Exp. Med 172: 1633-1641.
79. Badell E, Oouvray C, Moreno A, Soe S, van Rooijen N, et al. (2000) **Human malaria in immunocompromised mice: an in vivo model to study defense mechanisms against *Plasmodium falciparum*.** J. Exp. Med 192: 1653-1660.
80. Arnold L, Tyagi RK, Meija P, Swetman C, Gleeson J, et al. (2011) **Further improvements of the *P. falciparum* humanized mouse model.** PLoS ONE 6: e18045. doi:10.1371/journal.pone.0018045
81. Treutiger, C. J., I. Hedlund, H. Helmbj, J. Carlson, A. Jepson, P. Twumasi, D. Kwiatkowski, B. M. Greenwood, and M. Wahlgren. 1992. **Rosette formation in *Plasmodium falciparum* isolates and anti-rosette activity of sera from Gambians with cerebral or uncomplicated malaria.** Am. J. Trop. Med. Hyg. 46: 503–510.
82. Udeinya, I. J., L. H. Miller, I. A. McGregor, and J. B. Jensen. 1983. ***Plasmodium falciparum* strain-specific antibody blocks binding of infected erythrocytes to amelanotic melanoma cells.** Nature 303: 429–431.
83. Sugamura K, Asao H, Kondo M, Tanaka N, Ishii N, et al. (1996) **The interleukin-2 receptor gamma chain: its role in the multiple cytokine receptor complexes and T cell development in XSCID.** Annu. Rev. Immunol 14: 179-205.
84. Cao X, Shores EW, Hu-Li J, Anver MR, Kelsall BL, et al. (1995) **Defective lymphoid development in mice lacking expression of the common cytokine receptor gamma chain.** Immunity 2: 223-238.
85. Kester, K. E., D. A. McKinney, N. Tornieporth, C. F. Ockenhouse, D. G. Heppner, Jr., T. Hall, B. T. Wellde, K. White, P. Sun, R. Schwenk, et al; RTS,S Malaria Vaccine Evaluation Group. 2007. **A phase I/IIa safety, immunogenicity, and efficacy bridging randomized study of a two-dose regimen of liquid and lyophilized formulations of the candidate malaria vaccine RTS,S/ AS02A in malaria-naïve adults.** Vaccine 25: 5359–5366.
86. Persson KEM, McCallum FJ, Reiling L, Lister NA, Stubbs J, et al. (2008) **Variation in use of erythrocyte invasion pathways by *Plasmodium falciparum* mediates evasion of human inhibitory antibodies.** J. Clin. Invest 118: 342-351.

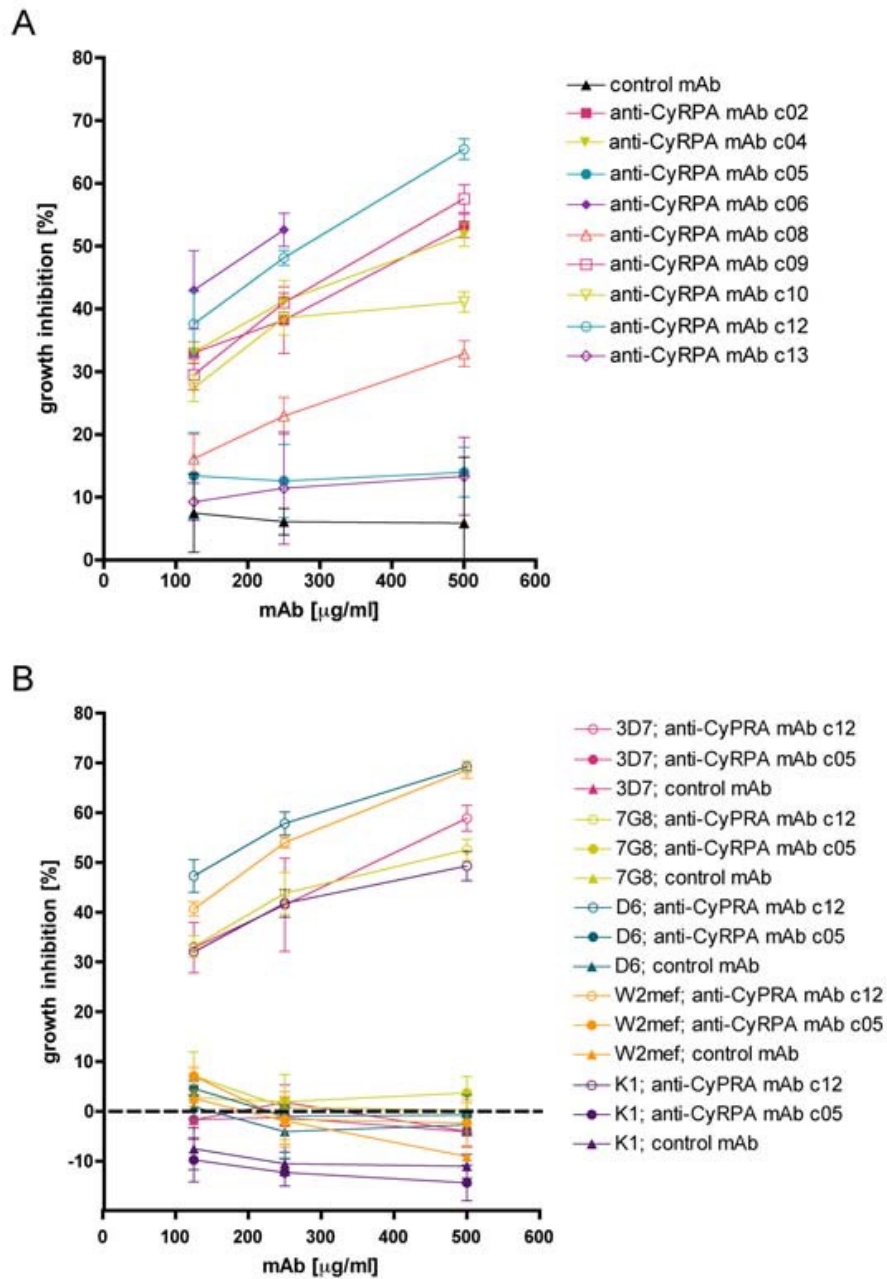
87. Nwuba RI, Sodeinde O, Anumudu CI, Omosun YO, Odaibo AB, et al. (2002) **The human immune response to *Plasmodium falciparum* includes both antibodies that inhibit merozoite surface protein 1 secondary processing and blocking antibodies.** Infect. Immun 70: 5328-5331.
88. Li C, Wang R, Wu Y, Zhang D, He Z, et al. (2010) **Epitope mapping of PfCP-2.9, an asexual blood-stage vaccine candidate of *Plasmodium falciparum*.** Malar. J 9: 94. doi:10.1186/1475-2875-9-94
89. Kedzierski L, Black CG, Coppel RL (2000) **Immunization with recombinant *Plasmodium yoelii* merozoite surface protein 4/5 protects mice against lethal challenge.** Infect. Immun 68: 6034-6037.
90. Bracho G, Zayas C, Wang L, Coppel R, Pérez O, et al. (2009) **AFCo1, a meningococcal B-derived cochleate adjuvant, strongly enhances antibody and T-cell immunity against *Plasmodium falciparum* merozoite surface protein 4 and 5.** Malar. J 8: 35. doi:10.1186/1475-2875-8-35
91. Wu T, Black CG, Wang L, Hibbs AR, Coppel RL (1999) **Lack of sequence diversity in the gene encoding merozoite surface protein 5 of *Plasmodium falciparum*.** Mol. Biochem. Parasitol 103: 243-250.
92. Kidgell C, Volkman SK, Daily J, Borevitz JO, Plouffe D, et al. (2006) **A systematic map of genetic variation in *Plasmodium falciparum*.** PLoS Pathog 2: e57.
93. Polley SD, Tetteh KKA, Lloyd JM, Akpogheneta OJ, Greenwood BM, et al. (2007) ***Plasmodium falciparum* merozoite surface protein 3 is a target of allele-specific immunity and alleles are maintained by natural selection.** J. Infect. Dis 195: 279-287.
94. Hodder AN, Crewther PE, Anders RF (2001) **Specificity of the protective antibody response to apical membrane antigen 1.** Infect. Immun 69: 3286-3294. doi:10.1128/IAI.69.5.3286-3294.2001
95. Kennedy MC, Wang J, Zhang Y, Miles AP, Chitsaz F, et al. (2002) **In vitro studies with recombinant *Plasmodium falciparum* apical membrane antigen 1 (AMA1): production and activity of an AMA1 vaccine and generation of a multiallelic response.** Infect. Immun 70: 6948-6960.
96. Kocken CHM, Withers-Martinez C, Dubbeld MA, van der Wel A, Hackett F, et al. (2002) **High-level expression of the malaria blood-stage vaccine candidate *Plasmodium falciparum* apical membrane antigen 1 and induction of antibodies that inhibit erythrocyte invasion.** Infect. Immun 70: 4471-4476.
97. Richards JS, Beeson JG (2009) **The future for blood-stage vaccines against malaria.** Immunol. Cell Biol 87: 377-390. doi:10.1038/icb.2009.27

Supplementary Material



Supplementary Figure 1. CyRPA resides intracellular in free merozoites.

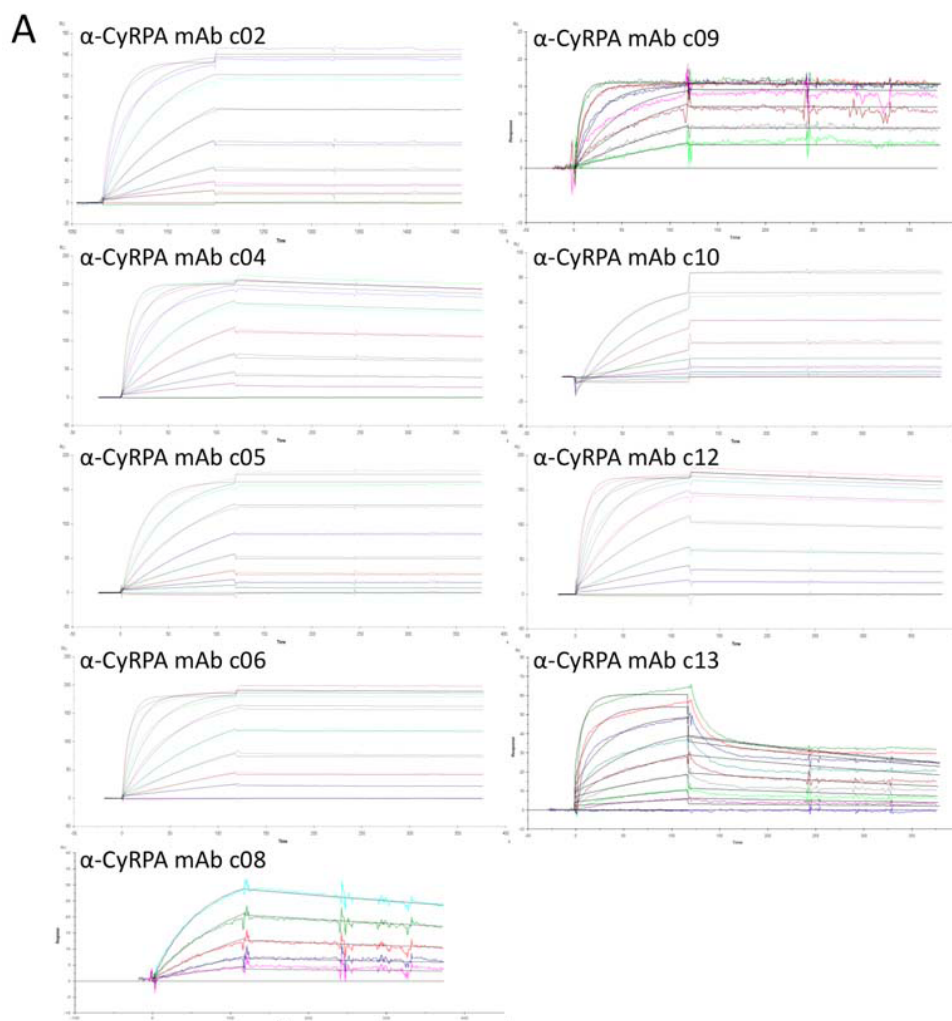
Indirect immunofluorescence staining of fixed (left) and un-fixed /right) merozoites with mAbs specific for GAPDH (green), MSP-1 (green) and CyRPA (red). Nuclei were stained with DAPI.



Supplementary Figure 2. Some, but not all anti-CyRPA mAbs inhibit parasite growth of various strains.

(A) Synchronous *P. falciparum* 3D7 blood stage parasites were cultured for two cycles in the presence of different concentrations of different purified anti-CyRPA mAbs. Percent parasite growth inhibition was calculated against the parasitemia of PBS control wells. Anti-6xHis-tag mAb was used as negative control mAb. Each symbol represents the mean of a triplicate experiment, and error bars indicate the standard deviation.

(B) Synchronous blood stage parasites of *P. falciparum* strain 3D7, 7G8, D6, W2mef and K1 were cultured for two cycles in the presence of different concentrations of purified anti-CyRPA mAb c12 or c05. Percent parasite growth inhibition was calculated against the parasitemia of PBS control wells. Anti-6xHis-tag mAb was used as negative control mAb. Each symbol represents the mean of a triplicate experiment, and error bars indicate the standard deviation.

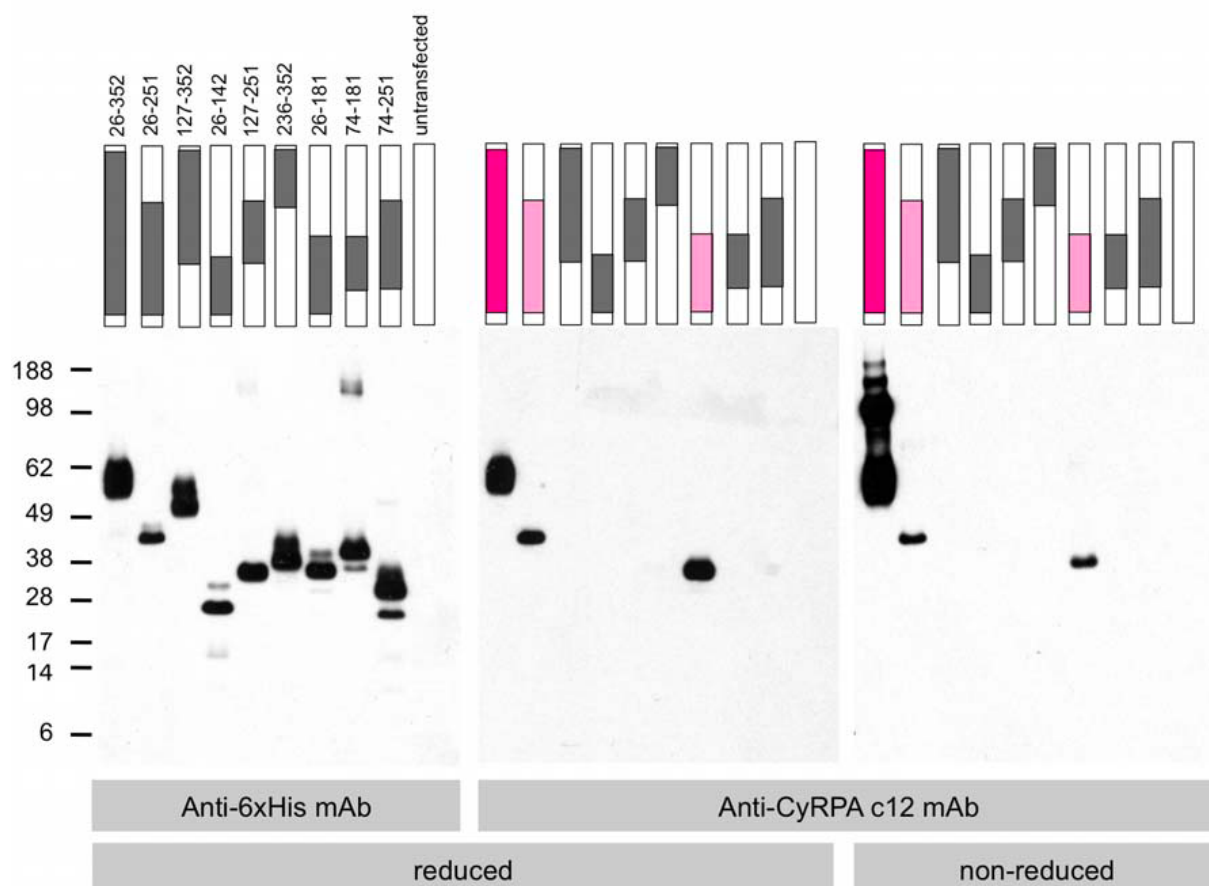


B

mAb	ka	kd	Rmax	KA	KD	Chi2
α -CyRPA mAb c02	1.68e5	9.35e-6	141	1.8e10	5.57e-11	6.35
α -CyRPA mAb c04	2.81e5	3.1e-4	208	9.04e8	1.11e-9	16.7
α -CyRPA mAb c05	1.13e5	1.28e-6	173	8.84e10	1.13e-11	6.53
α -CyRPA mAb c06	3.32e5	4.45e-5	191	7.46e9	1.34e-10	16.2
α -CyRPA mAb c08	4.04e4	7.4e-4	35	5.46e7	1.83e-8	0.48
α -CyRPA mAb c09	8.76e5	2.64e-5	16	3.32e10	3.01e-11	0.31
α -CyRPA mAb c10	6.1e4	4.67e-7	89	1.31e11	7.65e-12	0.90
α -CyRPA mAb c12	3.04e5	3.05e-4	176	9.96e8	1e-9	9.92
α -CyRPA mAb c13	N.A.	N.A.	N.A.	N.A.	N.A.	N.A.

Supplementary Figure 3. Surface Plasmon Resonance analysis of CyRPA binding to anti-CyRPA mAbs.

(A) SPR sensograms showing binding kinetics of CyRPA anti-CyRPA mAbs. A CM5 chip with immobilized anti-mouse IgG Abs was used to capture anti-CyRPA mAbs. Purified recombinant CyRPA was injected at concentrations of 400, 200, 100, 50, 25, 12.5, 6.25 and 3.13 nM (coloured lines, from top to bottom). Fitted curves for a 1:1 binding model is superimposed in black. RU, response units. (B) Summary of affinity constants for anti-CyRPA mAbs. Ka: on-rate, kd: off-rate, Rmax: response at complete saturation, KA: association constant, KD: dissociation constant. No fit could be obtained for mAb c13.



Supplementary Figure 4. Reactivity pattern of anti-CyRPA mAb c12 with fragments of the target antigen.

Lysates of HEK cells transiently transfected with expression plasmids encoding different CyRPA protein fragments were probed with anti-CyRPA mAbs. All nine mAbs recognized fragment 26-352 (dark pink), and all except mAb c10 recognized fragment 26-251 and fragment 26-181 (light pink). As an example, Western blots with anti-CyRPA mAb c12 are shown in the middle and right panel. As positive control lysates were probed with anti-6xHis-tag mAb (left panel). Relative molecular masses in kDa are indicated on the left.

Supplementary Table 1. Oligonucleotide sequence of used primers.

Primer Name	Sequence (5' to 3')
3888	AAAATTTTGTAGGAAATGTTGAGAA
3899	AAAACGATGACAAGTCATATCCTTC
3896	TGTCCTTGTATTTCGTGATATGTTTT
3903	TCATCATTTAATGTAGAAACATCTTGA
3900	TGACAATTACAAATTAGGTGTGCAA
3891	CAAATATGATGATTGTTGAATGGTT
3910	CCAATGCTAGCGGCATAAATTG
3911	ATAAGATAGCGGCCGCTTACCGTCATTTGAATAGAACCT
3912	ATACTAGCTAGCCGTAAGAAGGATATGACTTGTCCACAG
3913	ATAAGAATGCGGCCGCTTTCACATTATTGATGTTGTCTCCA
3886	GCTAGCGACCTGTCCTTTCACCTTTATGTTG
3887	GCGGCCGCGTTGTAATGCCCTGGGATG
3905	TCGGTACCTCGCGAATGC
3938	ATACTAGCTAGCGAGACCCATATCTACGTGCAG
3939	ATAAGAATGCGGCCGCCCGCAGATGAGGAAGTAC
3986	ATGCCATGGGCATAAATTGTGACAGCC
3941	CCGCTCGAGTTGTAATGCCCTGGGA
3987	CCGCTCGAGCCCGCAGATGAGGAA

Results Part 2

Generation of *Plasmodium falciparum* parasite-inhibitory antibodies by immunization with recombinantly expressed CyRPA

Malaria Journal 2016, **15**:161

Paola Favuzza^{1,2}, Simon Blaser^{1,2}, Anita M Dreyer^{1,2}, Guy Riccio^{1,2}, Marco Tamborrini^{1,2}, Ralf Thoma³, Hugues Matile³, Gerd Pluschke^{1,2§}

¹ Medical Parasitology and Infection Biology Department, Swiss Tropical and Public Health Institute, Basel, Switzerland

² University of Basel, Switzerland

³ Roche Pharmaceutical Research & Early Development, Small Molecule Research, Roche Innovation Center Basel, F. Hoffmann-La Roche Ltd., Basel, Switzerland

[§] Corresponding author

Abstract

Background

The pathogenesis of malaria is primarily associated with blood-stage infection and there is strong evidence that antibodies specific for parasite blood-stage antigens can control parasitaemia. This provides a strong rationale for incorporation of asexual blood-stage antigen components into an effective multivalent malaria subunit vaccine. Previously uncharacterized *Plasmodium falciparum* open reading frames, coding for new blood stage vaccine candidates, were selected on the basis of available genome-wide transcriptomic and proteomic data. This has led to the identification of the Cysteine-Rich Protective Antigen (PfCyRPA), which forms together with PfRH5 and PfRipr a multiprotein complex that is crucial for erythrocyte invasion.

Methods

Glycosylated and non-glycosylated variants of recombinant PfCyRPA were expressed and produced as secreted protein in mammalian cells. Adjuvanted formulations of purified PfCyRPA were tested to assess whether they can effectively elicit parasite inhibitory antibodies, and investigate whether or not the glycosylation status affects antibody binding. For this purpose, two sets of PfCyRPA-specific mouse monoclonal antibodies (mAbs) have been raised and evaluated for functional activity.

Results

Generated PfCyRPA-specific mAbs, irrespective of the immunogen's glycosylation status, showed substantial parasite in vitro growth-inhibitory activity due to inhibition of erythrocyte invasion by merozoites. Furthermore, passive immunization experiments in *P. falciparum* infected NOD-*scid* *IL2R γ ^{null}* mice engrafted with human erythrocytes demonstrated potent in vivo growth-inhibitory activity of generated mAbs.

Conclusions

Recombinantly expressed PfCyRPA tested as adjuvanted vaccine formulations in mice elicited antibodies that significantly inhibit *P. falciparum* asexual blood stage parasite growth both in vitro and in vivo. These findings render PfCyRPA a promising blood-stage candidate antigen for inclusion into a multicomponent malaria subunit vaccine.

Background

The World malaria report 2015 reported the reduction of malaria mortality rates by an impressive 48% between 2000 and 2015 as a result of a major scale-up of vector control interventions, diagnostic testing, and treatment with artemisinin - based combination therapy [1]. Despite these tremendous achievements, an estimated 214 million cases of malaria occurred globally in 2015, and the disease led to 438,000 deaths, mostly those of children under five years of age in Africa [1]. Limited efficacy achieved by subunit vaccine candidates, emerging anti-malarial drug resistances, along with reported insecticide resistances, underline the need of new tools to control and prevent malaria [2,3]. In this perspective, the development of an effective malaria vaccine is recognized as one of the most promising approaches to conquer the disease. Despite decades of research, an effective vaccine against malaria has remained elusive. Anti-malarial vaccines can break the parasite life cycle at different stages: infection-blocking vaccines targeting hepatic stages, anti-morbidity vaccines targeting the asexual blood stages, and transmission-blocking vaccines targeting the sexual stages. To achieve effective protection, the ideal malaria vaccine is thought to target several steps of the parasite life-cycle in a multistage combination vaccine [4].

Clinical and experimental data support the feasibility of developing an effective malaria vaccine. Adults living in malaria endemic areas rarely experience malaria episodes: partial protection of adults is mediated by naturally acquired immunity, and protects against symptomatic disease and high - density parasitaemia, but is not effective in offering sterile immunity [5]. Also, passive transfer of γ -globulin from semi-immune adults to malaria patients conferred a significant reduction of parasitaemia and recovery from clinical symptoms [6]. Those studies showed that immunity can be naturally acquired with exposure and indicated antibodies as crucial components of the protective immune response against asexual blood stage parasites. In this perspective, a multi-stage malaria vaccine should contain as one component antigen(s) that elicit antibody responses upon parasite presentation, leading to clearance of asexual blood stage parasites, and thus reducing the clinical symptoms.

Currently, with a total 25 projects in the pipeline [7], three candidate vaccines are in Phase 2B clinical trials and one, the pre-erythrocytic subunit vaccine RTS,S/AS01, has completed Phase 3 [8]. In infants aged 6-12 weeks at first vaccination with four doses of RTS,S reduced

the number of cases of clinical malaria by 26% to the end of the study over an follow-up of 38 months. Blood-stage vaccines, designed to elicit anti-invasion and anti-disease responses [9], are traditionally mainly based on a few protein candidate antigens: Apical Membrane Antigen 1 (AMA1) [10–12], Erythrocyte-Binding Antigen-175 (EBA-175) [13], Glutamate-Rich Protein (GLURP) [14,15], Merozoite Surface Protein (MSP) 1 [16], MSP2 [17,18] and MSP3 [19,20] and Serine Repeat Antigen 5 (SERA5) [21,22]. These immunodominant antigens, highly expressed on merozoites surface or within apical organelles, are involved in the invasion process. Unfortunately, AMA1 and MSP1, the most advanced blood-stage vaccines, have not demonstrated effective protection in African children [10,16,23], probably due to their highly polymorphic nature [24]. Genetic variability, extensive polymorphism and antigenic complexity in immunodominant antigens represent major obstacles in the development of an effective blood-stage malaria vaccine [25–27]. Identifying and designing antigens able to induce strain-transcending immune responses, which cover antigenic diversity remains a critical issue to be addressed. Since the *Plasmodium falciparum* genome was sequenced and annotated in 2002 [28], reverse vaccinology represents the most attractive strategy to rationally identify novel malaria vaccine candidates [29,30]. On the basis of the large-scale genomic, transcriptomic, proteomic and comparative data from *Plasmodium* spp. that have become available, new antigens with great potential as blood-stage vaccine candidates have been discovered [31].

Among the newly characterized proteins, the Cysteine Rich Protective Antigen (PfCyRPA) exhibited remarkable properties: PfCyRPA (i) elicits Abs that inhibit parasite growth in vitro and in vivo [32], (ii) is highly conserved among *P. falciparum* isolates [32], (iii) has limited natural immunogenicity, and (iv) forms together with the Reticulocyte-binding Homolog 5 (PfRH5) and the PfRH5-interacting Protein (PfRipr) a multiprotein complex crucial for *P. falciparum* erythrocyte invasion [33]. PfRH5 is currently regarded another leading blood-stage malaria vaccine candidate: it has been shown to induce invasion-inhibitory antibodies that are effective across common PfRH5 genetic variants and PfRH5-based vaccines can protect *Aotus* monkeys against virulent vaccine-heterologous *P. falciparum* challenges [34–37]. The PfCyRPA encoding gene *PFD1130w* is located in the subtelomeric region of chromosome 4 in close proximity to other genes playing a crucial role in the erythrocytes invasion, including *PFD1145c* that encodes for PfRH5 [36]. PfCyRPA is a 362-aa-long protein with a predicted molecular mass of 42.8 kDa, an N-terminal signal peptide, a C-terminal GPI-anchor motif and twelve cysteine residues, potentially involved in the formation

of six disulfide bridges. PfCyRPA was identified as a promising blood-stage malaria vaccine candidate exploiting a cell-based approach that utilizes antigens expressed on the surface of mammalian cells for mouse immunization [38]. Since antigen-loaded cells are not suitable for human immunization, we investigated whether invasion inhibitory anti-PfCyRPA antibodies could be raised by active immunization with purified recombinant PfCyRPA protein. In the present study, PfCyRPA was recombinantly-expressed in mammalian cells and adjuvanted vaccine formulations of purified PfCyRPA were tested for their potential to elicit antibodies that inhibit *P. falciparum* parasite growth in vitro and in vivo.

Methods

Bacterial strains and media

Escherichia coli strain Top10 (Life Technologies) was used for the amplification of plasmids. Bacteria were grown in LB medium containing 100 µg/ml ampicillin at 37°C.

Construction of expression plasmids

The expression vector which allows for the secretion of the recombinant PfCyRPA protein (aa 22-362) was generated by PCR-based mutagenesis [39–42] using the BVM_PFD1130W_FLAG_GP_His plasmid as template [38]. Briefly, a PCR product encompassing the bee-venom melittin secretion signal (BVM) and PfCyRPA aa 26-352 codon-optimized sequence, was amplified using GeneAmp® High Fidelity PCR System (Life Technologies) and primer 4325 (5'-CAACTCCGCCCCATTGACGCA-3') and 4326 (5'-GGTGTGGATGTTGTAAATGCCCTGGGA-3'). The hexa-his tag was amplified with primers 4329 (5'-GAGGAATTCCATCACCATCACCATCACTGATAA-3') and 4330 (5'-AGGGCGATGGCCCACTACGT-3'). A double-stranded oligonucleotide encoding for PfCyRPA aa 353-362 was generated by oligos-annealing employing the complementary oligonucleotides 4327 (5'-ATTTACAACATCCACACCATCTACTACGCCAACTACGAGGAATTCCATCACCAT-3') and 4328 (5'-ATGGTGATGGAATTCCTCGTAGTTGGCGTAGATGGTGTGGATGTTGTAAAT-3'). In a second step, a ligation PCR was performed with the outermost primer pair (4325 and 4330) using a mixture of the three previously generated PCR amplicons. Eventually, the recombined PCR product was recloned by NheI and XhoI (New England Biolabs) resulting in plasmid pcDNA3.1_BVM_CyRPA(26-362)_6xHis. This expression vector allows the expression of PfCyRPA with a hexa-His tag as secreted protein via the BVM signal peptide (designated G-CyRPA). It contains the secretion signal of bee-venom melittin, the coding sequence of the protein of interest and a hexa-His tag.

The expression vector coding for the non-glycosylated PfCyRPA (N-CyRPA) was generated by site-directed mutagenesis (GenScript) resulting in the expression plasmid pcDNA3.1_BMV_CyRPA(26-362/N145Q-N322Q-N338Q)_6xHis.

Culture of eukaryotic cells

FreeStyle 293-F cells (Thermo Fisher), a variant of human embryonic kidney cell line HEK cells, were cultured in suspension in serum-free medium (FreeStyle™ 293 Expression Medium, Thermo Fisher) at 37°C in a humidified incubator with 5% CO₂. Shake flask cultures were run in 1 L shake flasks (Corning, 120 rpm, 5 cm diameter) and 10 L cultures were performed in fully instrumented Wave bioreactors (Sartorius, Melsungen) under controlled conditions (30 rpm, pH 7.2, 30% DO).

Recombinant protein expression and purification

FreeStyle 293-F cells were transfected with pcDNA3.1_BVM_CyRPA(26-362)_6xHis and pcDNA3.1_BMV_CyRPA(26-362/N145Q-N322Q-N338Q)_6xHis plasmids using a riDOM-based transfection system [43]. Prior to transfection at 1.2×10^6 cells/ml, cells were diluted 1:2 with fresh culture medium and transfected with 0.4 mg/l expression plasmids and transfection reagents. Cell supernatants containing secreted proteins were typically harvested 72-96 hours post-transfection. Histidine-tagged proteins were purified by immobilized metal ion affinity chromatography (IMAC). The purity and integrity of the purified proteins were analysed by RP-HPLC on an Agilent 1290 Series with a Poroshell 300SB-C8, 1x75 mm column (Agilent). Chromatography was performed with a non-linear (H₂O + 0.01% TFA / Acetonitrile + 0.08% TFA) gradient system. The protein concentration was determined by measuring the OD₂₈₀ (1 Abs = 1 mg/ml). The purified recombinant proteins were identified as the expected G-CyRPA and N-CyRPA proteins by Western blot analysis with PfCyRPA-specific mAbs [32].

Expression of PfCyRPA fragments on the surface of HEK cells

293 HEK cells expressing PfCyRPA fragments on the cell surface were generated essentially as described previously by Dreyer *et al.* [32]. Briefly, DNA sequences coding for the fragments of PfCyRPA were amplified by PCR from a plasmid containing the full length and codon-optimized sequence of PfCyRPA. The amplicons were digested with restriction endonucleases NheI and NotI (New England Biolabs) and then ligated into a pcDNA3.1-based expression vector [38]. This expression vector allows to anchor the protein of interest on the cell surface via the transmembrane domain of mouse glycoporphin-A. In addition it contains the secretion signal of bee-venom melittin, a FLAG tag located extracellularly, and a hexa-His tag located in the cytosol. The 293 HEK cells were transfected with the different

expression vectors using JetPEI transfection reagent (PolyPlus) according to the manufacturer's instructions. Transient transfectants were harvested 48 hours post-transfection; cell lysates were generated as described below and used for Western blot analysis.

Immunization of mice

All procedures involving living animals were performed in strict accordance with the Rules and Regulations for the Protection of Animal Rights (Tierschutzverordnung) of the Swiss Federal Food Safety and Veterinary Office. The protocol was granted ethical approval by the Veterinary Office of the county of Basel-Stadt, Switzerland (Permit Numbers: 2375 and 2303). Specific pathogen-free HsdWin:NMRI outbred mice were purchased from Harlan Laboratories B.V. (The Netherlands) and used for immunizations studies. Sixteen mice were immunized intraperitoneally with 20 µg/injection of recombinant protein emulsified in aluminum hydroxide gel (Alhydrogel-2%, Brenntag Biosector) containing CpG ODN as immune enhancer [44]. The animals received three booster injections at two weeks intervals with the same antigen preparation. Two weeks after the last boost, blood was collected and the serum was tested for the presence of PfCyRPA-specific antibodies by ELISA and Western blot analysis.

Fusion and cell-based selection

The best immune responders were selected for fusion. These mice received an intravenous (i.v.) injection of 20 µg of antigen dissolved in PBS two days before the fusion. Mice were sacrificed and the spleen was removed. Splenocytes were fused to the myeloma cell partner (PAI mouse myeloma cells, derived from SP-20, Institute of Immunology, Basel) using polyethylene glycol 1500 (Roche Diagnostics). The fusion mix was plated into 96-well culture plates and hybridomas were selected by growing in HAT-medium supplemented with culture supernatant of mouse macrophages P388. Wells were screened for IgG production two weeks post-fusion by ELISA as described previously [38]. IgG-producing hybrids were further screened for PfCyRPA-specific IgG production by ELISA on recombinant PfCyRPA. Positive wells were cloned in HT-medium by limiting dilution to obtain monoclonal populations.

Antibody production and characterization

Identification of antibody subclasses was performed using a Mouse Monoclonal Antibody Isotyping Kit (ISO2, Sigma). For large-scale mAb production hybridoma cell lines were cultured in 500 ml roller-bottles (Corning). Monoclonal antibodies were purified by affinity chromatography using Protein A Sepharose (GE Healthcare).

***Plasmodium falciparum* blood stage culture**

Plasmodium falciparum strain 3D7 was cultured essentially as described previously [45]. The culture medium was supplemented with 0.5% AlbuMAX (Life Technologies) as a substitute for human serum [46]. Cultures were synchronized by sorbitol treatment [47]. Erythrocytes for passages were obtained from the Swiss Red Cross (Switzerland). *Plasmodium falciparum* merozoites were mechanically released from mature schizonts as previously described [48]. Briefly, late-stage parasites (40-46 h post-invasion) were purified by Percoll density gradient [49] and incubated with 10 μ M E-64 inhibitor (Sigma). After 6-8 h incubation, mature schizonts were filtered through 1.2 μ m filters to release merozoites mechanically. Then, merozoites were resuspended PBS and stored at -80 °C until further use.

ELISA

Detection of PfCyRPA-specific Abs in mouse sera by ELISA

ELISA Maxisorp plates (Nunc) were coated with 10 μ g/ml purified recombinant G-CyRPA or MUL3720 proteins. After blocking, plates were incubated with dilutions of mouse serum. Horseradish Peroxidase (HRP) conjugated goat anti-mouse γ -chain specific (SouthernBiotech) was used as secondary antibody and tetramethylbenzidine substrate was used as substrate (KPL). The reaction was stopped with 0.5M H₂SO₄ and the absorbance at 450 nm was measured using the Sunrise Absorbance Reader (Tecan). The cut-off value for calculation of endpoints titers was defined for each immunization group as:

$$\text{Average OD value control} + (2x \text{ Standard Deviation control})$$

Serum IgG endpoint titers were calculated as reciprocal values of the last dilution factor yielding an OD value higher than the cut-off. Data were processed and analysed using GraphPad Prism 6.0 (GraphPad).

Ab competition ELISA

Plates were coated with 10 µg/ml purified recombinant G-CyRPA protein; after blocking, plates were incubated with 10 µg/ml, 1 µg/ml, or 0 µg/ml of different anti-PfCyRPA mAbs. After 30 min, different biotinylated anti-PfCyRPA mAbs were added to each well resulting in a concentration of 1 µg/ml of labelled mAb. As the two antibodies compete for the same binding site, the signal is reduced because less biotinylated detection antibody is able to bind to PfCyRPA. Alkaline phosphatase-conjugated streptavidin (Southern Biotech) was used as detecting agent, and *p*-nitrophenyl phosphate substrate (Sigma) was used for development. The OD of the reaction product was measured at 405 nm. Anti-PfCyRPA antibodies with a signal reduction higher than 30% (compared to the absence of competitor) were considered as competing.

Western blotting analysis

Blood stage parasite lysates were prepared essentially as described previously by saponin lysis of *P. falciparum* 3D7-infected erythrocytes [45]. In brief, cultured parasites were washed once with PBS. Pelleted infected red blood cells were lysed in 20 volumes of 0.06% (w/v) saponin in PBS and incubated on ice for 20 min. Parasites were washed and the final pellet was resuspended in three volumes of PBS and stored at -80 °C until further use. RIPA-lysates were prepared by resuspending saponin pellets in three volumes of complete lysis buffer (1% NP40, 0.25% DOC, 10% glycerol, 2 mM EDTA, 137 mM NaCl, 20 mM Tris HCl pH 8.0, Protease Inhibitors) for 10 min on ice. The lysates were cleared by centrifugation at 15,000g for 10 min and the supernatant kept at -80°C until use. HEK cell lysate were prepared at 10⁷ cells/ml in Complete Lysis Buffer as described above. For SDS-PAGE, recombinant PfCyRPA, cell- or parasite lysates were resolved on precast 4-12% gradient gels (NuPAGE® Novex 4-12% Bis-Tris Gel, Life Technologies) with MES running buffer according to the manufacturer's directions. For analyses under reducing conditions, samples were reduced with 50mM_f dithiothreitol (DTT) and heated to a temperature of 70°C for 10 minute prior to loading. The proteins were electrophoretically transferred to nitrocellulose membrane using a dry-blotting system (iBlot, Life Technologies). After blocking the membrane, specific proteins were detected with appropriate dilutions of mAbs followed by HRP-conjugated goat anti-mouse IgG Abs (SouthernBiotech). Blots were developed using the ECL Western blotting detection reagents (Pierce).

Immunofluorescence staining of infected erythrocytes and free merozoites

For indirect immunofluorescence microscopy, smears of infected red blood cells or free merozoites were fixed in 60% methanol and 40% acetone for 2 min at -20°C, air-dried and blocked with 3% BSA in PBS. Parasites were probed with the following antibodies: biotin-labelled anti-PfCyRPA mAb SB3.3b and Alexa 568-labelled streptavidin (Invitrogen), Alexa 488-labelled mouse anti-GAPDH 1.4a mAb [50]. The slides were mounted in mounting medium containing DAPI (ProLong Gold antifade reagent with DAPI, Life Technologies). Fluorescence microscopy was performed on a Leica DM-5000B using a 60x oil immersion objective lens and documented with a Leica DFC345FX digital camera system. Images were processed using Leica Application Suite V4 (Leica) and Adobe Photoshop® CS6.

In vitro growth inhibition assay

In vitro growth inhibition assays with *P. falciparum* strain 3D7 were conducted essentially as described [51]. Each culture was set up in triplicate in 96-well flat-bottomed culture plates. The cells were analysed in a FACScan flow cytometer (Becton Dickinson) using CellQuest software. A total of 30,000 cells per sample were analysed. Percent inhibition was calculated from the mean parasitaemia of triplicate test and control wells as follows:

$$\text{Percent inhibition (\%)} = \frac{\text{control} - \text{test}}{(\text{control}/_{100})}$$

In vivo growth inhibition assay

Monoclonal antibodies were tested in the murine *P. falciparum* model essentially as described [32,52]. Human blood (0.75 ml) was administered daily by the i.v. or i.p. route. Mice received a single dose of mAbs formulation by i.v. injection. The following day, mice were infected with 3×10^7 parasitized erythrocytes. Parasitaemia was monitored daily by flow cytometry over six days (day four to nine after mAb injection). To measure serum levels of administered mAbs, serum samples were taken one and eight days after injection.

.

Results

Recombinant expression of PfCyRPA

For the production of correctly folded recombinant secreted PfCyRPA (aa. 26-362), we removed the GPI-anchor motif from the coding sequence of *PFD1130w* and expressed the ORF as hexa-Histidine (His-tag) fusion protein in the human embryonic kidney cell line FreeStyle 293-F cells. While the predicted molecular mass of the recombinant protein, designated G-CyRPA, was 40.9 kDa, a discrete band of about 48 kDa was detected both in SDS-PAGE and Western Blot analyses with a PfCyRPA-specific mAb (Fig. 1a and b). When analysed for the presence of N-glycosylation sites (NetNGlyc 1.0 Server) [53], three asparagine residues were predicted as potential sites for N-glycosylation (N145, N322 and N338) in human cells. Recombinant G-CyRPA was then treated with PNGase F, which enzymatically removes N-linked carbohydrate residues from proteins. As expected, this treatment reduced the size of G-CyRPA by about 8 kDa (see Additional file 1).

The shift in molecular mass after PNGase F treatment suggests that G-CyRPA is indeed N-glycosylated when recombinantly expressed in HEK cells. Therefore, a non-glycosylated variant of PfCyRPA, designated N-CyRPA, was generated by replacing the three asparagine residue potentially implicated in N-glycosylation with glutamine residues (N145Q, N322Q, N338Q). As expected, N-CyRPA expressed in HEK cells migrated, both in SDS-PAGE and Western Blot analyses with a PfCyRPA-specific mAb, as a discrete band of about 41 kDa (Fig. 1a and b, and Additional file 2).

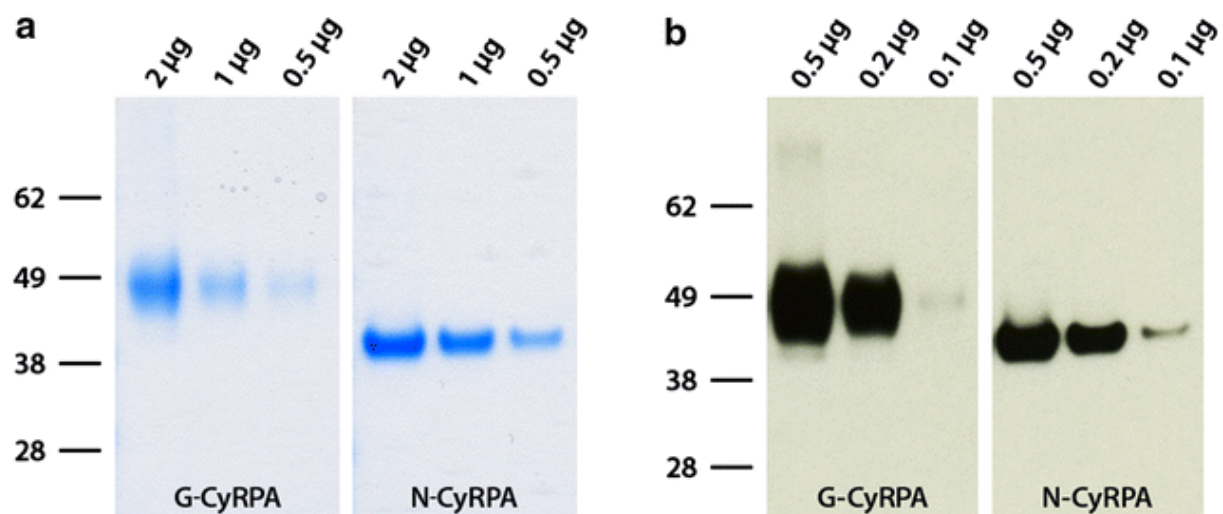


Fig. 1 Expression of recombinant PfCyRPA. Glycosylated (G) and non-glycosylated (N) recombinant PfCyRPA were expressed as His-tagged proteins in HEK cells and purified by affinity chromatography. The proteins were analyzed by denaturing/reducing gel electrophoresis (SDS-PAGE) and stained with Coomassie blue (**a**), and identified by Western blot analysis with the PfCyRPA-specific mAb Q8IF12 (**b**).

Immunogenicity of recombinant PfCyRPA and generation of PfCyRPA-specific mAbs

Mice were immunized three times with 20µg of recombinant G-CyRPA or N-CyRPA emulsified in aluminium hydroxide containing CpG ODN as immune enhancer [44]. After the third immunization, PfCyRPA-specific serum IgG endpoint titers were determined by indirect ELISA. All mice raised antibody responses against recombinant PfCyRPA, irrespective of the immunogen's glycosylation state ($p = 0.9591$, Mann-Whitney test, 95% confidence interval, two-tailed p value). As expected, mice raised also marginal antibody responses against the hexa-His tag, as indicated by a low antibody titer against the hexa-His tagged irrelevant protein MUL_3720 (Fig. 2a). Also, all immunized mice raised immune responses cross-reactive with *P. falciparum* endogenous PfCyRPA, as shown by Western blot analyses on late blood-stage parasite lysates (Fig. 2b).

Hybridoma cell lines producing PfCyRPA-specific mAbs were generated by fusing splenocytes of immunized mice with myeloma cells. Based on reactivity to recombinant PfCyRPA in ELISA, a panel of 11 anti-PfCyRPA mAbs was generated and tested for reactivity on recombinant and *P. falciparum* expressed PfCyRPA by Western blot analyses. 8/11 anti-PfCyRPA mAbs stained the recombinant PfCyRPA band and ten of them also stained either strongly (mAbs SB1.6, SB2.1, SB2.3, SB3.3 and SB3.9) or weakly (SB1.5, SB2.4, SB2.5, SB3.8 and SB3.8) a band of the size expected for PfCyRPA in *P. falciparum* schizont-stage lysate (Fig. 3, Table 1). In indirect immunofluorescence staining of asexual blood stage parasites, 9/11 mAbs were positive. mAb SB2.2 was positive in ELISA with recombinant PfCyRPA, but negative both in Western blot analysis and in IFA (Table 1). With the exception of mAb SB3.8, which in ELISA was reacting only to recombinant G-CyRPA, no general differences in binding properties, between anti-PfCyRPA mAbs produced against glycosylated or non-glycosylated recombinant PfCyRPA, were observed (Table 1). In indirect immunofluorescence and Western blotting analyses mAbs stained asexual blood stage parasites stage-specifically (Fig. 4, Table 1), since PfCyRPA is only expressed by schizonts and free merozoites [32]. As expected, the generated mAbs showed the characteristic pattern [32] consisting of a small spot toward the merozoite apical pole (see Additional file 3).

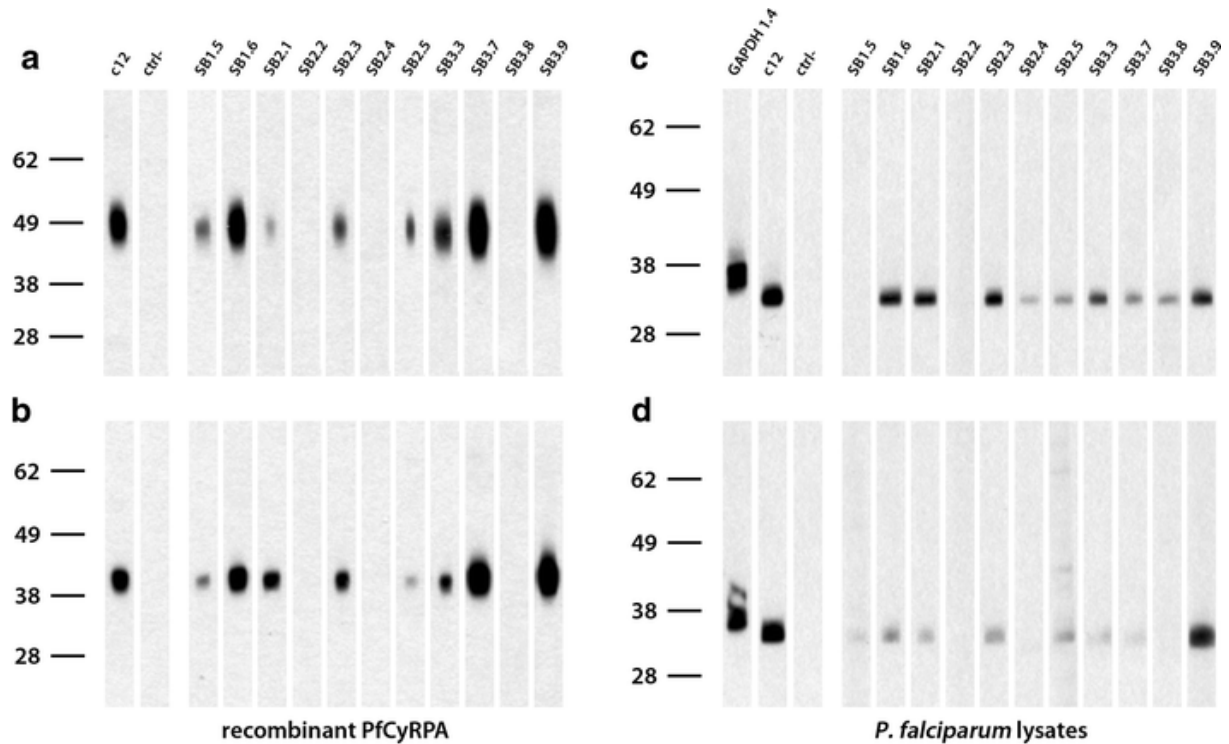


Fig. 3 Western blotting analysis of anti-PfCyRPA mAbs. Anti-PfCyRPA mAbs were tested by Western-blotting analysis on (a) recombinant G-CyRPA and (b) N-CyRPA (both sample were analysed under reducing conditions). Anti-PfCyRPA mAbs were also tested on *P. falciparum* 3D7 schizont-stage parasites under non-reducing (c) and reducing conditions (d). The anti-PfCyRPA mAb c12 and the anti-GAPDH mAb 1.4a were used as positive control [32,50]; the secondary antibody without primary antibody served as negative control.

Table 1 Summary of anti-PfCyRPA mAbs characterization

mAb	Immunization	ELISA		Western blotting analysis			IFA	GIA	Epitope group
		G-CyRPA	N-CyRPA	G-CyRPA	N-CyRPA	<i>P. falc.</i> 3D7	<i>P. falc.</i> 3D7	<i>P. falc.</i> 3D7	
SB1.5	G-CyRPA	+	+	+	+	+	-	partial	nd
SB1.6	G-CyRPA	+	+	+	+	+	+	yes	F
SB2.1	N-CyRPA	+	+	+	+	+	+	yes	F
SB2.2	N-CyRPA	+	+	-	-	-	-	partial	nd
SB2.3	N-CyRPA	+	+	+	+	+	+	yes	F
SB2.4	N-CyRPA	+	+	-	-	+	+	no	nd
SB2.5	N-CyRPA	+	+	+	+	+	+	partial	A
SB3.3	G-CyRPA	+	+	+	+	+	+	yes	F
SB3.7	G-CyRPA	+	+	+	+	+	+	partial	B
SB3.8	G-CyRPA	+	-	-	-	+	+	no	nd
SB3.9	G-CyRPA	+	+	+	+	+	+	no	E

Anti-PfCyRPA mAbs were characterized by ELISA (x, OD value higher than control anti-6xHis mAb HIS-6/9; -, OD value \leq control mAb), Western blotting analyses (x, staining; -, no staining; cf. Fig. 3), immunofluorescence assays (x, staining; -, no staining), growth inhibition assays (yes, GIA \geq 40%; no, GIA \leq 20%) and categorized into distinct epitope groups by epitope mapping experiments (cf. Table 2). G-CyRPA designates recombinant glycosylated PfCyRPA whereas N-CyRPA designates non-glycosylated recombinant PfCyRPA.

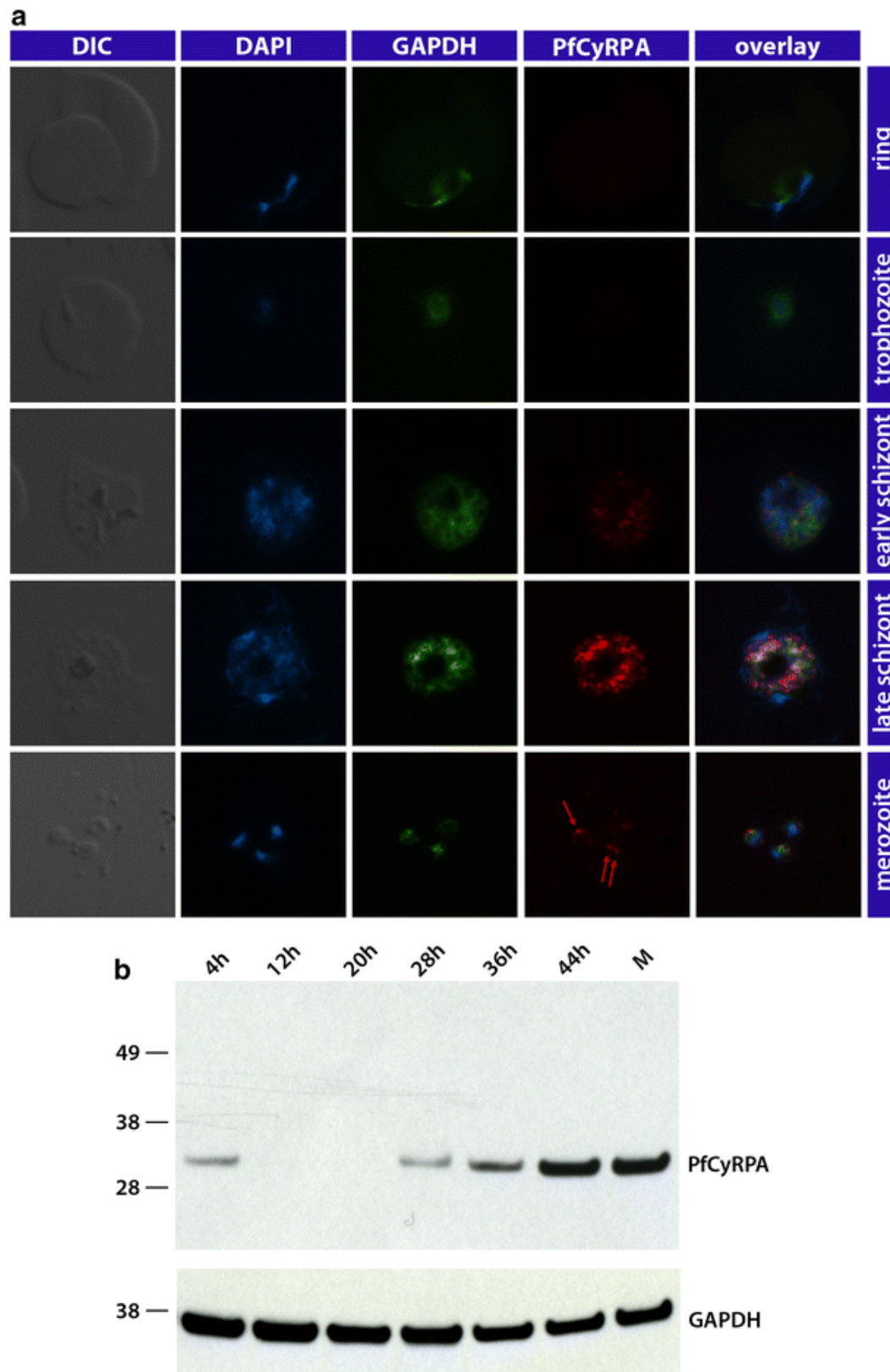


Fig. 4 Stage specific expression of PfCyRPA in late asexual blood stage parasites

(a) Indirect immunofluorescence staining of synchronized asexual blood stage parasites showed stage specific expression of PfCyRPA in schizont stages and free merozoites. Methanol/acetone fixed *P. falciparum* 3D7 parasites were probed with the anti-GAPDH mAb (green) and the anti-PfCyRPA mAb SB3.3 (red) as representative example. Nuclei were stained with DAPI (blue). Exposure times were identical for all pictures of the same channel. **(b)** Western blot analysis with lysates of tightly synchronized *P. falciparum* 3D7 blood-stage parasites with anti-PfCyRPA mAb SB1.6 (upper panel). The blot was probed for equal loading with an anti-GAPDH 1.4a mAb (lower panel). 4, 12, 20, 28, 36, 44: hours post-invasion; M: free merozoites.

Vaccine elicited anti-PfCyRPA mAbs inhibit parasite growth in vitro

For the analysis of the growth inhibitory activity of mAbs generated against the purified recombinant PfCyRPA, parasites were cultured for two cycles of merozoite invasion in the presence of anti-PfCyRPA mAbs at concentrations of 500, 250, and 125 µg/ml. Anti-PfCyRPA mAbs with parasite growth inhibitory activity higher than 40% at the concentration of 500 µg/ml were classified as inhibitory and those with an inhibitory effect ranging between 20 and 40%, were classified as partially inhibitory. Among the four inhibitory mAbs (SB1.6, SB2.1, SB2.3, and SB3.3), SB1.6 showed the highest activity by reducing parasite growth by $64 \pm 3.2\%$ when tested at a concentration of 500 µg/ml (Fig. 5, Table 1). Another four anti-PfCyRPA mAbs inhibited parasite growth partially, whereas three mAbs showed no inhibitory effect (Fig. 5, Table 1). All tested mAbs were produced and purified in the same way and results were reproducible in independent experiments and with independent mAb production batches (see Additional file 4).

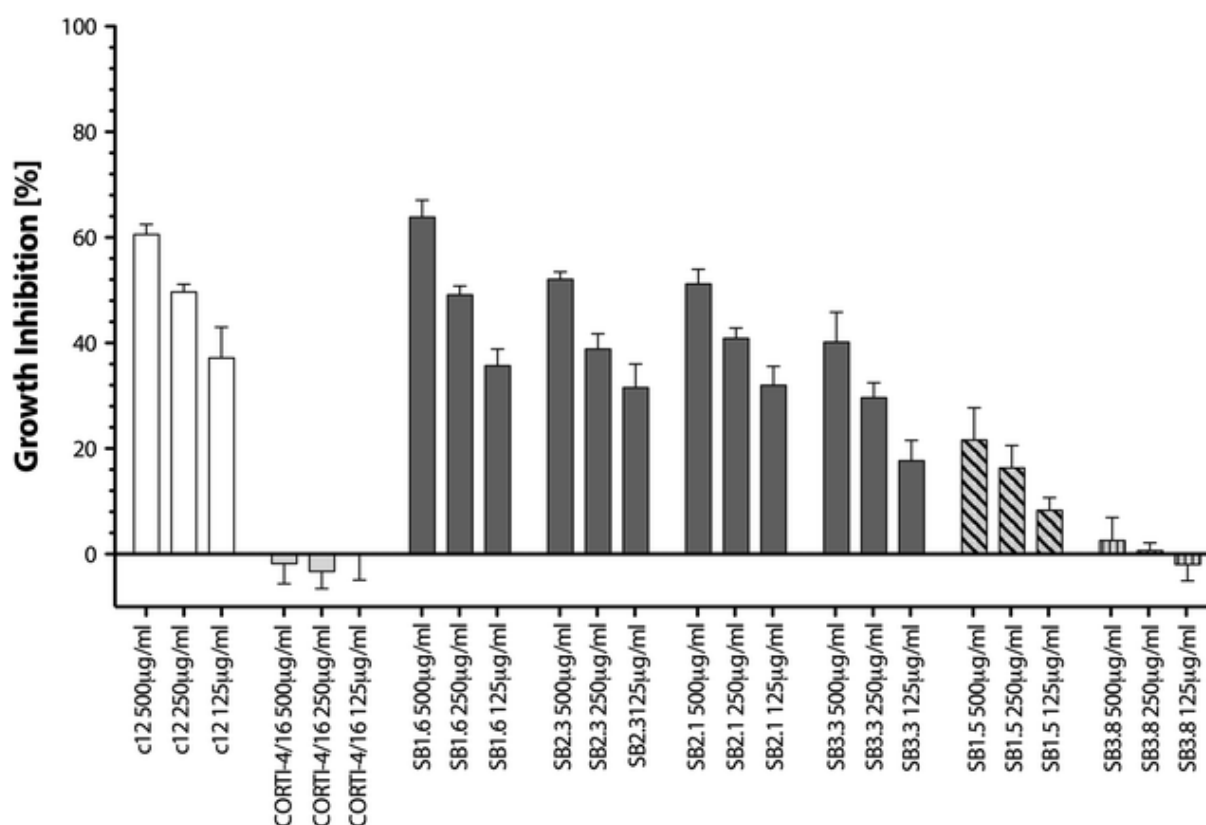


Fig 5. Vaccine elicited anti-PfCyRPA mAbs inhibit parasite growth in vitro. Synchronized *P. falciparum* 3D7 parasites were cultivated for 96 h in the presence of anti-PfCyRPA mAbs. The percentage of growth inhibition was calculated against the parasitaemia of PBS control wells. Each bar represents the mean of a triplicate experiment, and error bars indicate the SD. Anti-PfCyRPA mAbs SB1.6, SB2.3, SB2.1 and SB3.3 are growth inhibitory mAbs, mAb SB1.5 is shown as an example for a partially inhibitory mAb, and mAb SB3.8 as an example for a non-inhibitory mAb. The anti-cortisol mAb CORTI-4/16 was used as negative control and the anti-PfCyRPA mAb c12, which was produced after immunization with mammalian cells expressing recombinant PfCyRPA on their cell surface, as positive control [32].

Vaccine elicited anti-PfCyRPA mAbs inhibit parasite growth in vivo

The in vivo parasite inhibitory activity of the generated anti-PfCyRPA mAbs was evaluated in the *P. falciparum* SCID murine model [52] that employs non-myelodepleted NOD-scid *IL2R γ ^{null}* mice engrafted with human erythrocytes. Groups of three mice received 2.5 or 0.5 mg of PfCyRPA-specific mAbs, either mAb SB1.6 generated here, or the previously described [32] invasion-inhibitory mAb c12, by i.v. injection. The control group received the same volume of PBS. Mice were infected with parasitized erythrocytes one day after the antibody transfer and parasitaemia of all mice was monitored for six days (Fig. 6). In the control group, parasitaemia reached $22.9 \pm 1.7\%$ on day nine. Parasitaemia in mice having received 2.5 mg anti-PfCyRPA mAbs SB1.6 or c12 increased only marginally, reaching $2.2 \pm 1.4\%$ and $1.5 \pm 0.6\%$ on day nine after mAb injection, respectively. At the lower dose of 0.5 mg anti-PfCyRPA mAbs SB1.6 or c12 inhibited parasite growth to $10\% \pm 1.6\%$ and $12.8\% \pm 5.8\%$ parasitaemia, respectively (Fig. 6). Titration of administered mAbs in the serum of the passively immunized mice by ELISA showed that antibodies, although at reduced level, persisted over the entire study period. One day after mAb injection (2.5 mg dose), when mice were infected, PfCyRPA-specific mAb concentrations were estimated to be $295 \pm 0.3\%$ and $389 \pm 0.1\%$ $\mu\text{g/ml}$ of serum, for SB1.6 and c12, respectively. Eight days after mAb injection, at the end of the experiment, antibody concentrations had dropped down to $74 \pm 0.1\%$ and $83 \pm 0.2\%$ $\mu\text{g/ml}$, for SB1.6 and c12 respectively (see Additional file 5).

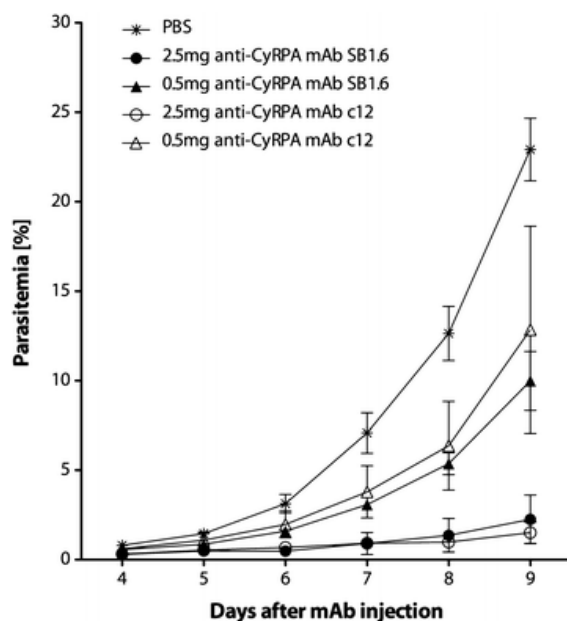


Fig. 6 Vaccine elicited anti-PfCyRPA mAbs inhibit parasite growth in vivo. NOD-scid *IL2R γ ^{null}* mice received purified anti-PfCyRPA mAbs by i.v. injection. Mice were then infected with *P. falciparum* 3D7 and parasitaemia was monitored over six days. Values are the mean parasitaemia in human erythrocytes in peripheral blood of three mice per group. Error bars indicate the SD. PBS was used as negative control, the anti-PfCyRPA mAb c12 as positive control [32].

Fine specificities of anti-CyRPA mAbs

The fine specificities of the generated anti-PfCyRPA mAbs were analysed by Ab-Ab competition ELISA on recombinant PfCyRPA. The *in vitro* growth-inhibitory anti-PfCyRPA mAbs SB1.6, SB2.1, SB2.3, and SB3.3 competed against each other for their antigen binding site (Table 2 A). These four mAbs did neither compete with the partially inhibitory mAbs SB2.5 and SB3.7 nor with the previously described parasite inhibitory anti-PfCyRPA mAb c12. Additionally, the reactivity of anti-PfCyRPA mAbs with overlapping protein fragments of PfCyRPA [32] was tested by Western blotting analysis (Figs. 7, 8b). With the exception of SB2.5, all tested anti-PfCyRPA mAbs reacted with fragment 26-251. All four inhibitory anti-PfCyRPA mAbs SB1.6, SB2.1, SB2.3, and SB3.3 recognized the same fragments, i. e. bound to fragment 74-251, but not to the truncated sub-fragments 26-142, 74-181, and 127-251, indicating that they recognize a conformational epitope present in fragment 74-251. Furthermore, the partially inhibitory mAbs SB3.7 and the control mAb c12 showed the same reactivity pattern. Based on the complementary results of both epitope classification assays we assigned the anti-PfCyRPA mAbs to four distinct epitope groups (Fig. 8b, c).

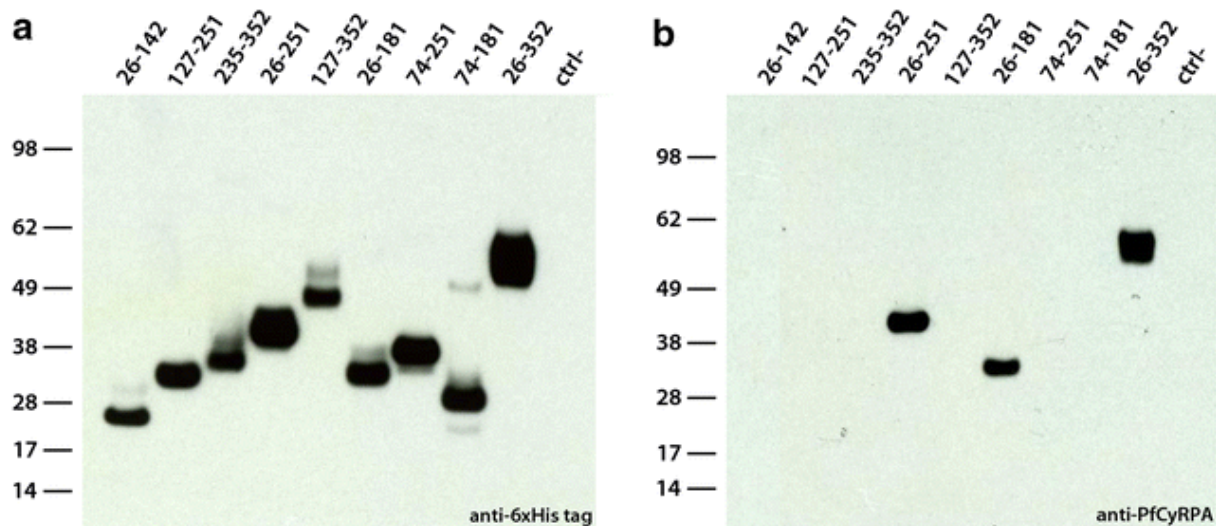
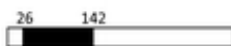










Fig. 7 Reactivity pattern of anti-PfCyRPA mAbs with recombinant PfCyRPA fragments. Anti-PfCyRPA mAbs were tested by Western blot analysis on lysates of HEK cells expressing recombinant PfCyRPA fragments. A lysate HEK cells transfected with empty plasmids served as negative control. Both samples were analysed under reducing conditions. **(a)** Reactivity pattern of anti-6xHis mAb HIS-6/9 as positive control for expression. **(b)** Reactivity pattern of anti-PfCyRPA mAb SB 3.7 as a representative example.

a Ab-Ab Competition ELISA								
Competing anti-PfCyRPA mAb	Detecting anti-PfCyRPA mAb							
	SB2.5	SB3.7	SB1.6	SB2.1	SB2.3	SB3.3	SB3.9	c12
SB2.5	x	-	-	-	-	-	x	-
SB3.7	-	x	-	-	-	-	-	x
SB1.6	-	-	x	x	x	x	-	-
SB2.1	-	-	x	x	x	x	-	-
SB2.3	-	-	x	x	x	x	-	-
SB3.3	-	-	x	x	x	x	-	-
SB3.9	x	-	-	-	-	-	x	-
Q8IF12	-	x	-	-	-	-	-	x

b Reactivity of anti-PfCyRPA mAbs with PfCyRPA fragments								
PfCyRPA fragment	Anti-PfCyRPA mAb							
	SB2.5	SB3.7	SB1.6	SB2.1	SB2.3	SB3.3	SB3.9	c12
	-	-	-	-	-	-	-	-
	-	-	-	-	-	-	-	-
	-	-	-	-	-	-	-	-
	-	-	-	-	-	-	-	-
	-	-	-	-	-	-	x	-
	-	-	x	x	x	x	x	-
	-	x	-	-	-	-	x	x
	-	x	x	x	x	x	x	x
	x	x	x	x	x	x	x	x

c Epitope group	A	B	F	F	F	F	E	B
d Parasite growth inhibition	part.	part.	yes	yes	yes	yes	no	yes

Fig. 8 Epitope specificities of anti-PfCyRPA mAbs. **(a)** Anti-PfCyRPA mAbs were tested in an Ab–Ab competition ELISA. *x* Ab competition (signal reduction higher than 30 %; measured values: min. 34 %, max. 91 % reduction), – no Ab competition (measured values: min. –10 %, max. 21 % reduction). **(b)** Reactivity of anti-PfCyRPA mAbs with recombinant PfCyRPA fragments were investigated by western blotting analyses performed on lysates of HEK cells expressing recombinant PfCyRPA fragments. *x* staining, – no staining (an example of the reactivity pattern is reported in Fig. 7b). **(c)** Anti-PfCyRPA mAbs were assigned to different epitope groups according to the results from the Ab–Ab competition ELISA and the epitope mapping experiment. **(d)** *P. falciparum* in vitro growth inhibition activity of mAbs.

Discussion

On the basis of available genome-wide transcriptomic and proteomic data, Dreyer *et al.* [38] have selected uncharacterized surface proteins, with specific expression in extracellular parasite stages, to evaluate their potential as blood stage vaccine candidate antigens. A panel of candidates was characterized (e.g. abundance, distribution and parasite growth inhibitory potential) using antigen-specific mAbs, which were generated exploiting a cell-based approach that utilizes antigen-expressing living cells for mouse immunization. This strategy has led to the identification of PfCyRPA as promising blood-stage malaria vaccine candidate: generated anti-PfCyRPA mAbs showed parasite *in vitro* and *in vivo* growth-inhibitory activity due to inhibition of merozoite invasion [32]. Since antigen-loaded mammalian cells are not suitable for human immunization, here it was investigated whether growth inhibitory anti-PfCyRPA Abs could be raised by active immunization with adjuvanted purified recombinant PfCyRPA protein. The expression of *Plasmodium* antigens in heterologous hosts as stable recombinant protein can be challenging. Since PfCyRPA is a cysteine-rich protein, disulfide bonds play an important role in its folding. Aiming at the production of a properly folded recombinant protein, a eukaryotic rather than a prokaryotic expression system was used. Since PfCyRPA was successfully expressed in a native conformation on the surface of HEK cells and raised parasites-cross reactive mAbs [32], the same mammalian expression platform was exploited for the production of secreted PfCyRPA. For this purpose, the expression plasmid coding for PfCyRPA was modified to produce the secreted version of the protein by removing the sequence coding for the transmembrane domain artificially used to display the protein on the cell surface. PfCyRPA was expressed and secreted into the cultivation medium in good quality and quantity (ca.18 mg/l), and the glycosylated recombinant protein was easily purified via the hexa-His tag. Since the protein glycosylation status may influence immunogenicity, we also produced a non-glycosylated version of PfCyRPA, but did not find a marked difference between the two proteins with respect to their immunogenicity. To dissect and characterize the properties of the elicited anti-PfCyRPA antibody response, mice immunized with either the glycosylated or the non-glycosylated recombinant protein were employed to generate a panel of eleven IgG mAbs reactive with recombinant PfCyRPA in ELISA. Nine of the generated mAbs were cross-reacting in indirect immunofluorescence analysis with *P. falciparum* asexual blood stage parasites, yielding a dotted staining pattern characteristic for PfCyRPA and ten of them stained a band of the size expected for PfCyRPA in Western blotting analysis with *P. falciparum* schizont stage lysate.

Four mAbs showed strong and another four partial parasite blood stage in vitro growth inhibitory activity. The parasite inhibitory activity of mAb SB1.6 showing the strongest in vitro activity was comparable to that of the previously described anti-PfCyRPA mAb c12 which was produced after immunization with mammalian cells expressing recombinant PfCyRPA on their cell surface [32]. The strongly growth inhibitory mAbs c12 and SB1.6 do not compete for antigen binding (Table 2), confirming that PfCyRPA harbours more than one target epitope for inhibitory antibodies, as already suggested by Dreyer *et al.* [32]. Structural analyses with antigen-antibody complexes are required to gain deeper insight into the targets and mode of action of these antibodies. Since orthologs of PfCyRPA are only present in the human malaria parasite *Plasmodium vivax* and the primate pathogens *Plasmodium knowlesi*, *Plasmodium cynomolgi*, and *Plasmodium reichenowi* [54–56], but are absent in *Plasmodium* species infecting rodents, conventional mouse models with rodent parasites cannot be used to evaluate the in vivo growth inhibitory activity of anti-PfCyRPA mAbs. Therefore, passive immunization experiments were performed exploiting an innovative *P. falciparum* SCID mouse model [32,52].

Non myelo-depleted NOD-*scid* *IL2R γ ^{null}* mice, engrafted with human erythrocytes to allow the growth of *P. falciparum*, received a single dose of anti-PfCyRPA mAbs via the i.v. route and were infected with *P. falciparum* 3D7 parasites on the subsequent day. In mice receiving SB1.6 mAb, a strong, dose-dependent parasite growth inhibitory effect was observed, reducing parasite's growth by about 90% (2.5 mg dose). The concentration of mAb SB1.6 in the circulation of the passively immunized mice which received the higher dose, was estimated to be 300 μ g/ml and 80 μ g/ml one and eight days after injection, respectively. Since SCID mice lack the adaptive immune system and have deficiencies in the innate immune system [57,58], the injected mAbs were the only circulating IgG, and this may enhance their clearance from the circulation. However, the measured serum concentration of PfCyRPA-specific antibody fall in the range of specific Abs that can be induced by appropriate vaccine formulations [8,37]. In this context, it should also be taken into account that immunizations with recombinant PfCyRPA (both antigen-loaded cells and adjuvanted purified proteins) generated anti-PfCyRPA mAbs with different fine specificity [32].

Hence, stronger inhibitory activities may be achieved in the context of active immunizations, where Abs specific for more than one inhibitory epitope are induced, and lower titers of total PfCyRPA-specific Abs may be required to confer substantial protection. As already described [32], anti-PfCyRPA mAbs reduce, but do not completely block, parasite growth by inhibiting a crucial invasion pathway of erythrocytes by merozoites. Invasion of host erythrocytes is a

complex and critical step in the life cycle of malaria parasites, and *P. falciparum* has evolved an abundance of antigenically diverse, and probably functionally redundant, merozoite surface proteins to facilitate parasite escape from host immune detection and ensure invasion via multiple pathways [59,60]. In this respect, marginal sequence polymorphisms and limited natural immunogenicity of PfCyRPA [32] suggest a critical function of PfCyRPA in erythrocytes invasion, which prevents sequence variation and accessibility to the immune system in the natural context. PfCyRPA has been recently identified as the anchor protein that tethers PfrRH5, and its interacting partner PfrRipr, to the surface of merozoites [33]. PfrRH5 has been shown to play a key role in the attachment of merozoites to the erythrocyte surface via the interaction with the host receptor basigin [61,62]. Interestingly, PfCyRPA and PfrRH5 genes are located in close proximity in the genome, have no substantial sequence polymorphisms, have demonstrated poor natural immunogenicity, and elicit potent and strain-transcending growth-inhibitory parasite antibodies [32,34]. Anti-PfCyRPA mAb concentrations required for substantial growth inhibition in GIA were higher than those reported for anti-basigin (1ug/ml) and anti-PfrRH5 (15ug/ml) mAbs, respectively [36]. This may be in part related to different assay formats, but also to other factors, such as accessibility of the antigens and kinetic and thermodynamic features of mAb binding. Reddy *et al.* [33] also reported a synergistic in vitro inhibitory activity for the combination of polyclonal anti-PfCyRPA and anti-PfrRH5 antibodies. Targeting simultaneously PfCyRPA and PfrRH5 seems to hinder parasite invasion more effectively than when blocking only one component of the multiprotein invasion complex. Taken together, these findings suggest that additional investigation are needed for an in depth characterization of the invasion complex, and make both PfCyRPA and PfrRH5 appealing candidates for the development of new anti-malarial vaccine strategies.

Conclusions

A vaccine formulation composed of adjuvanted recombinantly expressed PfCyRPA has been shown to elicit in mice high titers of antibodies that inhibit both in vitro and in vivo *P. falciparum* asexual blood stage parasite growth. These findings qualify PfCyRPA, a highly conserved and poorly immunogenic merozoite protein, as highly suitable candidate antigen for inclusion into a strain-transcending, multivalent malaria subunit vaccine.

Authors' contributions

PF was responsible for experimental design, performed the experiments and data analysis described in this study and drafted the manuscript. SB participated in the study design, performed the experiments and data analysis described in this study and helped to draft the manuscript. AMD contributed to the conception and design of the study. MT contributed to the experimental design and carried out the passive immunoprotection experiments in mice; GR contributed to the immunoprotection experiments in mice. RT contributed to mutant generation, participated in the study design and assisted in data analysis. HM contributed to the conception of the study, participated in its design and assisted in data interpretation. GP conceived the study, participated in the study design, coordinated the collaborations that made this study possible and revised the manuscript. All authors read and approved the final manuscript.

Acknowledgements

We thank Georg Schmid and Marcello Foggetta for cell transfections, and Bernard Gsell for the support in recombinant PfCyRPA purification and analysis.

Disclosures

The authors declare that they have no competing interests.

Funding

This study was supported by funds of the Uniscientia Stiftung.

References

1. WHO | World Malaria Report 2015 [Internet]. WHO. [cited 2016 Jan 15]. Available from: <http://www.who.int/malaria/publications/world-malaria-report-2015/report/en/>
2. Crompton PD, Pierce SK, Miller LH. Advances and challenges in malaria vaccine development. *J Clin Invest* [Internet]. 2010 Dec 1 [cited 2015 Feb 22];120(12):4168–78. Available from: <http://www.jci.org/articles/view/44423>
3. Marsh K, Kinyanjui S. Immune effector mechanisms in malaria. *Parasite Immunol*. 2006 Feb;28(1–2):51–60.
4. Doolan DL, Hoffman SL. Multi-gene vaccination against malaria: A multistage, multi-immune response approach. *Parasitol Today Pers Ed*. 1997 May;13(5):171–8.
5. Doolan DL, Dobaño C, Baird JK. Acquired immunity to malaria. *Clin Microbiol Rev*. 2009 Jan;22(1):13–36, Table of Contents.
6. Cohen S, McGregor IA, Carrington S. Gamma-globulin and acquired immunity to human malaria. *Nature* [Internet]. 1961 Nov 25 [cited 2015 Feb 22];192(4804):733–7. Available from: <http://www.nature.com/nature/journal/v192/n4804/abs/192733a0.html>
7. WHO | Tables of malaria vaccine projects globally [Internet]. WHO. [cited 2015 Jul 12]. Available from: http://www.who.int/immunization/research/development/Rainbow_tables/en/
8. RTS,S Clinical Trials Partnership. Efficacy and safety of RTS,S/AS01 malaria vaccine with or without a booster dose in infants and children in Africa: final results of a phase 3, individually randomised, controlled trial. *Lancet Lond Engl*. 2015 Jul 4;386(9988):31–45.
9. Moorthy VS, Good MF, Hill AVS. Malaria vaccine developments. *Lancet Lond Engl*. 2004 Jan 10;363(9403):150–6.
10. Sagara I, Dicko A, Ellis RD, Fay MP, Diawara SI, Assadou MH, et al. A randomized controlled phase 2 trial of the blood stage AMA1-C1/Alhydrogel malaria vaccine in children in Mali. *Vaccine*. 2009 May 18;27(23):3090–8.
11. Polhemus ME, Magill AJ, Cummings JF, Kester KE, Ockenhouse CF, Lanar DE, et al. Phase I dose escalation safety and immunogenicity trial of Plasmodium falciparum apical membrane protein (AMA-1) FMP2.1, adjuvanted with AS02A, in malaria-naïve adults at the Walter Reed Army Institute of Research. *Vaccine* [Internet]. 2007 May 22 [cited 2015 Oct 4];25(21):4203–12. Available from: <http://www.sciencedirect.com/science/article/pii/S0264410X07002976>
12. Laurens MB, Thera MA, Coulibaly D, Ouattara A, Kone AK, Guindo AB, et al. Extended Safety, Immunogenicity and Efficacy of a Blood-Stage Malaria Vaccine in Malian Children: 24-Month Follow-Up of a Randomized, Double-Blinded Phase 2 Trial. *PLoS ONE* [Internet]. 2013 Nov 18 [cited 2015 Oct 4];8(11):e79323. Available from: <http://dx.doi.org/10.1371/journal.pone.0079323>
13. El Sahly HM, Patel SM, Atmar RL, Lanford TA, Dube T, Thompson D, et al. Safety and immunogenicity of a recombinant nonglycosylated erythrocyte binding antigen 175 Region II malaria vaccine in healthy adults living in an area where malaria is not endemic. *Clin Vaccine Immunol CVI*. 2010 Oct;17(10):1552–9.
14. Esen M, Kremsner PG, Schleucher R, Gässler M, Imoukhuede EB, Imbault N, et al. Safety and immunogenicity of GMZ2 - a MSP3-GLURP fusion protein malaria vaccine candidate. *Vaccine*. 2009 Nov 16;27(49):6862–8.
15. Hermsen CC, Verhage DF, Telgt DSC, Teelen K, Bousema JT, Roestenberg M, et al. Glutamate-rich protein (GLURP) induces antibodies that inhibit in vitro growth of Plasmodium falciparum in a phase 1 malaria vaccine trial. *Vaccine*. 2007 Apr 12;25(15):2930–40.

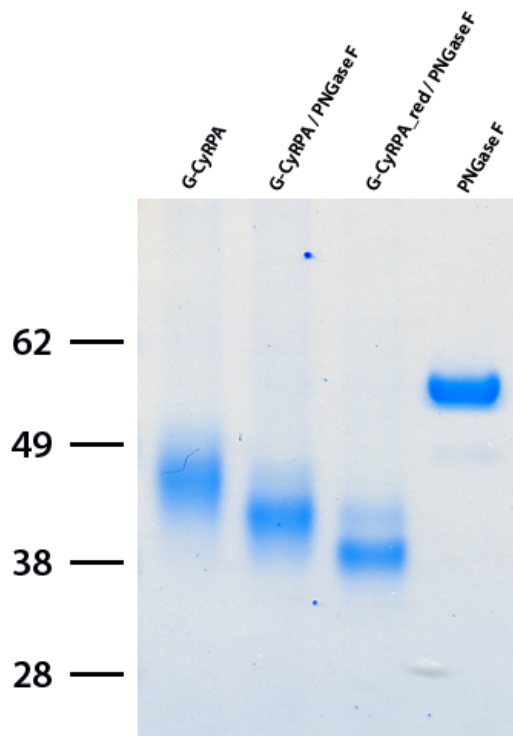
16. Ogutu BR, Apollo OJ, McKinney D, Okoth W, Siangla J, Dubovsky F, et al. Blood stage malaria vaccine eliciting high antigen-specific antibody concentrations confers no protection to young children in Western Kenya. *PloS One*. 2009;4(3):e4708.
17. Genton B, Betuela I, Felger I, Al-Yaman F, Anders RF, Saul A, et al. A recombinant blood-stage malaria vaccine reduces *Plasmodium falciparum* density and exerts selective pressure on parasite populations in a phase 1-2b trial in Papua New Guinea. *J Infect Dis*. 2002 Mar 15;185(6):820–7.
18. McCarthy JS, Marjason J, Elliott S, Fahey P, Bang G, Malkin E, et al. A Phase 1 Trial of MSP2-C1, a Blood-Stage Malaria Vaccine Containing 2 Isoforms of MSP2 Formulated with Montanide® ISA 720. *PLoS ONE* [Internet]. 2011 Sep 19 [cited 2015 Oct 4];6(9):e24413. Available from: <http://dx.doi.org/10.1371/journal.pone.0024413>
19. Audran R, Cachat M, Lurati F, Soe S, Leroy O, Corradin G, et al. Phase I malaria vaccine trial with a long synthetic peptide derived from the merozoite surface protein 3 antigen. *Infect Immun*. 2005 Dec;73(12):8017–26.
20. Jepsen MPG, Jogdand PS, Singh SK, Esen M, Christiansen M, Issifou S, et al. The Malaria Vaccine Candidate GMZ2 Elicits Functional Antibodies in Individuals From Malaria Endemic and Non-Endemic Areas. *J Infect Dis* [Internet]. 2013 Aug 1 [cited 2015 Jul 13];208(3):479–88. Available from: <http://jid.oxfordjournals.org/lookup/doi/10.1093/infdis/jit185>
21. Horii T, Shirai H, Jie L, Ishii KJ, Palacpac NQ, Tougan T, et al. Evidences of protection against blood-stage infection of *Plasmodium falciparum* by the novel protein vaccine SE36. *Parasitol Int*. 2010 Sep;59(3):380–6.
22. Palacpac NMQ, Ntege E, Yeka A, Balikagala B, Suzuki N, Shirai H, et al. Phase 1b Randomized Trial and Follow-Up Study in Uganda of the Blood-Stage Malaria Vaccine Candidate BK-SE36. Ellis RD, editor. *PLoS ONE* [Internet]. 2013 May 28 [cited 2015 Jul 13];8(5):e64073. Available from: <http://dx.plos.org/10.1371/journal.pone.0064073>
23. Spring MD, Cummings JF, Ockenhouse CF, Dutta S, Reidler R, Angov E, et al. Phase 1/2a study of the malaria vaccine candidate apical membrane antigen-1 (AMA-1) administered in adjuvant system AS01B or AS02A. *PloS One*. 2009;4(4):e5254.
24. Takala SL, Coulibaly D, Thera MA, Batchelor AH, Cummings MP, Escalante AA, et al. Extreme Polymorphism in a Vaccine Antigen and Risk of Clinical Malaria: Implications for Vaccine Development. *Sci Transl Med* [Internet]. 2009 Oct 14 [cited 2015 Jul 13];1(2):2ra5. Available from: <http://www.ncbi.nlm.nih.gov/pmc/articles/PMC2822345/>
25. Takala SL, Plowe CV. Genetic diversity and malaria vaccine design, testing and efficacy: preventing and overcoming “vaccine resistant malaria.” *Parasite Immunol* [Internet]. 2009 Sep 1 [cited 2015 Jul 13];31(9):560–73. Available from: <http://onlinelibrary.wiley.com/doi/10.1111/j.1365-3024.2009.01138.x/abstract>
26. Riley EM, Stewart VA. Immune mechanisms in malaria: new insights in vaccine development. *Nat Med* [Internet]. 2013 Feb [cited 2015 Jul 13];19(2):168–78. Available from: <http://www.nature.com/nm/journal/v19/n2/full/nm.3083.html>
27. Dzikowski R, Deitsch KW. Genetics of antigenic variation in *Plasmodium falciparum*. *Curr Genet*. 2009 Apr;55(2):103–10.
28. Gardner MJ, Hall N, Fung E, White O, Berriman M, Hyman RW, et al. Genome sequence of the human malaria parasite *Plasmodium falciparum*. *Nature* [Internet]. 2002 [cited 2015 Feb 22];419(6906):498–511. Available from: <http://www.nature.com/articles/nature01097>
29. Rappuoli R. Reverse vaccinology. *Curr Opin Microbiol* [Internet]. 2000 [cited 2015 Feb 22];3(5):445–450. Available from: <http://www.sciencedirect.com/science/article/pii/S1369527400001193>
30. Donati C, Rappuoli R. Reverse vaccinology in the 21st century: improvements over the original design: Reverse vaccinology in the 21st century. *Ann N Y Acad Sci* [Internet].

- 2013 May [cited 2015 Feb 22];1285(1):115–32. Available from:
<http://doi.wiley.com/10.1111/nyas.12046>
31. Proietti C, Doolan DL. The case for a rational genome-based vaccine against malaria. *Front Microbiol.* 2014;5:741.
 32. Dreyer AM, Matile H, Papastogiannidis P, Kamber J, Favuzza P, Voss TS, et al. Passive immunoprotection of *Plasmodium falciparum*-infected mice designates the CyRPA as candidate malaria vaccine antigen. *J Immunol Baltim Md 1950.* 2012 Jun 15;188(12):6225–37.
 33. Reddy KS, Amlabu E, Pandey AK, Mitra P, Chauhan VS, Gaur D. Multiprotein complex between the GPI-anchored CyRPA with PfrRH5 and PfrIpr is crucial for *Plasmodium falciparum* erythrocyte invasion. *Proc Natl Acad Sci [Internet].* 2015 Jan 27 [cited 2015 Feb 22];112(4):1179–84. Available from:
<http://www.pnas.org/lookup/doi/10.1073/pnas.1415466112>
 34. Douglas AD, Williams AR, Illingworth JJ, Kamuyu G, Biswas S, Goodman AL, et al. The blood-stage malaria antigen PfrRH5 is susceptible to vaccine-inducible cross-strain neutralizing antibody. *Nat Commun [Internet].* 2011 Dec 20 [cited 2015 Feb 22];2:601. Available from: <http://www.nature.com/doi/10.1038/ncomms1615>
 35. Bustamante LY, Bartholdson SJ, Crosnier C, Campos MG, Wanaguru M, Nguon C, et al. A full-length recombinant *Plasmodium falciparum* PfrRH5 protein induces inhibitory antibodies that are effective across common PfrRH5 genetic variants. *Vaccine [Internet].* 2013 Jan [cited 2015 Feb 21];31(2):373–9. Available from:
<http://linkinghub.elsevier.com/retrieve/pii/S0264410X12015812>
 36. Douglas AD, Williams AR, Knuepfer E, Illingworth JJ, Furze JM, Crosnier C, et al. Neutralization of *Plasmodium falciparum* Merozoites by Antibodies against PfrRH5. *J Immunol [Internet].* 2014 Jan 1 [cited 2015 Feb 22];192(1):245–58. Available from:
<http://www.jimmunol.org/cgi/doi/10.4049/jimmunol.1302045>
 37. Douglas AD, Baldeviano GC, Lucas CM, Lugo-Roman LA, Crosnier C, Bartholdson SJ, et al. A PfrRH5-Based Vaccine Is Efficacious against Heterologous Strain Blood-Stage *Plasmodium falciparum* Infection in Aotus Monkeys. *Cell Host Microbe.* 2015 Jan 14;17(1):130–9.
 38. Dreyer AM, Beauchamp J, Matile H, Pluschke G. An efficient system to generate monoclonal antibodies against membrane-associated proteins by immunisation with antigen-expressing mammalian cells. *BMC Biotechnol.* 2010;10:87.
 39. Lee J, Lee H-J, Shin M-K, Ryu W-S. Versatile PCR-mediated insertion or deletion mutagenesis. *BioTechniques.* 2004 Mar;36(3):398–400.
 40. Shevchuk NA. Construction of long DNA molecules using long PCR-based fusion of several fragments simultaneously. *Nucleic Acids Res [Internet].* 2004 Jan 21 [cited 2015 Feb 21];32(2):19e–19. Available from:
<http://nar.oxfordjournals.org/lookup/doi/10.1093/nar/gnh014>
 41. Barik S. [21] Site-directed mutagenesis by PCR: Substitution, insertion, deletion, and gene fusion. In: Sarkar G, editor. *Methods in Neurosciences [Internet].* Academic Press; 1995 [cited 2016 Jan 20]. p. 309–23. (PCR in Neuroscience; vol. 26). Available from:
<http://www.sciencedirect.com/science/article/pii/S1043947106800996>
 42. Wurch T, Lestienne F, Pauwels PJ. A modified overlap extension PCR method to create chimeric genes in the absence of restriction enzymes. *Biotechnol Tech [Internet].* 1998 [cited 2015 Feb 21];12(9):653–657. Available from:
<http://link.springer.com/article/10.1023/A:1008848517221>
 43. Québatte G, Kitas E, Seelig J. riDOM, a cell penetrating peptide. Interaction with phospholipid bilayers. *Biochim Biophys Acta BBA - Biomembr [Internet].* 2014 Mar [cited 2015 Oct 5];1838(3):968–77. Available from:
<http://www.sciencedirect.com/science/article/pii/S0005273613003787>

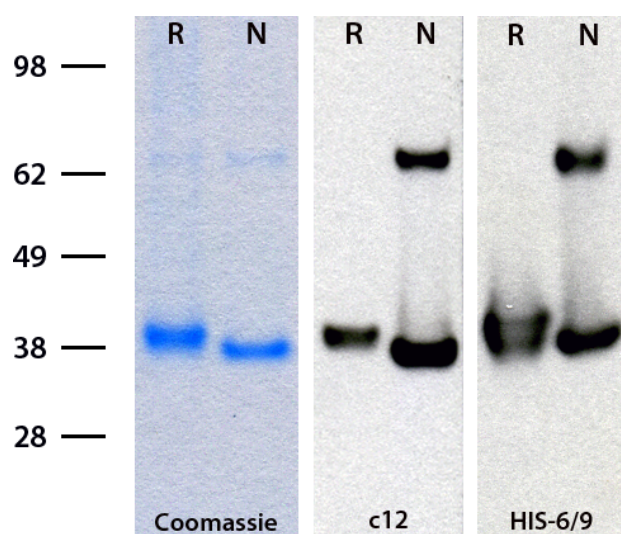
44. Davis HL, Weeratna R, Waldschmidt TJ, Tygrett L, Schorr J, Krieg AM, et al. CpG DNA is a potent enhancer of specific immunity in mice immunized with recombinant hepatitis B surface antigen. *J Immunol Baltim Md 1950*. 1998 Jan 15;160(2):870–6.
45. Lefkowitz I, Pernis B. *Immunological Methods*. Academic Press; 2014. 367 p.
46. Dorn A, Stoffel R, Matile H, Bubendorf A, Ridley RG. Malarial haemozoin/beta-haematin supports haem polymerization in the absence of protein. *Nature*. 1995 Mar 16;374(6519):269–71.
47. Lambros C, Vanderberg JP. Synchronization of *Plasmodium falciparum* erythrocytic stages in culture. *J Parasitol*. 1979 Jun;65(3):418–20.
48. Boyle MJ, Wilson DW, Richards JS, Riglar DT, Tetteh KKA, Conway DJ, et al. Isolation of viable *Plasmodium falciparum* merozoites to define erythrocyte invasion events and advance vaccine and drug development. *Proc Natl Acad Sci [Internet]*. 2010 Aug 10 [cited 2015 Feb 22];107(32):14378–83. Available from: <http://www.pnas.org/cgi/doi/10.1073/pnas.1009198107>
49. Rivadeneira EM, Wasserman M, Espinal CT. Separation and concentration of schizonts of *Plasmodium falciparum* by Percoll gradients. *J Protozool*. 1983 May;30(2):367–70.
50. Daubenberger CA, Tisdale EJ, Curcic M, Diaz D, Silvie O, Mazier D, et al. The N⁷-terminal domain of glyceraldehyde-3-phosphate dehydrogenase of the apicomplexan *Plasmodium falciparum* mediates GTPase Rab2-dependent recruitment to membranes. *Biol Chem*. 2003 Aug;384(8):1227–37.
51. Mueller MS, Renard A, Boato F, Vogel D, Naegeli M, Zurbriggen R, et al. Induction of parasite growth-inhibitory antibodies by a virosomal formulation of a peptidomimetic of loop I from domain III of *Plasmodium falciparum* apical membrane antigen 1. *Infect Immun*. 2003 Aug;71(8):4749–58.
52. Jiménez-Díaz MB, Mulet T, Viera S, Gómez V, Garuti H, Ibáñez J, et al. Improved murine model of malaria using *Plasmodium falciparum* competent strains and non-myelodepleted NOD-scid IL2R γ manu mice engrafted with human erythrocytes. *Antimicrob Agents Chemother*. 2009 Oct;53(10):4533–6.
53. Gupta R., Jung E., Brunak S. Prediction of N-glycosylation sites in human proteins. 2004.
54. Müller M, Schlagenhauf P. *Plasmodium knowlesi* in travellers, update 2014. *Int J Infect Dis [Internet]*. 2014;22:55–64. Available from: <http://dx.doi.org/10.1016/j.ijid.2013.12.016> http://ac.els-cdn.com/S1201971214000307/1-s2.0-S1201971214000307-main.pdf?_tid=3de7eb00-8ece-11e5-a284-00000aacb361&acdnat=1447945395_f755fd747177070a0b7e83cba023bddc
55. Ta TH, Hisam S, Lanza M, Jiram AI, Ismail N, Rubio JM. First case of a naturally acquired human infection with *Plasmodium cynomolgi*. *Malar J*. 2014;13:68.
56. Otto TD, Rayner JC, Böhme U, Pain A, Spottiswoode N, Sanders M, et al. Genome sequencing of chimpanzee malaria parasites reveals possible pathways of adaptation to human hosts. *Nat Commun*. 2014;5:4754.
57. Cao X, Shores EW, Hu-Li J, Anver MR, Kelsall BL, Russell SM, et al. Defective lymphoid development in mice lacking expression of the common cytokine receptor gamma chain. *Immunity*. 1995 Mar;2(3):223–38.
58. Sugamura K, Asao H, Kondo M, Tanaka N, Ishii N, Ohbo K, et al. The interleukin-2 receptor gamma chain: its role in the multiple cytokine receptor complexes and T cell development in XSCID. *Annu Rev Immunol*. 1996;14:179–205.
59. Cowman AF, Crabb BS. Invasion of red blood cells by malaria parasites. *Cell [Internet]*. 2006 [cited 2013 Jan 21];124(4):755–766. Available from: <http://www.sciencedirect.com/science/article/pii/S0092867406001814>

60. Cowman AF, Berry D, Baum J. The cellular and molecular basis for malaria parasite invasion of the human red blood cell. *J Cell Biol* [Internet]. 2012 Sep 17 [cited 2015 Aug 10];198(6):961–71. Available from: <http://jcb.rupress.org/content/198/6/961>
61. Baum J, Chen L, Healer J, Lopaticki S, Boyle M, Triglia T, et al. Reticulocyte-binding protein homologue 5 – An essential adhesin involved in invasion of human erythrocytes by *Plasmodium falciparum*. *Int J Parasitol* [Internet]. 2009 Feb [cited 2015 Feb 22];39(3):371–80. Available from: <http://linkinghub.elsevier.com/retrieve/pii/S0020751908003883>
62. Crosnier C, Bustamante LY, Bartholdson SJ, Bei AK, Theron M, Uchikawa M, et al. Basigin is a receptor essential for erythrocyte invasion by *Plasmodium falciparum*. *Nature* [Internet]. 2011 [cited 2013 Jan 21]; Available from: http://www.nature.com/nature/journal/vaop/ncurrent/full/nature10606.html?WT.mc_id=FBK_NPG
63. Moreno R, Pörtl-Frank F, Stüber D, Matile H, Mutz M, Weiss NA, et al. Rhoptry-associated protein 1-binding monoclonal antibody raised against a heterologous peptide sequence inhibits *Plasmodium falciparum* growth in vitro. *Infect Immun*. 2001 Apr;69(4):2558–68.
64. Marshall VM, Tieqiao W, Coppel RL. Close linkage of three merozoite surface protein genes on chromosome 2 of *Plasmodium falciparum*. *Mol Biochem Parasitol*. 1998 Jul 1;94(1):13–25.

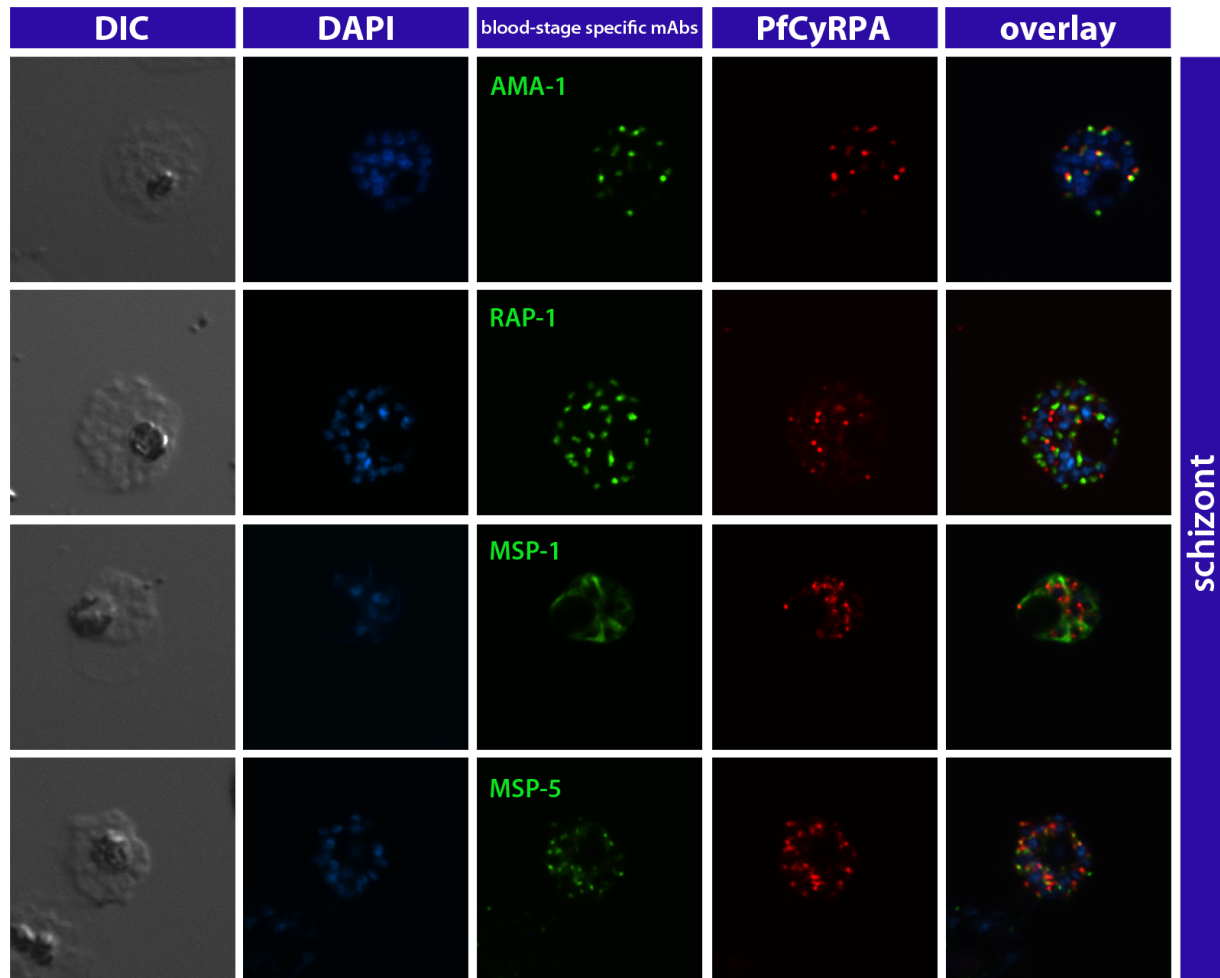
Additional files



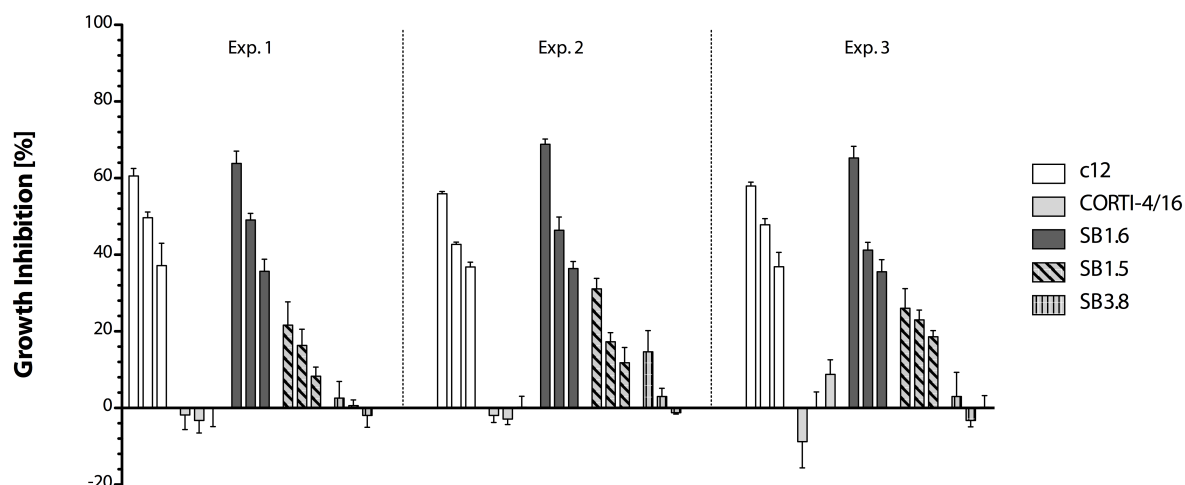
Additional file 1. PNGase F treatment of recombinant G-CyRPA. 1 mg/ml of native (second lane) or reduced with 50mM_r DTT (third lane) G-CyRPA was subjected for 16 h at room temperature to PNGase F at a final concentration of 0.05 mg/ml, and analysed by reducing SDS-PAGE (1 µg protein per lane). Lane 1: untreated G-CyRPA; lane 4: PNGase F.



Additional file 2. Recognition of N-CyRPA by PfCyRPA- and 6xHis-specific mAbs. Reducing (R) and non-reducing (N) SDS-PAGE of non-glycosylated PfCyRPA (N-CyRPA) detected by Coomassie-staining (blue) and Western blotting with anti-PfCyRPA mAb c12 and anti-6xHis mAb HIS-6/9 (black). Analyses under non-reducing conditions revealed both a monomeric and a dimeric form of PfCyRPA.



Additional file 3. Localization of PfCyRPA in late asexual blood stage parasites. Indirect immunofluorescence staining of *P. falciparum* 3D7 schizont stages. Methanol/acetone fixed parasites were co-immunostained with mAbs against PfCyRPA (red) and AMA-1 (marker for micronemes), RAP-1 (marker for rhoptry bulbs), MSP-1 or MSP-5 (marker for merozoite's surface) (green). Parasites were probed with the following primary or secondary antibodies: biotin-labeled anti-PfCyRPA mAb SB3.3b, Alexa 488-labeled mouse anti-AMA-1 DV5a mAb [51], Alexa 488-labeled mouse anti-RAP-1 5-2 mAb [63], anti-MSP-1 MC7.2 mAb (G. Pluschke, unpublished), anti-MSP-5 rabbit serum (MRA-320; Malaria Research and Reference Reagent Resource Center) [64], Alexa 568-labeled streptavidin (Invitrogen), Alexa 488-labeled goat anti-mouse IgG (H+L) Abs, and Alexa 488-labeled chicken anti-rabbit IgG (H+L) Abs (Invitrogen). Nuclei were stained with DAPI (blue). Exposure times were identical for all pictures of the same channel.



Additional file 4. In vitro parasite growth inhibitory activity of vaccine elicited anti-PfCyRPA mAbs was reproducible in independent experiments. Different batches of anti-PfCyRPA mAbs were produced and purified in the same way, and tested in independent in vitro growth inhibition assays. Reported are three independent experiments as representative examples of obtained results. Anti-PfCyRPA mAbs SB1.6 is shown as an example for an inhibitory mAb, mAb SB1.5 for a partially inhibitory mAb, and mAb SB3.8 for a non-inhibitory mAb. The anti-cortisol mAb CORTI-4/16 was used as negative control and the anti-PfCyRPA mAb c12 as positive control [32]. Each bar represents the mean of a triplicate experiment, and error bars indicate the SD.

Injected mAb	Injection dose	Day	PfCyRPA-specific IgG ($\mu\text{g/ml}$)	Total IgG ($\mu\text{g/ml}$)
SB1.6	2.5 mg	1	294.6 \pm 0.32	249.9 \pm 0.51
		8	74.2 \pm 0.09	58.1 \pm 0.09
	0.5 mg	1	63.4 \pm 0.07	57.9 \pm 0.07
		8	14.7 \pm 0.08	13.7 \pm 0.16
c12	2.5 mg	1	388.4 \pm 0.06	418.7 \pm 0.08
		8	82.7 \pm 0.16	89.0 \pm 0.13
	0.5 mg	1	55.9 \pm 0.10	65.1 \pm 0.11
		8	13.2 \pm 0.21	16.2 \pm 0.25

Additional file 5. Titration of administered mAbs in the serum of the passively immunized mice. The concentration of administered PfCyRPA-specific mAbs SB1.6 and c12 in the circulation was estimated by indirect ELISA on day one and eight after injection. For the detection of PfCyRPA-specific mAbs and total circulating IgGs, plates were coated with N-CyRPA or goat anti-mouse IgG (γ -chain specific) mAb (M1397, Sigma), respectively. After blocking, plates were incubated with dilutions of individual mouse serum. An HRP-conjugated goat anti-mouse IgG (γ -chain specific) Ab (A3673, Sigma) was used as secondary antibody and TMB as substrate. Standard curves were generated from known dilutions of SB1.6 and c12 mAbs and fit using a 4-PL logistic equation. Concentration of circulating mAbs was calculated by interpolating the absorbance values for the test sera from the standard curves. Reported values are means of three mice per group \pm SD.

Results Part 3

Structure of the malaria vaccine candidate antigen CyRPA and its complex with a parasite invasion inhibitory antibody

eLife 2017;10.7554/eLife.20383

Paola Favuzza^{1,2}, Elena Guffart³, Marco Tamborrini^{1,2}, Bianca Scherer^{1,2}, Anita M. Dreyer^{1,2}, Arne Rufer³, Johannes Erny³, Joerg Hoernschemeyer³, Ralf Thoma³, Georg Schmid³, Bernard Gsell³, Araceli Lamelas^{1,2,#a}, Joerg Benz³, Catherine Joseph³, Hugues Matile³, Gerd Pluschke^{1,2*}, and Markus G. Rudolph^{3*}

¹ Medical Parasitology and Infection Biology Department, Swiss Tropical and Public Health Institute, 4002 Basel, Switzerland

² University of Basel, 4001 Basel, Switzerland

³ Roche Pharmaceutical Research & Early Development, Small Molecule Research, Roche Innovation Center Basel, F. Hoffmann-La Roche Ltd, 4070 Basel, Switzerland

^{#a} Current Address: Red de Estudios Moleculares Avanzados, Instituto de Ecología A.C., Xalapa, 91070, México

* Corresponding authors

Correspondence regarding Immunology and Infectious Disease should be addressed to G.P.

(gerd.pluschke@unibas.ch) and that regarding Structural Biology to M.G.R. (markus.rudolph@roche.com)

Data deposition: The coordinates and structure factors have been deposited in the Protein Data Bank (accession codes 5ezi, 5ezl, 5ejj, 5ezn, and 5ezo).

Abstract

Invasion of erythrocytes by *Plasmodial* merozoites is a composite process involving the interplay of several proteins. Among them, the *Plasmodium falciparum* Cysteine-Rich Protective Antigen (PfCyRPA) is a crucial component of a ternary complex, including Reticulocyte binding-like Homologous protein 5 (PfRH5) and the RH5-interacting protein (PfRipr), essential for erythrocyte invasion. Here we present the crystal structures of PfCyRPA and of complex with the antigen-binding fragment of a parasite growth inhibitory antibody. PfCyRPA adopts a 6-bladed β -propeller structure with similarity to the classic sialidase fold, but it has no sialidase activity and fulfills a purely non-enzymatic function. Characterization of the epitope recognized by protective antibodies may facilitate design of peptidomimetics to focus vaccine responses on protective epitopes. Both *in vitro* and *in vivo* anti-PfCyRPA and anti-PfRH5 antibodies showed more potent parasite growth inhibitory activity in combination than on their own, supporting a combined delivery of PfCyRPA and PfRH5 in vaccines.

Keywords: CyRPA, Malaria vaccine candidate, sialidase, crystal structure, β -propeller, invasion inhibitory antibody.

Introduction

According to the World Health Organization 2015 Malaria Report (who.int/malaria/publications/world_malaria_report/en), malaria is estimated to have caused 214 million clinical cases and 438,000 deaths in 2015. The disease is transmitted by female *Anopheles* mosquitoes and caused by parasitic protozoans of the genus *Plasmodium*, of which *P. falciparum* and *P. vivax* are the most prevalent and *P. falciparum* is causing the most often fatal and medically most severe form of malaria. Debilitating clinical symptoms associated with the infection are caused by the multiplication of the asexual blood-stage parasites in erythrocytes. One of the most promising targets for malaria vaccine development is therefore at the stage where merozoites invade erythrocytes.

Invasion of host erythrocytes by merozoites is a complex process, conceptually divisible into four phases: (1) initial recognition of and reversible attachment to the erythrocyte membrane by the merozoite; (2) junction formation leading to irreversible attachment of the merozoite, parasitophorous vacuole formation, and release of the *Plasmodium* rhoptry-microneme secretory organelles are released; (3) invagination of the erythrocyte membrane around the merozoite, accompanied by the shedding of the merozoite's surface coat; (4) closing of the parasitophorous vacuole and resealing of the erythrocyte membrane mark the completion of merozoite invasion (Pinder et al., 2000). The initial recognition and the active invasion of erythrocytes depend on specific molecular interactions between parasite ligands and receptors on the host erythrocyte membrane. Although several ligand-receptor interactions have already been identified, the entire network of molecular interactions involved in invasion is not yet fully disentangled. In addition, *P. falciparum* merozoite proteins are antigenically highly diverse and in part functionally redundant, to facilitate parasite escape from host immune surveillance and to ensure erythrocyte invasion *via* alternative pathways (Cowman et al., 2012).

Most efforts in malaria blood stage vaccine research and development have historically concentrated on immuno-dominant, polymorphic antigens that contribute to the invasion of red blood cells by merozoites. Despite major efforts, blood stage vaccines based on merozoite surface antigens have so far shown limited efficacy in clinical trials (reviewed in (Halbroth and Draper, 2015)). Extensive antigenic polymorphism represents one major hurdle for the development of an effective blood-stage malaria vaccine (Takala et al., 2009; Dzikowski and Deitsch, 2009). Therefore, the identification of new candidate antigens that are able to induce broad strain-transcending immunity and that are not susceptible to 'vaccine resistance' has become a recent research focus.

Availability of pathogen genomes is facilitating the discovery of novel vaccine candidate antigens through ‘reverse vaccinology’ approaches (Rappuoli, 2001; Donati and Rappuoli, 2013). Sequencing and annotation of the *P. falciparum* genome (Gardner et al., 2002) has supported the identification of new blood stage vaccine candidate antigens (Conway, 2015; Proietti and Doolan, 2015), among which the *P. falciparum* Cysteine-Rich Protective Antigen (PfCyRPA) has a number of noteworthy properties. While PfCyRPA is highly conserved among a plethora of *P. falciparum* isolates, it also is poorly immunogenic in the context of natural exposure (Dreyer et al., 2012). Moreover, PfCyRPA-specific monoclonal antibodies (mAb) inhibit parasite growth both *in vitro* and *in vivo* by blocking merozoite invasion (Dreyer et al., 2012; Favuzza et al., 2016).

PfCyRPA is a 42.8 kDa protein of 362 residues with a predicted N-terminal secretion signal. Orthologs of PfCyRPA have been found in the genomes of the human malaria parasite *P. vivax* and the primate pathogens *P. knowlesi*, *P. cynomolgi*, and *P. reichenowi* (Figure 3-figure supplement 1), but not in the sequenced genomes of other *Plasmodium* species. *P. falciparum* PfCyRPA shares on average 42% sequence identity with its orthologs, but within different *P. falciparum* isolates PfCyRPA is highly conserved: just thirteen dimorphic amino acid positions (highlighted in Figure 3-figure supplement 1) were found in 227 *P. falciparum* field isolates (Manske et al., 2012), and only a single variant (Arg399 instead of Ser399) was found at a frequency of greater than 2%.

PfCyRPA is part of a multi-protein complex (Reddy et al., 2015; Volz et al., 2016) including also the PfRH5-interacting protein PfRipr and the reticulocyte binding-like homologous protein PfRH5, which binds to the erythrocyte receptor basigin (Baum et al., 2009; Crosnier et al., 2011; Chen et al., 2011b; Chen et al., 2014). PfRH5, PfCyRPA and PfRipr colocalize during parasite invasion at the junction between merozoites and erythrocytes. The complex seems to be required both for triggering Ca^{2+} release and establishment of tight junctions (Volz et al., 2016). While merozoites deficient in PfCyRPA or PfRH5 can still bind to erythrocytes, they do not attach irreversibly and cannot invade the host cells (Volz et al., 2016). Like PfCyRPA (Dreyer et al., 2012), PfRH5 induces invasion-blocking antibodies that are effective across common genetic variants (Douglas et al., 2011; Bustamante et al., 2013; Douglas et al., 2014).

‘Structural vaccinology’, a combination of immunological, structural, and bioinformatics approaches, is increasingly used for the design of improved vaccine antigens (Dormitzer et al., 2008; Cozzi et al., 2013; Malito et al., 2015). To this end the crystal structures of PfRH5 in complex with basigin and neutralizing inhibitory mAb have been determined (Chen et al.,

2014; Wright et al., 2014). Here, we describe the crystal structure of the promising vaccine candidate PfCyRPA alone and in complex with the antigen-binding fragment (Fab) of the parasite growth inhibitory mAb c12 (Dreyer et al., 2012). The structure of PfCyRPA represents a step toward elucidating its biological function. Furthermore, definition of the specific epitope–paratope interactions from the crystal structure of the PfCyRPA/c12 complex will support rational design of an epitope-focused PfCyRPA-based candidate vaccine.

Results

Fine specificities of anti-PfCyRPA antibodies

The finding that PfCyRPA and PfRH5 form a complex essential for parasite invasion prompted us to investigate the fine specificities of previously generated parasite inhibitory and non-inhibitory anti-PfCyRPA mAbs. The 16 anti-PfCyRPA mAbs available for analysis (Dreyer et al., 2012; Favuzza et al., 2016), showed six distinctive reactivity patterns with seven overlapping recombinant protein fragments of PfCyRPA, assigning them to the epitope groups A – F, with groups A, B, C and F comprising the parasite inhibitory and groups D and E the non-inhibitory mAbs (Figure 1). All mAbs bound to the full-length PfCyRPA (without the signal sequence; fragment 1). mAbs belonging to epitope group A exclusively bound this fragment, indicating that they recognize conformational epitopes not present in any of the shorter PfCyRPA sequence stretches. Lack of binding to fragments 2 and 7 indicates that the epitope may comprise sequences from both ends of the polypeptide chains. Epitope group B antibodies, including mAb c12, bound only to fragments 1, 2 and 3. Epitope group F mAbs bound to fragments 1, 2 and 5, but not to fragment 3, indicating that in contrast to group B, residues located in the sequence stretch between aa 181–251 are required for their binding. The single mAb c04 constitutes the epitope group C showing binding to fragment 7 (only in IFA, not confirmed by Western blotting analysis). The non-inhibitory mAbs clustered into the distinct epitope groups D and E.

Reactivity of anti-PfCyRPA mAbs with PfCyRPA fragments						
PfCyRPA fragment	Epitope group					
	A	B	C	D	E	F
1	x	x	x	x	x	x
2	–	x	x	x	x	x
3	–	x	x	x	x	–
4	–	–	–	–	–	–
5	–	–	–	x ^a	x	x
6	–	–	–	–	x	–
7	–	–	x ^a	–	–	–
Parasite growth inhibition	yes	yes	yes	no	no	yes

Figure 1. Binding of anti-PfCyRPA mAbs to fragments of PfCyRPA

Binding of sixteen mAbs to PfCyRPA fragments (black bars) expressed on the cell surface of HEK cells as assessed by Western blotting analysis and live-cell immunofluorescence staining. (x) indicates staining and (–) no staining; (^a) indicates no reactivity in Western blot analysis of HEK cell lysates. Expression on the surface of the HEK cells has been demonstrated for all PfCyRPA fragments by immunofluorescence analysis using anti-Histidine tag HIS-6/9 mAb (Figure 1-figure supplement 1). For reference, the seventeen residues constituting the epitope on PfCyRPA identified from the complex crystal structure with the Fab of mAb c12 is shown in all constructs as red bars. According to their reactivity pattern, anti-PfCyRPA mAbs were assigned to different epitope groups: **A:** c10, SB2.5; **B:** c02, c06, c08, c09, c12, SB3.7; **C:** c04; **D:** c05; **E:** c13, SB3.9; **F:** SB1.6, SB2.1, SB2.3, SB3.3.

The parasite growth inhibitory activity of anti-PfCyRPA antibodies is enhanced by anti-PfRH5 antibodies

Since it may prove useful to incorporate a combination of PfCyRPA and PfRH5 in a multivalent malaria vaccine, we investigated whether mAbs against these two vaccine candidate antigens have additive or synergistic effects. In a first step, we tested a combination of inhibitory mAbs against the two antigens in an *in vitro* parasite growth inhibition assay. Parasites were cultured for one cycle of merozoite invasion in the presence of the anti-PfCyRPA c12 mAb with or without the anti-PfRH5 BS1.2 mAb at concentrations of 500, 250, and 125 µg/mL. Either mAbs showed potent inhibitory activity, consistently reducing parasite growth of all four tested *P. falciparum* strains in a concentration-dependent manner and to the same extent as the well characterized inhibitory anti-MSP-1 mAb 12.10 (Blackman et al., 1990) (Figure 2A and Figure 2-figure supplement 1). When combining the anti-PfCyRPA c12 mAb with the anti-RH5 BS1.2 mAb, we found a significantly enhanced inhibitory activity: while mAbs c12 and BS1.2 at a concentration of 250 µg/mL inhibited growth by 21 ± 2.2% and 31 ± 4.6%, respectively, the combination of both mAbs (250 µg/mL each) inhibited growth by 59 ± 1.4%; (Figure 2A). The functional activity of both mAbs was not enhanced by the addition of a malaria-unrelated control mAb.

In a second step the *in vivo* parasite inhibitory activity of the mAbs was evaluated in the *P.*

falciparum SCID murine model that employs non-myelodepleted NODscidIL2R γ null mice engrafted with human erythrocytes (Dreyer et al., 2012; Jiménez-Díaz et al., 2009). Groups of three mice received 2.5 or 0.5 mg of mAbs c12 or BS1.2 or a combination of both mAbs by i.v. injection. The control groups received either 2.5 mg of an isotype-matched malaria-unrelated mAb or the same volume of PBS without Ab. Mice were infected with parasitized erythrocytes one day after the antibody transfer and parasitemia was subsequently monitored (Figure 2B). In the control groups parasitemia reached $19.6 \pm 0.8\%$ on day 9 after mAb injection. Parasitemia in mice having received 2.5 mg c12 or BS1.2 mAb increased only marginally, reaching 2.2 ± 0.5 and $2 \pm 0.3\%$ on day 9 after mAb injection, respectively. At the lower dose of 0.5 mg c12 and BS1.2 inhibited parasite growth to 10.1 ± 2.3 and $10.8 \pm 6.9\%$ parasitemia, respectively (Figure 2B). In accord with the *in vitro* data, parasitemia decreased significantly ($p = 0.0356$; unpaired t test, 95% confidence interval, two-tailed) and reached only $4.8 \pm 1.9\%$ on day 9 if mice received 0.5 mg of the anti-PfRH5 BS1.2 mAb in addition to 0.5 mg of the anti-PfCyRPA c12 mAb.

These results demonstrated that anti-PfCyRPA and anti-PfRH5 antibodies have an additive parasite growth inhibitory effect, justifying the combination of both antigens in a subunit vaccine. While the structure of PfRH5 in complex with an inhibitory antibody has been determined, structural information for PfCyRPA is lacking. We therefore we determined the crystal structures of PfCyRPA and its complex with the Fab of the growth inhibitory mAb c12.

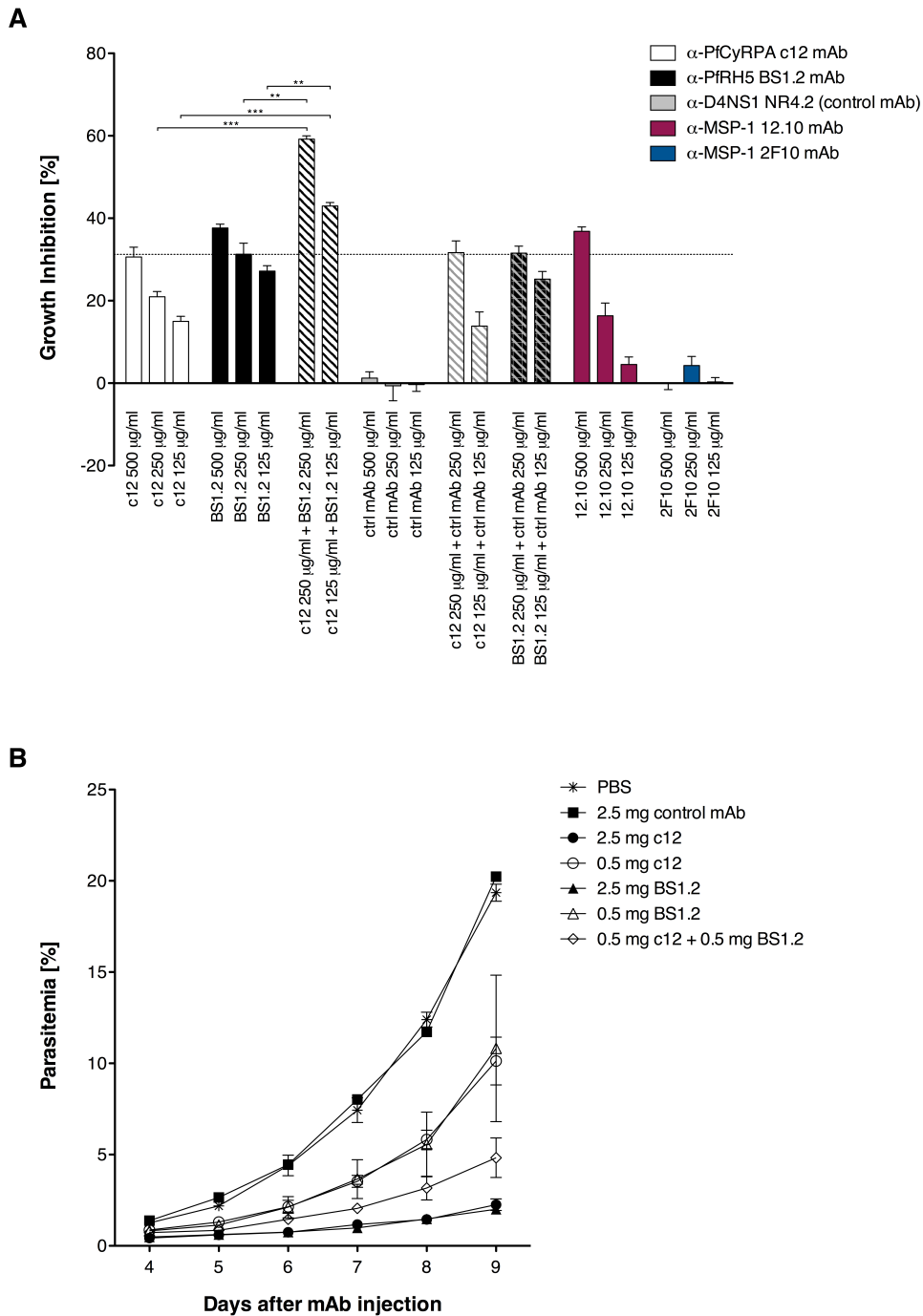


Figure 2. Anti-PfCyRPA and anti-PfRH5 mAbs have both *in vitro* and *in vivo* an additive inhibitory effect on parasite growth

(A) Growth inhibition *in vitro*. Synchronized *P. falciparum* 3D7 blood-stage parasites were cultured for one cycle of merozoite invasion (48 h) in the presence of anti-PfCyRPA c12 mAb, anti-PfRH5 BS1.2 mAb, and their combinations. An isotype-matched, malaria-unrelated mAb (NR4.2) (Rose et al., 2016) was used as negative control. Inhibitory and non-inhibitory anti-MSP-1 mAbs (12.10 and 2F10, respectively) were also included as reference (Blackman et al., 1990; Blackman et al., 1994). Percent parasite growth inhibition was calculated against the parasitemia of PBS control wells. Each bar represents the mean of a triplicate experiment, and error bars indicate the standard deviation (SD). Differences in parasite growth inhibition between mAbs c12 and BS1.2 alone and their combinations are statistically significant (unpaired t test with Welch's correction, 95% confidence interval, two-tailed p value).

(B) Growth inhibition *in vivo*. NODscidIL2R^{null} mice received purified anti-PfCyRPA c12 mAb and/or anti-PfRH5 BS1.2 mAb by i.v. injections. Mice were then infected with *P. falciparum* 3D7 and parasitemia was monitored over six days. Values represent the mean parasitemia in human erythrocytes in peripheral blood of three mice per group. Error bars indicate the SD. PBS and an unrelated control mAb were used as negative control.

Biophysical analysis and crystal structure of PfCyRPA

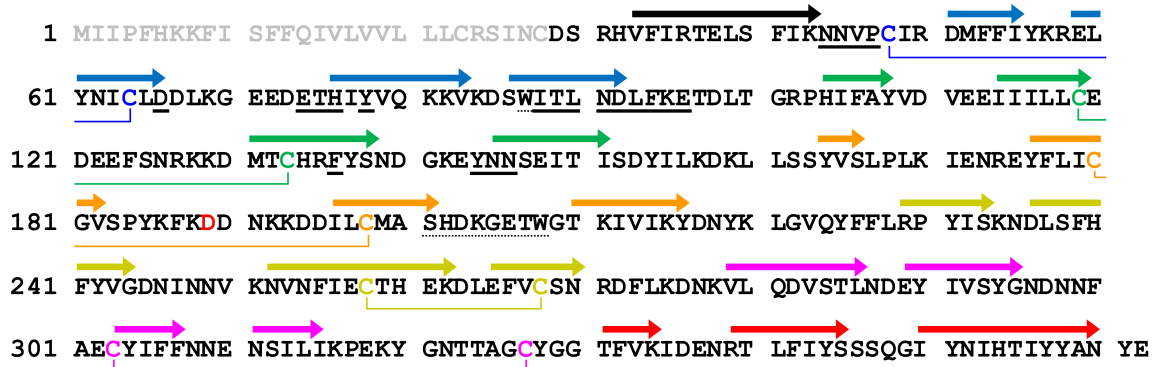
The far-UV CD spectrum of PfCyRPA is consistent with an all- β structure connected by loop regions and the absence of α -helices (Figure 3-figure supplement 2A). Mass spectrometric analysis of proteolytic fragments of PfCyRPA revealed at least four disulfide bonds that are sequential along the sequence (Figure 3-figure supplement 2B). Intrinsic fluorescence showed that the two Trp residues present in PfCyRPA are buried in the native state. Also, the disulfide bonds seem to be buried, because addition of 50 mM reducing agent had no significant effect on the fluorescence of PfCyRPA (Figure 3-figure supplement 2C). Taken together, these data are consistent with PfCyRPA forming a compact, disulfide-stabilized molecule of predominantly β -sheet structure.

In order to crystallize PfCyRPA, we needed to pre-treat the protein with Actinase E (Figure 4-figure supplement 1A). The crystal structure of PfCyRPA, determined to a resolution of 2.5 Å (detailed in Supplementary file 1), confirmed our biophysical analyses (Figure 3). PfCyRPA adopts a six-bladed β -propeller structure that buries the disulfide bonds and the Trp residues. Each blade of the propeller is constructed by a four-stranded anti-parallel β -sheet (Figure 3B). The five disulfide bonds in PfCyRPA are located within blades 2-6 (Figure 3A), stabilizing each individual blade. The first blade has no disulfide bond; it is formed by β -strands from the N- and C-terminal regions of PfCyRPA, potentially enabling conformational changes in PfCyRPA by opening and closing. A domain alignment search (DALI; (Holm and Rosenstrom, 2010)) for related structures revealed that PfCyRPA adopts a heavily modified sialidase/neuraminidase fold. The closest structural relative is the catalytic domain of *Vibrio cholerae* sialidase (Moustafa et al., 2004) (Figure 3C). The two proteins have only 9% sequence identity and the structures have a large root mean square distance (rmsd) of 3.7 Å over 285 residues, clearly showing that while the overall fold is similar, the structures are very different with respect to the inclination of the blades (Figure 3C) and the length and conformations of the surface loops connecting the β -strands (Figure 3D). PfCyRPA also contains a signature sequence motif for sialidases known as an Asp-box (201-SHDKGETW-208; conserved residues are underlined) (Roggentin et al., 1989), which serve structural roles in the β -propellers of sialidases. However, while bacterial sialidases contain between three to five Asp-boxes, PfCyRPA contains only a single one.

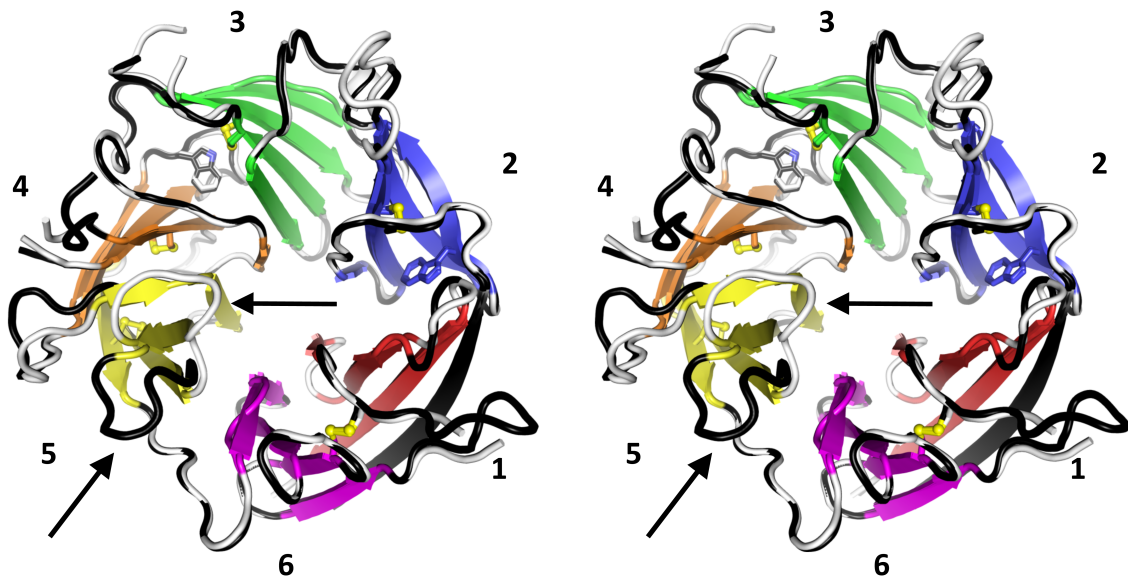
Two molecules of PfCyRPA are present in the asymmetric unit and have conformational differences in several surface loops, suggesting possible flexibility of these loops in solution (Figure 3B). From the point of peptidomimetics that could be derived from PfCyRPA for vaccine development, these surface loops connecting the blades on the back and front of the

β -propeller are natural candidates. Although some of the loops, e.g. in blade 5 (arrows in Figure 3B), have significant structural plasticity, it should be possible to stabilize them in a conformation suitable to raise an immune response.

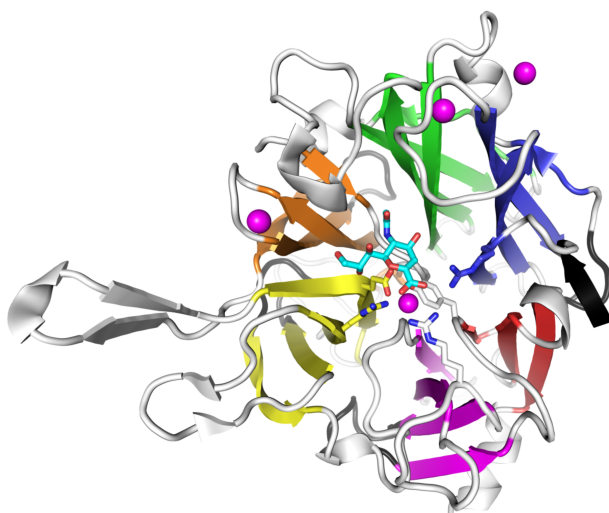
A



B



C



D

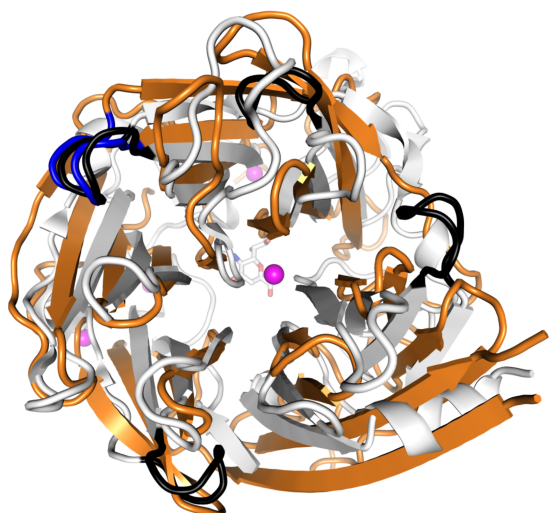


Figure 3. PfCyRPA adopts the neuraminidase fold

(A) Structure-sequence relationship of PfCyRPA. Indicated are an Actinase E cleavage site at Asp189 (red), a sialidase-typical Asp-box (dotted underlined), the two Trp residues (dotted underlined), and the sequential disulfide bonds (connected by lines and in same color). β -strands are shown as arrows colored according to the blade they form. The epitope recognized by mAb c12 is underlined in bold.

(B) Cross-eyed stereo view of the ribbon representation of a superposition of the two PfCyRPA molecules in the asymmetric unit with the blades numbered 1-6 from the N-terminus and colored individually. Blade 1 is made up of an N-terminal (black) and three C-terminal β -strands (red). One protomer is shown with white, the other with black loop regions, which may differ substantially (arrows in blade 5). The Trp and Cys residues are drawn as stick models.

(C) The same orientation of the catalytic domain of *Vibrio cholerae* sialidase (PDB-ID 1w0o), the next structural homolog of PfCyRPA with a DALI score of 18 ($Z < 5$ is structurally dissimilar). Sialic acid and residues in the *Vibrio* enzyme are displayed as balls and sticks. Structural Ca^{2+} ions are marked as magenta spheres. None of the residues necessary for metal ion binding, substrate binding, or catalysis is present in PfCyRPA.

(D) Superposition of PfCyRPA with the *V. cholerae* sialidase. While both proteins are 6-bladed β -propellers, the blades have very different angles, extents, and loop lengths and conformations connecting the β -strands. The four Asp-boxes in the bacterial sialidase (grey) are colored black. PfCyRPA (orange) has only a single Asp-box connecting the third and fourth β -strands in blade 3 (colored blue). Other β -strand connections are made by sequences unrelated to the Asp-box motif, in agreement with poor conservation of the Asp-box in other, e.g. viral, sialidases. The view in (D) is rotated by 180° about the horizontal axis compared to (B) and (C).

PfCyRPA has no sialidase activity

The sialidase fold of PfCyRPA and the presence of an Asp-box motif raised the question whether PfCyRPA exhibits sialidase activity. In view of the involvement of viral and microbial sialidases in the unmasking of cryptic host ligands, host cell adhesion, and invasion (Lewis and Lewis, 2012; Matrosovich et al., 2015), sialidase activity could make sense for PfCyRPA-mediated invasion of erythrocytes. We detected no sialidase activity, however, when we tested recombinant PfCyRPA for neuraminidase activity using a colorimetric assay (Figure 3-figure supplement 3). The active site of sialidases usually contains a triad of Arg residues that bind to the substrate, a Glu/Tyr pair where the acid acts as a general base to activate the Tyr nucleophile, and a hydrophobic pocket with a conserved Trp that accommodates the acetyl group of sialic acid (Buschiazzo and Alzari, 2008). In addition, many sialidases bind to Ca^{2+} ions, of which one is close to the active site and is bound by three main-chain carbonyl groups and oxygen atoms in the side-chains of Asn, Thr, and Asp. PfCyRPA contains none of the residues necessary for catalysis, nor does it harbor a Ca^{2+} binding site, providing structural correlates of the absence of sialidase activity in PfCyRPA. PfCyRPA and sialidases may have evolved from a common ancestor, or PfCyRPA could have evolved from a genuine sialidase to adopt other functionalities.

Characterization of the epitope recognized by the parasite growth inhibitory anti-PfCyRPA mAb c12

The parasite inhibitory anti-PfCyRPA c12 mAb binds tightly to PfCyRPA with a K_d of ca. 1 nM as determined by surface plasmon resonance analysis (Dreyer et al., 2012). This mAb recognizes PfCyRPA independent of its glycosylation, as revealed by Western blot analyses

(Figure 4A). Because of these favorable properties, we chose c12 for epitope mapping by determining the structure of a PfCyRPA/c12 complex. In a first step, we determined the crystal structure of c12 in isolation (Figures 4B and 4C). We obtained three different crystal forms containing a total of four crystallographically independent Fab molecules. Superposition of the structures showed very little structural plasticity of the CDR loops (Figure 4C), suggesting that they retain their structures upon epitope binding.

We then purified the PfCyRPA/c12 complex, analyzed it by limited proteolysis, and crystallized it. Actinase E treatment of the PfCyRPA/c12 complex resulted in the same proteolysis pattern as observed for PfCyRPA alone (Figure 4-figure supplement 1B), suggesting that the epitope for mAb c12 is distant from the Actinase E recognition site at Asp189. Actinase E treatment was not necessary to crystallize the PfCyRPA/c12 complex, however. We determined the crystal structure of the PfCyRPA/c12 complex at a resolution of 4.0 Å by molecular replacement using the individual high-resolution structures of c12 and PfCyRPA as search models (Figure 5A). Despite the limited resolution, novel molecular features were visible in the electron density maps of the complex, providing confidence in the relative orientation of PfCyRPA and c12 (Figure 5-figure supplement 1). First, the electron density visible for PfCyRPA after molecular replacement with c12 was used as a search model for structure determination of PfCyRPA alone (see Methods). This strategy would have been impossible had the placement of c12 been wrong. Second, a loop region that is absent in the PfCyRPA search model due to Actinase E proteolysis (see above) exhibits omit electron density in the PfCyRPA/c12 complex (Figure 4-figure supplement 1). Third, consistent with the similar conformations of the CDR loops in the individual c12 Fab structures (Figure 4) there are negligible conformational changes in the c12 CDR loops when bound to PfCyRPA. Similarly, the epitope conformation in PfCyRPA is very similar in the unbound and complexed form. Minor adjustments of side-chains were required during rebuilding of the complex structure. While the resolution of the PfCyRPA/c12 complex is limited and many side-chains lack clear electron density, as is typical for this resolution, knowledge of the relative orientation of PfCyRPA with respect to c12 in the complex is sufficient for designing peptidomimetics to target the immune response to the protective epitope.

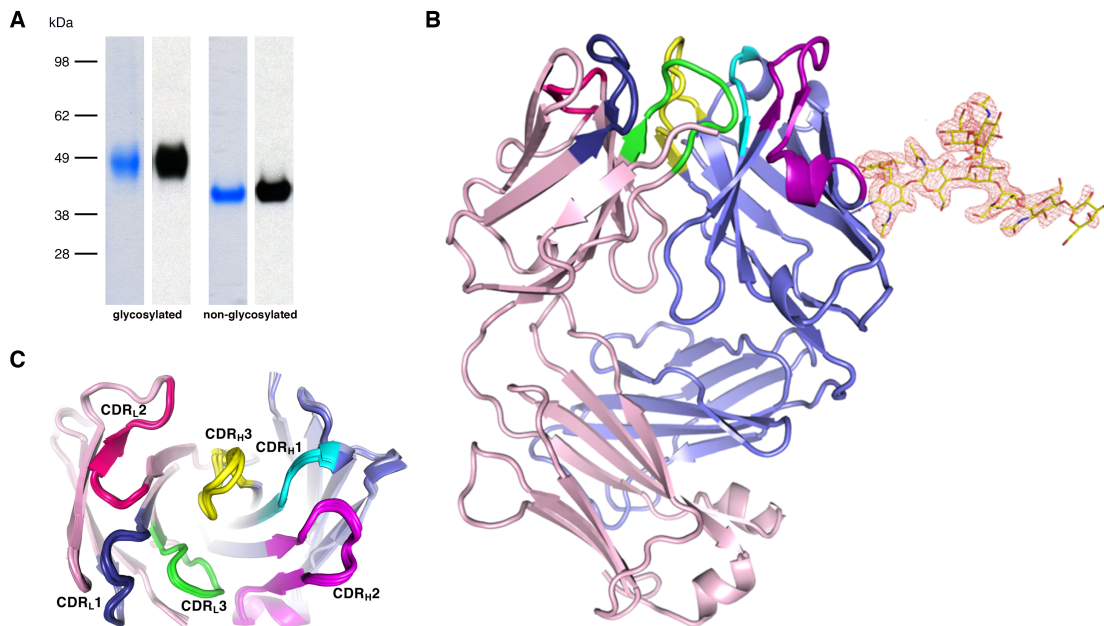


Figure 4. Recognition of PfCyRPA by the mAb c12 and structure of c12

(A) Reducing SDS-PAGE of glycosylated (left) and non-glycosylated (right) PfCyRPA detected by Coomassie-staining (blue) and Western blotting with mAb c12 (black). Recognition by c12 is independent of the glycosylation.

(B) Overview of the c12 structure with a glycan located at heavy-chain Asn37. mFo-DFc electron density for the glycan is shown as a red mesh drawn at the 3 rmsd level. The light and heavy chains are colored light pink and light blue, respectively. Heavy chain CDR1-3 are colored cyan, magenta, and yellow, and light chain CDR1-3 are drawn in dark blue, pink, and green.

(C) Comparison of the four c12 structures shows little conformational variability of the CDR loops. The four c12 molecules superimpose onto their variable V_HV_L di-domains with an average rmsd of 0.35 Å, which reveals a minor spread of the elbow angles between 133.1° and 135.8°. The high structural congruence indicates that the CDR conformations are genuine and not dominated by crystal contacts. The view is from above on top of the CDR loops.

The epitope recognized by mAb c12 is a surface composed of blade 2 and part of blade 3 of PfCyRPA (Figure 5A). The most frequent amino acid dimorphism of PfCyRPA at position 339 is thus located outside the epitope recognized by mAb c12, consistent with the observation that mAb c12 binds to *P. falciparum* independent of the PfCyRPA variant they express (Dreyer et al., 2012). mAb c12 buries a total surface area of 950 Å² on PfCyRPA with the major contributor being the light chain, which buries 520 Å², while the heavy chain buries only 430 Å². The surface complementarity coefficient *S_c* of the complex is 0.67, a typical value for antibody-antigen interactions (Lawrence and Colman, 1993); a value of one would denote perfect complementarity. The light chain also forms more potential hydrogen bonds to PfCyRPA than the heavy chain (Figure 5B). Seven hydrogen bonds are possible between PfCyRPA and the c12 light chain. Each side-chain of light chain CDR1 residues 50-RND-52 can form a hydrogen bond with the side-chains of PfCyRPA residues Asp66, Asn45, and Tyr78, respectively. A particularly large contribution to complex stability may stem from a salt bridge between PfCyRPA residue Asp66 and CDR1 residue Arg50, which by

mutagenesis was found to be true (see below), a further confirmation that the PfCyRPA/c12 complex structure is correct. In addition, the heavy chain contributes significantly to antigen binding. Tyr120 of heavy chain CDR3 can engage in two hydrogen bonds with the side-chains of PfCyRPA residues Asp92 in blade 2 and Tyr144 in blade 3, thus establishing a mini-network that bridges blade 2 and 3. Together with heavy chain CDR3 residue Tyr122, Tyr120 also forms numerous van der Waals interactions with Asn91, Lys95, Glu96, and Phe136, Tyr144, Asn145, and Asn146 (Figures 5B and 5C). A complete listing of the derived potential interactions is available in Supplementary file 2, which due to the limited resolution of the complex structure must remain tentative. What is clear from the structure is that mAb c12 recognizes a discontinuous epitope that contains at least seventeen residues distributed over four PfCyRPA sequence stretches (marked in Figure 3A).

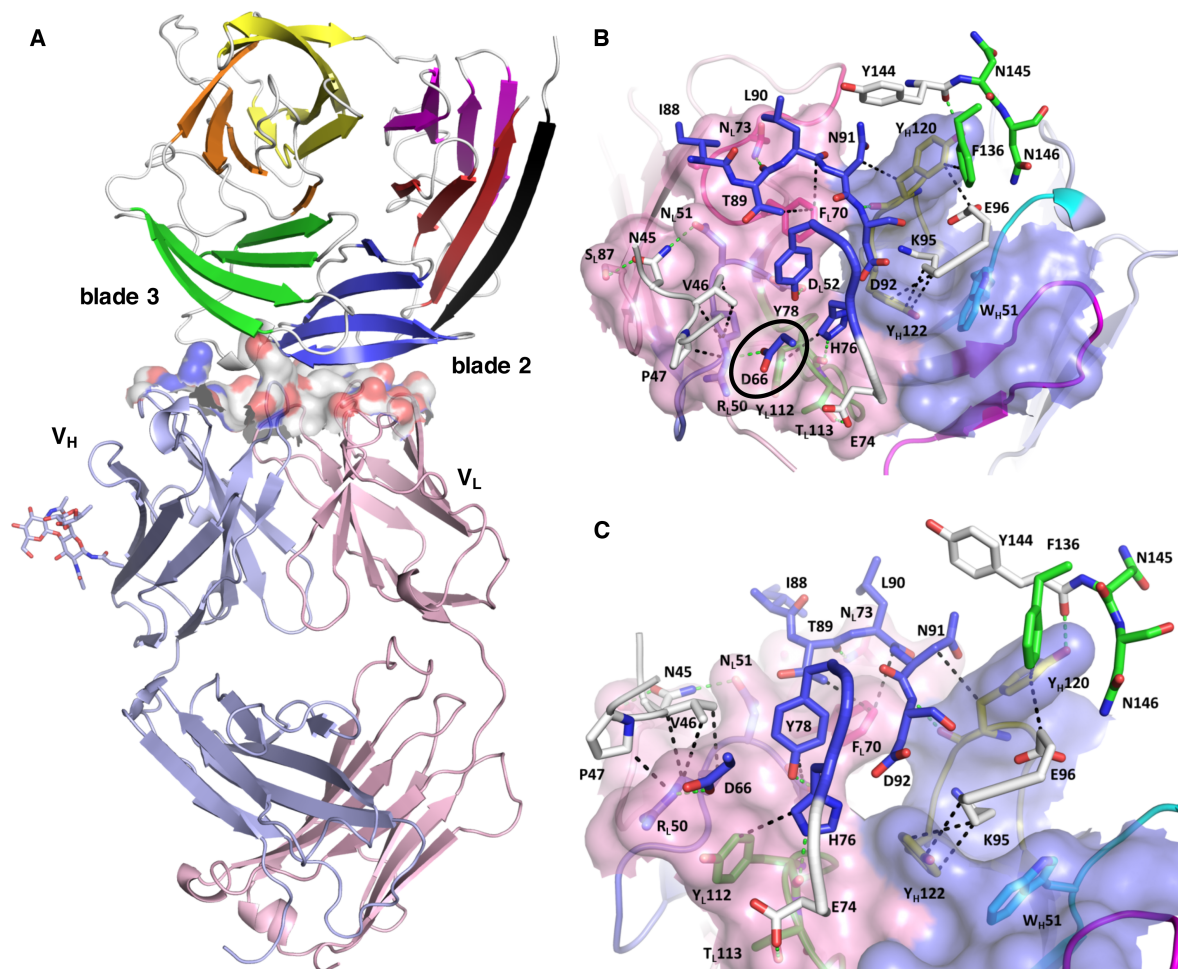


Figure 5. Structure of the PfCyRPA/c12 complex

(A) Overview showing that the majority of the interface is made by interactions between the light chain of c12 and blade 2 of PfCyRPA.

(B) Details of the interface viewed from top onto the CDR loops. The light and heavy chain surfaces buried by PfCyRPA are colored pink and blue, respectively. Possible hydrogen bonds and van der Waals interactions are indicated by dashed green and black lines. The CDR loops are color-coded as in Figure 4. The Asp66-Arg50 salt bridge is circled.

(C) Close-up of (B).

The epitope extracted from the complex structure matches the binding pattern of mAb c12 to the PfCyRPA fragments in our epitope analysis (Figure 1): only fragments 1-3 containing all the seventeen interaction sites were recognized by mAb c12. Furthermore, fragment 4, lacking three out of these seventeen residues (Tyr144, Asn145 and Asn146) and fragments 5 and 6, lacking four residues (Asn45, Val46, Pro47 and Asp66), were not recognized by mAb c12.

The PfCyRPA epitope recognized by mAb c12 was further verified by mutagenesis. The crystal structure suggests that Asp66 forms a salt bridge with Arg50 in the CDR1 loop of the c12 light chain (Supplementary file 2 and Figure 5-figure supplement 1). When Asp66 was changed to Lys, a capture ELISA detected significantly weaker binding of the mAb c12 to the Asp66Lys variant of PfCyRPA (Figure 6A). As expected, the Asp66Lys replacement did not affect binding of the control mAb SB1.6 (Figure 6B), which belongs to the unrelated epitope group F and is expected to engage in crucial interactions with PfCyRPA residues located between residues 181-251 (Figure 1).

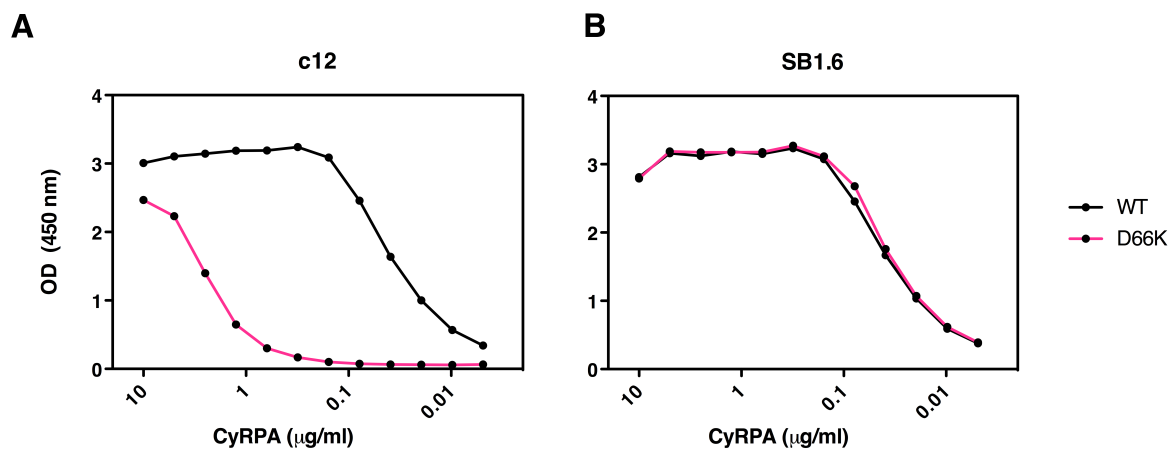


Figure 6. Identification of Asp66 as a key contact residue for PfCyRPA/c12 interaction

mAb binding to purified wild type PfCyRPA and an Asp66Lys single amino acid sequence variant was analyzed by capture-ELISA experiments. ELISA plates were coated with 10 µg/mL anti-PfCyRPA mAbs and then incubated with serial dilutions of wild-type PfCyRPA (WT) or an Asp66Lys variant (D66K); HRPO-labeled anti-Histidine tag mAbs were used as detection antibody.

(A) When compared to wild-type PfCyRPA, the Asp66Lys single amino acid exchange strongly reduced the binding to mAb c12 mAb (epitope group B; Figure 1).

(B) In contrast, the Asp66Lys amino acid exchange did not affect the binding of the mAb SB1.6, which belongs to epitope group F.

Discussion

PfCyRPA has been identified as a novel malaria blood stage vaccine target in an endeavor to test predicted *P. falciparum* open reading frames for the capacity to elicit parasite-inhibitory mAbs (Dreyer et al., 2010). PfCyRPA is stage-specifically expressed in late schizonts and elicits mAbs that inhibit parasite growth *in vitro* and in a *P. falciparum* experimental infection model based on NODscidIL2R γ null mice engrafted with human erythrocytes (Dreyer et al., 2012). Recent studies (Reddy et al., 2015) have placed PfCyRPA in a ternary complex with PfrH5 and PfrIpr that as a whole is essential for erythrocyte invasion (Volz et al., 2016). Like PfrH5 and PfrIpr (Baum et al., 2009; Chen et al., 2011b), PfCyRPA is refractory to genetic disruption (Reddy et al., 2015), and loss of PfCyRPA or PfrH5 function in conditionally expressing mutants blocks parasite growth due to the inability of merozoites to invade erythrocytes (Volz et al., 2016). Here we show that antibodies against PfrH5 and PfCyRPA have additive parasite growth inhibitory activity. Inclusion of both antigens into a multivalent subunit vaccine therefore represents an attractive strategy to prevent emergence of escape mutants. While an ortholog of PfCyRPA is also present in the genome of the human parasite *P. vivax*, an ortholog of PfrH5 has only been found so far in the genome of *P. reichenowi*, a chimpanzee malaria parasite closely related to *P. falciparum* (Otto et al., 2014). This may indicate a function of PfCyRPA beyond its role as a protein-binding platform in the ternary complex with PfrH5 and PfrIpr. While it has been claimed that PfCyRPA anchors the ternary complex through a GPI anchor to the parasite membrane (Reddy et al., 2015), recent results are not consistent with this suggestion (Volz et al., 2016). This inconsistency suggests that additional proteins might be involved in anchoring the complex to the parasite membrane and that PfCyRPA has an essential function other than that of an anchor. Further functional studies are required to elucidate the molecular mechanisms how the ternary complex is involved in the triggering of Ca²⁺ release and the establishment of tight junctions between the merozoite and the erythrocytes (Volz et al., 2016). In this context it may be relevant that the five sequential disulfide bonds of PfCyRPA are in blades 1-5, leaving blade 6 of the β -propeller structure without such a local stabilization. Blade 6 is constructed by β -strands from the N- and the C-terminus, and in principle could act as a gate to allow PfCyRPA to undergo substantial conformational changes.

Structural vaccinology defines epitopes from antigen-antibody complex crystal structures and thus allows the design of surrogate antigens that elicit protective humoral immune responses. The approach may be of particular use for pathogens that cause chronic infections by presenting immuno-dominant antigens and epitopes to the immune system, which, however,

only elicit non-protective antibody responses (Liljeroos et al., 2015; Loomis and Johnson, 2015; Robinson, 2013; Dormitzer et al., 2012). The structural studies of *Neisseria meningitidis* adhesin A and factor H binding protein (Malito et al., 2013), as well as of the *Staphylococcus aureus* manganese transport protein (Ahuja et al., 2015) represent remarkable examples in which crystal structure determination of antigens elucidated both the molecular mechanism of their biological functions and their immunological viability as vaccine antigens.

For the development of synthetic malaria subunit vaccines, conformationally stabilized and structurally optimized peptide antigens mimicking conserved protective epitopes (Mueller et al., 2003; Okitsu et al., 2007; James et al., 2006) may be more suitable components than entire recombinant proteins containing highly polymorphic immuno-dominant non-protective surface loops. Both PfCyRPA and PfRH5 elicit protective as well as non-protective antibodies (Dreyer et al., 2012; Douglas et al., 2011), making them candidates for structure-based approaches, that aim to focus the immune responses on protective epitopes.

Even at the comparatively moderate resolution of 4 Å, the crystal structure of the protective mAb c12 bound to PfCyRPA provides an ideal starting point for the design of a conformationally stabilized PfCyRPA-derived peptide antigen to elicit primarily protective antibodies. Particle-based antigen delivery systems such as virosomes (Cech et al., 2011; Pluschke and Tamborini, 2012) are highly suitable to support, by repetitive epitope display, the development of strong immune responses against peptidomimetics. The epitope recognized by mAb c12 is monomorphic and, like PfCyRPA in general, little immunogenic in the natural context. Focusing the vaccine-induced immune response on this PfCyRPA epitope may confer a strong protective effect.

Malaria vaccine candidates based on single-antigens have been uniformly unsuccessful and an effective subunit vaccine will likely have to include antigens from more than one stage of the parasite life cycle (pre-erythrocytic, liver stage, and blood stage components), as well as sexual blood-stage gametocyte or mosquito-stage parasite antigens as transmission-blocking components. The *Plasmodium* genome contains more than 5,000 open reading frames of which only < 0.5% have been tested as vaccine candidates, so careful selection of new targets for an optimized multi-valent vaccine is called for (Proietti and Doolan, 2015; Dups et al., 2014; Longley et al., 2015; Wu et al., 2015). PfCyRPA represents one of the most promising new blood stage vaccine candidate antigens identified with the support of –omics approaches, and there is renewed hope that an effective combination and formulation of such rationally selected antigens can lead to the development of a malaria subunit vaccine that offers high

level strain-transcending protection (Halbroth and Draper, 2015). With the availability of structural analyses for both PfCyRPA and PfRH5 in complex with an inhibitory antibody, structure-based approach is now possible. In view of the observed additive effect of antibodies, inclusion of immunogens representing both antigens in a subunit vaccine would make sense, thereby reducing the danger of selection of immune escape mutants.

Materials and Methods

Molecular biology

Plasmids were amplified in *E. coli* strain Top10 (Life Technologies) grown in LB medium under 100 µg/mL ampicillin selection. The expression vector for secretion of recombinant PfCyRPA was generated by PCR using the plasmid BVM_PFD1130W_FLAG_GP_His as template (Dreyer et al., 2010). The resulting expression vector pcDNA3.1_BVM_CyRPA(26-362)_His₆ encodes the bee-venom melittin (BVM) signal sequence to secrete PfCyRPA into the cultivation medium, and a C-terminal His₆-tag. Three asparagine residues (N145, N322, and N338) were predicted to be potential sites for N-glycosylation of PfCyRPA in mammalian cells. Since *Plasmodium* proteins are not glycosylated (Dieckmann-Schuppert et al., 1992), an expression vector coding for the PfCyRPA triple variant N145Q/N322Q/N338Q comprising residues 29-362 and containing no N-glycosylation sites was derived from the first vector by site-directed mutagenesis (GenScript). The expression vector coding for the PfCyRPA Asp66Lys single amino acid variant (D66K) was also generated by site-directed mutagenesis (GenScript) resulting in the expression plasmid pcDNA3.1_BMV_CyRPA(29-362/D66K)_His₆.

Monoclonal antibodies

Generation of anti-PfCyRPA mAbs has been described elsewhere (Dreyer *et al.* 2010; Favuzza *et al.* 2016). Anti-PfRH5 antibodies were generated using the same strategy as described by Dreyer et al. 2010.

Plasmodium falciparum blood stage culture

Plasmodium falciparum strains 3D7, K1, 7G8 and D6 were obtained from the Malaria Research and Reference Reagent Resource Center (MR4; Manassas, VA, USA) (MRA-102, -159, -154 and -285, respectively). Parasites were cultured essentially as described previously (Matile and Pink, 1990). The culture medium was supplemented with 0.5% AlbuMAX (Life Technologies) as a substitute for human serum (Dorn et al., 1995). Cultures were synchronized by sorbitol treatment (Lambros and Vanderberg, 1979). Erythrocytes for passages were obtained from the Swiss Red Cross (Switzerland).

In vitro growth inhibition assay

In vitro growth inhibition assays with *P. falciparum* strains 3D7, K1, 7G8 and D6 were conducted essentially as described (Persson et al., 2006). Each culture (trophozoite stage parasites, 0.5% hematocrit, 2% parasitemia) was set up in triplicate in 96-well flat-bottomed

culture plates. After 48 hours of incubation (one cycle of merozoite invasion), viable parasites were stained with hydroethidine and analyzed in a FACSscan flow cytometer (Becton Dickinson) using CellQuest software. A total of 50,000 cells per sample were analyzed. Percent inhibition was calculated from the mean parasitemia of triplicate test and control wells as:

$$\text{Percent inhibition (\%)} = \text{control} - \text{test} / (\text{control} / 100)$$

Parasitemia of control samples was also determined by counting GIEMSA stained parasites.

***In vivo* growth inhibition assay**

All procedures involving living animals were performed in strict accordance with the Rules and Regulations for the Protection of Animal Rights (Tierschutzverordnung) of the Swiss Federal Food Safety and Veterinary Office. The protocol was granted ethical approval by the Veterinary Office of the county of Basel-Stadt, Switzerland (Permit Numbers: 2375 and 2303). Monoclonal antibodies were tested in the murine *P. falciparum* model essentially as described (Dreyer et al., 2012; Jiménez-Díaz et al., 2009). Human erythrocytes (hE) were administered daily (0.75 mL) by the i.v. or i.p. route. Mice received a single dose of mAbs formulation by i.v. injection. The following day, mice were infected with 3×10^7 erythrocytes parasitized by *P. falciparum* PfNF54^{0230/N3}, a strain developed at GlaxoSmithKline (GSK) for growth in hE engrafted mice (Jiménez-Díaz et al., 2009). Parasitemia was monitored daily by flow cytometry over six days (day four to nine after mAb injection).

Protein production

FreeStyle 293-F cells (Invitrogen, R790-07), a variant of human embryonic kidney HEK cells, were cultured in suspension in serum-free medium (FreeStyle™ 293 Expression Medium, Thermo Fisher Scientific) at 37°C in a humidified incubator with 5% CO₂ in volumes of 1 L shake flasks (Corning; 120 rpm, 5 cm diameter) or 10 L wave bioreactors (Sartorius; 30 rpm, pH 7.2, 30% dissolved oxygen). Cells were diluted 1:2 with fresh culture medium and transfected at $1.2 \cdot 10^6$ cells/mL with 0.4 mg/L expression plasmid using a riDOM-based transfection system (Quebatte et al., 2014). 72 h post-transfection, cells were removed by filtration and the supernatant was concentrated with a 10K Pellicon 3 cassette (Millipore). The His₆-tagged recombinant proteins were purified by immobilized metal ion affinity chromatography on a HisTrap HP column (5 or 10 mL volume; GE-Healthcare) equilibrated with 50 mM HEPES/NaOH pH 7.2, 500 mM NaCl. After washing the column with the same buffer containing 20, 40 and 50 mM imidazole, the protein was eluted with a linear 50-500 mM imidazole gradient over 20 column volumes. The eluate was concentrated

by ultra-filtration (Amicon Ultra-4 Ultracel 10K) and applied to a HiLoad 16/600 Superdex 200 gel permeation column (GE-Healthcare) equilibrated with 50 mM Tris/HCl pH 7.4, 150 mM NaCl. Homogeneity of PfCyRPA was assessed by reversed-phase chromatography (RP-HPLC) on a Poroshell 300SB-C8 1x75 mm² column using a H₂O + 0.01% TFA / Acetonitrile + 0.08% TFA gradient, and was confirmed by LC/MS intact mass analysis. Protein yields were 17 mg and 10 mg per liter of culture for the glycosylated and non-glycosylated PfCyRPA, respectively.

Purified anti-PfCyRPA mAb c12 (Dreyer et al., 2012) was diluted to 0.5 mg/mL in 20 mM sodium phosphate pH 7.0 and cleaved overnight at 21°C with 0.01 mg/mL papain (Sigma-Aldrich) in a molar ratio of 1:20. The reaction was stopped with 0.001 mg/mL E64 inhibitor (Sigma-Aldrich) and the concentrated (Amicon Ultra-4 Ultracel 10K) hydrolysate was applied to a 1 x 5 cm² Toyopearl protein A (Tosoh Biosciences) column equilibrated in 20 mM sodium phosphate pH 7.0. The flow-through containing the Fab was concentrated and chromatographed on a 21.5 x 60 cm² TSKgel G3000SW column (Tosoh Bioscience) equilibrated with 20 mM bis-Tris propane/HCl pH 7.0, 200 mM NaCl. The purity of the Fab was determined by RP-HPLC as described above.

The complex of PfCyRPA with the Fab of mAb c12 (abbreviated as c12 in the following) was prepared with a 1.5-fold excess of PfCyRPA, which was incubated for 20 min at 21°C, concentrated as above and chromatographed *via* a Superdex 200 Increase 10/300 GL column (GE-Healthcare) equilibrated with 20 mM bis-Tris propane/HCl pH 7.0, 200 mM NaCl. Complex-containing fractions were pooled and analyzed for homogeneity by asymmetric flow field-flow fractionation with static multi-angle light scattering (SEC/AF4-MALS). For the expression of the Asp66Lys PfCyRPA variant and PFRH5, FreeStyle 293-F cells were cultured in suspension in serum-free medium (FreeStyle™ 293 Expression Medium, Thermo Fisher Scientific) at 37°C in a humidified incubator with 5% CO₂ in 125 mL shake flasks. Cells were diluted 1:2 with fresh culture medium and transfected at 10⁶ cells/mL with 0.5 mg/L expression plasmid using the 293fectin™ transfection reagent (Thermo Fisher Scientific). 72 h post-transfection, cells were removed by centrifugation, and the His₆-tagged recombinant Asp66Lys PfCyRPA variant was purified by immobilized metal ion affinity chromatography on a HisTrap HP column (1 mL volume; GE-Healthcare) equilibrated with 50 mM Na-phosphate buffer pH 7.2, 500 mM NaCl. After washing the column with the same buffer containing 20 mM imidazole, the protein was eluted (isocratic elution) with 500 mM imidazole over 5 column volumes.

FreeStyle 293-F cells were tested and shown to be free of mycoplasma using MycoAlert Mycoplasma detection kit (Lonza; LT07-318). Identity of cells was confirmed using STR-PCR (Qiagen; Investigator Idplex Pkus Kit, 381625) from genomic DNA purified using High Pure PCR Template Kit (Roche Applied Science 11796828001). The obtained profile was compared to the database available from DSMZ and found to match the HEK293 profile.

Expression of PfCyRPA fragments on the surface of HEK cells

293 HEK cells (ATCC, CRL-1573) expressing PfCyRPA fragments on the cell surface were generated essentially as described previously by (Dreyer et al., 2012). Briefly, DNA sequences coding for the fragments of PfCyRPA were amplified by PCR from the BVM_PFD1130W_FLAG_GP_His plasmid (Dreyer et al., 2010). These expression vectors allow the anchoring of the protein of interest on the cell surface via the transmembrane domain of mouse glycoporphin-A (GP). In addition they contain the secretion signal of bee-venom melittin (BMV), a FLAG tag located extracellularly, and a His₆-tag located in the cytosol. The 293 HEK cells were transfected with the different expression vectors using JetPEI transfection reagent (PolyPlus) according to the manufacturer's instructions. Transient transfectants were harvested 48 h post-transfection. HEK cell lysates were prepared at 10⁷ cells/mL in RIPA-Buffer (1 % NP40, 0.25 % DOC, 10 % glycerol, 2 mM EDTA, 137 mM NaCl, 20 mM Tris/HCl pH 8.0, plus protease inhibitors) and used for Western blot analysis as described in (Favuzza et al., 2016).

293 HEK cells were regularly tested by PCR with mycoplasma-specific primer GPO-1 (5'-ACTCCTACGGGAGGCAGCAGTA-3') and MGSO (5'-TGCACCATCTGTCACTCTGTTAACCTC-3') and shown to be mycoplasma-free.

Biophysical characterization of PfCyRPA

To locate the disulfide bonds in PfCyRPA, peptides derived from proteolysis under native conditions by the endo-proteases LysC, AspN, and trypsin were analyzed by UPLC-tandem mass spectrometry using a Dionex UltiMate3000 RRLC system (Thermo Scientific) coupled to a Synapt G2 HDMS mass spectrometer (Waters) with an electrospray ion source and working in resolution mode under default parameters. 10 µg PfCyRPA was hydrolyzed for several hours at 37°C with 0.3 µg of LysC, trypsin, or AspN. Peptides were separated on a Waters BEH130 C18 1.7 µm UPLC column (0.3x150 mm²) by a 5–45% gradient of acetonitrile in water containing 0.1% HCOOH at a flow rate of 10 µL/min over 90 min and eluted into the mass spectrometer. Data was analyzed using BiopharmaLynx software Ver.

1.3 (Waters). The data derived from the proteolysis are summarized in Figure 3-figure supplement 2.

The secondary structure composition of PfCyRPA was estimated by far-UV circular dichroism (CD) spectroscopy on a Jasco J-815 spectropolarimeter using 10 μ M PfCyRPA in phosphate buffered saline (PBS) at 20°C. A cell of 1 mm path length was used to record four spectra between 200 and 320 nm with a step size of 0.1 nm and an integration time of 1 s. The spectral average was corrected for buffer contributions.

Intrinsic tryptophan fluorescence of a 5 μ M PfCyRPA solution under native (PBS) and denaturing (70°C or PBS with 9 M urea) conditions was measured on an ISS PC-1 photon counting spectrofluorimeter (ISS, Inc.) at 20°C. Fluorescence emission was excited at 295 nm with 4.8 nm band width and path length 1 mm. Emission was monitored in 2 nm steps between 300 and 400 nm with a band width of 16 nm, a path length 5 mm, and an integration time of and 1 s.

Crystallization and data collection

All crystallization was done at 21°C in the sitting drop vapor diffusion setup using a Mosquito LCP crystallization robot (TTP Labtech). If not stated otherwise crystals were cryo-protected with paraffin oil and vitrified in liquid N₂. A non-glycosylated variant of PfCyRPA (residues Asp29–Glu362, N145Q/N322Q/N338Q) did not yield well-diffracting crystals unless pre-treated with proteases. 1 mg/mL PfCyRPA in 50 mM Tris/HCl pH 7.4, 150 mM NaCl was diluted 1:1 with 10 mM HEPES/NaOH pH 7.5, 500 mM NaCl, subjected for 16 h to a panel of twelve proteases (Hampton Research Proti-Ace Kit) at a final concentration of 0.01 mg/mL, and analyzed by reducing SDS-PAGE (Figure 4-figure supplement 1). Of the proteases that changed the apparent molecular mass of PfCyRPA, subtilisin and proteinase K produced multiple bands, while Glu-C, elastase, and thermolysin produced a single band of slightly smaller apparent molecular mass. The thermolysin-treated PfCyRPA was subjected to crystallization, yielding triclinic crystals upon mixing of 120 nL 7.3 mg/mL PfCyRPA in 50 mM Tris/HCl pH 7.4, 150 mM NaCl with 80 nL of precipitant consisting of 0.2 M LiOAc and 20% (w/v) PEG 3350. These crystals are consistent with four molecules per unit cell but did not diffract X-rays beyond a resolution of 3.3 Å. Actinase E-treatment of PfCyRPA results in a different proteolysis pattern with two bands of apparent molecular mass 17 kDa and 20 kDa (Figure 4-figure supplement 1). Thin, plate-shaped monoclinic crystals diffracting to a maximum resolution of about 2.5 Å were obtained from mixing of 100 or 140 nL 15 mg/mL Actinase E-treated PfCyRPA in 50 mM HEPES/NaOH pH 7.5, 150 mM NaCl with 100 nL

and 60 nL precipitants consisting of 0-0.5 M MgCl₂ and 20-25% PEG 3350. Crystals of the same habit were also obtained from 7.6 mg/mL PfCyRPA mixed with 19 % PEG 3350, 0.3 M MgCl₂ and additional 5 mM CaCl₂, SrCl₂, and BaCl₂. Data collected from crystals grown in the presence of the heavier cations were tested for anomalous and isomorphous information content for phasing, which turned out to be negative.

Fab of mAb c12 crystallized from several conditions and its structure was determined in three crystal settings. Crystals were obtained by mixing of 80 nL 16.6 mg/mL c12 in 20 mM bis-Tris propane/HCl pH 7.0, 200 mM NaCl with 120 nL of precipitants consisting of 1.6 M sodium citrate pH 6.5 (hexagonal crystal form) or 0.1 M HEPES/NaOH pH 7.0, 20% w/v PEG 8000 (monoclinic and orthorhombic crystal forms). Monoclinic crystals were cryo-protected with reservoir solution supplemented with 20% glycerol.

Needle-shaped crystals of the PfCyRPA/c12 complex were obtained by mixing 120 nL of a 15.1 mg/mL solution in 50 mM Tris/HCl pH 7.4, 150 mM NaCl with 80 nL reservoir consisting of 0.1 M Sodium citrate pH 5.5, 17 % w/v PEG 5000 MME, 0.2 M NDSB-201 (non-detergent sulfobetaine). Cryo-protection was achieved with reservoir solution supplemented with 20% ethylene glycol.

Diffraction data were collected at Swiss Light Source beamline PX-II on a Pilatus 6M single photon counting detector using 1 Å radiation over a total range of at least 180° in fine slicing mode ($\Delta\phi = 0.25^\circ$). Data were indexed, integrated, and scaled with XDS (Kabsch, 2010), except for data from the hexagonal form of c12, which was integrated with MOSFLM and scaled with AIMLESS (CCP4, 1994). The high resolution limit was chosen as the shell where the correlation coefficient for half datasets $CC_{1/2}$ dropped below 70%. Data sets were tested for internal symmetry by self-Patterson and self-rotation function analyses (not shown). Twinning was excluded based on L-values and second moments. Data collection and also refinement statistics are collected in S1 Table.

Structure determination and refinement

The presence of a short sequence motif in PfCyRPA that is characteristic for sialidases suggested that a six-bladed β -propeller might serve as a molecular replacement model. However, all attempts using several hundred β -propeller structures as search models both with and without loop regions and/or as poly-Ala models were unsuccessful. Sialidases often contain structural Ca²⁺ ions, which prompted co-crystallization of PfCyRPA with the earth alkali cations Ca²⁺, Sr²⁺, and Ba²⁺ for SIRAS phasing, but none of these provided useful derivatives. Attempts to phase the PfCyRPA diffraction data by sulfur-SAD were also

unsuccessful. Packing density estimations indicated two molecules of PfCyRPA in the monoclinic asymmetric unit. The PfCyRPA data could be phased by molecular replacement using the unexplained electron density of the PfCyRPA/c12 complex (see below) as a search model. The volume of density was separated using a mask, placed in a large cubic cell, and back transformed to yield structure factor amplitudes, which were then used in a PHASER (CCP4, 1994) molecular replacement search for two molecules. The solution had a non-random log-likelihood gain of LLG = 175 and the orientations of the two entities replicated the 180° two-fold NCS (non-crystallographic symmetry) estimated from the self-rotation function. Density averaging using PARROT (CCP4, 1994) and the NCS operator defined by the two PHASER solutions resulted in manually interpretable electron density maps. The final model has a discontinuity at Asp189, which is consistent with cleavage of a surface loop by Actinase E. A symmetry-related PfCyRPA occupies the space liberated by the cleaved loop, explaining the necessity of the proteolytic pre-treatment for crystal formation in this setting. The model was refined using automatically generated NCS restraints excluding diverging surface loop regions. 99.5% of all residues are in the favored regions of the Ramachandran plot. The hexagonal dataset of c12 (Supplementary file 1) was phased by molecular replacement using a homology model generated from the c12 sequence in MOE (Chemical Computing Group) as the search model. Separate searches for the variable and constant parts of the Fab were performed in PHASER, which, as anticipated, placed the V_HV_L and C_HC_L domain boundaries close to each other to generate a complete Fab. The final model has 99.2% of all residues in the favored regions of the Ramachandran plot. The monoclinic and orthorhombic c12 datasets were phased using the refined hexagonal c12 structure as molecular replacement search model. Both structures have 98% of their main-chain torsion angles in the favored region of the Ramachandran plot. Elbow angles were calculated with PHENIX (Adams et al., 2010).

According to the Matthews parameter the 4 Å dataset collected from the PfCyRPA/c12 crystal has enough space per asymmetric unit to harbor a single complex. Molecular replacement readily placed c12, and initial maps calculated from this partial solution revealed additional electron density at the tips of the Fab (Figure 5-figure supplement 1), which occupied a volume large enough to host PfCyRPA. The density resembled a β-propeller but was not interpretable due to the limited resolution of the data. However, this density provided enough phasing power to solve the 2.5 Å PfCyRPA structure (see above), showing that the placement of the Fab was correct. The same arrangement of V_HV_L and C_HC_L was obtained when using the V_HV_L and C_HC_L parts of the Fab as separate search models, indicating that the

elbow angle of c12 does not change upon binding to PfCyRPA. The final model of PfCyRPA was used to complete the molecular replacement phasing of the PfCyRPA/c12 complex (log-likelihood gain of >1260), density for which is shown in Figure 5-figure supplement 2. A loop region not present in the PfCyRPA model could be traced in the electron density of the complex (Panel B in Figure 5-figure supplement 1), establishing confidence in the correctness of the molecular replacement solution. The model of the complex was refined according to established protocols for lower resolution structures (DeLaBarre and Brunger, 2006), i.e. using simulated annealing, group ADP values, automatically assigned TLS definitions, secondary structure restraints, and external restraints provided by the higher resolution individual structures of PfCyRPA and c12. No real-space refinement was applied during building and refinement of the PfCyRPA/c12 complex. Strong geometric restraints were applied throughout model building of the PfCyRPA/c12 complex. All models were built with COOT (Emsley et al., 2010) and refined with PHENIX (Adams et al., 2010).

Author Contributions

Conception and design, PF, AMD, RT, JB, HM, GP and MGR; Acquisition of data, PF, EG, MT, BS, ACR, JE, JH, GS, BG, CJ and MGR; Analysis and interpretation of data, PF, EG, MT, BS, AMD, ACR, JE, JH, RT, GS, BG, AL, JB, CJ, HM, GP and MGR; Drafting or revising the article, PF, EG, MT, BS, AMD, ACR, JE, JH, RT, GS, BG, AL, JB, CJ, HM, GP and MGR.

Acknowledgements

We thank Marcello Foggetta and Martin Siegrist for cell transfection. We also thank the staff at the Swiss Light Source for beamline support and Expose GmbH for data collection.

References

- Adams PD, Afonine PV, Bunkoczi G, Chen VB, Davis IW, Echols N, Headd JJ, Hung LW, Kapral GJ, Grosse-Kunstleve RW, McCoy AJ, Moriarty NW, Oeffner R, Read RJ, Richardson DC, Richardson JS, Terwilliger TC, Zwart PH. 2010. PHENIX: a comprehensive Python-based system for macromolecular structure solution. *Acta Cryst D* **66**:213-21. doi:10.1107/S0907444909052925.
- Ahuja S, Rougé L, Swem DL, Sudhamsu J, Wu P, Russell SJ, Alexander MK, Tam C, Nishiyama M, Starovasnik MA, Koth CM. 2015. Structural analysis of bacterial ABC transporter inhibition by an antibody fragment. *Structure* **23**:713-23. doi:10.1016/j.str.2015.01.020.
- Baum J, Chen L, Healer J, Lopaticki S, Boyle M, Triglia T, Ehlgren F, Ralph SA, Beeson JG, Cowman AF. 2009. Reticulocyte-binding protein homologue 5 - an essential adhesin involved in invasion of human erythrocytes by *Plasmodium falciparum*. *Int J Parasitol* **39**:371-80. doi:10.1016/j.ijpara.2008.10.006.
- Blackman MJ, Heidrich HG, Donachie S, McBride JS, Holder AA. 1990. A single fragment of a malaria merozoite surface protein remains on the parasite during red cell invasion and is the target of invasion-inhibiting antibodies. *J Exp Med* **172**:379-82.
- Blackman MJ, Scott-Finnigan TJ, Shai S, Holder AA. 1994. Antibodies inhibit the protease-mediated processing of a malaria merozoite surface protein. *J Exp Med* **180**:389-93.
- Buschiazzo A, Alzari PM. 2008. Structural insights into sialic acid enzymology. *Curr Opin Chem Biol* **12**:565-72. doi:10.1016/j.cbpa.2008.06.017.
- Bustamante LY, Bartholdson SJ, Crosnier C, Campos MG, Wanaguru M, Nguon C, Kwiatkowski DP, Wright GJ, Rayner JC. 2013. A full-length recombinant *Plasmodium falciparum* PfRH5 protein induces inhibitory antibodies that are effective across common PfRH5 genetic variants. *Vaccine* **31**:373-79. doi:10.1016/j.vaccine.2012.10.106.
- CCP4. 1994. The Collaborative Computational Project Number 4, suite programs for protein crystallography. *Acta Cryst D* **50**:760-63.
- Cech PG, Aebi T, Abdallah MS, Mpina M, Machunda EB, Westerfeld N, Stoffel SA, Zurbriggen R, Pluschke G, Tanner M, Daubenberger C, Genton B, Abdulla S. 2011. Virosome-Formulated *Plasmodium falciparum* AMA-1 & CSP Derived Peptides as Malaria Vaccine: Randomized Phase 1b Trial in Semi-Immune Adults & Children. *PLoS One* **6**:e22273. doi:10.1371/journal.pone.0022273.
- Chen CKM, Chan N-L, Wang AHJ. 2011a. The many blades of the β -propeller proteins: conserved but versatile. *Trends Biochem Sci* **36**:553-61. doi:10.1016/j.tibs.2011.07.004.
- Chen L, Lopaticki S, Riglar DT, Dekiwadia C, Uboldi AD, Tham WH, O'Neill MT, Richard D, Baum J, Ralph SA, Cowman AF. 2011b. An EGF-like protein forms a complex with PfRh5 and is required for invasion of human erythrocytes by *Plasmodium falciparum*. *PLoS Pathog* **7**:e1002199. doi:10.1371/journal.ppat.1002199.

- Chen L, Xu Y, Healer J, Thompson JK, Smith BJ, Lawrence MC, Cowman AF. 2014. Crystal structure of PfRh5, an essential *P. falciparum* ligand for invasion of human erythrocytes. *Elife* **3**:e04187. doi:10.7554/eLife.04187.
- Chen Y, Barkley MD. 1998. Toward understanding tryptophan fluorescence in proteins. *Biochemistry* **37**:9976-82. doi:10.1021/bi980274n.
- Conway DJ. 2015. Paths to a malaria vaccine illuminated by parasite genomics. *Trends Genet* **31**:97-107. doi:10.1016/j.tig.2014.12.005.
- Cowman AF, Berry D, Baum J. 2012. The cellular and molecular basis for malaria parasite invasion of the human red blood cell. *J Cell Biol* **198**:961-71. doi:10.1083/jcb.201206112.
- Cozzi R, Scarselli M, Ferlenghi I. 2013. Structural vaccinology: a three-dimensional view for vaccine development. *Curr Top Med Chem* **13**:2629-37.
- Crosnier C, Bustamante LY, Bartholdson SJ, Bei AK, Theron M, Uchikawa M, Mboup S, Ndir O, Kwiatkowski DP, Duraisingh MT, Rayner JC, Wright GJ. 2011. Basigin is a receptor essential for erythrocyte invasion by *Plasmodium falciparum*. *Nature* **480**:534-7. doi:10.1038/nature10606.
- DeLaBarre B, Brunger AT. 2006. Considerations for the refinement of low-resolution crystal structures. *Acta Cryst D* **62**:923-32. doi:10.1107/S0907444906012650.
- Dieckmann-Schuppert A, Bender S, Odenthal-Schnittler M, Bause E, Schwarz RT. 1992. Apparent lack of N-glycosylation in the asexual intraerythrocytic stage of *Plasmodium falciparum*. *Eur J Biochem* **205**:815-25.
- Donati C, Rappuoli R. 2013. Reverse vaccinology in the 21st century: improvements over the original design. *Ann N Y Acad Sci* **1285**:115-32. doi:10.1111/nyas.12046.
- Dormitzer PR, Grandi G, Rappuoli R. 2012. Structural vaccinology starts to deliver. *Nat Rev Microbiol* **10**:807-13. doi:10.1038/nrmicro2893.
- Dormitzer PR, Ulmer JB, Rappuoli R. 2008. Structure-based antigen design: a strategy for next generation vaccines. *Trends Biotechnol* **26**:659-67. doi:10.1016/j.tibtech.2008.08.002.
- Dorn A, Stoffel R, Matile H, Bubendorf A, Ridley RG. 1995. Malarial haemozoin/beta-haematin supports haem polymerization in the absence of protein. *Nature* **374**:269-71. doi:10.1038/374269a0.
- Douglas AD, Williams AR, Illingworth JJ, Kamuyu G, Biswas S, Goodman AL, Wyllie DH, Crosnier C, Miura K, Wright GJ, Long CA, Osier FH, Marsh K, Turner AV, Hill AVS, Draper SJ. 2011. The blood-stage malaria antigen PfRH5 is susceptible to vaccine-inducible cross-strain neutralizing antibody. *Nat Commun* **2**:601. doi:10.1038/ncomms1615.

- Douglas AD, Williams AR, Knuepfer E, Illingworth JJ, Furze JM, Crosnier C, Choudhary P, Bustamante LY, Zakutansky SE, Awuah DK, Alanine DGW, Theron M, Worth A, Shimkets R, Rayner JC, Holder AA, Wright GJ, Draper SJ. 2014. Neutralization of *Plasmodium falciparum* Merozoites by Antibodies against PfRH5. *J Immunol* **192**:245-58. doi:10.4049/jimmunol.1302045.
- Dreyer AM, Beauchamp J, Matile H, Pluschke G. 2010. An efficient system to generate monoclonal antibodies against membrane-associated proteins by immunisation with antigen-expressing mammalian cells. *BMC Biotechnol* **10**:87. doi:10.1186/1472-6750-10-87.
- Dreyer AM, Matile H, Papastogiannidis P, Kamber J, Favuzza P, Voss TS, Wittlin S, Pluschke G. 2012. Passive immunoprotection of *Plasmodium falciparum*-infected mice designates the CyRPA as candidate malaria vaccine antigen. *J Immunol* **188**:6225-37. doi:10.4049/jimmunol.1103177.
- Dups JN, Pepper M, Cockburn IA. 2014. Antibody and B cell responses to *Plasmodium* sporozoites. *Front Microbiol* **5**:625. doi:10.3389/fmicb.2014.00625.
- Dzikowski R, Deitsch KW. 2009. Genetics of antigenic variation in *Plasmodium falciparum*. *Curr Genet* **55**:103-10. doi:10.1007/s00294-009-0233-2.
- Emsley P, Lohkamp B, Scott WG, Cowtan K. 2010. Features and development of Coot. *Acta Cryst D* **66**:486-501.
- Favuzza P, Blaser S, Dreyer AM, Riccio G, Tamborrini M, Thoma R, Matile H, Pluschke G. 2016. Generation of *Plasmodium falciparum* parasite-inhibitory antibodies by immunization with recombinantly-expressed CyRPA. *Malar J* **15**:161. doi:10.1186/s12936-016-1213-x.
- Gardner MJ, Hall N, Fung E, White O, Berriman M, Hyman RW, Carlton JM, Pain A, Nelson KE, Bowman S, Paulsen IT, James K, Eisen JA, Rutherford K, Salzberg SL, Craig A, Kyes S, Chan MS, Nene V, Shallom SJ, Suh B, Peterson J, Angiuoli S, Pertea M, Allen J, Selengut J, Haft D, Mather MW, Vaidya AB, Martin DM, Fairlamb AH, Fraunholz MJ, Roos DS, Ralph SA, McFadden GI, Cummings LM, Subramanian GM, Mungall C, Venter JC, Carucci DJ, Hoffman SL, Newbold C, Davis RW, Fraser CM, Barrell B. 2002. Genome sequence of the human malaria parasite *Plasmodium falciparum*. *Nature* **419**:498-511. doi:10.1038/nature01097.
- Halbroth BR, Draper SJ 2015. Recent Developments in Malaria Vaccinology. *Adv Parasitol*. Elsevier.
- Holm L, Rosenstrom P. 2010. Dali server: conservation mapping in 3D. *Nucleic Acids Res* **38**:W545-9. doi:10.1093/nar/gkq366.
- James S, Moehle K, Renard A, Mueller MS, Vogel D, Zurbriggen R, Pluschke G, Robinson JA. 2006. Synthesis, solution structure and immune recognition of an epidermal growth factor-like domain from *Plasmodium falciparum* merozoite surface protein-1. *ChemBioChem* **7**:1943-50. doi:10.1002/cbic.200600357.

- Jiménez-Díaz MB, Mulet T, Viera S, Gómez V, Garuti H, Ibáñez J, Alvarez-Doval A, Shultz LD, Martínez A, Gargallo-Viola D, Angulo-Barturen I. 2009. Improved murine model of malaria using *Plasmodium falciparum* competent strains and non-myelodepleted NOD-scid IL2R γ 0 mice engrafted with human erythrocytes. *Antimicrob Agents Chemother* **53**:4533-36. doi:10.1128/AAC.00519-09.
- Kabsch W. 2010. XDS. *Acta Cryst D* **66**:125-32.
- Lambros C, Vanderberg JP. 1979. Synchronization of *Plasmodium falciparum* erythrocytic stages in culture. *J Parasitol* **65**:418-20.
- Lawrence MC, Colman PM. 1993. Shape complementarity at protein/protein interfaces. *J Mol Biol* **234**:946-50. doi:DOI 10.1006/jmbi.1993.1648.
- Lewis AL, Lewis WG. 2012. Host sialoglycans and bacterial sialidases: a mucosal perspective. *Cell Microbiol* **14**:1174-82. doi:10.1111/j.1462-5822.2012.01807.x.
- Liljeroos L, Malito E, Ferlenghi I, Bottomley MJ. 2015. Structural and Computational Biology in the Design of Immunogenic Vaccine Antigens. *J Immunol Res* **2015**:156241. doi:10.1155/2015/156241.
- Longley RJ, Hill AV, Spencer AJ. 2015. Malaria vaccines: identifying *Plasmodium falciparum* liver-stage targets. *Front Microbiol* **6**:965. doi:10.3389/fmicb.2015.00965.
- Loomis RJ, Johnson PR. 2015. Emerging Vaccine Technologies. *Vaccines (Basel)* **3**:429-47. doi:10.3390/vaccines3020429.
- Malito E, Carfi A, Bottomley MJ. 2015. Protein Crystallography in Vaccine Research and Development. *Int J Mol Sci* **16**:13106-40. doi:10.3390/ijms160613106.
- Malito E, Faleri A, Lo Surdo P, Veggi D, Maruggi G, Grassi E, Cartocci E, Bertoldi I, Genovese A, Santini L, Romagnoli G, Borgogni E, Brier S, Lo Passo C, Domina M, Castellino F, Felici F, van der Veen S, Johnson S, Lea SM, Tang CM, Pizza M, Savino S, Norais N, Rappuoli R, Bottomley MJ, Masignani V. 2013. Defining a protective epitope on factor H binding protein, a key meningococcal virulence factor and vaccine antigen. *Proc Natl Acad Sci U S A* **110**:3304-9. doi:10.1073/pnas.1222845110.
- Manske M, Miotto O, Campino S, Auburn S, Almagro-Garcia J, Maslen G, O'Brien J, Djimde A, Doumbo O, Zongo I. 2012. Analysis of *Plasmodium falciparum* diversity in natural infections by deep sequencing. *Nature* **487**:375-9. doi:10.1038/nature11174.
- Matile H, Pink JR 1990. *Plasmodium falciparum* malaria parasite cultures and their use in immunology.: Academic Press.
- Matrosovich M, Herrler G, Klenk HD. 2015. Sialic Acid Receptors of Viruses. *Top Curr Chem* **367**:1-28. doi:10.1007/128_2013_466.
- Moustafa I, Connaris H, Taylor M, Zaitsev V, Wilson JC, Kiefel MJ, von Itzstein M, Taylor G. 2004. Sialic acid recognition by *Vibrio cholerae* neuraminidase. *J Bio Chem* **279**:40819-26. doi:10.1074/jbc.M404965200.

- Mueller MS, Renard A, Boato F, Vogel D, Naegeli M, Zurbriggen R, Robinson JA, Pluschke G. 2003. Induction of parasite growth-inhibitory antibodies by a virosomal formulation of a peptidomimetic of loop I from domain III of *Plasmodium falciparum* apical membrane antigen 1. *Infect Immun* **71**:4749-58.
- Okitsu SL, Silvie O, Westerfeld N, Curcic M, Kammer AR, Mueller MS, Sauerwein RW, Robinson JA, Genton B, Mazier D, Zurbriggen R, Pluschke G. 2007. A Virosomal Malaria Peptide Vaccine Elicits a Long-Lasting Sporozoite-Inhibitory Antibody Response in a Phase 1a Clinical Trial. *PLoS One* **2**:e1278. doi:10.1371/journal.pone.0001278.
- Otto TD, Rayner JC, Böhme U, Pain A, Spottiswoode N, Sanders M, Quail M, Ollomo B, Renaud F, Thomas AW, Prugnolle F, Conway DJ, Newbold C, Berriman M. 2014. Genome sequencing of chimpanzee malaria parasites reveals possible pathways of adaptation to human hosts. *Nat Commun* **5**:4754. doi:10.1038/ncomms5754.
- Persson KE, Lee CT, Marsh K, Beeson JG. 2006. Development and optimization of high-throughput methods to measure *Plasmodium falciparum*-specific growth inhibitory antibodies. *J Clin Microbiol* **44**:1665-73. doi:10.1128/JCM.44.5.1665-1673.2006.
- Pinder J, Fowler R, Bannister L, Dluzewski A, Mitchell GH. 2000. Motile systems in malaria merozoites: how is the red blood cell invaded? *Parasitol Today* **16**:240-5.
- Pluschke G, Tamborrini M. 2012. Development of a virosomal malaria vaccine candidate: from synthetic peptide design to clinical concept validation. *Fut Virol* **7**:779-90. doi:10.2217/fvl.12.74.
- Proietti C, Doolan DL. 2015. The case for a rational genome-based vaccine against malaria. *Front Microbiol* **5**:741. doi:10.3389/fmicb.2014.00741.
- Quebatte G, Kitas E, Seelig J. 2014. riDOM, a cell penetrating peptide. Interaction with phospholipid bilayers. *Biochim Biophys Acta* **1838**:968-77. doi:10.1016/j.bbamem.2013.10.017.
- Rappuoli R. 2001. Reverse vaccinology, a genome-based approach to vaccine development. *Vaccine* **19**:2688-91.
- Reddy KS, Amlabu E, Pandey AK, Mitra P, Chauhan VS, Gaur D. 2015. Multiprotein complex between the GPI-anchored CyRPA with PfRH5 and PfRipr is crucial for *Plasmodium falciparum* erythrocyte invasion. *Proc Natl Acad Sci U S A* **112**:1179-84. doi:10.1073/pnas.1415466112.
- Robinson JA. 2013. Max Bergmann lecture protein epitope mimetics in the age of structural vaccinology. *J Pept Sci* **19**:127-40. doi:10.1002/psc.2482.
- Roggentin P, Rothe B, Kaper J, Galen J, Lawrisuk L, Vimr E, Schauer R. 1989. Conserved sequences in bacterial and viral sialidases. *Glycoconj J* **6**:349-53. doi:10.1007/BF01047853.

- Rose N, Pinho-Nascimento CA, Ruggieri A, Favuzza P, Tamborrini M, Roth H, Baroni de Moraes MT, Matile H, Janisch T, Pluschke G, Roltgen K. 2016. Generation of monoclonal antibodies against native viral proteins using antigen-expressing mammalian cells for mouse immunization. *BMC Biotechnol* **16**:83. doi:10.1186/s12896-016-0314-5.
- Takala SL, Coulibaly D, Thera MA, Batchelor AH, Cummings MP, Escalante AA, Ouattara A, Traoré K, Niangaly A, Djimdé AA, Doumbo OK, Plowe CV. 2009. Extreme Polymorphism in a Vaccine Antigen and Risk of Clinical Malaria: Implications for Vaccine Development. *Sci Transl Med* **1**:2ra5. doi:10.1126/scitranslmed.3000257.
- Volz JC, Yap A, Sisquella X, Thompson JK, Lim NT, Whitehead LW, Chen L, Lampe M, Tham WH, Wilson D, Nebl T, Marapana D, Triglia T, Wong W, Rogers KL, Cowman AF. 2016. Essential Role of the PfRh5/PfRipr/CyRPA Complex during *Plasmodium falciparum* Invasion of Erythrocytes. *Cell Host Microbe* **20**:60-71. doi:10.1016/j.chom.2016.06.004.
- Wright KE, Hjerrild KA, Bartlett J, Douglas AD, Jin J, Brown RE, Illingworth JJ, Ashfield R, Clemmensen SB, de Jongh WA, Draper SJ, Higgins MK. 2014. Structure of malaria invasion protein RH5 with erythrocyte basigin and blocking antibodies. *Nature* **515**:427-30. doi:10.1038/nature13715.
- Wu Y, Sinden RE, Churcher TS, Tsuboi T, Yusibov V. 2015. Development of malaria transmission-blocking vaccines: from concept to product. *Adv Parasitol* **89**:109-52. doi:10.1016/bs.apar.2015.04.001.

Supplementary data

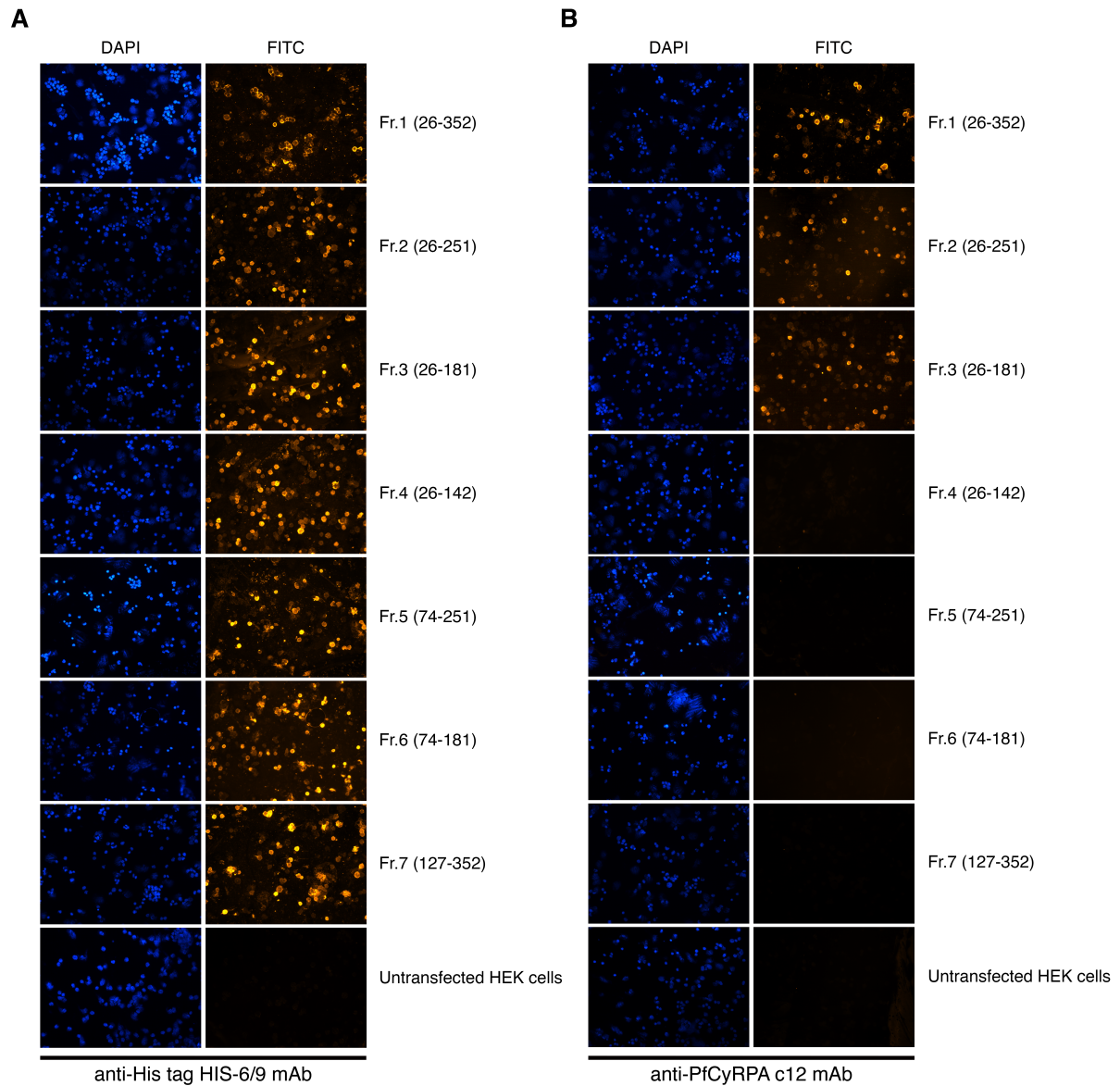


Figure 1-figure supplement 1. Cell-surface expression of PfCyRPA fragments on transiently transfected HEK cells

Fluorescence staining of HEK cells expressing PfCyRPA fragments on their surface after staining with (A) anti-His tag HIS-6/9 mAb or (B) anti-PfCyRPA c12 mAb and FITC-labelled anti-mouse IgG antibodies. Nuclei were stained with DAPI. Untransfected HEK cells served as negative control.

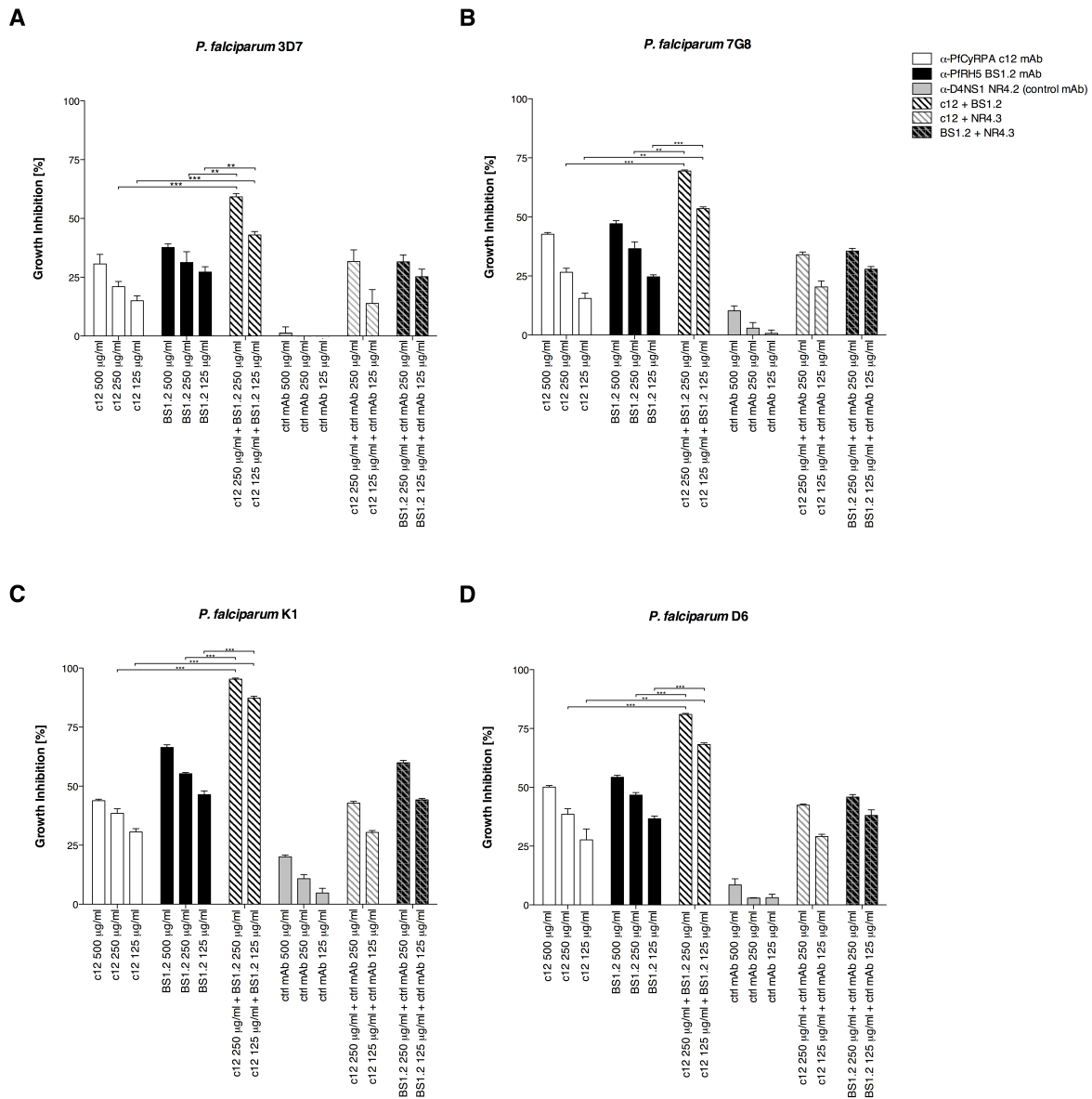


Figure 2-figure supplement 1. Anti-PfCyRPA and anti-PfRH5 mAbs inhibit parasite growth of various *P. falciparum* strains

Synchronized *P. falciparum* 3D7, 7G8, K1 and D6 (A, B, C, and D, respectively) blood-stage parasites were cultured for one life cycle in the presence of anti-PfCyRPA c12 mAb, anti-PfRH5 BS1.2 mAb, and their combinations. An isotype-matched, malaria-unrelated control mAb (NR4.2 mAb) was used as negative control. Percent parasite growth inhibition was calculated against the parasitemia of PBS control wells. Each bar represents the mean of a triplicate experiment, and error bars indicate the standard deviation (SD). Differences in parasite growth inhibition between mAbs c12 and BS1.2 alone and their combinations are statistically significant (unpaired t test with Welch's correction, 95% confidence interval, two-tailed p value).

```

P. fal.  MIIPFHKKFISFFQIVLVVLLCRSINCDSRHV-FIRTELSFIKNNVPCIRDMFFIYKRE 59
P. rei.  MIIPFNKKIISFFQIVLVVLLCRSIYCDSRHV-FIRTELSFVKNSVPCVGMFFIYKRE 59
P. kno.  MIVA---KIAILFFF-LLSCPTYLTNEESKQVILNDEITTTITSPVHCCIADTYFIFRNE 56
P. viv.  MIVT---KIAIFLFFFLFSFLRCLSTNTQSKNIIILNDEITTIKSPIHCCITDIYFLFRNE 57
P. cyn.  MIIQ---KIAILFFFVLR---CYLSTNIESKNIIILNDEIKTIKSPIHCCINEIYFLFQDE 54
      **:  * : : * : : * : : * : : * : : * : : * : : * : : * : : *

P. fal.  LYNICLDDDLKGEEDETHIYVQKKVKDSWITLNDLFKETDLTGRPHIFAYVDVEEIIILLC 119
P. rei.  LYNICSDFLRSEGDDPHIYVQKKVKDSWIIILFDLFKETDLTRRPHIFTYIDVEEIIILLC 119
P. kno.  LYKICIQHVNKGRTEIHVIVQKKAKNKWETKQKLFEDKMWFLHPFVFNQNDEIIILLVC 116
P. viv.  LYKTCIQHVIKGRTEIHVLVQKKINSTWETQTTLFKDHMWFELPSVFNFIHNDEIIIVICC 117
P. cyn.  LYKTCIQHVIRGRTEIHVLIQKQINSTWETQAKLFEDKLWFHVPSVFNFLVLDDEIIIVICC 114
      **:  * : : : * : : * : : * : : * : : * : : * : : * : : *

P. fal.  EDEEFSNRKKDMTCHRFYSNDGKEYnnSEITISDYILKDKLLSSYVSLPLKIENREYFLI 179
P. rei.  ENEEFGNRKKDLTCHRFYSNDGKEYNNSEITISDHILKDKILSSYASFPLRMKDQEYFLI 179
P. kno.  RYKGMT-KGEGVACDRWSSTGTNYNKGNIINIDAQALTKMNLDSYASFPIPKDKAIHI 175
P. viv.  RYKQRS-KREGTCKRWNSVTGTIYQKEDVQIDKEAFANKNLESYQSVPLTVKNKKFLLI 176
P. cyn.  RYKSVN-KKEGATCERWKSVTGTIYKESLQIG-ETFANKNIDSYASVPLKISKKKFLLI 172
      . : : : * : * * : : * : . : . * * * : : : : *

P. fal.  CGVSPYKFKDDNKDDILCMASHDKGETWGT-KIVIKYDNYKLGVQYFFLRPYISKNDLS 238
P. rei.  CGISPYKLKDETKKDNILCMASHDKGETWRT-KVVINYDEYKLGVQYFSLRPYISKNNLS 238
P. kno.  CGVHSYEQNVNQNNFISCLASEDKGTTWGDIKIHIYDQFQEGVPYFYLRPLVFNDEFG 235
P. viv.  CGILSYEYKTANKDNFISCVASEDKGRTWGT-KILINYEELQKGVPYFYLRPIIFGDEFG 235
P. cyn.  CGIHSYEQDSNKDNFISCIASEDKGATWRT-QIHINYEQFKGIPFYLRPLIFDDEFG 231
      **:  * : : . : : * * : * * * * * : : * * : : * : * * * * : : : .

P. fal.  FHFYVGDNINN-VKNVNFIECTHE-----KDLEFVCSNRD-FLKDNKVLQDVSTLNDEY 290
P. rei.  FHFYVGDNINN-VKNINFIECINE-----KDFEFTCSNKD-FLKVDKVLQDVSKLNDQY 290
P. kno.  FYLYSRISNNADRGGKYMKCILNPTNSRNKEYTFKCTNVN-LIKEDKSLQNITKLNGYY 294
P. viv.  FYFYSRISTNNTARGGNYMTCTLDVTNEGKKEYKFKCKHVS-LIKPDKSLQNVTKLNGYY 294
P. cyn.  FYFFSRISTINTGRGGNYMTCTPEAT----NEYKFICKDVNNLIKENKSLQNITKLSGYY 287
      * : : . * : : : * : : : * * . . : : * * * : : * * * : : *

P. fal.  IVSYGNDNNFAECYIFFNNENSILIKPEKYGnTTAGCYGGTFVKIDENRTLFIYSSSQGI 350
P. rei.  IVSYGNDNNFNECYIFFNNENSILIKPEKRGSKNGGCYGGKFVKIDEHRILFIYSSSQGI 350
P. kno.  VTSYAKKNFNECYLYYTENAIVVKPKVQNYELNGCYGGSFVKFNESKALFIYSTGHGV 354
P. viv.  ITSVYVKDNFNECYLYYTENAIVVKPKVQNDLNGCYGGSFVKLDESALFIYSTGYGV 354
P. cyn.  ITSVYVKDNFNECYLYYTEHNAIVVKPKVQNYDLNGCYGGSFVKLDEEDALFIYSTGHGV 347
      : . * * : : * * * : : : . * : : * : : * * * * * : : * * * * : : *

P. fal.  YNIHTIYYANYE 362
P. rei.  YNIHIIYYSNYE 362
P. kno.  QNIHTLHYARYE 366
P. viv.  QNIHTLYYTRYD 366
P. cyn.  QNIHTLHYTRYD 359
      *** : : * : * :

```

Figure 3-figure supplement 1. Sequence alignment of CyRPA orthologs

Sequence alignment of CyRPA orthologs from *P. falciparum* (*P. fal.*), *P. vivax* (*P. viv.*; PVX_090240), *P. knowlesi* (*P. kno.*; PKNH_0515800), *P. cynomolgi* (*P. cyn.*; PCYB_053730), and *P. reichenowi* (*P. rei.*; PRCDC_0421000). Full-length protein sequences (PlasmoDB; plasmodb.org/plasmo) were aligned with Clustal O (1.2.1). Asterisks indicate conserved positions, colons indicate strong biophysical conservation, and periods indicate weak biophysical conservation. Ten of the twelve Cys residues are conserved (same color code as in Figure 3). The predicted PfCyRPA secretion signal sequence (M1-C28) is indicated in boldface, and the predicted GPI-anchor motif (I353-E362) is underlined. The N-glycosylation sites that are used in human cells (N145, N322, and N338) are shown in lowercase and the non-synonymous SNPs (D73, D110, V165, P168, R174, F187, D236, N270, V292, N338, R339, L341, N352) are colored in red.

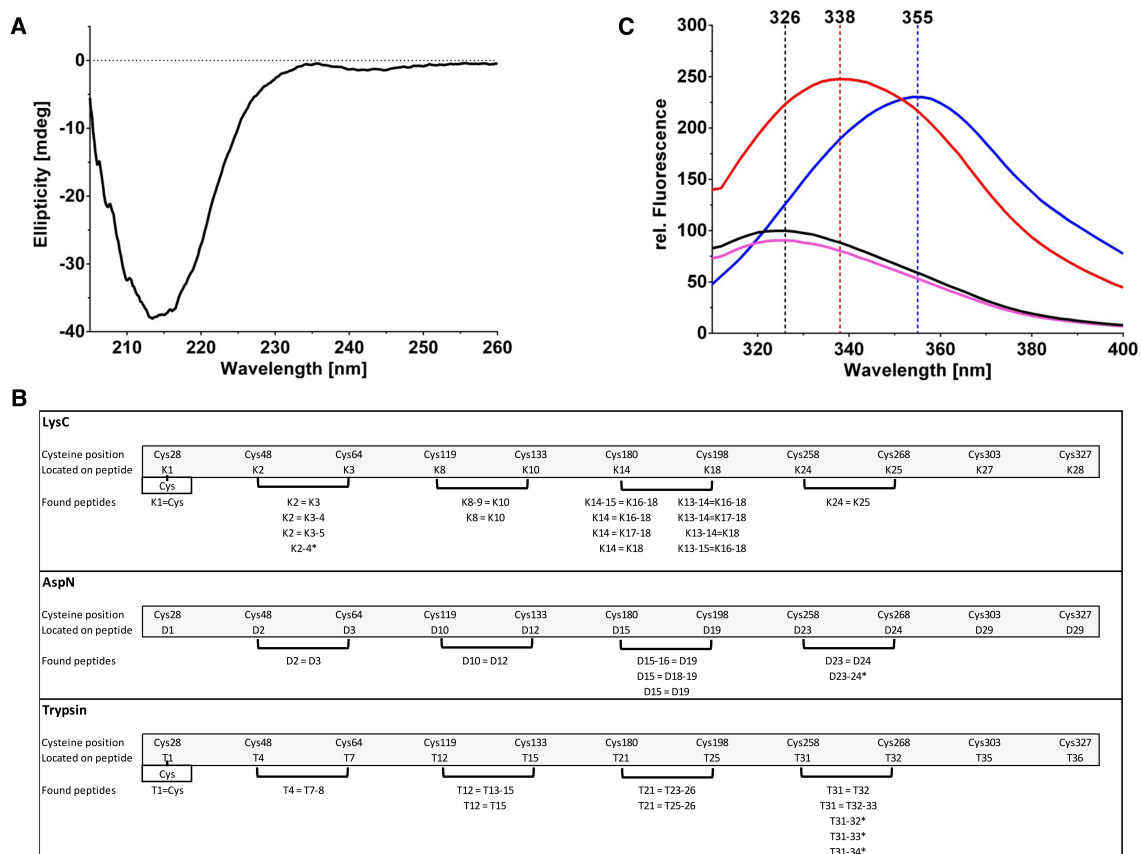


Figure 3-figure supplement 2. Biophysical analysis of PfCyRPA

(A) The CD spectrum of PfCyRPA shows a prominent minimum around 215 nm, consistent with a high content of β -secondary structure. The minimum is remote from the minima expected for helical (208 nm and 222 nm) and random coil (200 nm) structures.

(B) Identification of disulfide bonds in PfCyRPA. The peptide fragments are labeled K (LysC cleavage), D (AspN cleavage), and T (trypsin cleavage). A cut-off of 2% signal intensity was applied to separate highly populated from less populated fragments. Masses that correspond to two proteolytic peptides connected by disulfide bonds were repeatedly found (parentheses) when using different proteases. An equal sign (=) signifies a disulfide bond and a minus sign (-) signifies a skipped cleavage. For instance, the first disulfide bond between Cys48 and Cys64 was identified four times in the LysC hydrolysate: K2=K3 corresponds to the mass of the second and third expected proteolytic fragment linked by a disulfide bond. K2=K3-4 is the second expected LysC peptide (K2) disulfide-linked to a larger peptide (K3-K4) that still contains a LysC cleavage site but this site was not recognized by the enzyme. The same reasoning applies to K2=K3-5, where two LysC cleavage sites were not recognized. An asterisk (*) denotes a disulfide bond in a peptide. The K2-4* fragment has a mass corresponding to an un-cleaved and disulfide-linked peptide with two intact LysC cleavage sites that were not recognized. The last disulfide bond in PfCyRPA between Cys303/327 was not identified by any protease, possibly due to low abundance of the proteolytic fragments containing it.

(C) The fluorescence emission spectrum of native PfCyRPA (black) shows a maximum at 326 nm that shifts to 338 nm when heated to 70°C (red) or 355 nm when unfolded by 9 M urea (blue). Addition of 50 mM DTT (magenta) has no significant effect on the fluorescence, suggesting that the disulfide bonds are not solvent-accessible. The unusual finding that the Trp fluorescence quantum yield of the unfolded state is higher than in the native state indicates that the excited state of Trp is efficiently quenched by nearby residues in the native structure (Chen and Barkley, 1998).

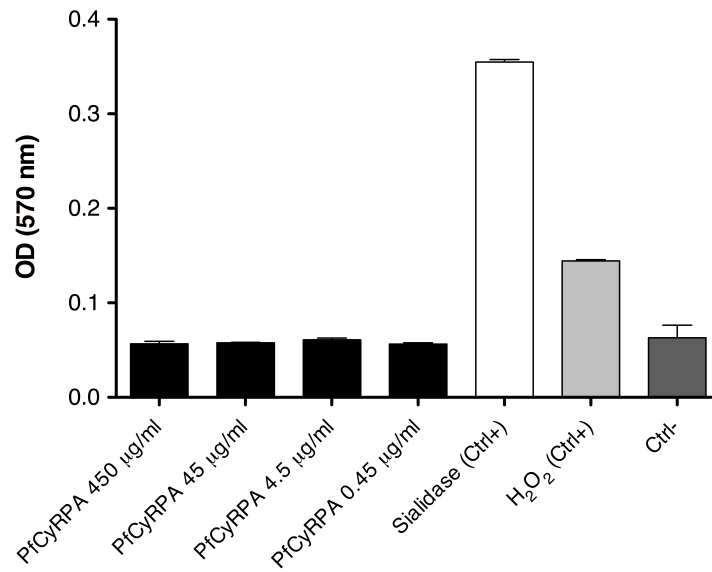


Figure 3-figure supplement 3. PfCyRPA lacks detectable sialidase activity in a functional assay

Sialidase activity was estimated using the Amplex Red Neuraminidase (Sialidase) assay kit (Molecular Probes, Inc.). The assay utilizes Amplex Red to detect H₂O₂ generated by galactose oxidase oxidation of desialiated galactose, the end product of sialidase activity. The H₂O₂ in the presence of HRP reacts with Amplex Red reagent to generate resorufin, the red fluorescent oxidation product, which was detected at 570 nm using the Sunrise Absorbance Reader (Tecan). PfCyRPA was mixed 1:1 (v/v) with the Amplex Red reagent/HRP/galactose oxidase/fetuin working solution (0.2U/mL HRP, 4U/mL galactose oxidase, 500 µg/mL fetuin), and the mixture was incubated at 37°C for 30 min in a light-protected container. Sialidase and H₂O₂ (supplied with the kit) were used as positive controls (Ctrl+); a no-sialidase sample as negative control (Ctrl-).

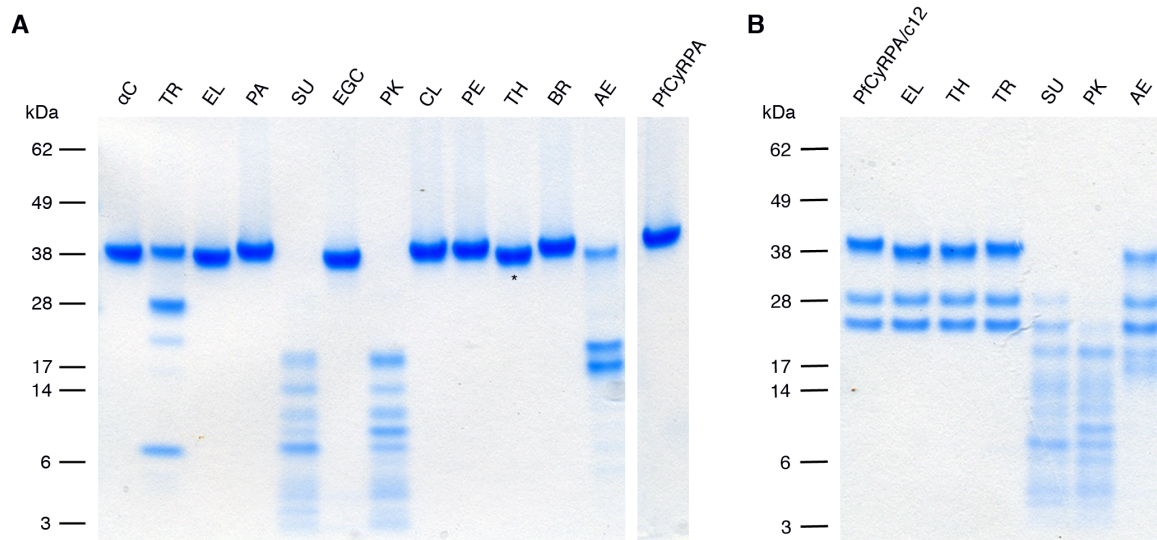


Figure 4-figure supplement 1. Limited proteolysis of PfCyRPA and the PfCyRPA/c12 complex

(A) PfCyRPA. (B) PfCyRPA/c12 complex. Proteases are abbreviated as: α C: α -Chymotrypsin; TR: Trypsin; EL: Elastase; PA: Papain; SU: Subtilisin; EGC: Endoproteinase Glu-C; PK: Proteinase K; CL: Clostripain; PE: Pepsin; TH: Thermolysin; BR: Bromelain; AE: Actinase E. The two bands around 28 kDa in (B) correspond to the Fab. Actinase E affects PfCyRPA irrespective of bound c12, yielding two major proteolysis products of apparent molecular weight 17 kDa and 20 kDa.

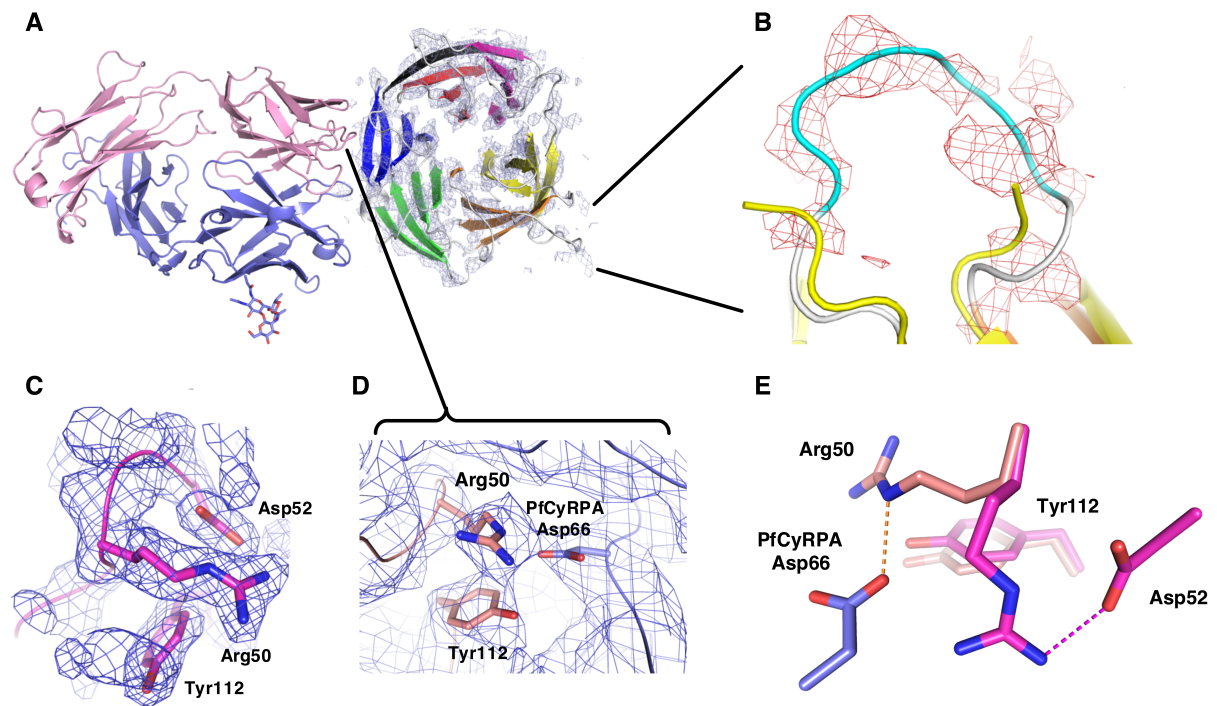


Figure 5-figure supplement 1. Electron density of the PfCyRPA/c12 complex

(A) Initial electron density at a resolution of 3.6 Å contoured at the 1 rmsd level for PfCyRPA after molecular replacement phasing of the PfCyRPA/c12 complex data with c12 as the search model. The light and heavy chains of c12 are colored pink and cyan, respectively. The final model of PfCyRPA (blades colored in the same pattern as in Figure 3A) is superimposed for reference but could not be traced using this map. This map fragment was cut out and used as starting model for molecular replacement of the PfCyRPA structure.

(B) Zoom of the loop region 186-KFKDDNK-192. This loop was cut at Asp189 by Actinase E. The loop opened and the sequence could not be completely traced in the isolated PfCyRPA structure (yellow). Difference electron density at a resolution of 3.6 Å contoured at the 1.8 rmsd level shows that the loop is intact in the PfCyRPA/c12 complex and can be traced in the electron density maps. The refined model of the complex (loop colored in cyan) is superimposed for reference.

(C) Region around Arg50 in the free c12 Fab structure 5ezj. 2mFo-DFc electron density is shown at the 1 rmsd level. Arg50 binds to nearby Asp52.

(D) This interaction is lost in the complex with PfCyRPA. Arg50 now binds to PfCyRPA residue Asp66 (light blue). 2mFo-DFc electron density is shown at the 0.8 rmsd level.

(E) Superposition of the structures from panels (C) and (D) shows the large movement of Arg50 in the free c12 Fab (magenta) *versus* its position in the complex with PfCyRPA (pink). By contrast, the conformation of Tyr112 does not change much.

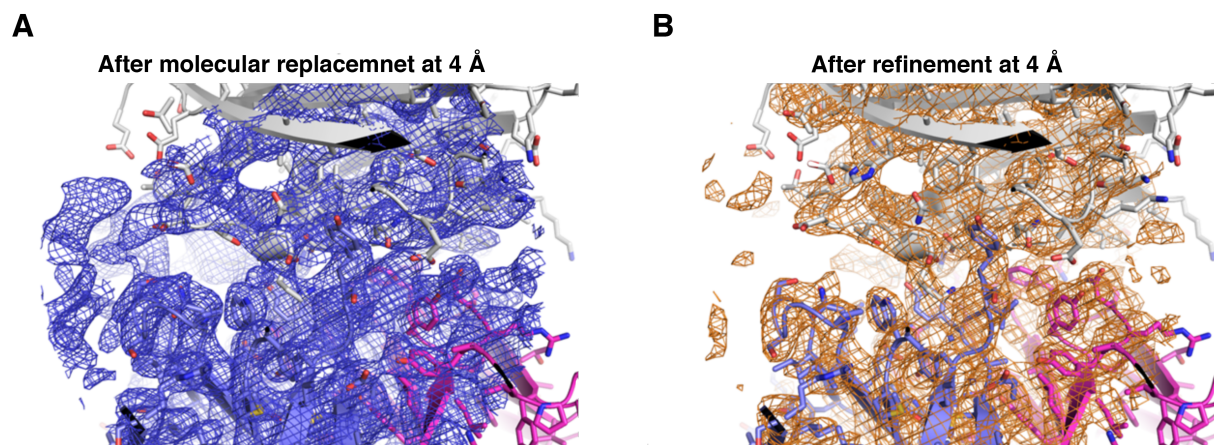


Figure 5-figure supplement 2. Electron density of the PfCyRPA/c12 complex at the interface

The final model of the PfCyRPA/c12 complex is shown. PfCyRPA is at the top, shown as a grey ribbon representation. Fab c12 is at the bottom with the light and heavy chain colored magenta and blue, respectively. 2Fo-Fc electron density at 4Å resolution is contoured at the 1 rmsd level at a radius of 22Å around the center of the image. The panel on the left-hand side shows the electron density after molecular replacement (A), while the panel on the right-hand side depicts the density after refinement (B).

Results Part 4

Evaluation of the conserved *Plasmodium falciparum* merozoite antigen PF14_0044 as candidate vaccine antigen

Malaria Journal 2017, ready for submission

Paola Favuzza^{1,2}, Anita M Dreyer^{1,2}, Araceli Lamelas^{1,2}, Hugues Matile³, Gerd Pluschke^{1,2§}

¹ Medical Parasitology and Infection Biology Department, Swiss Tropical and Public Health Institute, Basel, Switzerland

² University of Basel, Switzerland

³ Roche Pharmaceutical Research & Early Development, Small Molecule Research, Roche Innovation Center Basel, F. Hoffmann-La Roche Ltd., Basel, Switzerland

[§] Corresponding author

Abstract

Background

One key challenge for the development of a malaria subunit vaccine lies in the identification of suitable target antigens. Sequencing and annotation of the *Plasmodium falciparum* genome has disclosed the sequence of several thousand potential targets for malaria vaccine development, and reverse-vaccinology approaches offer the possibility to rationally select new targets from a large set of so far uncharacterized open reading frames (ORFs).

Methods

On the basis of available genome-wide transcriptomic and proteomic data, we selected previously uncharacterized *Plasmodium falciparum* ORFs and evaluated their potential as novel asexual blood-stage vaccine candidate antigens. For this purpose, we exploited a mammalian cell-based antigen expression platform for immunization of mice, raised antigen-specific mouse monoclonal antibodies (mAbs), and evaluated their parasite inhibitory activity.

Results

This strategy has led us to the identification of PF14_0044 as a potential asexual blood-stage candidate antigen for inclusion into a multi-component malaria subunit vaccine. While PF14_0044 -specific mAbs had only marginal parasite growth-inhibitory activity on their own, they showed a significant synergistic inhibitory activity in combination with previously described inhibitory anti-PfCyRPA mAbs.

Conclusions

Our findings demonstrate that for the selection of new malaria vaccine candidate antigens both the direct parasite growth inhibitory activity of target specific antibodies and their synergy with growth inhibitory antibodies against other antigens should be systematically evaluated.

Introduction

According to the latest estimates, there were about 212 million cases of malaria in 2015 and an estimated 429,000 deaths, mostly among children under five years of age in Africa [1]. Despite the remarkable improvements achieved in malaria control, which have led to a drastic reduction of malaria morbidity and mortality rates in the last decade, the development of an effective vaccine against malaria is still recognized as a most promising method for preventing and controlling malaria. However, complexity of the *Plasmodium* spp. parasite as well as the host response to the parasite has hindered the development of a highly effective vaccine until now. In spite of these challenges, field and clinical studies showed that some degree of clinical immunity can be acquired naturally with age and exposure [2] or induced by passive [3,4] or active immunization [5]. Those studies support the idea that a malaria vaccine is feasible and pointed out the importance of antibodies as crucial components of the immune response against blood stage parasites. Until recently, almost all efforts in malaria vaccine development have been focused on a selected panel of antigens recognized as immunodominant in the context of natural infection. These studies have primarily focused on the Circumsporozoite protein (CSP) for the pre-erythrocytic stage, and Merozoite Surface Protein-1 (MSP-1) and Apical Membrane Antigen-1 (AMA-1) for the blood stage, and investigated a variety of vaccine delivery systems [6–10]. However, despite major efforts, candidate subunit vaccines against malaria have shown limited efficacy in clinical trials [11–14]. This lack of success in single-antigen subunit based vaccines, led to the recognition that an effective malaria vaccine will likely need to be a multi-component, multi-stage vaccine [15]. Indeed, it is not unforeseen that single-antigen based vaccines failed to confer effective immune protection against a parasite with such a complex lifecycle, which expresses hundreds of stage-specific proteins, and that has evolved under the pressure of the human immune system for millennia [16]. Recent findings indicate that the search for new candidate antigens for a multivalent malaria vaccine should target parasite proteins that are not immunodominant in the context of natural infection [17,18]. For protection from clinical malaria immune recognition of multiple antigens might be required [15,19–21], suggesting that only a subunit vaccine incorporating several rationally selected key antigens would be effective. Since the full genome of *Plasmodium falciparum* 3D7 was sequenced and annotated in 2002 [22], major efforts have continued to improve availability of large-scale genomic, proteomic, transcriptomic and comparative data, including different *Plasmodium falciparum* strains and clinical isolates and other *Plasmodium* species [23]. These extensive data sets

offer valuable and powerful tools for rational search for new candidate antigens, and have made reverse vaccinology the most promising strategy for vaccine development [24,25]. We have identified one of the new most promising asexual blood-stage candidate antigens, the *Plasmodium falciparum* Cysteine-Rich Protective Antigen (PfCyRPA), based on a reverse vaccinology approach selecting so far uncharacterized blood-stage antigens and evaluating their potential as vaccine components [26]. PfCyRPA is a key component of a crucial invasion pathway of erythrocytes by merozoites [17,27] and is capable of eliciting antibodies that inhibit parasite growth in vitro and in vivo [28]. Along this line we have characterized in the present study the PF14_0044 protein with regard to stage-specific expression, localization and its potential to elicit parasite inhibitory antibodies.

Materials & Methods

Bacterial strains and media

Escherichia coli strain Top10 (Thermo Fisher Scientific) was used for the amplification of plasmids. Bacteria were grown at 37°C in LB medium containing 100 µg/ml ampicillin.

Construction of expression plasmids

Codon optimized synthetic sequence encoding *Plasmodium falciparum* PF14_0044 gene (GenScript) was subcloned into pcDNA3.1_BVM_FLAG_GP_His as previously described [26] resulting in expression plasmid pcDNA3.1_BVM_PF14_0044_FLAG_GP_6xHis. This expression vector allows for expression of the PF14_0044 as membrane-anchored protein. It contains the secretion signal of bee-venom melittin (BVM), the coding sequence of the protein of interest, a FLAG-tag, the mouse glycoporphin-A (GP) transmembrane domain (for membrane anchoring), and a hexa-His tag. The expression vector coding for the recombinant-secreted version of PF14_0044 was generated by site-directed mutagenesis (GenScript) resulting in expression plasmid pcDNA3.1_BMV_PF14_0044_6xHis. This expression vector allows the expression of PF14_0044 as secreted protein via the BVM signal peptide. It contains the secretion signal of BVM, the coding sequence of the protein of interest and an N-terminal hexa-His tag.

Culture of eukaryotic cells

FreeStyle 293-F cells (Thermo Fisher Scientific), a variant of human embryonic kidney cell line HEK cells, were cultured in suspension in serum-free medium (FreeStyle™ 293 Expression Medium, Thermo Fisher Scientific) supplemented with 30 mU Heparin at 37°C in a humidified incubator with 5% CO₂ in volumes of 3 L shake flasks (Corning, 100 rpm, 5 cm diameter).

Generation of transient HEK cell lines expressing PF14_0044

FreeStyle 293-F cells were transfected with pcDNA3.1_BVM_PF14_0044_FLAG_GP_6xHis plasmid using a riDOM-based transfection system [29]. Prior to transfection at 1.2×10^6 cells/ml, cells were diluted 1:2 with fresh culture medium and transfected with 0.4 mg/l expression plasmids and transfection reagents. Cells were harvested 48 hours post-transfection.

Immunofluorescence staining of methanol-fixed HEK cells

HEK cells were collected, washed with PBS, spotted on multiwell glass slides (Multitest slide, 12-well, 7 mm, MP Biomedicals), air-dried and fixed in ice-cold methanol for 10 min. Immunostaining was performed by incubating the wells with 50 µl of hybridoma culture supernatant, or an appropriate mAb diluted in 0.1% BSA-PBS, for 20 min in a humid chamber at 37°C. After washing, 50 µl of 20 µg/ml Alexa488-conjugated rabbit anti-mouse IgG (H+L) antibody (Thermo Fisher Scientific) diluted in 0.1% BSA-PBS was added and incubated for 20 min in a humid chamber at 37°C. After the final wash, the slides were mounted in 50% PBS-glycerol and covered with a coverslip. Stainings were assessed by fluorescence microscopy on a Zeiss Axioscop fluorescence microscope (Carl Zeiss AG).

Immune complex generation

Transiently transfected HEK cells were collected and washed twice with PBS. Cell lysate were prepared at 10^7 cells/ml in complete lysis buffer (1% NP40, 0.25% DOC, 10% glycerol, 2 mM EDTA, 137 mM NaCl, 20 mM Tris-HCl pH 8.0, Protease Inhibitors) for 10 min on ice. The lysate was cleared by centrifugation at 15,000g for 10 min at 4°C, and the supernatant kept at -80°C until use. For immune complex preparation, 1 mg of anti-His tag (His-6/9) mAb [26] was added to 50 ml of cell lysate and incubated over 3 days on an orbital shaker at 4°C. For immune complex purification, 1 ml of Protein G-coupled Sepharose beads (Sigma-Aldrich) was added and incubated under rotary agitation overnight at 4°C. The tubes were then centrifuged, the supernatants removed and the beads washed three times in NP40 Buffer (1% NP40, 10% glycerol, 2 mM EDTA, 137 mM NaCl, 20 mM Tris-HCl pH 8.0). To elute the immune complex, the resin was resuspended in 3 ml of Elution-Buffer (0.1M Glycine pH 2.8) containing 0.1% TX100. The eluate was collected by centrifugation and the pH neutralized with NaHCO₃, the buffer was exchanged to PBS-0.1% TX100 and the sample concentrated to 1 ml. Purified immune complex were kept at -80°C in fractions until use.

Immunization of mice

All procedures involving living animals were performed in strict accordance with the rules and regulations for the protection of animal rights (Tierschutzverordnung) of the Swiss Federal Food Safety and Veterinary Office. The protocol was granted ethical approval by the Veterinary Office of the county of Basel-Stadt, Switzerland (Permit numbers: 2375 and

2303). Specific pathogenfree HsdWin:NMRI outbred mice were purchased from Harlan Laboratories B.V. (The Netherlands) and used for immunizations studies.

Living cells immunization

Four Naval Medical Research Institute (NMRI) mice were immunized by intravenous (i.v.) injections of 10^6 transiently transfected HEK cells. Cells were thawed, washed and resuspended in 0.9% NaCl. Injections were accomplished on four consecutive days and, after two weeks, again on four consecutive days. Two weeks after the boost, blood was collected and the serum was tested for the presence of PF14_0044-specific antibodies by indirect Immunofluorescence assay (IFA) on HEK cells and Western blotting analysis on cell lysates.

Immune complex immunization

Four NMRI mice were immunized intraperitoneally (i.p.) with 20 μ g / injection of antigen emulsified in aluminum hydroxide gel (Alhydrogel-2%, Brenntag Biosector) containing CpG ODN as immune enhancer [30]. The animals received three booster injections at two weeks intervals with the same antigen preparation. Two weeks after the last boost, blood was collected and the serum was tested for the presence of PF14_0044-specific antibodies by IFA on HEK cells and Western blotting analysis on cell lysates.

Fusion and cell-based selection

The best immune responders were selected for fusion. Mice received two consecutive i.v. injections of 10^6 cells or single i.v. injection of 12.5 μ l of Immune complex in PBS two days before the fusion. Mice were sacrificed and spleens were removed. Splenocytes were fused to the myeloma cell partner (PAI mouse myeloma cells, derived from SP-20, Institute of Immunology, Basel) using polyethylene glycol 1500 (Roche Diagnostics) [31]. The fusion mix was plated in four 96-well culture plates at 10^7 cells/plate (remaining cells were aliquoted and frozen down as backup fusions) and hybridomas were selected by growing in HAT medium supplemented with culture supernatant of mouse macrophages P388. Wells were screened for IgG production two weeks post-fusion by ELISA as described previously [26]. IgG-producing hybrids were further screened for specific IgG production by IFA on methanol-fixed cells as described above. IFA-positive wells were cloned in HT medium by limiting dilution to obtain monoclonal populations.

Antibodies production and characterization

Identification of antibody subclasses was performed using a Mouse Monoclonal Antibody Isotyping Kit (ISO2, Sigma-Aldrich). For large-scale mAb production hybridoma cell lines were cultured in 500 ml roller-bottles (Corning). Antibodies were purified by affinity chromatography using Protein A Sepharose.

Plasmodium falciparum blood stage culture

Plasmodium falciparum strain 3D7 was cultured essentially as described previously [32]. The culture medium was supplemented with 0.5% AlbuMAX (Thermo Fisher Scientific) as a substitute for human serum [33]. Cultures were synchronized by sorbitol treatment [34]. Erythrocytes for passages were obtained from the Swiss Red Cross (Switzerland). *Plasmodium falciparum* merozoites were mechanically released from mature schizonts as previously described [35]. Briefly, late-stage parasites (40-46 h post-invasion) were purified by Percoll density gradient [36] and incubated with 10 μ M E-64 inhibitor (Sigma-Aldrich). After 6–8 h incubation, mature schizonts were filtered through 1.2 μ m filters to mechanically release merozoites. Then, merozoites were resuspended in PBS and stored at -80°C until further use.

Western blotting analysis

Blood stage parasite lysates were prepared essentially as described previously by saponin lysis of *Plasmodium falciparum* 3D7-infected erythrocytes [32]. In brief, cultured parasites were washed once with PBS. Pelleted infected red blood cells were lysed in 20 volumes of 0.06% (w/v) saponin in PBS and incubated on ice for 20 min. Parasites were washed in PBS and the final pellet was resuspended in 3 volumes of RIPA-Buffer and incubated for 10 min on ice. The lysate was cleared by centrifugation at 15,000g for 10 min at 4°C and the supernatant kept at -80°C until use. HEK cells lysate were produced at 10^7 cells/ml in RIPA-Buffer as described above. For SDS-PAGE recombinant PF14_0044, cell- or parasite lysates were resolved on precast 4-12% gradient gels (NuPAGE® Novex 4-12% Bis-Tris Gel, Thermo Fisher Scientific) with MES running buffer according to the manufacturer's directions. All samples were reduced with 50mM_f dithiothreitol (DTT) and heated to a temperature of 70°C for 10 minute prior to loading. The proteins were electrophoretically transferred to nitrocellulose membrane using a dry-blotting system (iBlot, Thermo Fisher Scientific). After blocking the membrane, specific proteins were detected with appropriate

dilutions of mAbs followed by Horseradish Peroxidase (HRP) conjugated goat anti-mouse IgG mAb (SouthernBiotech). Blots were developed using ECL Western blotting detection reagents (ECL Western Blotting Substrate, Pierce).

Immunofluorescence staining of infected erythrocytes and free merozoites

For indirect immunofluorescence microscopy, smears of infected red blood cells and isolated free merozoites were fixed in ice-cold 60% methanol and 40% acetone for 2 min at -20°C, air-dried and blocked with 3% BSA in PBS. Cells were probed with the following antibodies: biotinylated anti-PF14_0044 mAb 2/27, Alexa 488-labeled mouse anti-GAPDH 1.4a mAb [37], Alexa 568-conjugated streptavidin (Thermo Fisher Scientific). The slides were mounted in mounting medium containing DAPI (ProLong Gold antifade reagent with DAPI, Thermo Fisher Scientific). Fluorescence microscopy was performed on a Leica DM-5000B using a 60x oil immersion objective lens and documented with a Leica DFC345FX digital camera system. Images were processed using Leica Application Suite V4 (Leica) and Adobe Photoshop® CS6. For co-localization studies, cells were probed with the following antibodies: Alexa 568-labeled mouse anti-PF14_0044 mAb 2/27, Alexa 488-labeled mouse anti-RAP-1 5-2 mAb [38], Alexa 488-labeled mouse anti-AMA-1 DV5a mAb [39]. Fluorescence microscopy was performed on a API DeltaVision Core using a 100x oil immersion objective lens and documented with a Photometrics CoolSNAP HQ², interline transfer CCD. Images were processed using SoftWorx 4.1.2 and Adobe Photoshop® CS6.

In vitro growth inhibition assay

In vitro growth inhibition assays with *Plasmodium falciparum* strain 3D7 were conducted essentially as described [39]. Briefly, synchronous early trophozoites were diluted with fresh red blood cells to give a parasitemia of 0.5% and mixed with purified and sterile filtered mAbs. The final hematocrit in cultures was adjusted to 0.5%. Each culture was set up in triplicate in 96-well flat-bottomed culture plates. The cells were analyzed in a FACScan flow cytometer using CellQuest software (Becton Dickinson). A total of 30,000 cells per sample were analyzed. Percent inhibition was calculated from the mean parasitemia of triplicate test and control wells as follows:

$$\text{Percent inhibition (\%)} = \frac{\text{control} - \text{test}}{(\text{control}/100)}$$

Anti-PfCyRPA c12 mAb [17] was used as reference growth-inhibitory antibody. The anti-PfRON12 (*Plasmodium falciparum* rhoptry neck protein 12) mAb PF10-1/2, the anti-

PfSHLP2 (*Plasmodium falciparum* shewanella-like protein phosphatase 2) mAb PFL-2/30 and a malaria-unrelated anti-cortisol CORTI-4/16 mAb served as control antibodies.

Recombinant protein expression and purification

PF14_0044 (aa 21–290) was recombinantly expressed in mammalian cells employing the pcDNA3.1_BVM_PF14_0044_6xHis plasmid. When the PF14_0044 protein sequence was analyzed for the presence of N-glycosylation sites (NetNGlyc 1.0 Server) [Gupta et al. pers. comm.], one asparagine residue (N261) was predicted to be a potential site for N-glycosylation in human cells. To prevent the improper addition of glycans, which are absent from *Plasmodium* proteins [40], the potential N-linked glycosylation site (N-X-S/T, where X is not proline) was mutated by replacing the asparagine residue with glutamine (N261Q). The expression vector allows the secretion of the protein of interest in the cultivation medium: it contains the secretion signal of bee-venom melittin (BVM), the codon optimized coding sequence, and a C-terminal hexa-His tag. HEK cells were transfected as previously described and cell supernatant, containing secreted proteins, was harvested 72 hours post-transfection. Histidine-tagged proteins were purified by immobilized metal ion affinity chromatography (IMAC). The purity and integrity of the purified protein was analyzed by RP-HPLC on an Agilent 1290 Series with a Poroshell 300SB-C8, 1x75 mm column (Agilent). Chromatography was performed with a non-linear (H₂O + 0.01% TFA / Acetonitrile + 0.08% TFA) gradient system. The protein concentration was determined by measuring the OD₂₈₀ (1 Abs = 1 mg/ml). The purified recombinant protein was identified as the expected PF14_0044 protein by Western blotting analysis with PF14_0044-specific mAbs.

Detection of PF14_0044-specific Abs in human sera.

Human serum samples were derived from healthy individuals living along the Offin River in Ghana, a malaria endemic region [41]. ELISA plates (Maxisorp; Nunc) were coated with 1.5 µg/ml purified recombinant PF14_0044 protein produced in HEK cells. After blocking, plates were incubated with dilutions of human serum. HRPO-conjugated goat anti-human IgG γ chain specific (SouthernBiotech) was used as secondary Ab and tetramethylbenzidine substrate (KPL) was used for development. The reaction was stopped with 0.5 M H₂SO₄, and the OD was measured at 450 nm with a microplate absorbance reader (Sunrise Absorbance Reader; Tecan). Selected human serum samples were also tested for specificity by Western blotting analysis on recombinant PF14_0044; anti-PF14_0044 mAb 2/32 served as positive control.

Results

Sequence analysis of PF14_0044

The *PF14_0044* encoding gene (GeneID: 811626) is 873 bp long and located in the subtelomeric region of chromosome 14. Orthologs of *PF14_0044* are present in the genomes of *Plasmodium vivax* (PVX_086200), *Plasmodium knowlesi* (PKH_134220), *Plasmodium cynomology* (PCYB_135180), *Plasmodium reichenowi* (PRCDC_1404000), *Plasmodium berghei* (PBANKA_103740), *Plasmodium chabaudi* (PCHAS_103820), and *Plasmodium yoelii* (PY17X_1039800) with an average identity of 63.25% (see Additional file 1). To evaluate the genetic diversity of *PF14_0044* in *Plasmodium falciparum* we analyzed the gene sequences of 190 isolates (see Additional file 2) available on the plasmodia database PlasmoDB [42]. All sequences were identical to the *Plasmodium falciparum* 3D7 reference sequence with the exception of twelve non-synonymous single nucleotide polymorphism (SNP) and six deletions distributed along the gene (Fig. 1; see Additional file 2). The **nucleotide diversity**^a calculated for this population was $\text{Pi: } 0.00214$.

pfa13D7 PF14_0044	MIK VLLAVL FILIKLENI <u>IG</u> QDEKSVKNICVCDFTDKLNFLPLEKTKILCELKPO Y GEDI	60
	KIIANKEYEINCMNNSKVFCPLKDTFINNTNIKLYSPKLFHEIKDITHKGKNAALYYLKI	120
	DEEASDIFFFSCSIKPKQ V SLLEGEVRVNLKKHINEEYSIFN EED VHVCDFSKGNLDIT	180
	PSAGF Y LKNSRNVSCIYRVIPNKLFLIKLPKLDI V TEKLLPSIVNCLSEFSFINFTLKHV	240

Fig. 1 Amino acid sequence of *Plasmodium falciparum* PF14_0044. Amino acid residues of the predicted secretion signal sequences are indicated in boldface. Twelve non-synonymous SNPs (shaded in grey) and 6 deletions (underlined) are indicated.

Generation of anti-PF14_0044 monoclonal antibodies in mice

A HEK cell line expressing *Plasmodium falciparum* PF14_0044 as transmembrane protein was established by transient transfection. To ensure expression on the mammalian cell surface, the PF14_0044 sequence was codon-optimized for expression in human cells and the endogenous secretion signal sequences (aa. 1-20) was replaced by the secretion signal sequence of bee-venom melittin. For membrane anchoring the transmembrane domain encoding sequence of mouse glycoporphin-A was used and, to allow expression analysis, a FLAG tag was inserted N-terminally of the transmembrane domain and a hexa-His tag was placed at the C-terminus. Expression of recombinant PF14_0044 was confirmed by Western blotting analysis and immunofluorescence analysis (IFA) using an anti-His tag mAb [26]. The PF14_0044 expressing cells were used for (i) living cell immunization and (ii) generation of immune complexes derived from the lysate of the transfected HEK cells with an anti-His tag

mAb. NMRI mice received intravenous injections of living transfected HEK cells or intraperitoneal injections of immune complexes. Development of serum anti-PF14_0044 antibody titers was assessed by Western blotting analysis (Fig. 2). While discrete PF14_0044 bands were detected when lysates of PF14_0044 expressing cells were probed, no specific staining was observed in the control cell lysates.

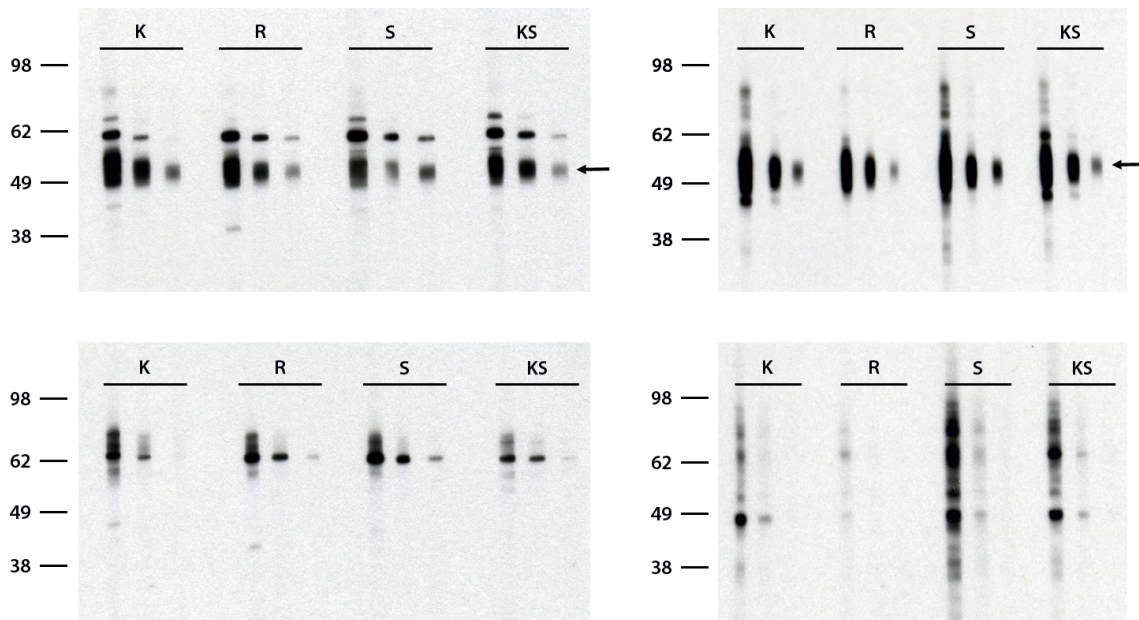


Fig. 2 Development of anti-PF14_0044 IgG response in mice. Western blotting analysis of sera from mice immunized with living cells (A) and immune complexes (B). Lysates of HEK cells transfected with PF14_0044 (upper panel) and control cell line (lower panel) were probed with serial dilution of sera from individual mice (S, R, K, KS). Sera were taken two weeks after second round of immunization.

Also in IFA, transfectants showed strong immunostaining compared to control cell lines. These data indicated that both formulations were highly immunogenic and that mice had mounted a strong humoral immune response specific for the recombinant PF14_0044. Spleen cells of two mice per group of immunization (living cells: R, S; immune complexes: K, R) were pooled and fused with PAI myeloma cells to generate B cell hybridomas. To identify hybridoma cells producing PF14_0044 specific antibodies, a two-step screening procedure was used. All cell culture wells were tested for IgG production by ELISA: between 80% (immune complex) and 90% (living cells) of tested wells were IgG-positive. Afterwards, supernatants of 12 IgG-producing wells were randomly selected from each plate (48 wells in total) for IFA screening. Transfected and control HEK cells spotted onto multiwell glass slides were stained with individual hybridoma supernatants and analyzed by fluorescence microscopy. Each fusion yielded numerous wells containing antibodies strongly reactive with transfectants but not reactive with control cells. From these wells, altogether eight hybridoma clones producing anti- PF14_0044 IgG were derived by limiting dilution (Table 1). To

determine whether the mAbs generated against heterologously expressed PF14_0044 would bind to the endogenous protein of *Plasmodium falciparum* parasites, we performed IFA and Western blotting analysis using cultivated blood-stage parasites (Fig. 3, Table 1). All eight generated anti-PF14_0044 mAbs stained specifically late blood-stage parasites in IFA, whereas just one of them (PF14-2/32) was positive in Western blotting analysis on parasite lysate.

Table 1. Specificities of generated anti-PF14_0044 mAbs.

Immunization	mAb	IgG class	Western blotting analysis		IFA	
			PF14_0044 HEK-293	<i>P. falciparum</i> 3D7	PF14_0044 HEK-293	<i>P. falciparum</i> 3D7
Living cells	1/21	IgG2b	-	-	+	+
	1/40	IgG2b	+	-	+	+
	1/44	IgG1	+	-	+	+
Immune Complex	2/14	IgG1	+	-	+	+
	2/20	IgG1	+	-	+	+
	2/27	IgG1	+	-	+	+
	2/32	IgG1	+	+	+	+
	2/44	IgG1	+	-	+	+

Anti-PF14_0044 mAbs were characterized by Western blotting analyses and immunofluorescence assays performed on HEK cells expressing recombinant PF14_0044 and *Plasmodium falciparum* 3D7 schizont stages.

Stage-specific expression and localization of PF14_0044 in schizonts and free merozoites

The *PF14_0044* gene encodes a 290-aa-long protein with a predicted molecular mass of 33.3 kDa. Using highly synchronized asexual blood-stage parasite cultures, we assessed the expression profile of PF14_0044 in *Plasmodium falciparum* across the intraerythrocytic developmental cycle (Fig. 3A). In Western blotting analysis, a discrete band of ~40 kDa was detected in schizonts and free merozoites but not in rings and early trophozoites. Stage-specific expression in schizont stages and free merozoites was confirmed by indirect immunofluorescence staining of synchronized blood-stage parasites with the anti-PF14_0044 mAb 2/27 (Fig. 3B). To determine the localization of PF14_0044 in schizont stages more accurately, we performed co-localization studies using Abs specific for the micronemes (AMA-1) [43] and the rhoptry bulbs (RAP-1) [44]. Schizonts showed a dotted staining pattern with PF14_0044-specific mAbs, neither co-localizing with rhoptry bulbs nor with micronemes (Fig. 4).

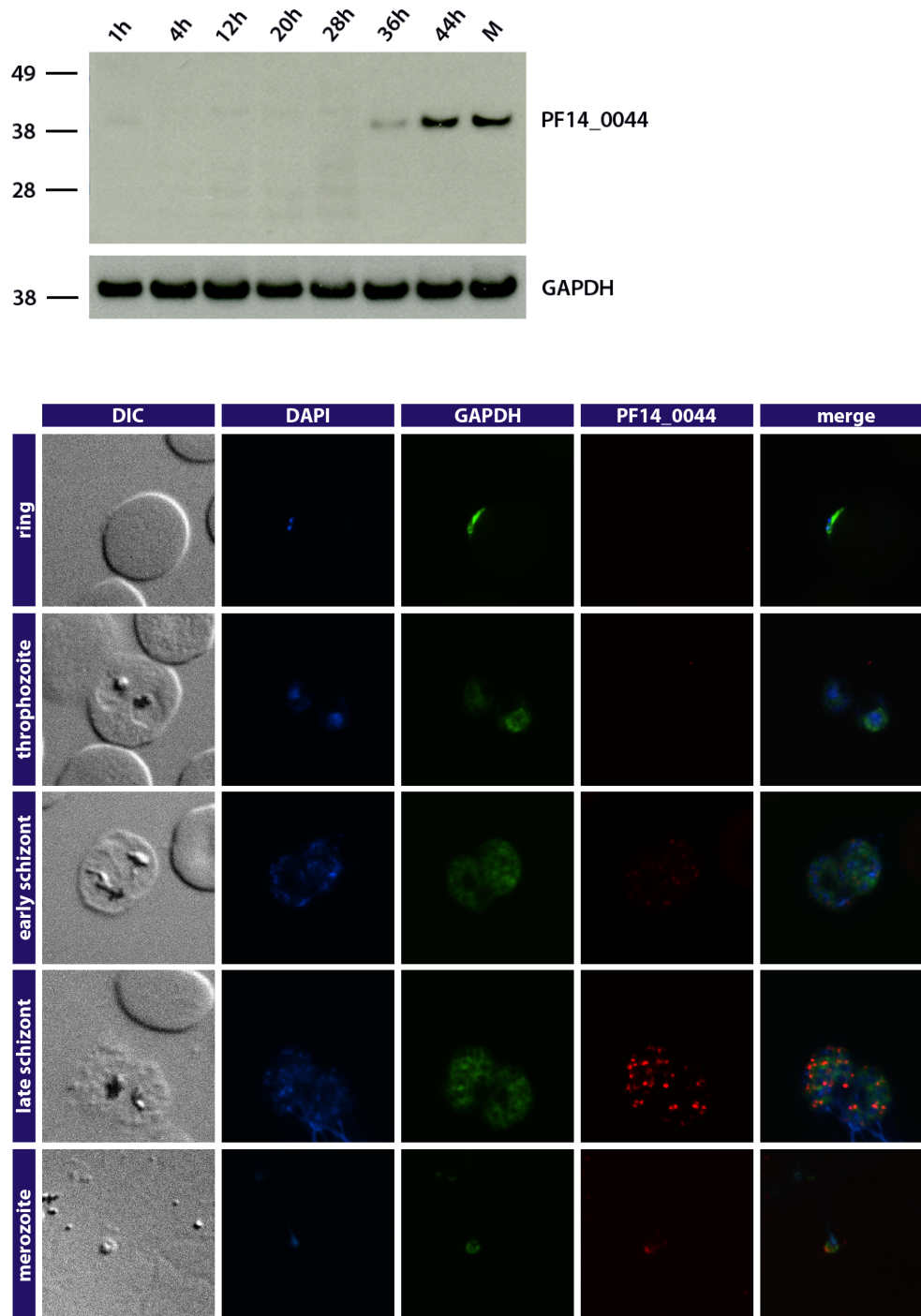


Fig. 3 Stage specific expression of PF14_0044 in late asexual blood stage parasites. **(A)** Western blot analysis of lysates of tightly synchronized *Plasmodium falciparum* 3D7 asexual blood stage parasites 1, 4, 12, 20, 28, 36, 44 hours post-invasion and of free merozoites (M) with anti-PF14_0044 mAb 2/32 (upper panel). The blot was probed for equal loading with an anti-GAPDH mAb (lower panel). **(B)** Indirect immunofluorescence stainings of tightly synchronized asexual blood stage parasites confirmed stage specific expression in schizont stages and free merozoites. Methanol/acetone fixed *Plasmodium falciparum* 3D7 parasites were probed with anti-PF14_0044 mAb 2/27 (red) and anti-GAPDH mAb (green). Exposure times were identical for all pictures of the same channel.

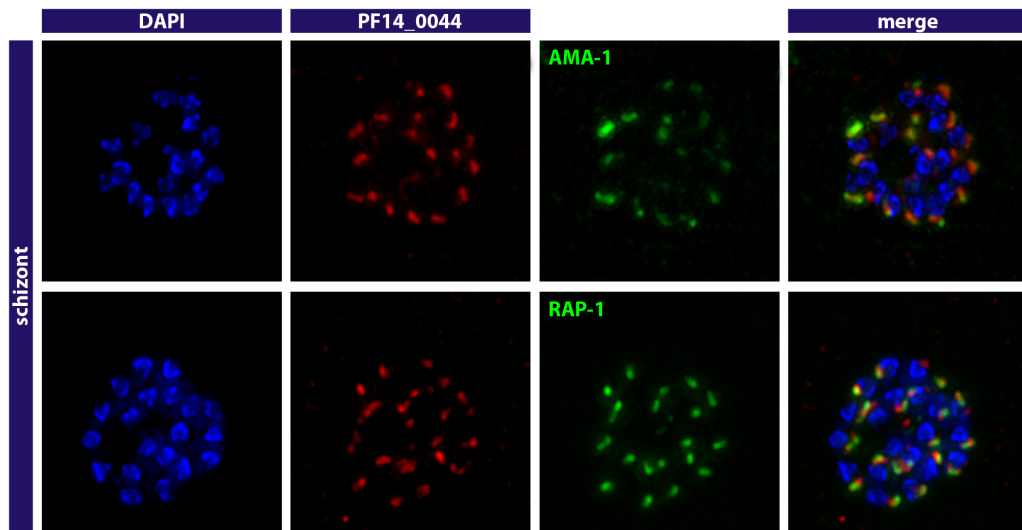


Fig. 4 Localisation of PF14_0044 to the merozoite apex by immunofluorescence staining
Plasmodium falciparum 3D7 schizont stages were co-immunostained with anti-PF14_0044 mAb 2/27 (red) and AMA-1 (marker for micronemes) or RAP-1 (marker for rhoptry bulbs) (green). Nuclei were stained with DAPI (blue).

Synergistic effect of anti-CyRPA and anti-PF14_0044 mAbs in an *in vitro* growth inhibition assay

Considering the expression profile and the apical localization of PF14_0044, we tested anti-PF14_0044 mAbs for *in vitro* parasite growth inhibitory activity. Growth inhibition assays were conducted with *Plasmodium falciparum* 3D7 parasites for two cycles of merozoite invasion. None of the anti-PF14_0044 mAbs showed more than marginal growth inhibitory activity even at a concentration as high as 500 $\mu\text{g/ml}$ (Fig. 5A). However, a significant synergistic inhibitory activity was measured when combining the growth inhibitory anti-PfCyRPA mAb c12 [17,26,28] with the anti-PF14_0044 mAb PF14-1/44 (Fig. 5A). This synergistic effect was observed for all eight generated anti-PF14_0044 mAbs (Fig. 4B), but with none of the tested control antibodies specific for the *Plasmodium falciparum* antigens PfRON12 and PfSHLP2 (PF10-1/2 and PFL-2/30 mAbs, respectively), or malaria-unrelated anti-cortisol CORTI-4/16 mAb (Fig. 4A). All tested mAbs were produced and purified in the same way and results were reproducible in independent experiments and with independent mAb production batches.

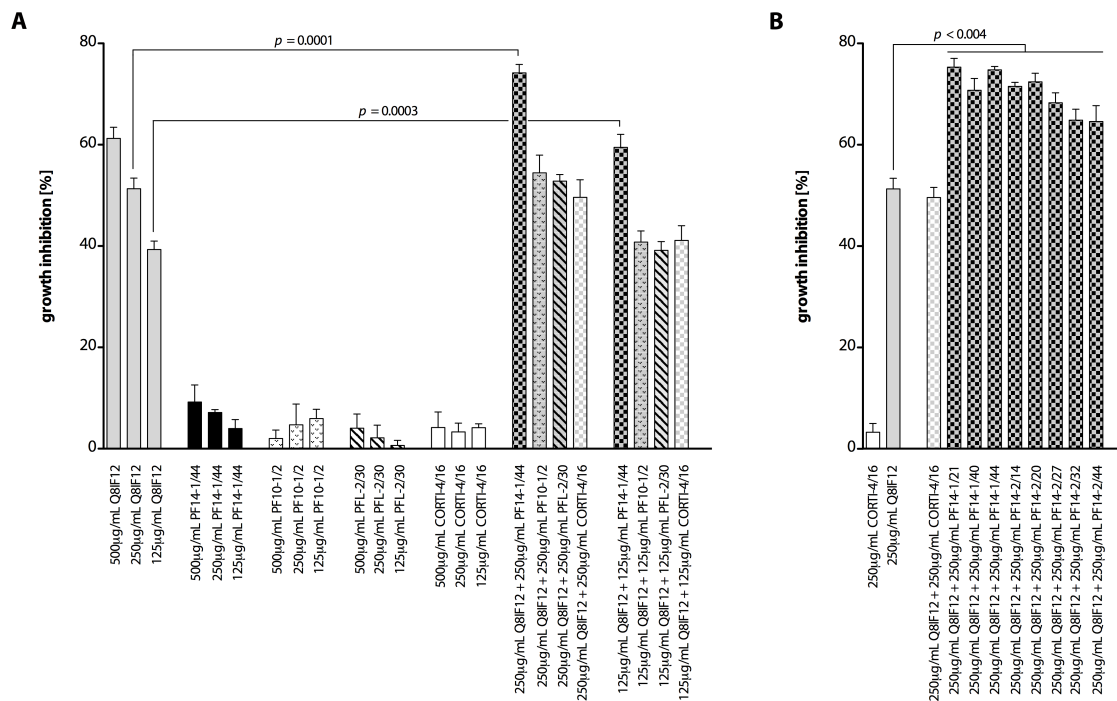


Fig. 5 Synergistic inhibitory activity of anti-CyRPA and anti-PF14_0044 mAbs. (A, B) Synchronized *Plasmodium falciparum* 3D7 blood-stage parasites were cultured for two cycles in the presence of combinations of different mAbs. Percent parasite growth inhibition was calculated against the parasitemia of PBS control wells. Anti-CyRPA Q8IF12 mAb [17] was used as reference growth-inhibitory antibody; anti-PfRON12 PF10-1/2 mAb, anti-PfSHLP2 PFL-2/30 mAb, and a malaria-unrelated anti-cortisol CORTI-4/16 mAb served as control antibodies. Each bar represents the mean of a triplicate experiment, and error bars indicate the SD. Significant differences in parasite growth inhibition are indicated (unpaired t test, 95% confidence interval, two-tailed p value). All mAbs tested were produced and purified in the same manner and results were reproducible in independent experiment and with independent mAb production batches.

Natural immunogenicity of PF14_0044

To examine if natural exposure to *Plasmodium falciparum* leads to the development of anti-PF14_0044 Abs, human sera were analyzed by ELISA for their reactivity with purified recombinant PF14_0044 (Fig. 6A). Selected samples were further analyzed for specificity by Western blotting analysis (Fig. 6B). Sera were collected from healthy individuals living along the Offin River in Ghana, where *Plasmodium falciparum* is highly endemic [1,41]. Among 81 randomly tested sera, 21 (25.9 %) showed the presence of IgG specific for recombinant PF14_0044 protein (Fig. 5A). Selected samples among ELISA-positive and negative samples, were further analyzed by Western blotting on recombinant PF14_0044 confirming the specificity of the serological response (Fig. 6B). In similar analyses >60% of sere were positive for AMA-1 and MSP-3, reflecting the strong exposure of the population to *Plasmodium falciparum* [41].

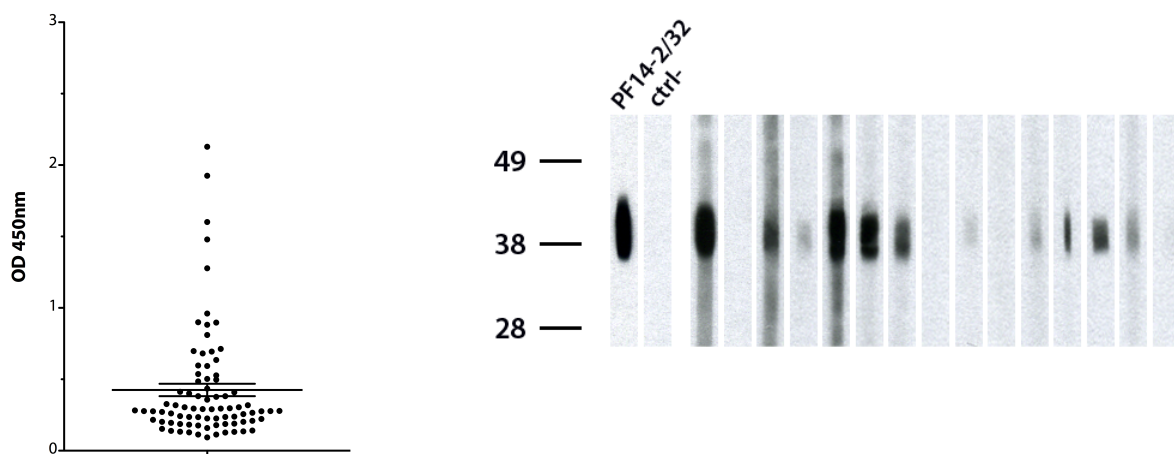


Fig. 6 Analysis of serum from malaria-exposed individuals for presence of PF14_0044-specific IgG. (A) Reactivity of human sera from 81 randomly selected individuals living along the Offin River in Ghana (malaria exposed) with recombinant PF14_0044 assessed by ELISA. Shown are IgG levels expressed as OD at 450 nm of serum samples diluted 1:400 (mean OD_{450} 0.93 ± 0.1 for positive and 0.25 ± 0.01 for negative samples). Horizontal lines designate means and SEM of responses. (B) Western blot analysis of recombinant PF14_0044 with selected 15 human sera; anti-PF14_0044 mAb 2/32 served as positive control.

Discussion

Despite being preventable and treatable, malaria still represents a massive global public health problem, threatening the lives of 3.2 billion people around the world [45]. Substantial improvements have been achieved in malaria control over the past decade as result of major investments in vector control, chemoprevention, diagnostic testing and treatment. To pursue the goal of reducing malaria case incidence and mortality rates globally by at least 90% in 2030 (compared to 2015) [46], the development and introduction of a malaria vaccine with protective efficacy of at least 75% would be an important addition to the arsenal of preventive tools. However, the complexity of the malaria parasite makes the development of an effective malaria vaccine a very difficult task. Despite many decades of intense research and development effort, there is currently no malaria vaccine commercially available. A number of vaccine candidates, with different modes of action and in different formulations, are currently in various stages of pre-clinical and clinical evaluation [14]. Among them, the most advanced is the pre-erythrocytic subunit vaccine RTS,S/AS01 which has completed Phase 3 [6]. Although immunodominant antigens induce very strong antibody responses, they typically vary antigenically to escape immune pressure and therefore possess substantial polymorphisms. Malaria vaccines based on immunodominant and polymorphic antigens have the risk of limited efficacy and protection, suggesting that the key protective malarial antigens might be the non-immunodominant antigens [47,48]. The research for novel malaria vaccine candidate antigens has received a great incentive from the genome-wide transcriptomic and proteomic data that have become available since the publication of the *Plasmodium falciparum* genome [22]. Since then, major efforts have been invested in the annotation of the *Plasmodium falciparum* genome. Nevertheless, the vast majority of the proteins are still not characterized. Therefore, we used a reverse vaccinology-based strategy to selected uncharacterized ORFs and evaluate their potential as asexual blood-stage vaccine candidate antigens [26]. Among the characterized proteins, PfCyRPA exhibited outstanding properties, demonstrating the utility of systematic genome-wide approaches for vaccine antigen selection [17,28]. Antibodies specific for PfCyRPA showed a strong parasite growth inhibitory activity by targeting the process of merozoite invasion into RBCs. Indeed, PfCyRPA has recently been identified as the key component of an essential complex on the surface of invading merozoites: PfCyRPA interacts with the RH5-interacting protein (PfRipr) and the Reticulocyte binding-like Homologous protein 5 (PfRH5), which binds the basigin receptor on the erythrocyte surface [27]. Anti-PfCyRPA and anti-PfRH5 mAbs inhibit, but do not

completely block, parasite growth by interfering with a crucial pathway for invasion of erythrocytes by merozoites [17,28,49]. *Plasmodium falciparum* merozoites are described to use alternative invasion pathways to evade Ab-mediated immunity [50] and the use of a PfCyRPA/PfRH5-independent invasion pathway of limited efficiency could explain persistence of infection associated with a reduced multiplication rate. In addition to the great potential shown by PfCyRPA and PfRH5 as vaccine candidate on their own [17,18,28], a synergistic in vitro inhibitory activity has also been reported for the combination of polyclonal anti-PfCyRPA and anti-PfRH5 antibodies [27]. Hence, it remains essential to identify next-generation vaccine candidate antigens and systematically assess their potential to induce antibodies that act synergistically when administered in multi-antigen formulations. To identify novel target antigens for protective immune responses, available genome-wide transcriptomic and proteomic data of the intra-erythrocytic stages of *Plasmodium falciparum* [2] were analyzed to pick out additional antigens potentially implicated in erythrocyte invasion. Candidate antigens were selected according to four main criteria: (i) expression peak in schizont and merozoite stages [51,52], (ii) mass spectrometry evidence for expression in detectable amounts, (iii) predicted signal peptide and/or a single transmembrane domain/GPI anchor attachment site (secreted and cell surface exposed proteins) [53–55], (iii) suitability for recombinant expression (molecular mass below 100 kDa and devoid of long stretches of repetitive amino acids). Although heterologous protein production has now become relatively easy and successful for proteins of diverse origins, the functional expression of plasmodial proteins has remained problematic [56]. The plasmodial proteome is enriched in proteins with high molecular weight (> 50 kDa), basic isoelectric point (pI > 6), and presence of low complexity regions [57]. For the expression, characterization and functional analysis of membrane-associated plasmodial proteins we favored an eukaryotic expression platform and expressed them on the surface of transfected mammalian cells, bypassing any need for purification of the recombinant proteins [26]. For the characterization of selected candidate antigens we (I) generated mammalian cell lines expressing high levels of the target antigen as His-tagged, transmembrane proteins; (II) used the transfected living cells, or immune complexes derived from them, for immunization of mice; (III) generated B cell hybridoma cell lines for the production of target antigen-specific mAbs. Among three recently investigated antigens (PF10_0166, PFL0300c, PF14_0044), PF14_0044 showed interesting features. A panel of eight mAbs was generated and employed to assess localization and stage-specific expression pattern of PF14_0044 in blood-stage parasites. In agreement with available transcriptional data, showing elevated transcript levels in late stages of the

asexual blood cycle of *Plasmodium falciparum* with maximal expression measured at 40 to 48h post invasion [51,52,58], we observed for PF14_0044 a stage-specific expression in schizonts and free merozoites. Similarly to PfCyRPA, it localized to a merozoites apical structure distinct from rhoptry bulbs and micronemes. However, in contrast to many anti-PfCyRPA antibodies, none of the anti-PF14_0044 mAbs significantly inhibited the growth of *Plasmodium falciparum* 3D7, but showed even at high concentrations only marginal growth inhibitory activity. However, a strong synergistic effect was observed when anti-PF14_0044 mAbs were combined with parasite growth inhibitory anti-PfCyRPA mAbs (Fig. 5). Here a greater inhibitory activity was observed than dose-wise additivity (unpaired *t* test, 95% confidence interval, two-tailed *p* value). To further investigate the detected synergy, for each combination of antibodies we also calculated the predicted GIA that would be achieved by the two components having an independent, additive effect by using the definition of Bliss additivity [59–61]. The observed growth inhibition was significantly higher than the predicted values at both concentrations of 250 µg/ml and 125 µg/ml ($p < 0.01$ and $p < 0.03$ respectively; 2-way ANOVA with Bonferroni post-hoc testing, 95% confidence interval). Given the complexity of *Plasmodium falciparum* erythrocyte invasion mechanisms [62,63], PfCyRPA-specific and PF14_0044-specific antibodies may exert a synergistic effect by acting ‘in series’, inhibiting successive stages of invasion or, alternatively, they may act ‘in parallel’, inhibiting redundant invasion processes [60]. Also, similarly to PfCyRPA, natural immunogenicity of PF14_0044 appears to be limited (Fig. 6) and, sequence analyses indicate that PF14_0044 have low nucleotide diversity^a and no substantial sequence polymorphisms, reducing the risk of limited efficacy and protection. It has been shown that relatively high titers of antigen-specific antibodies are required to achieve protective effects in animal malaria models [64–67]. Despite the improvements in vaccine delivery systems and adjuvant formulations [68,69], convincing protective immunity in humans has not been achieved yet. One of the strategies to achieve effective protection appears to be to assess the potential of candidate antigens to induce antibodies that act synergistically, lowering the individual titers needed for parasite neutralization [70].

Conclusions

Given the complexity of *Plasmodium falciparum* erythrocyte invasion mechanism and the extensive genetic diversity found in many *Plasmodial* antigens, the identification of new candidate antigens, able to induce broad strain-transcending immunity, has become an eager research focus. Here it is shown that PF14_0044-specific mAbs act synergistically with PfCyRPA-specific antibodies and thus enhancing the growth inhibitory effect. Our findings support the concept of rational genome-based selection of next-generation vaccine candidates.

Key words

Malaria, blood-stage vaccines, parasite growth inhibition.

Abbreviations

CyRPA: Cysteine-Rich Protective Antigen; PfCyRPA *Plasmodium falciparum* CyRPA; PfRH5: *Plasmodium falciparum* reticulocyte binding-like homologous protein 5; PfRipr: PfRH5-interacting protein; CSP: Circumsporozoite protein; MSP: Merozoite surface protein; AMA: Apical membrane protein.

Authors' contributions

PF was responsible for experimental design, performed the experiments and data analysis described in this study and drafted the manuscript. AMD contributed to the conception and design of the study. AL contributed to the bioinformatics analyses. HM contributed to the conception of the study, participated in its design and assisted in data interpretation. GP conceived the study, participated in the study design, coordinated the collaborations that made this study possible and revised the manuscript. All authors read and approved the final manuscript.

Acknowledgements

We thank Georg Schmid and Elvira Da Silva for cell transfections, Doris Zulauf for technical assistance concerning hybridoma cell generation and Bernard Rutten for mAb purification.

Disclosures

The authors declare that they have no competing interests.

Funding

This work was supported by a research grant from the Swiss National Science Foundation (310000-116337/1).

Endnotes

^a**Nucleotide diversity**, in molecular genetics, measures the degree of polymorphism within a population. Nei and Li in 1979 [71] introduced a commonly used measure of nucleotide diversity, defined as the average number of nucleotide differences per site between any two DNA sequences chosen randomly from the sample population.

References

1. WHO | World Malaria Report 2016 [Internet]. [cited 2017 Feb 1]. Available from: <http://www.who.int/malaria/publications/world-malaria-report-2016/en/>
2. PlasmoDB: The Plasmodium Genomics Resource [Internet]. [cited 2016 Jun 7]. Available from: <http://plasmodb.org/plasmo/>
3. Cohen S, McGregor IA, Carrington S. Gamma-globulin and acquired immunity to human malaria. *Nature*. 1961 Nov 25;192(4804):733–7.
4. Sabchareon A, Burnouf T, Ouattara D, Attanath P, Bouharoun-Tayoun H, Chantavanich P, et al. Parasitologic and clinical human response to immunoglobulin administration in falciparum malaria. *Am J Trop Med Hyg*. 1991 Sep;45(3):297–308.
5. Moreno A, Joyner C. Malaria vaccine clinical trials: what's on the horizon. *Curr Opin Immunol*. 2015 Aug;35:98–106.
6. RTS,S Clinical Trials Partnership. Efficacy and safety of RTS,S/AS01 malaria vaccine with or without a booster dose in infants and children in Africa: final results of a phase 3, individually randomised, controlled trial. *Lancet Lond Engl*. 2015 Jul 4;386(9988):31–45.
7. Remarque EJ, Faber BW, Kocken CHM, Thomas AW. Apical membrane antigen 1: a malaria vaccine candidate in review. *Trends Parasitol*. 2008 Feb;24(2):74–84.
8. Ogutu BR, Apollo OJ, McKinney D, Okoth W, Siangla J, Dubovsky F, et al. Blood stage malaria vaccine eliciting high antigen-specific antibody concentrations confers no protection to young children in Western Kenya. *PLoS One*. 2009;4(3):e4708.
9. Sagara I, Dicko A, Ellis RD, Fay MP, Diawara SI, Assadou MH, et al. A randomized controlled phase 2 trial of the blood stage AMA1-C1/Alhydrogel malaria vaccine in children in Mali. *Vaccine*. 2009 May 18;27(23):3090–8.
10. Laurens MB, Thera MA, Coulibaly D, Ouattara A, Kone AK, Guindo AB, et al. Extended Safety, Immunogenicity and Efficacy of a Blood-Stage Malaria Vaccine in Malian Children: 24-Month Follow-Up of a Randomized, Double-Blinded Phase 2 Trial. *PLoS ONE*. 2013 Nov 18;8(11):e79323.
11. Schwartz L, Brown GV, Genton B, Moorthy VS. A review of malaria vaccine clinical projects based on the WHO rainbow table. *Malar J*. 2012;11(11):10–1186.
12. Hoffman SL, Vekemans J, Richie TL, Duffy PE. The march toward malaria vaccines. *Vaccine*. 2015 Nov 27;33 Suppl 4:D13–23.
13. Goodman AL, Draper SJ. Blood-stage malaria vaccines - recent progress and future challenges. *Ann Trop Med Parasitol*. 2010 Apr;104(3):189–211.
14. WHO | Tables of malaria vaccine projects globally [Internet]. WHO. [cited 2017 Apr 18]. Available from: http://www.who.int/immunization/research/development/Rainbow_tables/en/
15. Doolan DL, Hoffman SL. Multi-gene vaccination against malaria: A multistage, multi-immune response approach. *Parasitol Today*. 1997 May;13(5):171–8.
16. Liu W, Li Y, Learn GH, Rudicell RS, Robertson JD, Keele BF, et al. Origin of the human malaria parasite *Plasmodium falciparum* in gorillas. *Nature*. 2010 Sep 23;467(7314):420–5.
17. Dreyer AM, Matile H, Papastogiannidis P, Kamber J, Favuzza P, Voss TS, et al. Passive immunoprotection of *Plasmodium falciparum*-infected mice designates the CyRPA as candidate malaria vaccine antigen. *J Immunol Baltim Md 1950*. 2012 Jun 15;188(12):6225–37.
18. Douglas AD, Williams AR, Illingworth JJ, Kamuyu G, Biswas S, Goodman AL, et al. The blood-stage malaria antigen PfRH5 is susceptible to vaccine-inducible cross-strain neutralizing antibody. *Nat Commun*. 2011 Dec 20;2:601.

19. Osier FHA, Fegan G, Polley SD, Murungi L, Verra F, Tetteh KKA, et al. Breadth and Magnitude of Antibody Responses to Multiple Plasmodium falciparum Merozoite Antigens Are Associated with Protection from Clinical Malaria. *Infect Immun*. 2008 May 1;76(5):2240–8.
20. Crompton PD, Kayala MA, Traore B, Kayentao K, Ongoiba A, Weiss GE, et al. A prospective analysis of the Ab response to Plasmodium falciparum before and after a malaria season by protein microarray. *Proc Natl Acad Sci*. 2010 Apr 13;107(15):6958–63.
21. Daou M, Kouriba B, Ouédraogo N, Diarra I, Arama C, Keita Y, et al. Protection of Malian children from clinical malaria is associated with recognition of multiple antigens. *Malar J*. 2015 Feb 5;14(1):56.
22. Gardner MJ, Hall N, Fung E, White O, Berriman M, Hyman RW, et al. Genome sequence of the human malaria parasite Plasmodium falciparum. *Nature*. 2002;419(6906):498–511.
23. Proietti C, Doolan DL. The case for a rational genome-based vaccine against malaria. *Front Microbiol*. 2014;5:741.
24. Rappuoli R. Reverse vaccinology. *Curr Opin Microbiol*. 2000;3(5):445–450.
25. Donati C, Rappuoli R. Reverse vaccinology in the 21st century: improvements over the original design: Reverse vaccinology in the 21st century. *Ann N Y Acad Sci*. 2013 May;1285(1):115–32.
26. Dreyer AM, Beauchamp J, Matile H, Pluschke G. An efficient system to generate monoclonal antibodies against membrane-associated proteins by immunisation with antigen-expressing mammalian cells. *BMC Biotechnol*. 2010;10:87.
27. Reddy KS, Amlabu E, Pandey AK, Mitra P, Chauhan VS, Gaur D. Multiprotein complex between the GPI-anchored CyRPA with PfRH5 and PfRipr is crucial for *Plasmodium falciparum* erythrocyte invasion. *Proc Natl Acad Sci*. 2015 Jan 27;112(4):1179–84.
28. Favuzza P, Blaser S, Dreyer AM, Riccio G, Tamborrini M, Thoma R, et al. Generation of Plasmodium falciparum parasite-inhibitory antibodies by immunization with recombinantly-expressed CyRPA. *Malar J*. 2016;15:161.
29. Québatte G, Kitas E, Seelig J. riDOM, a cell penetrating peptide. Interaction with phospholipid bilayers. *Biochim Biophys Acta BBA - Biomembr*. 2014 Mar;1838(3):968–77.
30. Davis HL, Weeratna R, Waldschmidt TJ, Tygrett L, Schorr J, Krieg AM, et al. CpG DNA is a potent enhancer of specific immunity in mice immunized with recombinant hepatitis B surface antigen. *J Immunol Baltim Md 1950*. 1998 Jan 15;160(2):870–6.
31. Köhler G, Milstein C. Continuous cultures of fused cells secreting antibody of predefined specificity. 1975. *J Immunol Baltim Md 1950*. 2005 Mar 1;174(5):2453–5.
32. Matile H, Pink JR. Plasmodium falciparum malaria parasite cultures and their use in immunology. In: *Immunological methods*. Volume IV. Edited by Lefkovits I, Pernis B. San Diego: Academic Press; 1990. p. 221-234.
33. Dorn A, Stoffel R, Matile H, Bubendorf A, Ridley RG. Malarial haemozoin/beta-haematin supports haem polymerization in the absence of protein. *Nature*. 1995 Mar 16;374(6519):269–71.
34. Lambros C, Vanderberg JP. Synchronization of Plasmodium falciparum erythrocytic stages in culture. *J Parasitol*. 1979 Jun;65(3):418–20.
35. Boyle MJ, Wilson DW, Richards JS, Riglar DT, Tetteh KKA, Conway DJ, et al. Isolation of viable Plasmodium falciparum merozoites to define erythrocyte invasion events and advance vaccine and drug development. *Proc Natl Acad Sci*. 2010 Aug 10;107(32):14378–83.

36. Rivadeneira EM, Wasserman M, Espinal CT. Separation and concentration of schizonts of *Plasmodium falciparum* by Percoll gradients. *J Protozool.* 1983 May;30(2):367–70.
37. Daubenberger CA, Tisdale EJ, Curcic M, Diaz D, Silvie O, Mazier D, et al. The N^o-terminal domain of glyceraldehyde-3-phosphate dehydrogenase of the apicomplexan *Plasmodium falciparum* mediates GTPase Rab2-dependent recruitment to membranes. *Biol Chem.* 2003 Aug;384(8):1227–37.
38. Moreno R, Pörtl-Frank F, Stüber D, Matile H, Mutz M, Weiss NA, et al. Rhoptry-associated protein 1-binding monoclonal antibody raised against a heterologous peptide sequence inhibits *Plasmodium falciparum* growth in vitro. *Infect Immun.* 2001 Apr;69(4):2558–68.
39. Mueller MS, Renard A, Boato F, Vogel D, Naegeli M, Zurbriggen R, et al. Induction of parasite growth-inhibitory antibodies by a virosomal formulation of a peptidomimetic of loop I from domain III of *Plasmodium falciparum* apical membrane antigen 1. *Infect Immun.* 2003 Aug;71(8):4749–58.
40. Dieckmann-Schuppert A, Bender S, Odenthal-Schnittler M, Bause E, Schwarz RT. Apparent lack of N-glycosylation in the asexual intraerythrocytic stage of *Plasmodium falciparum*. *Eur J Biochem.* 1992 Apr 1;205(2):815–25.
41. Ampah KA, Nickel B, Asare P, Ross A, De-Graft D, Kerber S, et al. A Sero-epidemiological Approach to Explore Transmission of *Mycobacterium ulcerans*. *PLoS Negl Trop Dis.* 2016 Jan 25;10(1):e0004387.
42. Aurrecochea C, Brestelli J, Brunk BP, Dommer J, Fischer S, Gajria B, et al. PlasmoDB: a functional genomic database for malaria parasites. *Nucleic Acids Res.* 2009 Jan;37(Database issue):D539–43.
43. Healer J, Crawford S, Ralph S, McFadden G, Cowman AF. Independent translocation of two micronemal proteins in developing *Plasmodium falciparum* merozoites. *Infect Immun.* 2002 Oct;70(10):5751–8.
44. Howard RF, Narum DL, Blackman M, Thurman J. Analysis of the processing of *Plasmodium falciparum* rhoptry-associated protein 1 and localization of Pr86 to schizont rhoptries and p67 to free merozoites. *Mol Biochem Parasitol.* 1998 Apr 1;92(1):111–22.
45. WHO | World Malaria Report 2015 [Internet]. WHO. [cited 2016 Jan 15]. Available from: <http://www.who.int/malaria/publications/world-malaria-report-2015/report/en/>
46. WHO | Global Technical Strategy for Malaria 2016–2030 [Internet]. WHO. [cited 2016 Jun 7]. Available from: http://www.who.int/malaria/areas/global_technical_strategy/en/
47. Doolan DL. *Plasmodium* immunomics. *Int J Parasitol.* 2011 Jan;41(1):3–20.
48. Chia WN, Goh YS, Rénia L. Novel approaches to identify protective malaria vaccine candidates. *Front Microbiol* [Internet]. 2014 Nov 17 [cited 2015 Apr 21];5. Available from: <http://www.ncbi.nlm.nih.gov/pmc/articles/PMC4233905/>
49. Douglas AD, Williams AR, Knuepfer E, Illingworth JJ, Furze JM, Crosnier C, et al. Neutralization of *Plasmodium falciparum* Merozoites by Antibodies against PfrH5. *J Immunol.* 2014 Jan 1;192(1):245–58.
50. Persson KEM, McCallum FJ, Reiling L, Lister NA, Stubbs J, Cowman AF, et al. Variation in use of erythrocyte invasion pathways by *Plasmodium falciparum* mediates evasion of human inhibitory antibodies. *J Clin Invest.* 2008 Jan 2;118(1):342–51.
51. Bozdech Z, Llinás M, Pulliam BL, Wong ED, Zhu J, DeRisi JL. The transcriptome of the intraerythrocytic developmental cycle of *Plasmodium falciparum*. *PLoS Biol.* 2003 Oct;1(1):E5.
52. Llinás M, Bozdech Z, Wong ED, Adai AT, DeRisi JL. Comparative whole genome transcriptome analysis of three *Plasmodium falciparum* strains. *Nucleic Acids Res.* 2006;34(4):1166–73.
53. Eisenhaber B, Bork P, Eisenhaber F. Prediction of potential GPI-modification sites in proprotein sequences. *J Mol Biol.* 1999 Sep 24;292(3):741–58.

54. Eisenhaber B, Bork P, Eisenhaber F. Post-translational GPI lipid anchor modification of proteins in kingdoms of life: analysis of protein sequence data from complete genomes. *Protein Eng.* 2001 Jan 1;14(1):17–25.
55. Petersen TN, Brunak S, von Heijne G, Nielsen H. SignalP 4.0: discriminating signal peptides from transmembrane regions. *Nat Methods.* 2011 Oct;8(10):785–6.
56. Birkholtz L-M, Blatch G, Coetzer TL, Hoppe HC, Human E, Morris EJ, et al. Heterologous expression of plasmodial proteins for structural studies and functional annotation. *Malar J.* 2008;7:197.
57. Wootton JC. Non-globular domains in protein sequences: automated segmentation using complexity measures. *Comput Chem.* 1994 Sep;18(3):269–85.
58. Le Roch KG, Zhou Y, Blair PL, Grainger M, Moch JK, Haynes JD, et al. Discovery of gene function by expression profiling of the malaria parasite life cycle. *Science.* 2003 Sep 12;301(5639):1503–8.
59. Williams AR, Douglas AD, Miura K, Illingworth JJ, Choudhary P, Murungi LM, et al. Enhancing Blockade of Plasmodium falciparum Erythrocyte Invasion: Assessing Combinations of Antibodies against PfRH5 and Other Merozoite Antigens. Riley EM, editor. *PLoS Pathog.* 2012 Nov 8;8(11):e1002991.
60. Bliss CI. The Toxicity of Poisons Applied Jointly. *Ann Appl Biol.* 1939 Aug 1;26(3):585–615.
61. Greco WR, Bravo G, Parsons JC. The search for synergy: a critical review from a response surface perspective. *Pharmacol Rev.* 1995 Jun;47(2):331–85.
62. Cowman AF, Crabb BS. Invasion of red blood cells by malaria parasites. *Cell.* 2006;124(4):755–766.
63. Cowman AF, Berry D, Baum J. The cellular and molecular basis for malaria parasite invasion of the human red blood cell. *J Cell Biol.* 2012 Sep 17;198(6):961–71.
64. Dutta S, Sullivan JS, Grady KK, Haynes JD, Komisar J, Batchelor AH, et al. High antibody titer against apical membrane antigen-1 is required to protect against malaria in the Aotus model. *PloS One.* 2009;4(12):e8138.
65. Lyon JA, Angov E, Fay MP, Sullivan JS, Girourd AS, Robinson SJ, et al. Protection Induced by Plasmodium falciparum MSP142 Is Strain-Specific, Antigen and Adjuvant Dependent, and Correlates with Antibody Responses. *PLoS ONE.* 2008 Jul 30;3(7):e2830.
66. Miura K, Zhou H, Diouf A, Moretz SE, Fay MP, Miller LH, et al. Anti-Apical-Membrane-Antigen-1 Antibody Is More Effective than Anti-42-Kilodalton-Merozoite-Surface-Protein-1 Antibody in Inhibiting Plasmodium falciparum Growth, as Determined by the In Vitro Growth Inhibition Assay. *Clin Vaccine Immunol CVI.* 2009 Jul;16(7):963–8.
67. Thera MA, Doumbo OK, Coulibaly D, Laurens MB, Ouattara A, Kone AK, et al. A field trial to assess a blood-stage malaria vaccine. *N Engl J Med.* 2011 Sep 15;365(11):1004–13.
68. Cassan SC de, Draper SJ. Recent advances in antibody-inducing poxviral and adenoviral vectored vaccine delivery platforms for difficult disease targets. *Expert Rev Vaccines.* 2013 Apr 1;12(4):365–78.
69. Hodgson SH, Choudhary P, Elias SC, Milne KH, Rampling TW, Biswas S, et al. Combining Viral Vectored and Protein-in-adjuvant Vaccines Against the Blood-stage Malaria Antigen AMA1: Report on a Phase 1a Clinical Trial. *Mol Ther.* 2014 Dec;22(12):2142–54.
70. Osier FH, Mackinnon MJ, Crosnier C, Fegan G, Kamuyu G, Wanaguru M, et al. New antigens for a multicomponent blood-stage malaria vaccine. *Sci Transl Med.* 2014 Jul 30;6(247):247ra102-247ra102.

71. Nei M, Li WH. Mathematical model for studying genetic variation in terms of restriction endonucleases. *Proc Natl Acad Sci U S A*. 1979 Oct;76(10):5269–73.

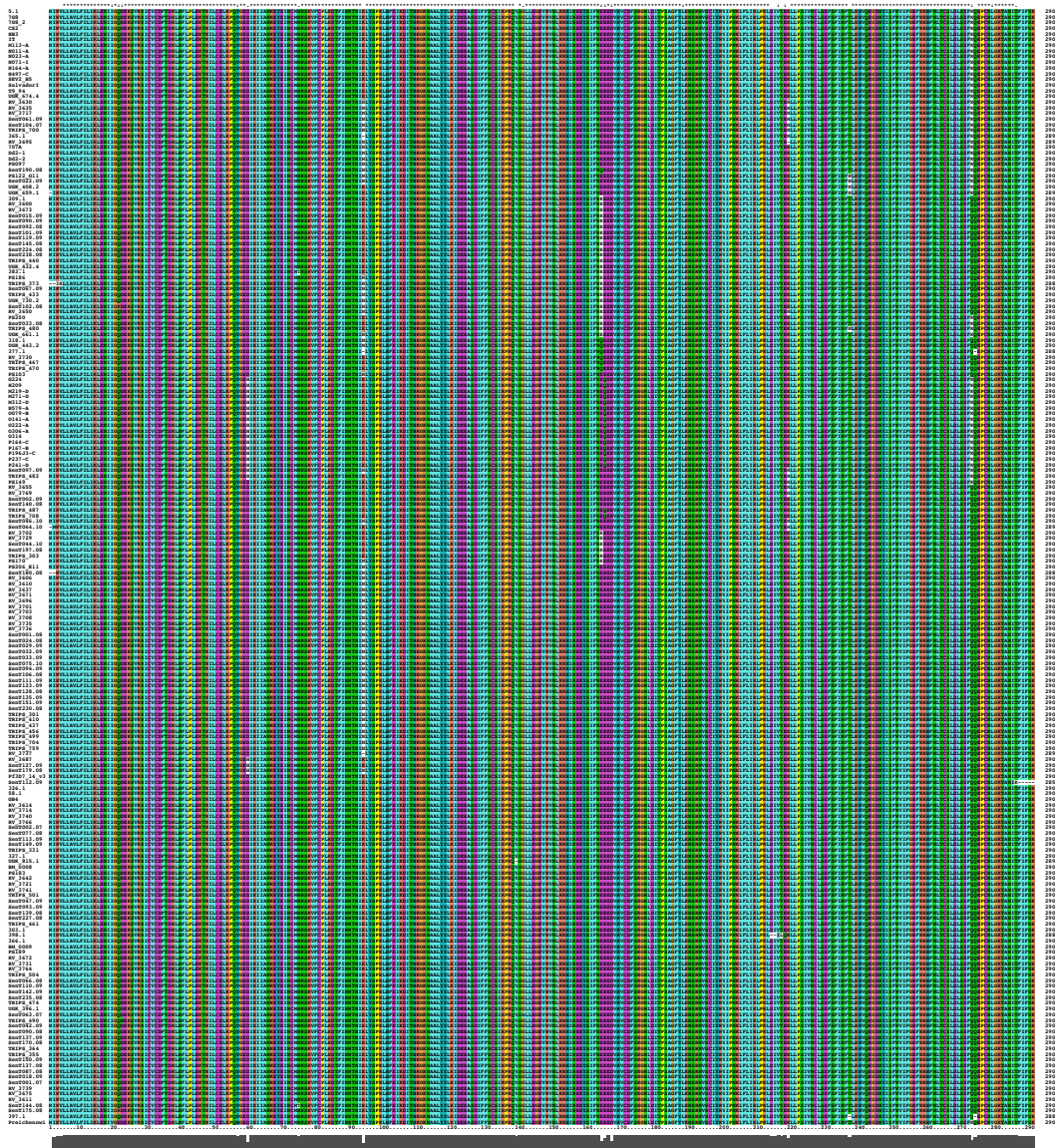
Additional file 2. *Plasmodium falciparum* strains and isolates analysed for SNPs evaluation (<http://plasmodb.org/plasmo/>)

(5.1, 7G8, 7G8_2, CS2, HB3, IT, M113-A, N011-A, N023-A, N071-I, N164-A, N497-C, SEV2_H5, SalvadorI, T9_94, UGK_674.4, RV_3630, RV_3635, RV_3717, SenT061.09, SenT104.07, TRIPS_700, 365.1, RV_3695, 707A, Dd2-1, Dd2-2, PS097, SenT190.08, PS122_G11, SenT022.09, UGK_408.2, UGK_659.1, 309.1, RV_3600, RV_3673, SenT015.09, SenT090.09, SenT092.08, SenT101.09, SenT119.09, SenT145.08, SenT224.08, SenT238.08, TRIPS_440, UGK_432.4, 383.1, PS186, TRIPS_373, SenT067.09, TRIPS_433, UGK_730.2, SenT102.08, RV_3650, PS250, SenT033.08, TRIPS_480, UGK_661.1, 318.1, UGK_443.2, 377.1, RV_3730, TRIPS_467, TRIPS_470, PS103, G224, H209, M219-D, M271-D, M312-D, N579-A, O079-B, O141-A, O222-A, O306-A, O314, P164-C, P167-B, P196J3-C, P237-C, P241-D, SenT097.09, TRIPS_482, PS149, RV_3655, RV_3769, SenT002.09, SenT140.08, TRIPS_487, TRIPS_708, SenT046.10, SenT064.10, RV_3702, RV_3729, SenT044.10, SenT197.08, TRIPS_303, PS170, PS206_E11, SenT180.08, RV_3606, RV_3610, RV_3637, RV_3671, RV_3696, RV_3701, RV_3703, RV_3708, RV_3735, RV_3736, SenT001.08, SenT024.08, SenT029.09, SenT032.09, SenT033.09, SenT075.10, SenT094.09, SenT106.08, SenT111.09, SenT123.09, SenT128.08, SenT135.09, SenT151.09, SenT230.08, TRIPS_301, TRIPS_410, TRIPS_437, TRIPS_456, TRIPS_499, TRIPS_704, TRIPS_759, RV_3737, RV_3687, SenT127.09, SenT179.08, Pf3D7_14_v3, SenT112.09, 326.1, 58.1, GB4, RV_3614, RV_3714, RV_3740, RV_3766, SenT002.07, SenT077.08, SenT113.09, SenT149.09, TRIPS_331, 327.1, UGK_815.1, BM_0008, PS183, RV_3642, RV_3721, RV_3741, TRIPS_501, SenT047.09, SenT093.09, SenT139.08, SenT227.08, TRIPS_461, 303.1, 398.1, 366.1, BM_0009, PS189, RV_3672, RV_3731, RV_3764, TRIPS_504, SenT066.08, SenT110.09, SenT142.09, SenT235.08, TRIPS_474, UGK_396.1, SenT063.07, TRIPS_490, SenT042.09, SenT090.08, SenT137.09, SenT170.08, TRIPS_364, TRIPS_355, SenT150.09, SenT137.08, SenT087.08, SenT018.09, SenT001.07, RV_3739, RV_3675, RV_3611, SenT144.08, SenT175.08, 397.1, *P. reichenowi*)

CLUSTAL 2.1 MULTIPLE SEQUENCE ALIGNMENT

File: PF14_004.gene_all.ps
Page 1 of 1

Date: Mon Nov 16 13:54:37 2015



Additional file 2. Amino acid sequence alignment of PF14_0044 in a population of 190 *P. falciparum* isolates. To evaluate the sequence diversity of PF14_0044 in a population of *P. falciparum* we analyze the sequences of 190 isolates provided by the database Plasmodb (<http://plasmodb.org/plasmo/>). All sequences obtained were identical to the *P. falciparum* 3D7 reference sequence with the exception of 12 non-synonymous single nucleotide polymorphism (SNP) and 6 deletions distributed along to the gene (873bp).

Discussion

Vaccination represents an elegant approach to induce an adaptive immune response in non-immune individuals by presenting antigenic determinants of a pathogen to the immune system without inducing the adverse effects of disease. Vaccination is one of the most effective medical interventions in history and helped to eliminate most of the life-threatening diseases that caused millions of deaths and severe morbidity (1, 2).

The intentional inoculation of healthy people to protect them against the onset of diseases dates back to the 16th century, when variolation (blowing powdered smallpox material, usually variola scabs, up the nostrils) was practiced in China.

Rational vaccination began in the 18th Century when Edward Jenner protected humans from smallpox by administering material from humans infected with cowpox (3). In the 19th Century, Pasteur, Koch, Ramon and Mérieux pioneered the development of live-attenuated or killed vaccines as well as inactivated toxins to protect against rabies, cholera, plague and typhoid. Additional major vaccine developments in the 20th Century provided protection against diphtheria, tetanus, pertussis, polio, meningococci and pneumococci hepatitis and influenza.

In the 21st Century vaccination continues to play a crucial role in global public health system (Tab. 1). Nevertheless, many important infections are not yet preventable by vaccination, including, respiratory syncytial virus (RSV), human immunodeficiency virus (HIV), malaria, tuberculosis and ebola.

Discussion

Table 1 – Outline of the development of human vaccines

Live attenuated	Killed whole organisms	Purified proteins or polysaccharides	Genetically engineered
18th Century			
Smallpox (1798)			
19th Century			
Rabies (1885)	Typhoid (1896)		
	Cholera (1896)		
	Plague (1897)		
Early 20th Century, first half			
Tuberculosis (BCG) (1927)	Pertussis (1926)	Diphtheria toxoid (1923)	
Yellow fever (1935)	Influenza (1936)	Tetanus toxoid (1926)	
	Rickettsia (1938)		
20th Century, second half			
Polio (oral) (1963)	Polio (injected) (1955)	Anthrax secreted proteins (1970)	Hepatitis B surface antigen recombinant (1986)
Measles (1963)	Rabies (cell culture) (1980)	Meningococcus polysaccharide (1974)	Lyme OspA (1998)
Mumps (1967)	Japanese encephalitis (mouse brain) (1992)	Pneumococcus polysaccharide (1977)	Cholera (recombinant toxin B) (1993)
Rubella (1969)	Tick-borne encephalitis (1981)	Haemophilus influenzae type B polysaccharide (1985)	
Adenovirus (1980)	Hepatitis A (1996)	H. influenzae type b conjugate (1987)	
Typhoid (Salmonella TY21a) (1989)	Cholera (WC-rBS) (1991)	Typhoid (Vi) polysaccharide (1994)	
Varicella (1995)	Meningococcal conjugate (group C) (1999)	Acellular pertussis (1996)	
Rotavirus reassortants (1999)		Hepatitis B (plasma derived) (1981)	
Cholera (attenuated) (1994)			
Cold-adapted influenza (1999)			
21st Century			
Rotavirus (attenuated and new reassortants) (2006)	Japanese encephalitis (2009) (Vero cell)	Pneumococcal conjugates* (heptavalent) (2000)	Human papillomavirus recombinant (quadrivalent) (2006)
Zoster (2006)	Cholera (WC only) (2009)	Meningococcal conjugates* (quadrivalent) (2005)	Human papillomavirus recombinant (bivalent) (2009)
		Pneumococcal conjugates* (13-valent) (2010)	Meningococcal group B proteins (2013)

* Capsular polysaccharide conjugated to carrier proteins.

Adapted from Plotkin S. 2014 (2)

Towards an effective malaria vaccine

Research for malaria vaccine development started in the middle of the 20th century, based on the observation that (I) partially protective immune responses eventually develop in people who experience and survive repeated malaria episodes during early childhood (4), and that (II) passive transfer of purified immunoglobulins from semi-immune adults can protect malaria-naïve children (5).

The first success in malaria vaccine development was achieved in 1973, when Clyde et al. reported that immunization with radiation-attenuated sporozoites could protect humans against challenge with fully infectious sporozoites (6), demonstrating the feasibility of developing a malaria vaccine capable to induce sterile protective immunity. Since then, progress toward developing malaria vaccines has moved forward as result of major advances in science and vaccine technologies (Tab. 2).

Table 2 – Major steps towards subunit and whole parasite malaria vaccines (6–20)

Date	Advances in vaccine development	References
1948	Immunisation of monkeys against malaria with killed parasites in adjuvants	[6]
1967	Mice protected from <i>P. berghei</i> by inoculation of irradiation-attenuated sporozoites by the bite of infected mosquitoes	[7]
1973	Humans protected from <i>P. falciparum</i> by inoculation of irradiation-attenuated sporozoites by the bite of infected mosquitoes	[8]
1981	Mice protected against a rodent parasite by immunisation with purified MSP1	[9]
1983	Expression of <i>P. falciparum</i> antigens as heterologous proteins in <i>E. coli</i>	[10]
1987	First human clinical trials with subunit (PfCS protein) malaria vaccines	[11,12]
1988	Partial protection of rhesus monkeys from a <i>P. knowlesi</i> blood-stage challenge with purified Pk AMA1	[13]
2001	RTS,S shown to have some efficacy in semi-immune adult men in The Gambia	[14]
2002	First field trial with a recombinant subunit blood-stage vaccine; Combination B in Papua New Guinea	[15]
2002	Immunity to <i>P. falciparum</i> induced in humans by administration of ultra-low doses of infected erythrocytes	[16]
2005	Mice protected against sporozoite challenge by infection with genetically-attenuated <i>P. berghei</i> sporozoites	[17]
2009	Multi-centre Phase III trial of RTS,S commences in Africa	[18]
2009	Sanaria's radiation-attenuated sporozoite vaccine (PfSPZ) first administered to human volunteers	[19]
2009	WRAIR AMA1 vaccine protects against malaria caused by a subset of <i>P. falciparum</i> genotypes in a Phase I/IIb trial in Mali	NCT00460525* [20]

* Clinical Trial Registration Number.

Adapted from Anders 2011 (21)

Today, the malaria vaccine development field is a dynamic and fertile ground of scientific endeavor. Increased funding and research are driving the discovery of new antigens and vaccine technologies, and many more malaria vaccine candidates are moving through the development pipeline (Tab. 3) (22).

Among them, the most advanced vaccine, the pre-erythrocytic subunit vaccine RTS,S/AS01, has completed a Phase III clinical trial but only limited clinical efficacy has been reported (23). To improve RTS,S efficacy, alternative vaccination regimens and adjuvants systems are being explored (i.e. NCT02207816 - booster doses of the vaccine using AS01E as adjuvant system, and Tab. 3).

Table 3 – Malaria vaccine clinical trials pipeline (24–43)

Antigen	Vaccine platform	References
<i>P. falciparum</i> CSP (RTS,S)	VLP-in-adjuvant	[24, 25]
<i>P. falciparum</i> CSP + <i>P. falciparum</i> AMA-1	DNA/Ad5 prime-boost regimen	[26, 27]
<i>P. falciparum</i> CSP	Ad35 vectored	[28, 29]
<i>P. falciparum</i> CSP + RTS,S	Ad35 vectored/VLP-in-adjuvant prime-boost regimen	NCT01366534*
<i>P. falciparum</i> ME-TRAP	ChAd63/MVA prime-boost regimen	[30–33]
<i>P. falciparum</i> ME-TRAP + RTS,S	ChAd63/MVA vectored + VLP-in-adjuvant coadministration	NCT02252640*
<i>P. falciparum</i> CelTOS	Protein-in-adjuvant	NCT02174978*
<i>P. falciparum</i> radiation-attenuated sporozoites	Whole organism	[34, 35]
<i>P. falciparum</i> genetically-attenuated sporozoites	Whole organism	[36]
<i>P. falciparum</i> sporozoite inoculation under prophylaxis	Whole organism	[37, 38]
<i>P. falciparum</i> MSP-1 / <i>P. falciparum</i> AMA-1	ChAd63/MVA prime-boost regimens	[39, 40]
<i>P. falciparum</i> AMA-1 (FMP2.1)	Protein-in-adjuvant	[41, 42]
<i>P. falciparum</i> AMA-1 (DiCo)	Protein-in-adjuvant	NCT02014727*
<i>P. falciparum</i> hybrid GLURP + MSP-3 (GMZ2)	Protein-in-adjuvant	[43]
<i>P. falciparum</i> Pfs25-EPA	Conjugated vaccine	NCT02334462*
<i>P. falciparum</i> Pfs230-EPA	Conjugated vaccine	NCT02334462*
<i>P. vivax</i> CSP (VMP001)	Protein-in-adjuvant	NCT01157897*
<i>P. vivax</i> DBP	ChAd63/MVA prime-boost regimen	NCT01816113*

* Clinical Trial Registration Number.

Adapted from Moreno & Joyner. 2015 (44)

Although efficacy and durability of the pre-erythrocytic RTS,S vaccine are far from ideal, the information gathered in 30 years of research efforts has paved the way for the progress of second generation malaria vaccines and has provided continued support for the development of novel subunit vaccines against *Plasmodium*.

Nonetheless, more research is needed for realizing the goals set by the WHO in the context of the Malaria Vaccine Technology Roadmap (45), which establishes the vision of licensing, by 2030, a vaccine against both *P. falciparum* and *P. vivax* with (I) protective efficacy of at least 75% against clinical malaria and (II) transmission-blocking effects.

Key hurdles to achieving an effective malaria vaccine include (I) antigenic diversity and variability of *Plasmodial* parasites, (II) lack of reliable and predictive animal models, and (III) limited availability of safe and efficient antigen delivery systems / adjuvants.

Subunit vaccines: implication for malaria vaccine development

Clinical immunity to malaria develops slowly and is short lived. This is mainly due to the extensive diversity found in *Plasmodium* antigens, which provides a mechanism to escape host immune detection and drug treatments (46). The antigenic diversity in *P. falciparum* arises from three main mechanisms: (I) classical antigenic variation that allows a clonal lineage of *P. falciparum* to express successive alternate forms of an antigen on the surface of the infected RBCs, (II) allelic polymorphisms that arose from host immune selection, and (III) phenotypic variation in which different strains express different combinations of functional ligands that bind to specific receptors on the erythrocyte surface. Besides, not all antigens are immunologically equivalent and *P. falciparum*, like many other pathogens, seems to hide from immune surveillance functionally essential and conserved domains while leading host's immune responses toward immunodominant hyper-variable epitopes (47).

Such an antigenic complexity is the major reason why progress towards a highly effective subunit vaccine has been so slow. Several merozoite surface proteins, and numerous proteins released from the merozoite apical organelles, have been described for having roles in the process of erythrocyte invasion (48). All these proteins represent potential vaccine candidates to elicit anti-invasion and anti-disease responses (49), but only few of them have reached the stage of clinical trials evaluation.

Until recently, almost all efforts in malaria vaccine development have been focused on a confined panel of antigens recognized as immunodominant in the context of natural infection. These studies have primarily focused on the Circumsporozoite protein (CSP) for the pre-erythrocytic stage, and Merozoite Surface Protein-1 (MSP-1) and Apical Membrane Antigen-1 (AMA-1) for the blood stage, and investigated a variety of vaccine delivery systems (23, 42, 50–53). However, despite major efforts, candidate subunit vaccines against malaria have shown limited efficacy in clinical trials, contributing to some discouragement with the recombinant protein subunit approach (54–56).

Although immunodominant antigens induce very strong antibody responses, they are favored to vary antigenically to escape immune pressure and therefore possess substantial

polymorphisms. Hardly surprising, extensive polymorphism has been observed for both MSP1 and AMA1 (57, 58), which might explain the limited efficacy reported in clinical trials. Approaches to overcome the problem of antigenic diversity in recombinant protein vaccines against *P. falciparum* include the (I) combination of several unrelated antigens or (II) multiple allelic forms of an antigen, (III) use of chimeric proteins or (III) mutagenized antigens.

Also, out of many potential vaccine antigens identified in *P. falciparum* some are much less polymorphic than MSP1 and AMA1, and could induce a more broadly protective immune response (59–61). Therefore, a promising strategy to overcome the risk of limited efficacy and protection, associated with antigenic diversity, may rely on non-immunodominant and more conserved vaccine antigens (62, 63).

The research for novel protective malarial antigens has received a great incentive from the genome-wide transcriptomic (64–67) and proteomic data (68–72) that have become available since the publication of the *P. falciparum* genome (73).

These extensive datasets offer valuable and powerful tools for rational search for new candidate antigens (74), and uncharacterized proteins with great potential as blood-stage vaccine candidates have been discovered (75).

Among them, the asexual blood-stage vaccine candidate antigen CyRPA, described in this thesis, is highly conserved. DNA sequencing of selected *P. falciparum* strains and field isolates from different geographic regions identified only two distinct PfCyRPA haplotypes differing by a single amino acid dimorphism of no functional importance. At sequence level, the high conservation could indicate that either PfCyRPA is not under strong selective pressure or that other evasion strategies, which do not involve diversification, apply for this protein.

Also, natural immunogenicity of PfCyRPA appears to be very moderate - sera of malaria-exposed adults basically contained no PfCyRPA-specific Abs. In released merozoites, PfCyRPA shows an intracellular localization and is thought to be accessible to the host immune surveillance for limited time only. Nevertheless, PfCyRPA showed to be accessible by inhibitory antibodies during the short period of invasion in both *in vitro* and *in vivo* growth inhibition assays (GIAs).

Developing malaria vaccines in the –omics era

The sequencing of the first bacterium genome in 1995 (76) had a great impact in pathogen's biology understanding and brought vaccine development into a new era. The concept of reverse vaccinology was introduced by Rappuoli in 2000 (77) and is based on the screening of the entire pathogenic genome to identify genes encoding proteins with the appealing features of potential vaccine targets (i.e., surface-exposed, secreted, highly conserved among strains). Once selected, ideal candidates are recombinantly expressed and used to immunize mice for evaluating immunogenicity and eventual protective efficacy. This strategy allows for the identification of a broad spectrum of vaccine candidates independent of abundance and natural immunogenicity.

The classical strategy, in malaria vaccine development, of inducing robust immune responses against a selected panel of antigens recognized as immunodominant in the context of natural infection, has been poorly fruitful. Most of the efforts should now be put toward a different approach: induce broad immune responses against a large number of parasite antigens, not necessarily recognized as immunodominant in the context of natural infection, in order to mimic and overtake the immunity induced by the whole parasite.

Rational genome-based identification of new candidate antigens has developed into a research focus (78, 79), and post-genomic tools have already begun to demonstrate their power to accelerate and enhance malaria vaccine development through the identification of potential novel subunit vaccine candidates (80–85).

To identify novel target antigens for protective immune responses, we analyzed available genome-wide transcriptomic and proteomic data of the intra-erythrocytic stages of *P. falciparum* (86) to pick out additional antigens potentially implicated in erythrocyte invasion. Candidate antigens were selected according to four main criteria: (I) expression peak in schizont and merozoite stage (65, 87), (II) mass spectrometry evidence, (III) predicted signal peptide and/or a single transmembrane domain/GPI anchor attachment site (secreted and cell surface exposed proteins) (88–90), (III) suitability for recombinant expression (molecular mass below 100 kDa and devoid of long stretches of repetitive amino acids). For the expression, characterization and functional analysis of membrane-associated *plasmodial* proteins we favored an eukaryotic expression platform and expressed them on the surface of transfected mammalian cells, bypassing any need for purified recombinant protein (91). For the characterization of selected candidate antigens we (I) generated mammalian cell lines expressing high levels of target antigen as His-tagged, transmembrane proteins; (II) used the

transfected living cells, or immune complexes derived from them, for immunization of mice; (III) generated B cell hybridoma cell lines for the production of target antigen-specific mAbs. This reverse vaccinology-based strategy (91) led us to the identification of the asexual-blood stage malaria vaccine candidate PfCyRPA: PfCyRPA-specific mAbs showed a strong parasite *in vitro* and *in vivo* growth inhibitory activity by targeting the process of merozoite invasion into erythrocytes (92, 93).

PfCyRPA is part of a multi-protein complex (94, 95) including also the PfrH5-interacting protein PfrRipr and the reticulocyte binding-like homologous protein PfrH5, which binds to the erythrocyte receptor basigin

Both anti-PfCyRPA and anti-PfrH5 mAbs strongly inhibit, but do not completely impede, parasite growth (92, 93, 96). *P. falciparum* merozoites are described to use alternative invasion pathways to evade Ab-mediated immunity (97) and the use of a PfCyRPA/PfrH5-independent invasion pathway of limited efficiency could explain persistence of parasitemia. Reddy et al. (94) reported a synergistic *in vitro* inhibitory activity for the combination of polyclonal anti-PfCyRPA and anti-PfrH5 antibodies, and we could show that monoclonal antibodies specific for PfrH5 and PfCyRPA have both *in vitro* and *in vivo* additive parasite growth inhibitory activity (98).

The additive inhibition produced by the combination of PfCyRPA and PfrH5 antibodies suggests that blocking two essential molecular interactions within the same invasion pathway (i.e. PfrH5-basigin binding and PfrH5/PfCyRPA complex formation) impede parasite growth more efficiently than when targeting only a single interaction. Also, in view of the observed additive effect, inclusion of both antigens into a multivalent subunit vaccine would represent an attractive strategy to prevent emergence of escape mutants.

Taken together, these findings draw the attention to the identification of additional antigens that may exert a synergistic effect by acting ‘in parallel’, inhibiting redundant invasion processes, or ‘in series’, inhibiting successive stages of invasion (99).

Among additional uncharacterized antigens, investigated in the framework of this thesis, PF14_0044 showed interesting features: none of the generated anti-PF14_0044 mAbs significantly inhibited the growth of *P. falciparum* 3D7, but a synergistic *in vitro* inhibitory activity was observed when anti-PF14_0044 were combined with anti-PfCyRPA mAbs. Given the complexity of *P. falciparum* erythrocyte invasion mechanism (48, 100), we could speculate that anti-PF14_0044 interfere with an invasion pathway of limited efficiency, and PfCyRPA- and PF14_0044-specific antibodies act ‘in parallel’ inhibiting redundant invasion processes. These fascinating hypotheses wait to be proved in the context of a broader panel of

invasion-related antigens. Hence, beside the identification of next-generation vaccine candidates, the systematic assessment of their potential to induce antibodies that act synergistically when administered in multi-antigen formulations remains essential (101).

Up to date, development of *P. vivax* vaccines has lagged behind that of *P. falciparum* owing to the knowledge gaps on the biology of this parasite and to the lack of reliable *in vitro* culture system (102, 103). Following the shift from malaria control to elimination and eradication (104, 105), *P. vivax* has been put at the forefront of the malaria research agenda and systems biology approaches using high-throughput technologies will greatly support the identification of vaccine candidates for *P. vivax*.

From reverse to structural vaccinology: a prospective for malaria vaccine development

Despite the improvements in vaccine delivery systems and adjuvant formulations, convincing protective immunity in humans has not been achieved yet. Efficacious immune response does not require recognition of the entire antigenic protein, but single or multiple selected epitopes may be sufficient to induce protective immunity.

Over the past decade, advances in X-ray crystallography and genetic engineering, have inaugurated the era of ‘structural vaccinology’, a combination of immunological, structural biology and bioinformatics approaches, in which the insights provided by high resolution structural analysis are used to design improved vaccine antigens (106–108). Detailed three-dimensional (3D) structure, domain organization, and dynamics of surface proteins of pathogens offer precious information that can guide the design of effective vaccines.

The ultimate goal of involving protein crystallography into vaccine research is the structural characterization of candidate antigens, either alone or in complexes with Fab (fragment antigen-binding) of neutralizing antibodies. The determination of such co-crystal structures represents the most powerful technique that allows a visually immediate and highly detailed definition of the epitope–paratope interface. Thus, epitope mapping has become one of the most relevant applications of protein crystallography in the field of vaccine research.

The structural studies of *Neisseria meningitidis* NadA (Neisseria adhesin A) and fHbp (factor H binding protein) (109, 110), and *Staphylococcus aureus* MntC (111) represent remarkable examples of crystal structure determination of vaccine antigens that, in turn, provided useful

information to elucidate both the molecular mechanism of their biological functions, and their immunological properties as vaccine antigens.

Another important target of structural vaccinology is to present the identified and characterized protective determinants in a stabilized and optimized conformation, in order to direct the immune response towards the neutralizing epitopes (112). Indeed, epitope-focused and scaffold-based vaccines, where neutralizing epitopes are grafted into unrelated scaffold proteins for conformational stabilization, have recently demonstrated their concrete applicability in HIV and RSV vaccine design and development (113, 114).

Taken together, these findings have raised hope that the rational design of vaccines for impervious pathogens, which have been so far refractory to vaccine development *via* traditional approaches, may become feasible (115).

In the studies described in this thesis, monoclonal antibodies specific for PfCyRPA were generated by immunization of mice with recombinantly expressed protein, either as antigen-loaded living cells or soluble protein-in-adjuvant. Raised PfCyRPA-specific mAbs inhibit merozoite invasion to different extent depending on their unique specificity (92, 93). Since induced PfCyRPA-specific antibodies can be invasion inhibitory or non-inhibitory, an optimized PfCyRPA-based vaccine should be designed to maximize induction of inhibitory responses. This possibly implies the design of protein surface loops comprising epitopes associated with protection (116).

We therefore investigated the crystal structure of PfCyRPA. Diffracting PfCyRPA crystals were obtained and the 3D structure has been solved, providing precious information that will facilitate the identification of the protective epitopes responsible for parasite-inhibitory immune responses (98).

Prospects for a PfCyRPA-based malaria vaccine

Recombinant protein-in-adjuvant formulations of PfCyRPA have been shown to elicit in mice high titers of antibodies that inhibit in a dose-dependent manner *P. falciparum* asexual blood stage parasite growth, both *in vitro* and *in vivo*.

Although lower doses showed moderate growth inhibitory effects, only doses of 2.5 mg PfCyRPA-specific mAb considerably inhibited parasite growth in mice. The protective effect of a PfCyRPA-based vaccine may therefore depend on the ability to induce and maintain high titers of inhibitory antibodies. The concentration of PfCyRPA-specific mAb in the circulation of the passively immunized mice (receiving the 2.5 mg mAb/mouse dose) was estimated to be

300 $\mu\text{g}/\text{mL}$ at the day of infection. For most human vaccines specific antibody concentrations from $<1 \mu\text{g}/\text{mL}$ to $\sim 200 \mu\text{g}/\text{mL}$ are sufficient to confer protection. However, it is feasible to induce much higher concentrations of specific antibodies, as shown by phase II studies of RTS,S adjuvanted with AS02 and AS01, where serum concentrations of CSP-specific antibody in the range mg/mL could be induced in malaria-naïve adults (117, 118). Furthermore, polyclonal antibodies induced by active immunization may have higher affinities compared to monoclonal antibodies, and might also exert additive or synergistic activity. Hence, vaccine-induced antibody concentration required for protection of humans may be lower than the concentration of mAbs required for parasite growth inhibition in the SCID-mouse model.

However, full-length recombinant proteins may primarily elicit immune responses against hyper-variable and functionally not relevant antigenic determinants hampering the development of parasite-inhibitory immune responses. This obstacle can be overcome by the use of synthetic peptidomimetics with native-like folds, which mirror those antigen domains capable of inducing protective antibodies. Optimized peptidomimetics can be then delivered on the surface of immunostimulating reconstituted influenza virosomes (IRIVs), which function both as carrier and adjuvant system (119, 120). IRIVs are in vitro-assembled non-replicating virus-like particles that mimic the structure and function of the parental influenza virus, but lack viral genetic material. Clinical studies (121) have demonstrated that IRIVs represent an optimal vaccine formulation for eliciting strong immune responses (either CD4 T/B-cell and/or CD8 T-cell immune responses) against synthetic peptide loaded on their surface. Also, and most importantly, distinct peptidomimetics can be anchored on the surface of IRIVs and different populations of antigen-loaded virosomes can be combined to formulate multi-component subunit vaccines. Hence, IRIVs represent a modular and extremely versatile antigen delivery system.

In this thesis, the 3D structure of PfCyRPA in complex with an inhibitory antibody has been elucidated (98). Diffracting PfCyRPA/Fab crystals were obtained producing a well-detailed definition of the epitope–paratope interactions.

PfCyRPA adopts a six-bladed β -propeller fold and presumably acts as a binding platform to tether on the merozoite surface other proteins essential for the invasion process. β -propellers are quite successful structural modules (122): examples of six-bladed β -propellers include sialidases (123, 124) and protein ligand binding (125, 126), signaling (127), and structural (128) functions. The extension of β -sheets by attachment of β -strands from different proteins is a common protein-protein interaction motif. Outermost β -strands of several blades in

PfCyRPA are exposed to solvent and, although the interaction surfaces are not very large, may represent potential binding site for other proteins.

PfCyRPA is a crucial component of a multiprotein complex that as a whole is essential for erythrocyte invasion (94, 129, 130). While it has been claimed that PfCyRPA anchors the ternary complex through a GPI anchor to the parasite membrane (94), recent results are not consistent with this suggestion (129, 130). These studies confirmed that CyRPA is a secreted protein, which directly interacts with PfRH5 and PfRipr, while the invasion complex is tethered to the merozoite surface by the GPI-linked protein P113 (130). In this light, secreted PfCyRPA would bind the P113-PfRH5-basigin complex and recruit PfRipr to the invasion complex, acting as a protein-protein binding platform essential for the assembly of the invasion complex.

PfCyRPA, PfRH5 and PfRipr colocalize during parasite invasion at the junction between merozoites and erythrocytes. The complex seems to be required both for triggering Ca^{2+} release and establishment of tight junctions: while merozoites deficient in PfCyRPA or PfRH5 can still bind to erythrocytes, they do not attach irreversibly and cannot invade the host cells (129). However, further functional studies are required to elucidate the molecular mechanisms how the invasion complex is involved in erythrocytes invasion (129). In this context it may be relevant that the five sequential disulfide bonds of PfCyRPA are in blades 1-5, leaving blade 6 of the β -propeller structure without such a local stabilization. Blade 6 is composed of β -strands from the N- and the C-terminus, and in principle could act as a gate to allow PfCyRPA to undergo substantial conformational changes.

The crystal structure of PfCyRPA, together with the already elucidated structure of PfRH5 (131), provides the structural insight into the multiprotein invasion complex. Also, the structure of PfCyRPA in complex with the inhibitory antibody c12 identified the protective protein surface epitopes to guide the rational design of next generation malaria vaccines against the blood-stage parasites.

Synthetic peptide chemistry and sequential rounds of structural optimization of selected peptides, together with immunological profiling, will allow us to design optimal peptidomimetics, which stably mirror the native structure of the corresponding inhibitory epitopes, to be incorporated into IRIVs and elicit parasite blood-stage growth-inhibitory antibodies.

The generation of optimized peptidomimetics is eagerly awaited for evaluating the potential of a virosomal, epitope-focused PfCyRPA-based candidate vaccine.

Conclusion

In this thesis, we exploited the great potential of genomics and other ‘omics’ sciences for the rational design of novel malaria subunit vaccine candidates. Our strategy was based on (I) the selection of hypothetical parasite proteins that are accessible to host immune surveillance by antibodies, (II) their functional characterization using antigen-specific monoclonal antibodies, and (III) their high-resolution structural analysis employing X-ray crystallography.

Our findings lead to the following key conclusions:

1. The cell-based immunization approach for the generation of antigen-specific and parasite cross-reactive mAbs represents a rapid and reliable tool for candidate antigen screening. The strategy can be applied to a wide range of cell-surface proteins.
2. Selected antigens can be easily expressed in a second step in HEK cells as soluble recombinant proteins and tested as adjuvanted vaccine formulations.
3. The *P. falciparum* NOD/scid-IL2Ry^{null} mouse model represents an unprecedented system to evaluate *in vivo* the functional potencies of raised malaria-specific Abs.
4. Reverse vaccinology is an excellent strategy for the identification of novel malaria vaccine targets and structural vaccinology constitutes the most promising approach for the design of optimal vaccine formulations.
5. Among the characterized candidate proteins, PfCyRPA has been identified as potential component for inclusion in a subunit malaria blood-stage vaccine: it (I) is target of potent parasite growth-inhibitory antibodies, (II) is highly conserved among *P. falciparum* isolates, and (III) has limited natural immunogenicity.
6. PfCyRPA adopts a six-bladed β -propeller fold and acts as a crucial binding platform to bridge different merozoite surface proteins and assemble the invasion complex, essential for the invasion process into erythrocytes. The crystal structure identified the inhibitory epitopes and will guide the rational design of next generation epitope-focused malaria blood-stage vaccine.

The rational application of the described strategy could lead to the identification and characterization of additional potential *P. falciparum* and *P. vivax* vaccine targets.

Results support the concept to apply reverse and structural vaccinology approaches for the selection of promising candidates and for the design of an effective multivalent malaria subunit vaccine.

References

1. Plotkin SA, Plotkin SL (2011) The development of vaccines: how the past led to the future. *Nat Rev Microbiol* 9(12):889–893.
2. Plotkin S (2014) History of vaccination. *Proc Natl Acad Sci U S A* 111(34):12283–12287.
3. Jenner E (1778) An Inquiry into the Causes and Effects of the Variolae Vaccinae, a Disease discovered in some of the Western Counties of England, particularly Gloucestershire, and known by the name of the Cow Pox. *Lond Sampson Low*. Available at: <http://www.christies.com/lotfinder/books-manuscripts/jenner-edward-an-inquiry-into-the-5084227-details.aspx> [Accessed November 7, 2015].
4. Doolan DL, Dobaño C, Baird JK (2009) Acquired immunity to malaria. *Clin Microbiol Rev* 22(1):13–36, Table of Contents.
5. Sabchareon A, et al. (1991) Parasitologic and clinical human response to immunoglobulin administration in falciparum malaria. *Am J Trop Med Hyg* 45(3):297–308.
6. Clyde DF, Most H, McCarthy VC, Vanderberg JP (1973) Immunization of man against sporozite-induced falciparum malaria. *Am J Med Sci* 266(3):169–177.
7. Freund J, Thomson KJ (1948) Immunization of monkeys against malaria by means of killed parasites with adjuvants. *Am J Trop Med Hyg* 28(1):1–22.
8. Nussenzweig RS, Vanderberg J, Most H, Orton C (1967) Protective immunity produced by the injection of x-irradiated sporozoites of plasmodium berghei. *Nature* 216(5111):160–162.
9. Holder AA, Freeman RR (1981) Immunization against blood-stage rodent malaria using purified parasite antigens. *Nature* 294(5839):361–364.
10. Kemp DJ, et al. (1983) Expression of Plasmodium falciparum blood-stage antigens in Escherichia coli: detection with antibodies from immune humans. *Proc Natl Acad Sci U S A* 80(12):3787–3791.
11. Herrington DA, et al. (1987) Safety and immunogenicity in man of a synthetic peptide malaria vaccine against Plasmodium falciparum sporozoites. *Nature* 328(6127):257–259.
12. Ballou WR, et al. (1987) Safety and efficacy of a recombinant DNA Plasmodium falciparum sporozoite vaccine. *Lancet Lond Engl* 1(8545):1277–1281.
13. Deans JA, et al. (1988) Vaccination trials in rhesus monkeys with a minor, invariant, Plasmodium knowlesi 66 kD merozoite antigen. *Parasite Immunol* 10(5):535–552.
14. Bojang KA, et al. (2001) Efficacy of RTS,S/AS02 malaria vaccine against Plasmodium falciparum infection in semi-immune adult men in The Gambia: a randomised trial. *Lancet Lond Engl* 358(9297):1927–1934.
15. Genton B, et al. (2002) A recombinant blood-stage malaria vaccine reduces Plasmodium falciparum density and exerts selective pressure on parasite populations in a phase 1-2b trial in Papua New Guinea. *J Infect Dis* 185(6):820–827.
16. Pombo DJ, et al. (2002) Immunity to malaria after administration of ultra-low doses of red cells infected with Plasmodium falciparum. *Lancet Lond Engl* 360(9333):610–617.
17. Mueller A-K, Labaied M, Kappe SHI, Matuschewski K (2005) Genetically modified Plasmodium parasites as a protective experimental malaria vaccine. *Nature* 433(7022):164–167.
18. Cohen J, Nussenzweig V, Nussenzweig R, Vekemans J, Leach A (2010) From the circumsporozoite protein to the RTS, S/AS candidate vaccine. *Hum Vaccin* 6(1):90–96.

19. Hoffman SL, et al. (2010) Development of a metabolically active, non-replicating sporozoite vaccine to prevent *Plasmodium falciparum* malaria. *Hum Vaccin* 6(1):97–106.
20. Thera MA, et al. (2011) A field trial to assess a blood-stage malaria vaccine. *N Engl J Med* 365(11):1004–1013.
21. Anders RF (2011) The case for a subunit vaccine against malaria. *Trends Parasitol* 27(8):330–334.
22. WHO | Tables of malaria vaccine projects globally WHO. Available at: http://www.who.int/immunization/research/development/Rainbow_tables/en/ [Accessed July 12, 2015].
23. RTS,S Clinical Trials Partnership (2015) Efficacy and safety of RTS,S/AS01 malaria vaccine with or without a booster dose in infants and children in Africa: final results of a phase 3, individually randomised, controlled trial. *Lancet Lond Engl* 386(9988):31–45.
24. Stoute JA, et al. (1997) A Preliminary Evaluation of a Recombinant Circumsporozoite Protein Vaccine against *Plasmodium falciparum* Malaria. *N Engl J Med* 336(2):86–91.
25. The RTS,S Clinical Trials Partnership (2014) (2014) Efficacy and Safety of the RTS,S/AS01 Malaria Vaccine during 18 Months after Vaccination: A Phase 3 Randomized, Controlled Trial in Children and Young Infants at 11 African Sites. *PLoS Med* 11(7):e1001685.
26. Chuang I, et al. (2013) DNA prime/Adenovirus boost malaria vaccine encoding *P. falciparum* CSP and AMA1 induces sterile protection associated with cell-mediated immunity. *PloS One* 8(2):e55571.
27. Tamminga C, et al. (2013) Human adenovirus 5-vectored *Plasmodium falciparum* NMRC-M3V-Ad-PfCA vaccine encoding CSP and AMA1 is safe, well-tolerated and immunogenic but does not protect against controlled human malaria infection. *Hum Vaccines Immunother* 9(10):2165–2177.
28. Creech CB, et al. (2013) Randomized, placebo-controlled trial to assess the safety and immunogenicity of an adenovirus type 35-based circumsporozoite malaria vaccine in healthy adults. *Hum Vaccines Immunother* 9(12):2548–2557.
29. Ouédraogo A, et al. (2013) A Phase 1b Randomized, Controlled, Double-Blinded Dosage-Escalation Trial to Evaluate the Safety, Reactogenicity and Immunogenicity of an Adenovirus Type 35 Based Circumsporozoite Malaria Vaccine in Burkinaabe Healthy Adults 18 to 45 Years of Age. *PLoS ONE* 8(11):e78679.
30. Dudareva M, et al. (2009) Prevalence of serum neutralizing antibodies against chimpanzee adenovirus 63 and human adenovirus 5 in Kenyan Children, in the context of vaccine vector efficacy. *Vaccine* 27(27):3501–3504.
31. Kimani D, et al. (2014) Translating the immunogenicity of prime-boost immunisation with ChAd63 and MVA ME-TRAP from malaria naïve to malaria-endemic populations. *Mol Ther*. doi:10.1038/mt.2014.109.
32. Ewer KJ, et al. (2013) Protective CD8+ T-cell immunity to human malaria induced by chimpanzee adenovirus-MVA immunisation. *Nat Commun* 4:2836.
33. Hodgson SH, et al. (2015) Evaluation of the efficacy of ChAd63-MVA vectored vaccines expressing circumsporozoite protein and ME-TRAP against controlled human malaria infection in malaria-naïve individuals. *J Infect Dis* 211(7):1076–1086.
34. Seder RA, et al. (2013) Protection against malaria by intravenous immunization with a nonreplicating sporozoite vaccine. *Science* 341(6152):1359–1365.
35. Epstein JE, Richie TL (2013) The whole parasite, pre-erythrocytic stage approach to malaria vaccine development: A review. *Curr Opin Infect Dis* 26(5):420–428.

36. Spring M, et al. (2013) First-in-human evaluation of genetically attenuated *Plasmodium falciparum* sporozoites administered by bite of *Anopheles* mosquitoes to adult volunteers. *Vaccine* 31(43):4975–4983.
37. Bijker EM, et al. (2014) Cytotoxic markers associate with protection against malaria in human volunteers immunized with *Plasmodium Falciparum* Sporozoites. *J Infect Dis* 210(10):1605–1615.
38. Nahrendorf W, et al. (2014) Memory B-Cell and Antibody Responses Induced by *Plasmodium falciparum* Sporozoite Immunization. *J Infect Dis* 210(12):1981–1990.
39. Sheehy SH, et al. (2012) ChAd63-MVA-vectored blood-stage malaria vaccines targeting MSP1 and AMA1: assessment of efficacy against mosquito bite challenge in humans. *Mol Ther J Am Soc Gene Ther* 20(12):2355–2368.
40. Hodgson SH, et al. (2014) Combining Viral Vectored and Protein-in-adjuvant Vaccines Against the Blood-stage Malaria Antigen AMA1: Report on a Phase 1a Clinical Trial. *Mol Ther* 22(12):2142–2154.
41. Polhemus ME, et al. (2007) Phase I dose escalation safety and immunogenicity trial of *Plasmodium falciparum* apical membrane protein (AMA-1) FMP2.1, adjuvanted with AS02A, in malaria-naïve adults at the Walter Reed Army Institute of Research. *Vaccine* 25(21):4203–4212.
42. Laurens MB, et al. (2013) Extended Safety, Immunogenicity and Efficacy of a Blood-Stage Malaria Vaccine in Malian Children: 24-Month Follow-Up of a Randomized, Double-Blinded Phase 2 Trial. *PLoS ONE* 8(11):e79323.
43. Jepsen MPG, et al. (2013) The Malaria Vaccine Candidate GMZ2 Elicits Functional Antibodies in Individuals From Malaria Endemic and Non-Endemic Areas. *J Infect Dis* 208(3):479–488.
44. Moreno A, Joyner C (2015) Malaria vaccine clinical trials: what's on the horizon. *Curr Opin Immunol* 35:98–106.
45. WHO | Malaria vaccine technology roadmap WHO. Available at: http://www.who.int/immunization/topics/malaria/vaccine_roadmap/en/ [Accessed November 8, 2015].
46. Volkman SK, et al. (2007) A genome-wide map of diversity in *Plasmodium falciparum*. *Nat Genet* 39(1):113–119.
47. Akram A, Inman RD (2012) Immunodominance: A pivotal principle in host response to viral infections. *Clin Immunol* 143(2):99–115.
48. Cowman AF, Berry D, Baum J (2012) The cellular and molecular basis for malaria parasite invasion of the human red blood cell. *J Cell Biol* 198(6):961–971.
49. Moorthy VS, Good MF, Hill AVS (2004) Malaria vaccine developments. *Lancet Lond Engl* 363(9403):150–156.
50. Remarque EJ, Faber BW, Kocken CHM, Thomas AW (2008) Apical membrane antigen 1: a malaria vaccine candidate in review. *Trends Parasitol* 24(2):74–84.
51. Ogutu BR, et al. (2009) Blood stage malaria vaccine eliciting high antigen-specific antibody concentrations confers no protection to young children in Western Kenya. *PloS One* 4(3):e4708.
52. Sagara I, et al. (2009) A randomized controlled phase 2 trial of the blood stage AMA1-C1/Alhydrogel malaria vaccine in children in Mali. *Vaccine* 27(23):3090–3098.
53. Spring MD, et al. (2009) Phase 1/2a study of the malaria vaccine candidate apical membrane antigen-1 (AMA-1) administered in adjuvant system AS01B or AS02A. *PloS One* 4(4):e5254.
54. Schwartz L, Brown GV, Genton B, Moorthy VS (2012) A review of malaria vaccine clinical projects based on the WHO rainbow table. *Malar J* 11(11):10–1186.
55. Hoffman SL, Vekemans J, Richie TL, Duffy PE The march toward malaria vaccines. *Vaccine*. doi:10.1016/j.vaccine.2015.07.091.

56. Goodman AL, Draper SJ (2010) Blood-stage malaria vaccines - recent progress and future challenges. *Ann Trop Med Parasitol* 104(3):189–211.
57. Barry AE, Schultz L, Buckee CO, Reeder JC (2009) Contrasting population structures of the genes encoding ten leading vaccine-candidate antigens of the human malaria parasite, *Plasmodium falciparum*. *PLoS One* 4(12):e8497.
58. Takala SL, Plowe CV (2009) Genetic diversity and malaria vaccine design, testing and efficacy: preventing and overcoming “vaccine resistant malaria.” *Parasite Immunol* 31(9):560–573.
59. Dzikowski R, Deitsch KW (2009) Genetics of antigenic variation in *Plasmodium falciparum*. *Curr Genet* 55(2):103–110.
60. Takala SL, et al. (2009) Extreme Polymorphism in a Vaccine Antigen and Risk of Clinical Malaria: Implications for Vaccine Development. *Sci Transl Med* 1(2):2ra5.
61. Riley EM, Stewart VA (2013) Immune mechanisms in malaria: new insights in vaccine development. *Nat Med* 19(2):168–178.
62. Doolan DL (2011) *Plasmodium* immunomics. *Int J Parasitol* 41(1):3–20.
63. Chia WN, Goh YS, Rénia L (2014) Novel approaches to identify protective malaria vaccine candidates. *Front Microbiol* 5. doi:10.3389/fmicb.2014.00586.
64. Le Roch KG, et al. (2003) Discovery of gene function by expression profiling of the malaria parasite life cycle. *Science* 301(5639):1503–1508.
65. Bozdech Z, et al. (2003) The transcriptome of the intraerythrocytic developmental cycle of *Plasmodium falciparum*. *PLoS Biol* 1(1):E5.
66. Otto TD, et al. (2010) New insights into the blood-stage transcriptome of *Plasmodium falciparum* using RNA-Seq. *Mol Microbiol* 76(1):12–24.
67. López-Barragán MJ, et al. (2011) Directional gene expression and antisense transcripts in sexual and asexual stages of *Plasmodium falciparum*. *BMC Genomics* 12:587.
68. Florens L, et al. (2002) A proteomic view of the *Plasmodium falciparum* life cycle. *Nature* 419(6906):520–526.
69. Florens L, et al. (2004) Proteomics approach reveals novel proteins on the surface of malaria-infected erythrocytes. *Mol Biochem Parasitol* 135(1):1–11.
70. Lasonder E, et al. (2008) Proteomic profiling of *Plasmodium* sporozoite maturation identifies new proteins essential for parasite development and infectivity. *PLoS Pathog* 4(10):e1000195.
71. Acharya P, et al. (2009) A glimpse into the clinical proteome of human malaria parasites *Plasmodium falciparum* and *Plasmodium vivax*. *Proteomics Clin Appl* 3(11):1314–1325.
72. Hall N, et al. (2005) A comprehensive survey of the *Plasmodium* life cycle by genomic, transcriptomic, and proteomic analyses. *Science* 307(5706):82–86.
73. Gardner MJ, et al. (2002) Genome sequence of the human malaria parasite *Plasmodium falciparum*. *Nature* 419(6906):498–511.
74. Singh SP, Khan F, Mishra BN (2010) Computational characterization of *Plasmodium falciparum* proteomic data for screening of potential vaccine candidates. *Hum Immunol* 71(2):136–143.
75. Proietti C, Doolan DL (2014) The case for a rational genome-based vaccine against malaria. *Front Microbiol* 5:741.
76. Fleischmann RD, et al. (1995) Whole-genome random sequencing and assembly of *Haemophilus influenzae* Rd. *Science* 269(5223):496–512.
77. Rappuoli R (2000) Reverse vaccinology. *Curr Opin Microbiol* 3(5):445–450.
78. Doolan DL, Apte SH, Proietti C (2014) Genome-based vaccine design: the promise for malaria and other infectious diseases. *Int J Parasitol* 44(12):901–913.
79. Schussek S, Trieu A, Doolan DL (2014) Genome- and proteome-wide screening strategies for antigen discovery and immunogen design. *Biotechnol Adv* 32(2):403–414.

80. Doolan DL, et al. (2008) Profiling humoral immune responses to *P. falciparum* infection with protein microarrays. *Proteomics* 8(22):4680–4694.
81. Gilson PR, et al. (2006) Identification and stoichiometry of glycosylphosphatidylinositol-anchored membrane proteins of the human malaria parasite *Plasmodium falciparum*. *Mol Cell Proteomics MCP* 5(7):1286–1299.
82. Sanders PR, et al. (2007) Identification of protein complexes in detergent-resistant membranes of *Plasmodium falciparum* schizonts. *Mol Biochem Parasitol* 154(2):148–157.
83. Crompton PD, et al. (2010) A prospective analysis of the Ab response to *Plasmodium falciparum* before and after a malaria season by protein microarray. *Proc Natl Acad Sci* 107(15):6958–6963.
84. Crosnier C, et al. (2013) A Library of Functional Recombinant Cell-surface and Secreted *P. falciparum* Merozoite Proteins. *Mol Cell Proteomics MCP* 12(12):3976–3986.
85. Zenonos ZA, Rayner JC, Wright GJ (2014) Towards a comprehensive *Plasmodium falciparum* merozoite cell surface and secreted recombinant protein library. *Malar J* 13(1):93.
86. PlasmoDB: The *Plasmodium* genome resource Available at: <http://plasmodb.org/plasmo/> [Accessed April 8, 2015].
87. Llinás M, Bozdech Z, Wong ED, Adai AT, DeRisi JL (2006) Comparative whole genome transcriptome analysis of three *Plasmodium falciparum* strains. *Nucleic Acids Res* 34(4):1166–1173.
88. Eisenhaber B, Bork P, Eisenhaber F (1999) Prediction of potential GPI-modification sites in proprotein sequences. *J Mol Biol* 292(3):741–758.
89. Eisenhaber B, Bork P, Eisenhaber F (2001) Post-translational GPI lipid anchor modification of proteins in kingdoms of life: analysis of protein sequence data from complete genomes. *Protein Eng* 14(1):17–25.
90. Petersen TN, Brunak S, von Heijne G, Nielsen H (2011) SignalP 4.0: discriminating signal peptides from transmembrane regions. *Nat Methods* 8(10):785–786.
91. Dreyer AM, Beauchamp J, Matile H, Pluschke G (2010) An efficient system to generate monoclonal antibodies against membrane-associated proteins by immunisation with antigen-expressing mammalian cells. *BMC Biotechnol* 10:87.
92. Dreyer AM, et al. (2012) Passive immunoprotection of *Plasmodium falciparum*-infected mice designates the CyRPA as candidate malaria vaccine antigen. *J Immunol Baltim Md 1950* 188(12):6225–6237.
93. Favuzza P, et al. (2016) Generation of *Plasmodium falciparum* parasite-inhibitory antibodies by immunization with recombinantly-expressed CyRPA. *Malar J* 15:161.
94. Reddy KS, et al. (2015) Multiprotein complex between the GPI-anchored CyRPA with PfRH5 and PfRipr is crucial for *Plasmodium falciparum* erythrocyte invasion. *Proc Natl Acad Sci* 112(4):1179–1184.
95. Volz JC, et al. (2016) Essential Role of the PfRh5/PfRipr/CyRPA Complex during *Plasmodium falciparum* Invasion of Erythrocytes. *Cell Host Microbe* 20(1):60–71.
96. Douglas AD, et al. (2014) Neutralization of *Plasmodium falciparum* Merozoites by Antibodies against PfRH5. *J Immunol* 192(1):245–258.
97. Persson KEM, et al. (2008) Variation in use of erythrocyte invasion pathways by *Plasmodium falciparum* mediates evasion of human inhibitory antibodies. *J Clin Invest* 118(1):342–351.
98. Favuzza P, et al. (2017) Structure of the malaria vaccine candidate antigen CyRPA and its complex with a parasite invasion inhibitory antibody. *eLife* 6:e20383.

99. Williams AR, et al. (2012) Enhancing Blockade of Plasmodium falciparum Erythrocyte Invasion: Assessing Combinations of Antibodies against PfrRH5 and Other Merozoite Antigens. *PLoS Pathog* 8(11):e1002991.
100. Cowman AF, Crabb BS (2006) Invasion of red blood cells by malaria parasites. *Cell* 124(4):755–766.
101. Osier FH, et al. (2014) New antigens for a multicomponent blood-stage malaria vaccine. *Sci Transl Med* 6(247):247ra102-247ra102.
102. Galinski MR, Meyer EVS, Barnwell JW (2013) Plasmodium vivax: modern strategies to study a persistent parasite's life cycle. *Adv Parasitol* 81:1–26.
103. Noulin F, Borlon C, Van Den Abbeele J, D'Alessandro U, Erhart A (2013) 1912-2012: a century of research on Plasmodium vivax in vitro culture. *Trends Parasitol* 29(6):286–294.
104. Alonso PL, et al. (2011) A Research Agenda to Underpin Malaria Eradication. *PLoS Med* 8(1):e1000406.
105. The malERA Consultative Group on Basic Science and Enabling Technologies (2011) A Research Agenda for Malaria Eradication: Basic Science and Enabling Technologies. *PLoS Med* 8(1):e1000399.
106. Dormitzer PR, Ulmer JB, Rappuoli R (2008) Structure-based antigen design: a strategy for next generation vaccines. *Trends Biotechnol* 26(12):659–667.
107. Dormitzer PR, Grandi G, Rappuoli R (2012) Structural vaccinology starts to deliver. *Nat Rev Microbiol* 10(12):807–813.
108. Loomis R, Johnson P (2015) Emerging Vaccine Technologies. *Vaccines* 3(2):429–447.
109. Malito E, et al. (2014) Structure of the meningococcal vaccine antigen NadA and epitope mapping of a bactericidal antibody. *Proc Natl Acad Sci U S A* 111(48):17128–17133.
110. Malito E, et al. (2013) Defining a protective epitope on factor H binding protein, a key meningococcal virulence factor and vaccine antigen. *Proc Natl Acad Sci U S A* 110(9):3304–3309.
111. Ahuja S, et al. (2015) Structural analysis of bacterial ABC transporter inhibition by an antibody fragment. *Struct Lond Engl* 23(4):713–723.
112. Cozzi R, Scarselli M, Ferlenghi I (2013) Structural vaccinology: a three-dimensional view for vaccine development. *Curr Top Med Chem* 13(20):2629–2637.
113. Azoitei ML, et al. (2014) Computational design of protein antigens that interact with the CDR H3 loop of HIV broadly neutralizing antibody 2F5. *Proteins* 82(10):2770–2782.
114. Correia BE, et al. (2014) Proof of principle for epitope-focused vaccine design. *Nature* 507(7491):201–206.
115. Malito E, Carfi A, Bottomley M (2015) Protein Crystallography in Vaccine Research and Development. *Int J Mol Sci* 16(6):13106–13140.
116. Pluschke G, Tamborrini M (2012) Development of a virosomal malaria vaccine candidate: from synthetic peptide design to clinical concept validation. *Future Virol* 7(8):779–790.
117. Kester KE, et al. (2007) A phase I/IIa safety, immunogenicity, and efficacy bridging randomized study of a two-dose regimen of liquid and lyophilized formulations of the candidate malaria vaccine RTS,S/AS02A in malaria-naïve adults. *Vaccine* 25(29):5359–5366.
118. Leroux-Roels G, et al. (2014) Evaluation of the immune response to RTS,S/AS01 and RTS,S/AS02 adjuvanted vaccines: randomized, double-blind study in malaria-naïve adults. *Hum Vaccines Immunother* 10(8):2211–2219.

119. Westerfeld N, Pluschke G, Zurbriggen R (2006) Optimized Malaria-antigens delivered by immunostimulating reconstituted influenza virosomes. *Wien Klin Wochenschr* 118(19–20 Suppl 3):50–57.
120. Moser C, Müller M, Kaeser MD, Weydemann U, Amacker M (2013) Influenza virosomes as vaccine adjuvant and carrier system. *Expert Rev Vaccines* 12(7):779–791.
121. Cech PG, et al. (2011) Virosome-Formulated Plasmodium falciparum AMA-1 & CSP Derived Peptides as Malaria Vaccine: Randomized Phase 1b Trial in Semi-Immune Adults & Children. *PLoS ONE* 6(7):e22273.
122. Chen CK-M, Chan N-L, Wang AH-J (2011) The many blades of the β -propeller proteins: conserved but versatile. *Trends Biochem Sci* 36(10):553–561.
123. Varghese JN, McKimm-Breschkin JL, Caldwell JB, Kortt AA, Colman PM (1992) The structure of the complex between influenza virus neuraminidase and sialic acid, the viral receptor. *Proteins* 14(3):327–332.
124. von Itzstein M (2007) The war against influenza: discovery and development of sialidase inhibitors. *Nat Rev Drug Discov* 6(12):967–974.
125. Fujihashi M, Peapus DH, Kamiya N, Nagata Y, Miki K (2003) Crystal structure of fucose-specific lectin from *Aleuria aurantia* binding ligands at three of its five sugar recognition sites. *Biochemistry (Mosc)* 42(38):11093–11099.
126. Fath S, Mancias JD, Bi X, Goldberg J (2007) Structure and Organization of Coat Proteins in the COPII Cage. *Cell* 129(7):1325–1336.
127. Bosanac I, et al. (2009) The structure of SHH in complex with HHIP reveals a recognition role for the Shh pseudo active site in signaling. *Nat Struct Mol Biol* 16(7):691–697.
128. Abergel C, et al. (1999) Structure of the Escherichia coli TolB protein determined by MAD methods at 1.95 Å resolution. *Structure* 7(10):1291–1300.
129. Volz JC, et al. (2016) Essential Role of the PfRh5/PfRipr/CyRPA Complex during Plasmodium falciparum Invasion of Erythrocytes. *Cell Host Microbe* 20(1):60–71.
130. Galaway F, et al. (2017) P113 is a merozoite surface protein that binds the N terminus of Plasmodium falciparum RH5. *Nat Commun* 8:14333.
131. Wright KE, et al. (2014) Structure of malaria invasion protein RH5 with erythrocyte basigin and blocking antibodies. *Nature* 515(7527):427–430.

**PERSONAL
INFORMATION****Paola Favuzza**

📍 Petersgraben 15, 4051 Basel, Switzerland

☎ +41 61 284 82 51 📠 +41 78 904 43 20

✉ paola.favuzza@unibas.ch ✉ paolafavuzza@gmail.com

🌐 <http://www.swisstph.ch/>

| Sex Female | Date of birth 24 Feb 1986 | Nationality Italian | Civil Status Nubile

ACADEMIC EDUCATION

- Jul 2011–Dec 2015 PhD in Microbiology
Molecular Immunology, Medical Parasitology and Infection Biology
Swiss Tropical and Public Health Institute (Swiss TPH), Basel (Switzerland)
- Oct 2007–Mar 2010 MSc in Biotechnology for Industry and Scientific Research (110/110 cum Laude et Mentio).
University of Palermo, Palermo (Italy).
- Oct 2004–Oct 2007 BSc in Biotechnology (110/110 cum Laude et Mentio).
University of Palermo, Palermo (Italy)

RESEARCH EXPERIENCE

- Jan 2016–Present Postdoctoral Scientific Collaborator
Medical Parasitology and Infection Biology, Swiss Tropical and Public Health Institute
(Swiss TPH), Basel (Switzerland)
Molecular Immunology. Malaria vaccine development.
- Mar 2013–Present Visiting Researcher
F. Hoffmann - La Roche Ltd., Basel (Switzerland)
Production of Monoclonal Antibodies. Protein purification and crystallization.
- Jul 2011–Dec 2015 Experimental PhD thesis:
'From reverse to structural vaccinology: profiling of CyRPA as new Plasmodium falciparum
malaria vaccine candidate antigen.'
Swiss Tropical and Public Health Institute, Basel (Switzerland).
F. Hoffmann - La Roche Ltd., Basel (Switzerland)
- Oct 2008–Jul 2009 Internship and Experimental MSc thesis:
'Phenol Hydroxylase from Trichosporon cutaneum: Gene Cloning and Protein Expression in
Heterologous Hosts.'
FHNW, University of Applied Sciences Northwestern Switzerland; School of Life Sciences,
Basel (Switzerland).
- May 2007–Jul 2007ent Internship and Experimental Bsc thesis:
'Study of mutation occurring to the Perforin gene (PRF1) in lymphoma patients.'
Dept. of Experimental Oncology and Clinical Application (DOSAC) c/o "La Maddalena",
University of Palermo (Italy).

WORK EXPERIENCE

- Jun 2010–May 2011 Trainee in Analytical Sciences
Novartis Pharma AG (NIBR), Basel (Switzerland)
- Quality control analysis of recombinant proteins: HPLC, LC-ESI-MS; ULPC-ESI-MS/MS; UPLC-ESI-QToF-MS/MS; MALDI-TOF/TOF; N-Terminal Sequencing.
- Development of HPLC-MS based methods for the characterization of N-Glycosylated proteins and Immunoprecipitation assays for Abs and ADCs.

PERSONAL SKILLS

- Mother tongue Italian
- Other languages English: proficient user
CEFR (Common European Framework of Reference for Languages) - C1
IELTS (International English Language Testing System) - score 7.5 (Apr 2017)
German: basic user
- Laboratory skills
- DNA extraction, purification, amplification, hybridization, sequencing and analysis;
 - Bacterial, Yeast and Mammalian cells culture methods; methods in Malaria research (*P. falciparum*);
 - Recombinant protein expression, extraction, purification, crystallization, structural and functional characterization;
 - Hybridoma cell lines generation and monoclonal antibodies (mAbs) production, purification, structural and functional characterization;
 - Molecular immunology methods: WB, ELISA, IFA, FACS;
 - Animal work: immunization and treatment of mice (s.c., i.p., i.m. p.o.), blood collection in mice;
 - Databases analysis.
- Computer skills
- Good knowledge of bioinformatics software and on-line tools for nucleic acids and proteins analysis;
 - Good knowledge of the Microsoft Office package, Adobe Photoshop, GraphPad Prism;
 - Good knowledge of MAC OS X (10.11) and MS Windows (XP, 7).
- Interests Skiing, Diving, Cooking
- Driving licence A1, A, B

PUBLICATIONS

Favuzza P, Dreyer AM, Lamelas A, Matile H, Pluschke G: **Evaluation of the conserved *Plasmodium falciparum* merozoite antigen PF14_0044 as candidate vaccine antigen.** *Malaria Journal*, Ready for submission.

Favuzza P, Guffart E, Tamborrini M, Scherer B, Dreyer AM, Rufer AC, Erny J, Hoernschemeyer J, Thoma R, Schmid G, Gsell B, Lamelas A, Benz J, Joseph C, Matile H, Pluschke G and Rudolph MG: **Structure of the malaria vaccine candidate antigen CyRPA and its complex with a parasite invasion inhibitory antibody.** *eLife* 2017; 10.7554/eLife.20383

Favuzza P, Blaser S, Dreyer AM, Riccio G, Tamborrini M, Thoma R, Matile H, Pluschke G: **Generation of *Plasmodium falciparum* parasite-inhibitory antibodies by immunization with recombinantly-expressed CyRPA.** *Malaria Journal* 2016, 15:161.

Favuzza P, Blaser S, Dreyer AM, Tamborrini M, Matile H, Pluschke G: **Novel approaches for the identification and profiling of new *Plasmodium falciparum* antigens as promising blood-stage candidates for inclusion in a malaria subunit vaccine.** *Trop Med Int Health* 2015, **20**(Suppl 1):1–147.

Favuzza P, Dreyer AM, Wittlin S, Matile H, Pluschke G: **Cysteine-Rich Protective Antigen (CyRPA) as promising blood-stage candidate protein for inclusion in a malaria subunit vaccine.** *Malaria Journal* 2012, **11**(Suppl 1):P30.

Dreyer AM, Matile H, Papastogiannidis P, Kamber J, Favuzza P, Voss TS, Wittlin S, Pluschke G: **Passive immunoprotection of *Plasmodium falciparum*-infected mice designates the CyRPA as candidate malaria vaccine antigen.** *J Immunol* 2012, **188**:6225–6237.

CONFERENCES

ICTMM 2016: International Congress for Tropical Medicine and Malaria 2016

Melbourne, Australia. September 2016.

Oral presentation: ‘From reverse to structural vaccinology: profiling of CyRPA as promising *Plasmodium falciparum* malaria vaccine candidate antigen’.

BioMalPar XII: Biology and Pathology of the Malaria Parasite

EMBL Heidelberg, Germany. May 2016.

Oral presentation: ‘From reverse to structural vaccinology: profiling of CyRPA as promising *Plasmodium falciparum* malaria vaccine candidate antigen’.

Co-chair of the Scientific Session “Immunology I”.

ETCMIH 2015- 9th European Congress on Tropical Medicine and International Health

Basel, Switzerland. September 2015.

Oral presentation: ‘Novel approaches for the identification and profiling of new *Plasmodium falciparum* antigens as promising blood-stage candidates for inclusion in a malaria subunit vaccine’.

Trop Med Int Health 2015, **20**(Suppl 1):1–147.

Advancing Vaccines in the Genomics Era (T1)

Rio de Janeiro, Brazil. November 2013.

Poster presentation: ‘Novel approaches for the identification and profiling of new *Plasmodium falciparum* candidate vaccine antigens’.

Challenges in malaria research

Basel, Switzerland. October 2012.

Poster presentation: ‘Cysteine-Rich Protective Antigen (CyRPA) as promising blood-stage candidate protein for inclusion in a malaria subunit vaccine’.

Malaria Journal 2012, **11**(Suppl 1):P30.

TEACHING EXPERIENCES

- | | |
|-------------------|--|
| Feb 2015–Feb 2016 | Supervision of an MSc student. ‘Generation and characterization of parasite inhibitory monoclonal antibodies against the malaria blood stage vaccine candidate PfRH5’.
Master Infektionsbiologie, University of Basel, Switzerland. |
| Feb 2014–Feb 2015 | Supervision of an MSc student. ‘Cysteine-Rich Protective Antigen (CyRPA) as promising blood-stage candidate antigen for inclusion in a malaria subunit vaccine’.
Master Infektionsbiologie, University of Basel, Switzerland. |

Lectures and Seminars

Advanced Immunology of Infections

Master Infektionsbiologie, University of Basel, Switzerland. May 2016.

‘From reverse to structural vaccinology’.

Advances in Infection Biology, Epidemiology and Global Public Health

Master Infektionsbiologie, University of Basel, Switzerland. Autumn semester 2015.

‘Novel approaches for the identification and profiling of new *Plasmodium falciparum* antigens as promising blood-stage candidates for inclusion in a malaria subunit vaccine’.

Advanced Immunology of Infections

Master Infektionsbiologie, University of Basel, Switzerland. Spring semester 2013.

‘Reverse vaccinology: a new opportunity to identify novel malaria vaccine candidates’.